Role of the minimal inertia axis in the kinaesthetic control of unconstrained 3D movements

Clint Hansen

UNIVERSITE PARIS-SUD

ÉCOLE DOCTORALE : *ED 456*
Laboratoire de *CIAMS*

DISCIPLINE
« Sciences du Sport, de la Motricité et du Mouvement Humain »

THÈSE DE DOCTORAT

soutenue le 04/07/2013

par

Clint HANSEN

Role of the minimal inertia axis in the kinesthetic control of unconstrained 3D movements

Directeur de thèse :	Brice ISABLEU	MCF-HDR, Université Paris Sud
Co-directeur de thèse :	Philippe GORCE	PR, Université du Sud Toulon Var
Co-encadreur de thèse :	Nasser REZZOUG	MCF, Université du Sud Toulon Var

Composition du jury :

Président du jury :		
Rapporteurs :	Frédéric MARIN	PR, Université de Compiègne
	Emmanuel GUIGON	MCF-HDR, UMPC CNRS
Examinateurs :	Benoît BARDY	PR, Université de Montpellier

Acknowledgements

I would like to express my gratitude to my supervisors, Dr. Brice Isableu, Dr. Nasser Rezzoug and Professor Philippe Gorce. We had profitable scientific conversations during my Ph.D. study in France and they were always ready and present to discuss the project and execution.

I would like to thank the committee members, Dr. Guigon and Professor Marin, who have provided their feedback in their function as Rapporteurs. Also I would like to thank Professor Bardy who accepted to assist at the defense of this dissertation.

My gratitude is also extended to all my colleagues. Thanks for the help to the secretaries and the technical staff. Being involved in such a multicultural environment, as the Faculty of Sport Science, has been a real enriching experience. The present work has been granted by the Ministère de l'Enseignement Supérieur et de la Recherche.

1 Introduction 15
1.1 Motivation 15
1.2 Research goals 15
1.3 Summary of chapters 16
2 Literature and hypotheses 21
2.1 Introduction 21
2.2 Bernstein problem 21
2.3 Reference system 22
2.4 Motor control strategies 23
2.4.1 Computational motor control strategy 24
2.4.1.1 Internal Models 24
2.4.1.2 Forward models 26
2.4.1.3 Inverse models 28
2.4.1.3.1 Synthesis 29
2.4.1.3.2 Internal feedback 29
2.4.1.4 Cost functions 30
2.4.1.5 Optimal Control 32
2.4.1.6 Summary 33
2.4.2 Ecological and nonlinear dynamical systems approaches on perception and action 33
2.4.2.1 Proprioception and kinesthesia 36
2.4.2.2 Body schema 37
2.4.2.3 Inertia Tensor 39
2.4.2.4 Inertia Tensor and proprioception 40
2.4.2.5 Role of the inertia tensor in pointing movements 40
2.4.2.6 Role of the inertia tensor during rotation movements 43
2.5 Synthesis 46
2.6 Problematic 47
3 Biomechanical Model 51
3.1 Introduction 51
3.2 Anatomical background 51
3.2.1 Measuring human movement 52
3.2.2 Motion Capture Measurement Devices 53

3.3 Biomechanical model 55
3.3.1 Degrees of freedom 55
3.3.2 Shoulder 56
3.3.3 Elbow 56
3.3.4 Wrist 56
3.3.5 Global Reference System and Marker Set 57
3.3.6 Upper-body model segments 58
3.3.7 Upper-body model joints 60
3.3.8 Joint Angles Computation 61
3.4 Inertia tensor 63
3.4.1 Body Segment Inertial Parameters (BSIP) 64
3.4.1.1 Regression model 65
3.4.1.2 Geometric model 65
3.4.1.3 Dynamic estimation models 65
3.4.2 Chosen BSIP estimation technique 66
3.5 Computation of the rotation axes 66
3.5.1 Upper-limb inertia tensor and center of mass position in the global frame 69
3.5.2 Upper-limb forward model 70
3.5.3 Upper-limb COM position in the global frame 71
3.5.4 Upper-limb inertia tensor at the shoulder expressed in the global frame 72
3.5.5 e_3, SH-CM and SH-EL axes computation 73
3.6 Inverse dynamics 74
3.6.1 DH convention 75
3.6.2 Decomposition of the inverse dynamics computation 77
3.6.3 Validation of the inverse dynamics calculations 79
4 Hypotheses and Transition 83
5 Effect of velocity, sensory, gravity torque, arm dominance, initial instruction during purposeless (non-athletic) rotation movements tasks 91
5.1 Velocity-dependent changes of rotational axes during the control of unconstrained 3D arm motions depend on initial instruction on limb position. 91
5.1.1 Introduction 91
5.1.2 Results 97
5.1.3 Discussion 101
5.1.4 Conclusion 104
5.1.5 Executive Summary 105

5.2 Differences in the control of unconstrained 3D arm motions of the dominant and the non-dominant arm. 107
5.2.1 Introduction 107
5.2.2 Methods 109
5.2.3 Results 112
5.2.4 Discussion 118
5.2.5 Conclusion 121
5.2.6 Executive Summary 122
5.3 Differences in the control of unconstrained 3D arm motions due to gravitational torque 124
5.3.1 Introduction 124
5.3.2 Methods 126
5.3.3 Results 129
5.3.4 Discussion 135
5.3.5 Conclusion 138
5.3.6 Executive Summary 139
6 Effect of precision demands: maximizing precision in athletic skills 143
6.1. Precision throwing tasks and the control of unconstrained 3D arm motions 143
6.1.1. Introduction 143
6.1.2. Methods 145
6.1.3. Results 147
6.1.4. General discussion 156
6.1.5. Conclusion 158
6.1.6. Executive Summary 159
6.2. Differences between experts and novices in the control of unconstrained 3D throwing motions Darts Novices vs. Experts 161
6.2.1. Introduction 161
6.2.2. Methods 162
6.2.3. Results 165
6.2.4. Discussion 172
6.2.5. Conclusion 175
6.1.1 Executive Summary 176
7 Effect of velocity demands: Maximizing velocity in athletic skills. The axis of rotation changes during overarm throwing 181
7.1 The axis of rotation changes during the over arm throwing. 181

7.1.1 Introduction 181
7.1.2 Methods 183
7.1.3 Results 186
7.1.4 Discussion 193
7.1.5 Conclusion 195
7.1.6 Executive Summary 196
8 Effect of spatial and velocity demands. Maximizing both precision and velocity in athletic skills 201
8.1 The axis of rotation changes during the tennis service. 201
8.1.1 Introduction 201
8.1.2 Methods 203
8.1.3 Results 205
8.1.4 Discussion 210
8.1.5 Conclusion 212
8.1.6 Executive Summary 213
8.2 Intercepting balls and the control of unconstrained 3D arm motions 215
8.2.1 Introduction 215
8.2.2 Methods 216
8.2.3 Results 220
8.2.4 Discussion 229
8.2.5 Executive Summary 232
9 General Discussion 237
9.1 Role of minimal inertia axis e_3 238
10 Limitations 245
10.1 Technological Limitations 245
10.2 BSIP Estimation 245
10.3 Rotation axes computation 246
10.4 Biomechanical model 246
10.5 Experimental limitation 247
10.6 Simulations 247
10.7 Inter individual differences 248
11 Perspective 251
12 Conclusion 255
13 References 256

List of Figures

Figure 1 Successive positions of the right hand and a hammer during striking with a chisel (Bernstein, 1967, Chapter 2 page 16-17). 22
Figure 2 The sensoriomotor loop acan be divided into three stages. These three stages are represented in the CNS as internal models, known as the inverse model, forward dynamic model and forward sensory model respectively. 26
Figure 3 Relationship between grip force and load force. 27
Figure 4 A shows trajectories without perturbations. B shows the initial pertubations, causing large movement variations. C shows the trajectories with the perturbation after learning sessions and D shows the after effects of the trajectories when the perturbations are stopped. 28
Figure 5 The experimental setup proposed by Pagano (1996) to separate the geometric (SH-EL) and the e_3 axis. 41
Figure 6 This figure shows the experiments of van de Langenberg to seperate the CM and e3 axis. To do so, masses were attached to two rods with different distances on the forearm. 42
Figure 7 In 2009, Isableu et al. proposed an experiment that allowed to naturally separate the rotation axes during cyclic rotations of the arm. 44
Figure 8 Anatomical model of the human upper body 52
Figure 9 Example of a motion capture session including eight cameras and one force plate. 54
Figure 10 Example Marker Setup of the Upper-Body 57
Figure 11 Reference frames and notations to describe the upper-limb kinematics (Wu et al., 2005) (A—arm, F—forearm, H—hand). Oi designs the origin of segment i (i_A, F, or H). pij designs the vector between the origins of segment i and j. Vector gi defines the vector from the origin of segment i to its center of mass (CoM) Gi expressed in the frame of segment i. Ggi defines the position of the CoM of segment i in the global frame. Rij denotes the rotation matrix from frame i to frame j. 59
Figure 12 shows the directions of the principal moments of inertia of each upper body segment. 73
Figure 13 Schematic representations of the biomechanical multi-articulated upper limb model 76
Figure 14 The robot with DOF used for the inverse dynamics computation using the DH convention 80
Figure 15 Results of the validation study. No differences could be found between the computations of the DH convention and the analytical model. 80
Figure 16 Experimental setup A) shows the Elb90 and the Elb140 configuration B) shows the rotation axes 95
Figure 17 Angular separation between the rotation axes due to the elbow angle. 95
Figure 18 Angular variability of the rotation axes during the eyes open conditions 99
Figure 19 Angular variability of the rotation axes during the eyes closed conditions 99
Figure 20 Angular variability of the rotation axes during the active elbow fast condition comparison between dominant and nondominant arm 114
Figure 21 Angular variability of the rotation axes during the active elbow slow condition comparison between dominant and nondominant arm 115

Figure 22 Angular variability of the axes during the active elbow eyes open condition comparison between dominant and nondominant arm 116
Figure 23 Angular variability of the axes during the active elbow eyes closed condition comparison between dominant and nondominant arm 116
Figure 24 Complexity index of the postural sway in A/P direction during slow arm rotations. 117
Figure 25 Experimental conditions, from 0° to 135° shoulder elevation 126
Figure 26 Movement frequency and elbow angle during the eight experimental condition .. 129
Figure 27 The angular variability of the rotation axes due to the shoulder elevation angles 131
Figure 28 The angular variability of the rotation axes due to the shoulder elevation angles and velocity conditions 132
Figure 29 Angular variability of the rotation axes for each subject 134
Figure 30 Experimental setup 146
Figure 31 Average scores of the subjects throwing performance 148
Figure 32 shows the axial shoulder rotation kinematic parameters of 10 representative throws made by subject 8 aligned on the moment of darts release indicated by the vertical line. 148
Figure 33 shows the shoulder elevation kinematic parameters of 10 representative throws made by subject 8 aligned on the moment of darts release indicated by the vertical line. ... 149
Figure 34 shows the plan of elevation kinematic parameters of 10 representative throws made by subject 8 aligned on the moment of darts release indicated by the vertical line. ... 149
Figure 35 shows the elbow kinematic parameters of 10 representative throws made by subject 8 aligned on the moment of darts release indicated by the vertical line. 150
Figure 36 Mean hand heights at ToR during the six throwing conditions 151
Figure 37 Decomposed torque at the elbow joint. The trials are aligned on the ToR, indicated by the vertical black line. 152
Figure 38 Angular variability of the rotation axes during the six throwing conditions 154
Figure 39 Individual angular variability of the rotation axes during the six throwing conditions 155
Figure 40 Torque predictions of a dart throwing movement while stabilizing the SH-EL, SH-CM and the SH-e_3 axis 164
Figure 41 Differences the angular amplitude and the angular velocity amplitude between the novice and expert dart throwers 166
Figure 42 Dynamic differences between novices and experts regarding the maximal torque values during the throwing movement 167
Figure 43 Differences between novices and experts regarding the axial shoulder net torque 168
Figure 44 Differences of the angular variability of the rotation axes between novices and experts 170
Figure 45 Angular variability of the rotation axes of each subject 171
Figure 46 An example of the overarm throw in team handball of the different phases and characteristic points during the throw (Modified from (Meister, 2000)) 184
Figure 47 Velocity profiles of the hand of a representative subject over the 20 trials 186
Figure 48 Peak velocity, acceleration and jerk profiles of the shoulder, elbow and the hand 186

Figure 49 Axial shoulder rotation angle as a function of elbow flexion/extension angle [°]. This figure shows the individual throwing patterns of each subject. 188
Figure 50 Axial shoulder rotation net torque as a function of elbow flexion/extension torque. This figure shows the individual throwing patterns of each subject. 188
Figure 51 Angular variability of the rotation axes during each throwing phase. 190
Figure 52 Individual angular variability of the rotation axes for each subject in each throwing phase. 191
Figure 53 Contribution of the INT and MUS to NET torque during the three throwing phases shown for the shoulder axial rotation 192
Figure 54 Peak Velocity of the shoulder, elbow, wrist and racket during the tennis serve ... 206
Figure 55 Individual velocity profiles of the shoulder, elbow, wrist and racket 206
Figure 56 Angular variability of the rotation axes during each tennis serve phase. 208
Figure 57 Individual angular variability of the rotation axes for each subject in each tennis serve phase. 209
Figure 58 Contribution of the MUS and INT to NET torque during the four tennis serve phases 210
Figure 59 Initial set up of the subjects 217
Figure 60 Interception heights of the experimental setup 218
Figure 61 Subject 1 Hand movement traces 221
Figure 62 Subject 1 Elbow movement traces 222
Figure 63 Contribution of the INT and MUS torque do the interception task 224
Figure 64 Angular variability of the rotational axes throughout the nine conditions 227
Figure 65 Inter individual differences throughout conditions 228

List of Tables

Table 1 Anatomical landmarks and sequences used for the calculation of the relative angles between each segment. The coordinate system Xg, Yg, Zg is the global coordinate system according to Wu et al (Wu et al., 2005). 62
Table 2 Scaling factors for the position of the center of mass (Dumas et al., 2007) 67
Table 3 Scaling factors for the position of the center of mass (Dumas et al., 2007) 67
Table 4 Scaling factors for tensor of inertia (Dumas et al., 2007). 68
Table 5 Mass, length, COM and inertia tensor for one subject 68
Table 6 Table of Denavit-Hartenberg parameters associated with each DOF of the model 77
Table 7 Mean(SD) rotation axes variability across conditions and subjects. 97
Table 8 Manova results 98
Table 9 Angular Variability of the angular displacement of the axes (mean ± sd) 113
Table 10 MANOVA table 130
Table 11 Angular Variability of the angular displacement of the axes (mean ± std) 130
Table 12 Angular variability of the rotation axes during the six throwing conditions. 153
Table 13 MANOVA table 153
Table 14 Angular variability of the rotation axes during the dart throwing 169
Table 15 MANOVA table 169
Table 16 MANOVA table 189
Table 17 Mean (SD) rotation axes variability across conditions and subjects. 189
Table 18 Mean (SD) rotation axes variability across conditions and subjects 207
Table 19 Velocity conditions and time to contact 219
Table 20 MANOVA table 225
Table 21 shows the mean angular variability of the axes in the three velocity conditions and the three height configuration respectively. 225
Table 22 Task dependent experiments 237

Nomenclature list

$\mathbf{R}_{Gi}$	Rotation matrix from the global frame to frame *i*.
${}^{G}\mathbf{I}_{i}^{CoM}$	Inertia tensor of segment *i* at the segment CoM expressed in the global frame (superscript ^{G}).
${}^{i}\mathbf{I}_{i}^{CoM}$	Inertia tensor of segment *i* at the segment CoM expressed in the local frame (superscript ^{i}).
$\mathbf{R}_{Gi}$	Rotation matrix from the global frame to frame *i*.
${}^{G}\mathbf{I}_{i}^{CoM}$	Inertia tensor of segment *i* at the segment CoM expressed in the global frame (superscript ^{G}).
${}^{i}\mathbf{I}_{i}^{CoM}$	Inertia tensor of segment *i* at the segment CoM expressed in the local frame (superscript ^{i}).
${}^{G}\mathbf{I}_{i}^{SH}$	Inertia tensor of segment i at the shoulder expressed in the global frame.
${}^{G}\mathbf{I}_{i}^{CoM}$	Inertia tensor of segment i at its CoM expressed in the global frame.
m_i	Mass of segment i.
${}^{G}\mathbf{g}_{i}$	$${}^{G}\mathbf{g}_{i} = \begin{bmatrix} {}^{G}g_{Xi} & {}^{G}g_{Yi} & {}^{G}g_{Zi} \end{bmatrix}^{T}$$
$\mathbf{T}_{ij}$	(4x4) that gives the pose (position and orientation) of frame j with respect to frame i
$\mathbf{R_{01}}$	SCS of the upper-arm
$\mathbf{R_{02}}$	SCS of the forearm
$\mathbf{R_{03}}$	SCS of the Hand
$\mathbf{R_{02}^{T}}$	the superscript T on the right side of a SCS denotes the fact that the matrix is transposed
$\mathbf{e_1}$, $\mathbf{e_2}$, $\mathbf{e_3}$	eigenvectors of the inertia matrix
$\boldsymbol{\Theta}$	Vector joint angle
DOF	Degrees of freedom
ROM	Range of motion
SCS	Segment Coordinate System
SH-EL	geometrical articular rotation axis
SH-CM	Center of mass based rotation axis
SH-e3	Inertia-based rotation axis
MIT	Minimum Inertia Trajectory
MIR	Minimum Inertia Resistance
COP	Center of pressure
CoM	Center of Mass

Chapter 1

1 Introduction

1.1 Motivation

The human body constantly completes voluntary and non-voluntary movements. While non-voluntary movements are not controlled by the motor cortex, voluntary movements are triggered by axons, running into the corticospinal tract to connect with motor neurons in the spinal cord. Voluntary movements take a large amount of energy expenditure in daily life and, therefore, saving energy by slight changes in the movement control is important. Movements such as taking a cup of coffee from the table demand detailed trajectory planning of the extremities that take into account the possible redundancy of degrees of freedom (DOF) (Bernstein, 1967). Multiple theories deal with the phenomenon of trajectory planning, including Latash (2008). Recently a new theory has been proposed dealing with the resistance to change any physical object in that state of motion (Bernardin et al., 2005). More precisely, the minimum inertia resistance principle (MIR) investigates the role of minimum axes of rotation in motor control (Isableu et al., 2009); (Bernardin et al., 2005); (Pagano and Turvey, 1995); (van de Langenberg et al., 2007; van de Langenberg et al., 2008). While the MIR has been successfully identified with respect to proprioception during pointing tasks (Pagano and Turvey, 1995), its has not yet been clearly identified during unconstrained 3D movements. The model has not yet been validated with experimental data but has been theoretically demonstrated to have an influence on the inverse dynamics of the upper extremities (Isableu et al., 2009).

1.2 Research goals

The overall aim of this dissertation is to develop experimental conditions that validate the MIR principle and its biomechanical role during unconstrained 3D movements and propose methods that will possibly facilitate movement planning and learning. It is clear that computational models have the potential to simulate the outcome of specific research questions in biomechanics and motor control on inter- or intracellular level. Still the models have no “Raison d'être” when not rigorously validated against experimental data. In this research, the objective is to validate this model using experimental results, and the experimental data has been analyzed depending on the specific research question. Second, experimental settings are developed to show the influence of the MIR principle during basic and applied

research. The possible impact in basic research has already shown(Isabeu et a., 2009), but only additional experiments, including complex multi articulated 3D movements with different ranges of motion and velocities, can validate the theory over a range of different experiments. As a final point, limitations of the experimental as well as the modeling protocol are presented in the context of different motor control strategies with special emphasis to the study of the MIR principle.

1.3 Summary of chapters

The structure of this dissertation has been organized to answer the essential question when developing experimental studies to validate a motor control theory. The main objective of Chapter 2 is to provide a working knowledge base that will serve as reference to the experiments and topics covered in the remaining Chapters. Chapter 2 discusses motor control theories and provides further information for developing experimental research questions and validating a motor control theory. This chapter places particular emphasis on theapplication of the computations on diverse multi articulated movements of the upper limbs. Motor control theories are critically discussed and compared with the proposed MIR principle.

Chapter 3 discusses the biomechanical functions of the model and provides the computation background and further motivation for developing more detailed and sophisticated models. Subjects such as the computational model and validation studies as well as data processing techniques are presented. Chapter 3 also discusses the development and validation of a subject-specific model of the torso, arm, forearm and the hand. In this dissertation, experimental models are developed and validated to study the kinematics and dynamics of the upper body, specifically the arm. Computational predictions of joint torque were validated by direct comparison to experimentally measured computations using kinematic data from a motion capture system as input. The influence of measured and assumed computation model outputs such as kinematics, joint torque and body segment inertial parameters were assessed and compared to results from the literature.

Chapter 4 spans a bridge between the theoretical background to the experiments proposed in Chapter 5 through 8 and lays out the formulation of the hypotheses of the different experiments. The main objective is to provide a Leitmotif, based on

previous results and the outcome of each conducted experiment. While the results of each study have shed light to previously proposed research hypotheses, the application of the gained results automatically leads to further hypotheses. Consequently, the initial research hypothesis has been tested against a variety of changing constraints using individual research protocols.

Subsequently, Chapter 5 presents three conducted research studies covering the topic of the “Effect of velocity, sensory, gravity torque, arm dominance, initial instruction during purposeless (non-athletic) rotation movements’ tasks”. Chapter 6 deals with two experimental studies related to the “Effect of precision demands: “maximizing precision” in athletic skills”. Chapter 7 will tackle research questions regarding the “Effect of velocity demands: Maximizing velocity in athletic skills. The axis of rotation changes during overarm throwing”. After having evaluated the effects of velocity demands Chapter 8 examines the “Effect of spatial and velocity demands: Maximizing both precision and velocity in athletic skills”. Every study will follow the guidelines of a research article being subdivided in Introduction, Methods, Results and Discussion/Conclusion.

Regardless of the formulated and introduced research hypotheses, following each study, the main points and hypotheses will be highlighted and used to guide the research interest to the next study as proposed in the Leitmotif (Chapter 4).

The gained conclusions from the studies of Chapter 5 through 8 are synthetized, discussed and compared with findings from the literature. Differences in the present results with related motor control theories are reported and possible clinical and physiological implications of these data are discussed. Chapter 9 concludes with a discussion of the challenges involved following specific motor control theories and makes recommendations in the context of future efforts.
Finally, Chapter 10 summarizes the entire dissertation by highlighting the important contributions that were made to the field motor control along with a discussion of limitations (Chapter 11) and future research directions (Chapter 12).

Chapter 2

2 Literature and hypotheses

2.1 Introduction

The purpose of this chapter is to present the context of the study developed in this dissertation regarding the role of the minimum inertia resistance axis during 3D uncontrolled movements. In the first part, we will introduce the main problem and will review the main approaches to study motor control including the computational, ecological and dynamic approaches. Then, the background relative to the minimum inertia resistance (MIR) principle is detailed and its relevant features in the control of human movements are discussed. The last part of this chapter describes the hypotheses related to this dissertation.

Motor Control in general tries to explain information processing related to activities carried out by the central nervous system (CNS) that organize the musculoskeletal system to create coordinated movements and skilled actions. To coordinate movements the focus can be put on biomechanical, neuromuscular, control and functional levels. Motor control models have the potential to explain movement and behavior pattern for living subjects (Bernstein, 1967). However, based on the variety of theories available in the literature, experimental data can probably be explained by multiple theories and some models do not have the ability to predict or explain movement patterns with sufficient accuracy (see (Guigon, 2010) & (Gielen, 2009)).

2.2 Bernstein problem

Bernstein (1967) observed that the same motor task can be performed in multiple ways with specific characteristics. The observation of a kinematically redundant system led to the formulation of the degrees of freedom (DOF) problem. The question arises how the CNS decides which solution is the most suitable.

The musculoskeletal system and its control can be characterized by two fundamental properties: redundancy and variability. The planning and control of movements of the upper limb leads to an "ill-posed" problem, because the motor system has more variables to tune than necessary to execute a predefined task (Kawato 1993). An infinite number of possibilities exist to move the finger along a trajectory from a start to an end position in Cartesian space. In addition, to follow a given path, there are endless combinations of joint configuration.The same joint trajectory can be obtained by an infinite number of muscle activation patterns. This property of the musculoskeletal system is called redundancy or motor abundance.

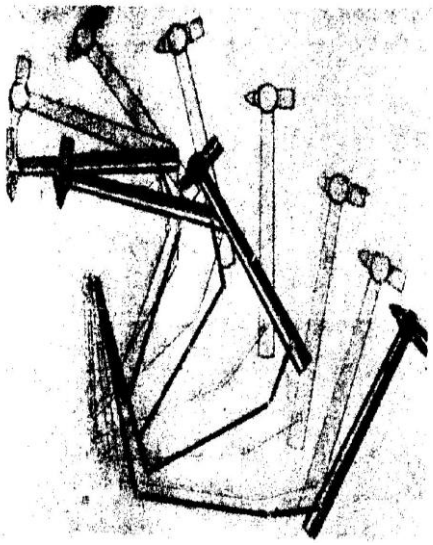

Figure 1 Successive positions of the right hand and a hammer during striking with a chisel (Bernstein, 1967, Chapter 2 page 16-17).

An initial experiment of Bernstein showed redundancy during hitting a chisel with a hammer. The endpoint position of the hammer hitting the chisel can stay unaffected but due to the kinematic redundancy the movement pattern alters without affecting the endpoint precision. Highly complex movements are organized as integral units and changes in one part of the motion lead to corresponding changes in the movement (Latash, 1998). The question arises how the CNS decides which solution is the most suitable.

2.3 Reference system

Before a movement can be performed, the task and the target need to be integrated in the motor planning. In order to do a voluntary movement the perception, cognition and the action play major roles. Being aware of one's environment helps to take cognitive decisions, that can be translated into actions (Newell A. and Simon H.A, 1972). The actions are transformation from motor commands which are governed by the physics of the environment, the musculoskeletal system and sensory receptors (Wolpert and Ghahramani, 2000).

The perception of the environment and the target are very important in the decision making and execution of a task. It has been shown that the brain does not specify a movement in terms of a final position (Desmurget and Prablanc, 1997); (van den

Dobbelsteen et al., 2001) but rather in terms of a vector (Vindras and Viviani, 1998); (Vindras et al., 2005). Following this idea, the target and the effector need to be expressed in a mutual reference frame to compute the vector (Gielen, 2009). Varying theories have been developed that show that a common reference frame can be coded in a visual, auditory and/or tactile centered frame. Also the mutual reference frame can be head-centered or expressed in somatosensory coordinates, respectively (Gielen, 2009). Also the coding seems to be time dependent and the reference frame may change between movement planning and the movement execution. In early stages of the movement planning, eye-centered coordinates are preferred (Batista et al., 1999); (Medendorp et al., 2003);(Admiraal et al., 2004) over proprioceptive coordinates in the absence of visual cues (Berkinblit et al., 1995); (van Beers et al., 1999b; van Beers et al., 2002); (Gielen, 2009) in tasks involving specified endpoints. Many studies have provided evidence for an endpoint coded approach and the endpoint can be coded in shoulder-centered coordinates (Flanders (Flanders and Soechting, 1992); (McIntyre et al., 1998); (Soechting and Flanders, 1989; Soechting and Lacquaniti, 1989) (van den Dobbelsteen et al., 2001), hand-centered coordinates (Sainburg et al., 2003); (Vindras et al., 2005), eye-centered coordinates (Henriques et al., 1998) (McIntyre et al., 1997); (Medendorp and Crawford, 2002); (Vetter et al., 1999), and even in multiple frames of reference (Lemay and Stelmach, 2005); (McIntyre et al., 1998)

Recently McGuire and Sabes (2009) proposed the multiple reference frames hypothesis for the optimal use of available sensory information. This hypothesis explains task-dependent reweighting of sensory cues. The authors claimed that movements are always represented in multiple reference frames, independent of the task, and it is the statistical reliability of these representations that determines their relative weighting. Also, only multiple reference frames in the model can be accounted for using a reweighting of visual feedback of the hand as a result of the target type.

2.4 Motor control strategies

The identification of physical parameters that can act as collective variables to simplify the control of joint DOFs (Bernstein, 1967) is a subject of continued controversy and the following subchapter is devoted to introduce three motor control strategies that provide solutions to the motor redundancy problem.

2.4.1 Computational motor control strategy

Computational motor control combines applications and quantitative tools to study biological movement control. In general terms, the models try to explain movements based on assumptions of the nervous systems state, movement laws and internal processes.

Along the lines of the introduction of Jordan and Wolpert (1999), the motor system can be considered as a system with inputs and outputs. The inputs are the motor commands emanating from the controller within the CNS and the outputs are the sensory feedback signals. As not all signals in CNS are known, an additional set of state variables has to be estimated .

In computational motor control, knowledge about the state of the system is not trivial and many factors complicate the system. Franklin & Wolpert (2011) showed that the computation outcome depends on multiple factors, including the redundancy in the human system due to the DOFs of the joints and the muscle contribution but also noise. To understand how information is treated and how the movement is performed, the computational approach uses internal models to explain the preparation and execution of movements. Internal models predict the consequences of motor commands and model the relationship between actions and their consequences (Wolpert and Flanagan, 2001).

In the following subchapter we will discuss two important points in computational motor control. First internal models are presented, which are neural processes simulating the response of the motor system in order to estimate the outcome of a motor command. In the second part, the functions are presented that measure the cost of a movement. The trajectories are assumed to be solutions of an optimal control problem whose cost has to be determined. Also, some examples will be given on how a movement could be considered as optimal by minimizing specific costs.

2.4.1.1 Internal Models

In order to control movements, the motor commands have to be converted into physical action. Jordan and Wolpert (1999) showed that internal models are neural processes simulating the sensorimotor response of the motor system. Internal

models are important because they allow for the control of the motor system using constant interactions of the body as an input to estimate the necessary motor commands.

Executing a movement is the cause of an internal representation of the movement. Movement planning and the movement itself can be divided into motion planning, processing of the information, and the estimation of the required motor commands. The internal representation involving perception, cognition and action is called internal model. Kawato et al. (1987) introduced the internal model principle in order to explain human movements and to understand the physical outcome of motor commands.Internal models can model the relationship between actions and their consequences (Wolpert and Flanagan, 2001).

Before predicting the consequences, motor commands have to be adapted depending on the movement context. Wolpert and Ghahramani (2000) showed that the sensorimotor loop can be divided into three stages. The first stage of the sensorimotor loop specifies the motor command generated by the CNS given the state and a particular task (Figure. 2, top). The second stage determines how the state changes given by the motor command (Figure. 2, right). The third state closes the loop by specifying the sensory feedback given by its new state (Figure. 2, left).

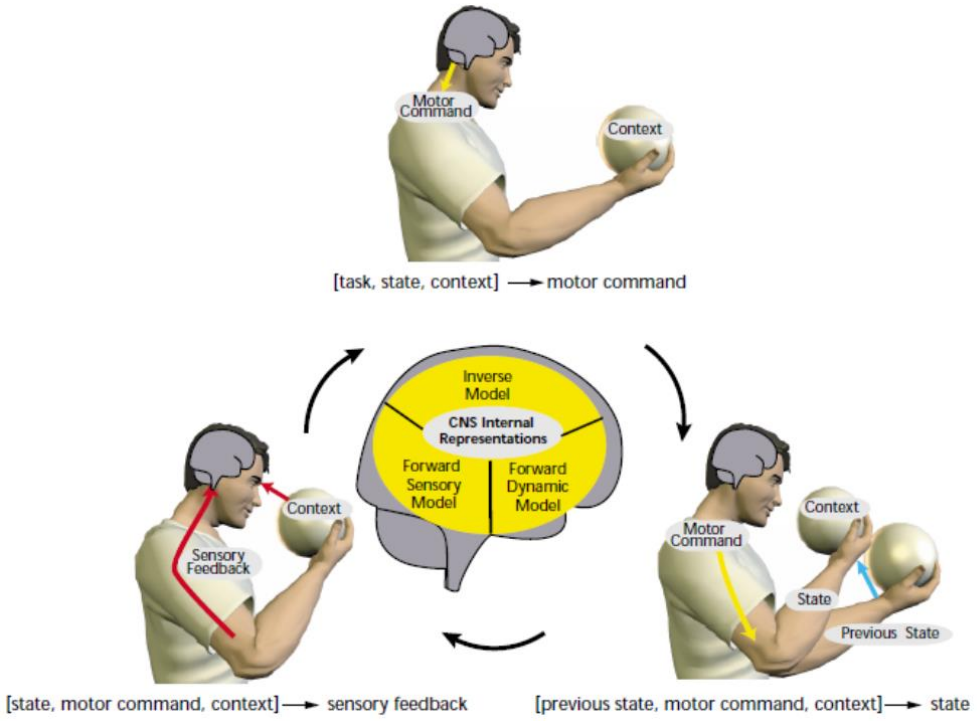

Figure 2 The sensoriomotor loop acan be divided into three stages. These three stages are represented in the CNS as internal models, known as the inverse model, forward dynamic model and forward sensory model respectively.

These models help to explain how the system may be controlled and counteracts perturbation to ensure robust control. Internal models can be subdivided into forward models and inverse models.

2.4.1.2 Forward models

The forward model delivers information about the causal relationship between actions and their consequences. It is very useful to predict the behavior of a system. For example taking the current state of the arm including its position, velocity and input such as control, it is possible to predict the future position and velocity of the arm.

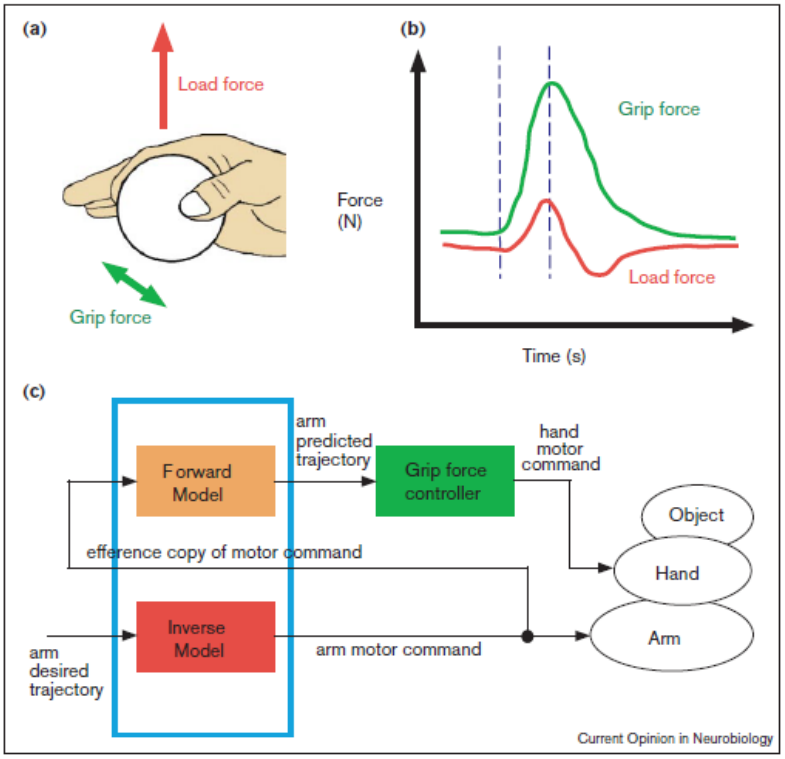

Figure 3 Relationship between grip force and load force.

Kawato (1999) showed the existence of forward models in the coordination between reaching and grasping. To prevent an object from slipping during a movement, a grip force must be exerted to compensate for the load force. Thus, holding a ball with the tips of the index finger and thumb on either side (Figure 3a), the grip force is accurately controlled (Figure 3b). The grip force must be greater than the minimum grip force needed in order to prevent the ball from falling. This grip-force–load-force coupling is explained by a framework that contains both the inverse and forward models of the arm.

Forward models may be of potential utility to solve particular problems in motor control (Wolpert et al., 1995). Indeed, they may be useful because sensorimotor delays are too high to allow efficient feedback control during fast movements. Therefore, it could be interesting to predict the outcome of an action before the sensory information is available. They could be used to predict and cancel the sensory effect of movement. During a learning process they can provide information because they allow to project errors between the actual and desired sensory response in errors in motor commands. Similarly, the sensory consequences can be

predicted without effectively executing the task therefore providing information for mental practice.

2.4.1.3 Inverse models

In contrast to direct models, inverse model characterize the relationship between desired consequences and corresponding actions. To give an example, the dynamics of the arm such as the trajectory are translated into appropriate control inputs to drive the arm along this trajectory.

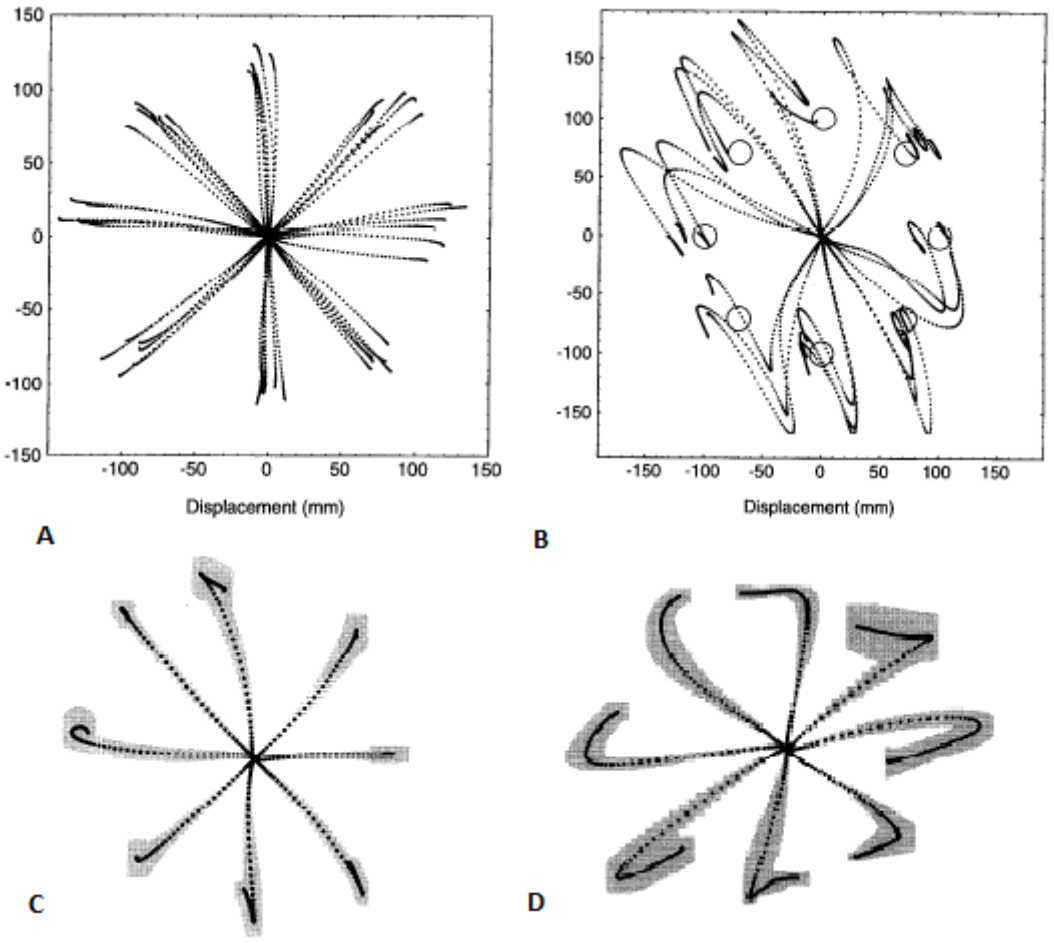

Figure 4 A shows trajectories without perturbations. B shows the initial pertubations, causing large movement variations. C shows the trajectories with the perturbation after learning sessions and D shows the after effects of the trajectories when the perturbations are stopped.

Shadmehr and Mussa-Ivaldi (1994) showed the existence of inverse models during planar arm pointing movements with perturbations (Figure 4). The participants of the study encountered dynamical perturbation during the pointing task. While the first

perturbation led to large movement variability, with training and constant perturbation the pointing movement returned to normal shape. However, when the perturbations are stopped, the movements show after-effects resulting in perturbed movement trajectories. The after-effects indicate that an inverse model of the system dynamics has been modified with training and the desired trajectory was successfully translated into the appropriate control commands.

2.4.1.3.1 Synthesis

Forward models can predict sensory consequences from efferent copies of issued motor commands. The estimated sensory sensations and the actually measured information serve as a control if, for example, the hand follows the proper trajectory (Gielen, 2009). That information can be used as an inverse internal model (Franklin et al., 2003) to determine the feed forward motor commands, which are based on learnt mean dynamics and an impedance controller to assist in the formation of the inverse dynamics.

2.4.1.3.2 Internal feedback

Internal errors in sensory-motor systems are common due to sensory noise, movement execution faults and inaccurate task specification (Faisal et al., 2008). To overcome such errors, sensory feedback is necessary to compare the actual and the desired performance. Movement modification is based on the sensory feedback and any difference between intended and actual movement is corrected whenever an error is detected. Especially in tasks related with terminal accuracy the correction leads to improved terminal accuracy and reductions of the arm trajectory variability, despite the fact that the variability of motor patterns (EMGs and torques) increased with co-contraction (Seidler-Dobrin and Stelmach, 1998; Laursen et al., 1998; Gribble et al., 2003; Osu et al., 2004)

The crux of the feedback is the time delay. Even though the movement might be corrected, the delayed response execution will lead to a different performance profile as expected. When changing the movement pattern during a reaching movement the usual bell-shaped velocity profile will be modified. This results in a longer

deceleration phase (Nagasaki, 1989), such that the trajectory deviates from the bell-shaped velocity profile (Plamondon et al., 1993).

Another method for overcoming motor error is through adapt action and learning. If the same movement is performed multiple times, the feedback will in turn influence the feed forward signal and motor learning will have taken place (Houk et al., 1996). This led to the suggestion that the learning of the inverse model could be done more quickly and more efficiently by simulating these tasks with the forward model (Kawato et al., 1987), (Miall and Wolpert, 1996). Also, previous experiences will contribute to an internal representation of the body (Massion, 1994) as shown when controlling the body position in space for stability and orientation (Shumway-Cook and Woollacott, 2007). Also, vestibular and proprioceptive changes (Kandel et al., 2000) have to be taken into account to anticipate disturbances to the postural control system arising as a consequence of movement (Aruin et al., 2001).

2.4.1.4 Cost functions

Due to the musculoskeletal redundancy, several solutions exist in end effector-, joint- and muscle space to execute a particular motor task. Among the infinite number of solutions, the idea has emerged that the chosen movement and the control of the CNS might optimize a particular variable such as effort, smoothness, etc.

In order to estimate whether or not a movement can be considered as efficient, parameters have been introduced to quantify its efficiency according to a particular cost function. From a certain point of view, cost functions assume that all movements are efficient. Over the years, many of them have been introduced in motor control in order to estimate which parameter is optimized. Brown and Rosenbaum (2002) proposed that planning criteria depend on geometric constraints (such as Listing's law, the law of Donders), a coupling between effectors, properties of the neuro-motor device (such as the theory of equilibrium point), cost reduction such as the minimization of torques.

The optimal principle is based on the assumption that the CNS system chooses one solution among those possible by minimizing its cost. A number of models are based on this principle and have been introduced over the years based on kinematic and dynamic variables and have been grouped under the term "optimal control"

(Pontryagin et al., 1962); (Kirk, 1970), (Bryson and Ho, 1975). In the context of human movement the two models need to be mentioned, the "minimum jerk" model (Flash and Hogan, 1985) which promotes the generation of a fluid motion by minimizing the derivative of acceleration (jerk) of the endpoint and the "minimum torque change" model (Uno et al., 1989). The "minimum torque change" model promotes the generation of a movement that minimizes the variation of developed joint torques.

Despite the similarity of certain movement characteristics provoked by these models, one of the major challenges is to understand how the neural substrate encodes the cost function such as the integral of the jerk or the variation of the torque over time.

Thus, other models are, physiologically speaking, directly related to muscle control and may contain more plausible criteria. In particular, they propose to minimize the variance of the final position of the end effector of a kinematic chain in the case where the effects of motor noise are proportional to the intensity of the considered motor command (Harris and Wolpert, 1998; Todorov and Jordan, 2002; Todorov, 2004, 2005). Finally, other models have been proposed to minimize muscle work based on mathematical analyses that predict the inactivation of certain muscles during the movement (Berret et al., 2008).

The goal of optimization based models of motion is that the models try to understand how movements are planned and executed.

2.4.1.5 Optimal Control

After having introduced cost functions, the question arises which cost function optimizes the human movement and how it is chosen. As already pointed out, the human system is undergoing constant changes and influenced by its current physiological shape. One of the ambitions in motor control is to find solutions that could be optimal, but what are optimal solutions? A solution to kinematic redundancy could likely be found in the framework of the optimal control theory.

Todorov and Jordan (2002) introduced that the CNS uses a minimal intervention principle in which noise/errors are not corrected if they do not influence the goal of the task. As soon as the task is affected, it is quickly corrected. Irrelevant noise is ignored because attempts to correct such errors may lead to new errors that influence the goal. Thus the best solution is to leave them alone. As a result, patterns of movement variability are not random, but show an organizational dependency on the task goal (Scholz and Schoner, 1999). Following this approach, motor control is viewed as the mastering of state-dependent dynamics in the presence of state- and control-dependent noise (Todorov, 2005). The optimal control strategy states that a unique solution to an ill-posed problem can generally be obtained as the solution that corresponds to the minimum of a cost function. However, the optimal solution is not general as the biological system tries to produce motor commands, that optimise behaviour with respect to biologically-relevant task goals (Diederichsen et al., 2009).

Rigoux and Guigon (2012) proposed a model of decision making based on the costs and benefits of the task and Berret et al. (2011) showed that an inverse optimal control methodology is able to identify the cost function that best replicates the participants' behaviour during a task with target redundancy.

A hybrid composite of cost functions mixing mechanical energy expenditure and joint smoothness was found to be close to the solutions of an optimal control problem, relying on a composite cost function mixing mechanical energy expenditure and joint smoothness. A combination of cost functions could lead to an optimal control but individuals may have different hybrid models when performing a motor task.

Based on the choice of the cost function, a movement could be considered as optimal. This would be a biased approach because each individual has specific

movement patterns. The origin of these patterns can be manifold. Habits, social conventions and health issues will affect the movement. The calculation of cost functions depends on the combination of external task demands and internal constraints and the outcome of an applied cost function to the movement may be different between individuals.

2.4.1.6 Summary

Trying to understand how movements are planned and executed is a very challenging task. One of the drawbacks of the computational approach is that depending on the studied parameter, an explanation is always based on assumptions that may have falsified the results. The introduction of optimal control mechanisms in motor control is an interesting approach to determine the cost function that fits best the movement but inter-individual differences will not allow a generalization of the results.

Parallel to the computational approach another control strategy has been developed, the ecological and dynamical approach.

2.4.2 Ecological and nonlinear dynamical systems approaches on perception and action

The ecological approach to perception and action is a perception-guided (Gibson, 1966) strategy. To perform an action or motor task, task-specific perceptual information is required. The organization of the movement itself is task and environment dependent and the perceptive information will support the action necessary to achieve the movement goal.

Sensory inputs are constantly perceived and the human processes the different kinds of sensory information to interact with its environment. The input that arrives at the receptors of an organism corresponds to the properties and changes of the environment and the body (Gibson, 1966). As perception is directly coupled with action, perception and action always influence each other creating a perception-action cycle.

The directly coupled perception-action follows the idea that physical invariants (Michaels and Carello, 1981) are also perceived continuously leading to information about possible actions and interactions with the environment. To detect these physical constants or invariants does not need internal representations and the idea that perception directly influences the action is contrary to computational approaches using internal models to interact with the environment. The general assumption is that perception is defined through laws that specify the action (Turvey, 1990; Turvey et al., 1981).

Direct perception (Gibson, 1979) is a functional approach because humans perceive their environment and act depending on the sensory information and properties of the environment. The properties provide a variety of opportunities to interact with the environment and are known as affordances (Gibson, 1966; Gibson, 1979). Turvey et al. (1999) defined affordance as the complementary relations between the environment and the human.

The relation between the perception of the environment and the action strongly depends on the environment itself. Changing ecological invariants or adding constraints will alter the physical characteristics of the action (Araújo et al., 2004).

Relations between individuals and the environment also depend on the individuals' perception of the environment, taking into account its individual motor capabilities (Turvey et al., 1999)

Interesting examples for the ecological approach are the tau and the bearing angle theory. In order to intercept an object flying towards an individual, Lee (1976) originally formulated the tau hypothesis. He suggested that movement initiation and deceleration could be controlled using the time to arrival. The tau theory or hypothesis is based on the control of behavior using perceptual information from the environment. This ecological approach to movement control implies that a simple variable such as tau is an affordance that the environment is providing and can be used to control movements (Gibson, 1979).

Another example is the constant bearing angle theory. This theory has applications in the predator-prey models in animal biology (Firestone and Warren, 2010) but also in

the behavioral dynamics of intercepting a moving target (Fajen and Warren, 2007).The basic idea is that during an interception task, the direction of a target with respect to one's body stays constant. A successful interception will occur when the movement is performed at correct velocity and the approach angle of the object is constant.

So far, the ecological approach was briefly introduced focusing on one of the main concepts the perception-action coupling.
A similar approach is based on a non-dynamic solution to understand coordination and biological systems. It can be understood and described as self-organizing systems because of their capability to organize themselves according to an emerging set of extrinsic and intrinsic stresses applied to the system (Kelso, 1995). Self-organization is a key factor in motor control and describes a spontaneous formation of spatial, temporal, and spatiotemporal structures that emerge from the constraints and the possibilities of the human body.

The framework of the dynamical system approach is based on the findings from Schöner and Kelso (1988) and describes that spatiotemporal patterns can emerge spontaneously from interactions between coupled subsystems. This approach, however, simplifies the control of movements because the computation aspects are replaced by self-organization. In fact, the internal and external constraints reduce the potential solutions available to control and regulate the movement and led to the emergence of a self-organized behavior. Stoffregen and Bardy (2001) showed that motion relative to different physical referents will structure some ambient arrays but not others. In other words the information, which defines the action, is structured by the set of the energies contained in the overall array.
The ecological approach to perception and action assumes that the relation between potential sensory stimulation and physical reality is ambiguous and that a relation between potential sensory stimulation and reality exist (Stoffregen and Bardy, 2001). As previously mentioned, specific reference frames are required in movement control and perception depends on physical referents or invariants. From the ecological perspective, it is important to determine how an organism detects information in the environment that is relevant to action. What form does the information take, and how

is the information used to modify and control movements. Not only the interaction with the environment is important but being aware of one's position during movement is an essential ability in the control of motor tasks and often called proprioception.

2.4.2.1 Proprioception and kinesthesia

The ability of being aware of one's position during movement is essential and often referred to as proprioception or kinesthesia. In the following subchapter the two concepts are briefly introduced and explained.

Both concepts are used to define the capacity of an organization to access movement configurations of their own body (Edin, 2001) which may lead to confusion. Each term must have a distinct definition to prevent misunderstanding (Scheerer, 1987).

Proprioception can be defined as "The sense of the relative position of neighboring parts of the body and strength of effort being employed in movement" (Mosby (Anderson, 1994). The term proprioception leads back to Sherrington (1906) who defines information from muscles and the vestibular system as the source of proprioception. Contemporarily, it is described as the sensations of the muscles, tendons, joints, skin, eyes and the vestibular apparatus.

Kinesthesia on the other hand has been defined as "the sense that detects bodily position, weight, or movement of the muscles, tendons, and joint but also the sensation of moving in space" (The American Heritage® Medical Dictionary, (Houghton Mifflin Company (COR), 2007)).

Kinesthesia is associated with distinct classes of sensory receptors. It is also related to the muscles, joints and skin receptors (Proske et al., 2000) and contributes to improve the knowledge of the position and movements of the body.

Losing parts of the sensory feedback mechanisms due to accidents or severe illnesses has been shown to affect the perception and control of movements. Patients with cerebellar affections have difficulties to compensate for dynamic interaction

forces (Topka et al., 1998). Also patients with a loss or reduced back proprioception, lose the ability to adjust their movement to unexpected load, and cannot maintain constant joint angles without using visual cues (Rothwell et al., 1982); (Sanes et al., 1985). Similar results were reported during movements with the goal to hit a target (Ghez et al., 1995; Sainburg, 2005).

The integration of visual-kinesthetic cues can be more beneficial because the visual feedback from the eyes has been shown to improve the signal-to-noise ratio by reducing uncertainty present in each of the sensory modalities (van Beers et al., 1998; van Beers et al., 1999a; van Beers et al., 1999b; van Beers et al., 1996). This means that visual-kinesthetic cues play a major role when kinesthetic or proprioceptive feedback is not available.

To conclude this brief introduction, the representation of the body can either happen using only visual-, or kinesthetic cues but an integration of both can help to improve the representation of the body in egocentric space.

2.4.2.2 Body schema

The representation of the own body is important in everyday life especially when interacting with somebody else or the environment. The following subchapter explains the concept of body schema. Body schema is the constant representation of the positions of body parts in egocentric space during movement and used for spatial organization (Haggard and Wolpert, 2005). It also provides information about the configuration of the segments in egocentric space and the shape of the body surface.

The body schema provides the basis of biological motion and vice versa so the biological motion exhibits invariant features, i.e. parameters that do not significantly change with movement as size, speed, load and direction (Soechting and Lacquaniti, 1981; Lacquaniti et al., 1982);(Atkeson and Hollerbach, 1985);(Papaxanthis et al., 2003). Identifying these physical invariants to understand the proprioceptive control of motor performance is an important topic in motor control and is under ongoing discussion (Riley et al., 2005);(Riley and Pagano, 2003);(Garrett et al.,

1998);(Pagano and Turvey, 1998);(Bernardin, 2005);(van de Langenberg et al., 2008);(van de Langenberg et al., 2007);(Pagano, 2000).
A number of these features were described for point-to-point (e.g. reaching, (Soechting and Flanders, 1991) and continuous (e.g. drawing and handwriting, (Lacquaniti et al., 1983) and other movements of the upper limb (Berret et al., 2011).

Turvey and Carello (2011), reviewed the concept of body schema and due to the hierarchical disposition of our limbs e.g. upper-arm, forearm and hand, the proprioception can be accounted for as body schema and the perception of the limbs is coupled with the inertial parameters that have been shown to be invariant.

According to Pagano and Turvey (1995), our ability to perceive the spatial orientation of a limb via kinesthetic inputs is tied to the inertial parameters. Moreover they showed that the perception of the spatial orientation is tied to the eigenvector ($\mathbf{e_3}$) of the inertia tensor ($\mathbf{I_{ij}}$) (i.e. the resistance to rotation) and is known to play a significant role in dynamic touch. The inertia tensor ($\mathbf{I_{ij}}$) quantifies an object's resistances to angular rotation in various directions that result from the object's mass distribution.

The dynamic touch can be described as the perception of objects properties using haptic information. It is the perception of how an object is oriented and how it’s mass is distributed relative to the body (Pagano, 2000). Grasping an object can become quite a challenge if we have no information’s about its mass, length and shape. Taking the example of a probe, if the probes mass is symmetrically distributed, no adaption has to be made to successfully lift the rod from the floor. On the other hand, if the mass is asymmetrically distributed, without being told, instantaneous adaptations have to be made to point with a probe (Turvey and Carello, 2011; Turvey et al., 1989). Turvey et al. (1989) showed in their experiments that geometric properties such as the length and mass of objects as well as the inertia moment (Solomon and Turvey, 1988) have an influence on the perception of the object.
The inertia tensor is not only the relevant mechanical quantity to which such perception is tied (see (Carello and Turvey, 2000), for a review) but also research in dynamic touch demonstrates the viability of Gibson's 'ecological' approach, and it underscores the role of $\mathbf{I_{ij}}$ as one such perceptual invariant (Pagano, 2000);.

2.4.2.3 Inertia Tensor

Gibson (1966), proposed the theory of dynamic touch that describes the capability of human beings to understand and detect invariants of physical quantities, which characterize an object using haptic information.

This approach (Jones, 1986) confirmed that in the absence of vision, the object's mass is used to discriminate its properties such as the center of mass (COM) and the inertial parameters. Solomon and Turvey (1988) suggested that also in the absence of vision, the inertia tensor plays a major role, identifying the invariants of a handled object. Taking this example a step further (Pellionisz and Llinas, 1985), the perception of the limbs, depends on the inertia tensor, i.e. the resistance to rotation.

The inertia tensor is a 3 x 3 symmetric matrix which contains the moments and products of inertia of an object with respect to an axis of rotation (Turvey and Carello, 2011). A major emphasis has been given to the three principal moments (eigenvalues) and three principal directions (eigenvectors) of the inertia tensor that define the symmetry axes of the object according to the mass distribution (a detailed explanation is given in Chapter 3).

The mechanical resistance to rotation is an important factor during the manipulation of objects or the limbs. Since movements of our limbs are fundamentally based on rotations (Turvey et al., 1989), results of earlier experiments show that the properties such as length, mass and the moments of inertia of an object can be perceived haptically. The perception is based on mechanical stimuli (Solomon and Turvey, 1988; Turvey et al., 1989; Turvey et al., 1992) that are physically associated with the quantification of the rotation resistance. The implication of this invariant dynamical parameter may be essential to the concept of dynamic touch rather than varying parameters as displacement, velocity, or torque (Pagano and Turvey, 1995). The inertia tensor was identified as the relevant mechanical quantity to which such perception is tied (Carello, 2004).

Proceeding this hypothesis, the principal moments of inertia as well as the eigenvectors provide information about an object such as length (Fitzpatrick et al., 1994) (Pagano et al., 1993), (Turvey et al., 1989), shape (Burton et al., 1990) and weight (Amazeen et al., 1995). The eigenvectors are the principal moments of inertia with respect to the axes of symmetry of the object, around which the mass of the

object is symmetrically distributed. The principal axes of a rigid body and specifically of the moment of inertia tensor are described by these eigenvectors. Extracting the eigenvectors ($\mathbf{e_1}$, $\mathbf{e_2}$, $\mathbf{e_3}$) of the inertia matrix in motor control, was initially proposed by (Pagano et al., 1994). The eigenvectors include the axes of maximal ($\mathbf{e_1}$) and minimal ($\mathbf{e_3}$) resistance to rotational acceleration (Pagano and Turvey, 1995). They also deduced that rotations around the axis $\mathbf{e_3}$ would be favorable, as the products of inertia are zero, which led to the minimum inertia resistance principle (Isableu et al., 2009).

2.4.2.4 Inertia Tensor and proprioception

Movement of our body can be controlled on a proprioceptive basis. The term proprioception leads back Sherrington (1906) who, unlike Bastian (1880), excludes the information from cutaneous receptors but includes information from muscles and vestibular system as the source of proprioception. When interacting with an object that has manipulated geometric properties such as the length, mass and the inertia moment (Solomon and Turvey, 1988), experiments have shown direct adaptations during the interaction due to an altered perception of the object. The inertia tensor has been previously identified as a physical invariant and the question arises if rotations around inertia based axes change the perception of the movement.

Proprioceptive control of our movements can be organized by exploiting different axes of rotation. Each axis has its specific physical meaning and the exploitation of the axes may depend on the constraints of the coordination pattern during motor tasks (Isableu et al., 2009);(Riley et al., 2005);(Bernardin et al., 2005).

2.4.2.5 Role of the inertia tensor in pointing movements

The identification of physical invariants as the inertia tensor in the proprioceptive control of motor skills is currently under ongoing discussion (Riley et al., 2005);(Pagano, 2000);(Pagano and Turvey, 1995);(Bernardin et al., 2005);(van de Langenberg et al., 2007; van de Langenberg et al., 2008). Exploiting this variable helps to detect the minimum inertia resistance axis (Arya, 1998) which minimizes rotational resistance during angular acceleration (Pagano and Turvey, 1995); (Isableu et al., 2009);(Bernardin et al., 2005).

To initially test the role of the inertia tensor in the perception of the direction of body segments, (Pagano and Turvey, 1995; Pagano et al., 1996a) set up several experiments. The experiments were based on the same principle and one of the goals was to separate the geometrical axis from the $\mathbf{e_3}$ axis (Figure 5).

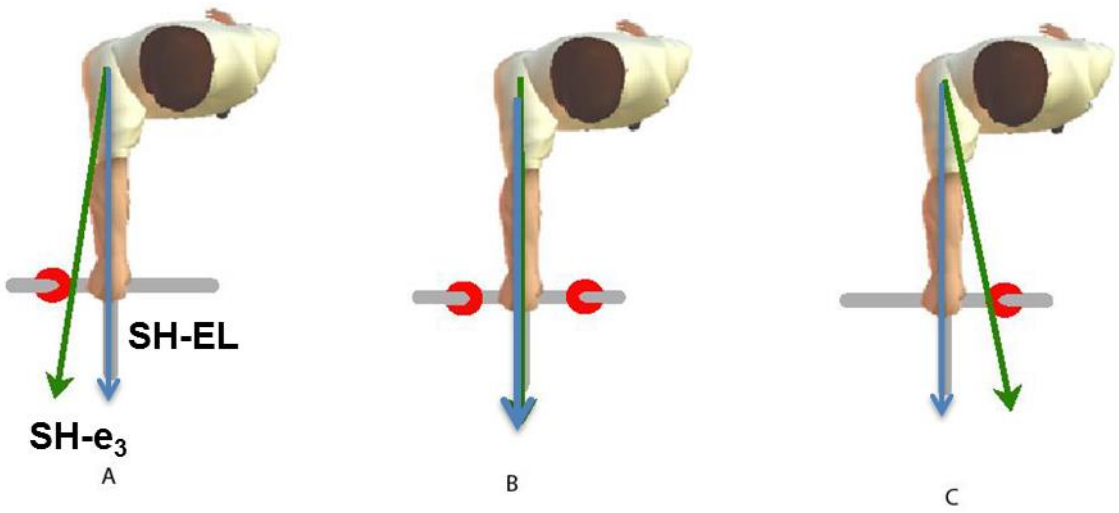

Figure 5 The experimental setup proposed by Pagano (1996) to separate the geometric (SH-EL) and the e_3 axis.

The authors examined the contribution of $\mathbf{e_3}$ during a single joint pointing gesture. To separate both axes, the direction of the eigenvector was changed by adding masses to an object held in the hand of the participants. When the masses are added symmetrically $\mathbf{e_3}$ coincides with the geometric axis of the arm. Positioning the masses asymmetrically results in a separation of both axes. The subjects were asked to point to targets while the mass distribution of the held object was changed. The results of this study show that the perception of the orientation of the arm changes with deviations of the eigenvector $\mathbf{e_3}$. The direction and importance of these errors depends on the magnitude of the deviation of $\mathbf{e_3}$. The results have been shown to be reproductive in various tasks using the same paradigm (Riley and Turvey, 2001; Garrett et al., 1998);(Bernardin et al., 2005). Later work generalized these findings to unconstrained 3D multi-joint arm movements at spontaneous velocity involving both the shoulder and the elbow (Bernardin et al., 2005).

However, the role of $\mathbf{e_3}$ has been questioned (Craig and Bourdin, 2002; Gueguen et al., 2004), especially because the center of mass (CM) and the $\mathbf{e_3}$ axes appear to be confounding variables and the role of each has not been sufficiently proved (Kingma et al., 2004; van de Langenberg et al., 2008).

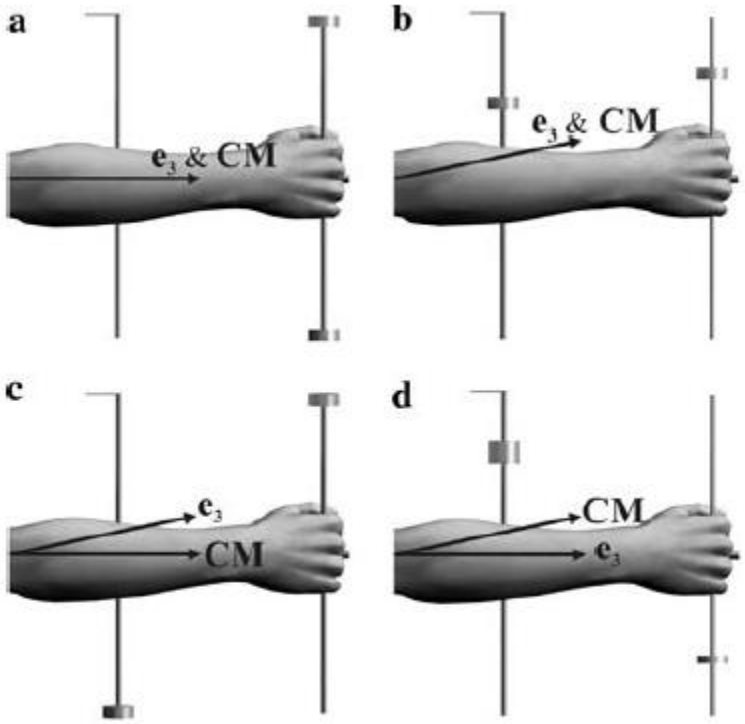

Figure 6 This figure shows the experiments of van de Langenberg to seperate the CM and e3 axis. To do so, masses were attached to two rods with different distances on the forearm.

To unravel the role of $\mathbf{e_3}$ and CM, (van de Langenberg et al., 2007; van de Langenberg et al., 2008), separated $\mathbf{e_3}$, CM and the geometrical vector of the arm (Figure 6), and provided evidence that CM may mainly be used in kinesthetic control, and not $\mathbf{e_3}$. Bernardin et al. (2005) showed the coherence of the findings regarding CM and $\mathbf{e_3}$ in movements performed at spontaneous velocity. Later work generalized these findings to unconstrained 3D multi-joint arm movements involving both the shoulder and the elbow (Bernardin et al., 2005).

Even though, it has been initially confirmed that the kinesthetic perception of limb direction varies as a function of $\mathbf{e_3}$ during rotations about the shoulder (Pagano and Turvey, 1995; Riley and Turvey, 2001; Riley et al., 2005) and the elbow (Garrett et al., 1998), attaching masses to manipulate and reorient $\mathbf{e_3}$ and the CM axis of the

arm, van de Langenberg (2007; 2008) provided evidence that the CM may be preferred over $\mathbf{e_3}$ in kinesthesia.

They also relativized the initially proposed role of the inertia tensor. However, the nature of his experiments cannot definitively reject the role of $\mathbf{e_3}$. The movement tasks were constrained to the horizontal plane, thus greatly limiting the rotations around $\mathbf{e_3}$ (van de Langenberg et al., 2008),(van de Langenberg et al., 2007); (Pagano and Turvey, 1995); (Bernardin et al., 2005).

As a matter of fact, large individual differences have been reported in the past experiments investigating the role of the inertia tensor in pointing or wielding tasks (Garrett et al., 1998);(Kingma et al., 2004);(Bernardin et al., 2005);(Withagen and Michaels, 2005);(van de Langenberg et al., 2008) which could also cover general strategies favoring the inertia tensor.

All precedent experiments that have tested the role of $\mathbf{e_3}$ showed experimental limitations and the constraints put on the subjects may have led to confound variables such as the CM and $\mathbf{e_3}$. The movements performed in the experiments neither controlled the velocity of the movement nor involved rotations. One of the major drawbacks of the experiments is that movements were not performed around $\mathbf{e_3}$ or the CM axis so no clear conclusions can be drawn by these experiments when studying the role of $\mathbf{e_3}$ during unconstrained 3D movements.

2.4.2.6 Role of the inertia tensor during rotation movements

Isableu et al. (2009) recently tested the role of the inertia tensor in a task involving an internal-external cyclic rotation of the shoulder performed at different velocities. The authors found that the rotation axis of a multi-articulated limb system may change from a geometrical articular axis (SH-EL) to a mass or inertia-based axis as the velocity and acceleration of the limb increased.

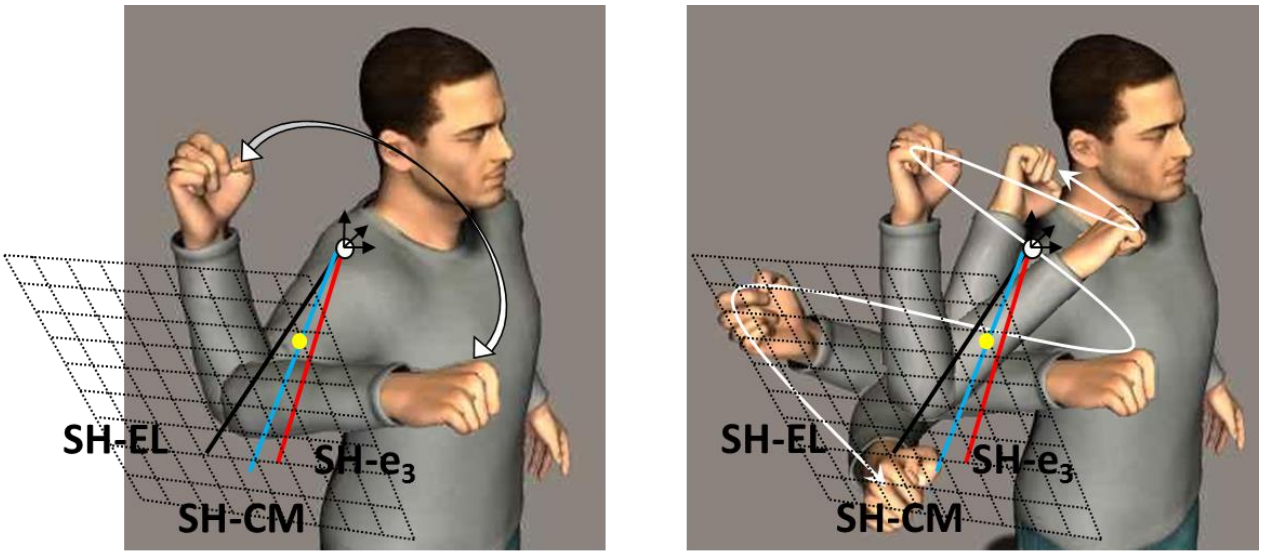

Figure 7 In 2009, Isableu et al. proposed an experiment that allowed to naturally separate the rotation axes during cyclic rotations of the arm.

The purpose of this study was to examine whether the minimum inertia resistance (MIR) principle (i.e., the spontaneous velocity-dependent change of rotation axes toward axes known to reduce inertial resistances and muscle torque) governs internal-external rotations at a fast velocity (Figure 7). The results are the first to provide evidence that the rotation axis of a multi-articulated limb system may change from a geometrical articular axis to a mass or inertia-based axis as the velocity and acceleration of the limb increase.

They also identified that the relevant mass/inertia-based axis forms a compromise between static and dynamic joint torques i.e. a SH-CM/$\mathbf{e_3}$ trade-off axis. Higher velocities and accelerations amplify the effects of inertia. When arm rotations are performed around other axes than $\mathbf{e_3}$, the inertia products augment and rotations are performed with higher torque. The authors also showed that rotation axes specifically determine the contribution of muscle, interaction and gravity torque to net torque and the magnitude of joint rotation. Rotations about $\mathbf{e_3}$ have been shown to minimize the contribution of muscle torque to net torque by using the interaction torque to assist motion compared to rotations about the center of mass (SH-CM) or joint (SH-EL) axes (Isableu et al., 2009).

As a consequence the contribution of interaction torque increased and the contribution of muscle torque was reduced. The results can be interpreted within the theoretical assumption that dynamic adaptive controls of complex systems exploit the biomechanical and physical interactions that minimize complex neuro-computational information processing and attention resources.

In general changing the axes of rotation (CM/$\mathbf{e_3}$) has an influence on the coordination of muscle and interaction torques and may be an efficient control strategy for 3D multi-articulated that avoids an intervention of the CNS which matches (Todorov, 2004).

Even though the contribution of muscle torque is reduced when exploiting the minimum inertia resistance axis, inter-individual differences have been found to emerge three control patterns. The exploitation of other axes than $\mathbf{e_3}$ in demanding tasks with large accelerations did not show the motor behavior, as it would have been hypothesized in the dynamical approach where additional constraints would self-organize towards general solutions, like the exploitation of the minimum inertia resistance axis.

2.5 Synthesis

To summarize, the presented models have one common point. As the human body reveals too many options and possibilities to move, all motor control models lay their focus on specific target areas and automatically reduce the dimensionality of the movement. Computational approaches assume that the perception and control of movements is based on cost functions while the dynamic and ecological approaches claim that solutions emerge due to acting constraints as physical invariants to control the execution of an action. However, the reduction of the dimensions and the explanations are limited because no cost functions or generalizable explanations (Berret et al., 2011) can be given on how and why subjects move differently. A strategy that may be followed by one person does not automatically relate to another person which brings us back to the minimum intervention principle of (Todorov and Jordan, 2002).

In the context of the inertia tensor, Isableu et al. (2009) showed that rotations around the eigenvector $\mathbf{e_3}$ not only minimize the resistance to rotational acceleration but also minimize the active torque compared to other rotation axes during the cyclic shoulder rotations.

The exploitation of $\mathbf{e_3}$ during rotational movements could be also accounted for a cost function as they are models that are based on the assumption that the CNS seeks to minimize a specific cost (Assaf, 2004). Optimization models attempt to identify the mechanisms implemented by the CNS as internal models that allow for the performance of a motor task while reducing errors and investing the least energy possible.

However, in highly redundant systems such as the human body the choice of motor commands is not trivial. An exploitation of an invariant such as a specific rotation axis, could also be a way to optimize the control and the performance during 3D movements involving rotations.

2.6 Problematic

This thesis focuses on the recently introduced MIR principle (Pagano and Turvey, 1995);(Isableu et al., 2009) in the coordination of upper-body movements. In the second chapter of this thesis, we were able to show the research background and the development of the MIR principle over the last years in movement control. Some research has been conducted to show the influence of the inertia tensor on the perception of the movement but also on one's limbs during the movement. The role of the inertia tensor is not necessarily the only invariant as the experiments of van de Langenberg et al. (2007; 2008) have shown. The influence of the CM has been found to be more pertinent than the role of the inertia tensor. However, during their experiments no rotation movements were performed and Isableu et al. (2009) showed a change of rotation axes during dynamic rotational movements of the arm. The exploitation of CM/$\mathbf{e_3}$ in the fast velocity conditions shows that the inertia tensor may be especially important when the inertia becomes very large due to high angular accelerations. The orientation and perception of the minimum inertia resistance axis can be seen as an ecological solution because it is the principal axes of inertia with the minimal resistance to rotational acceleration and could authorize its direct perception to control one's action.

As the inertia tensor has been proposed to play a major role in the perception, orientation and control of our actions (Garrett et al., 1998);(Pagano and Turvey, 1995; Pagano and Turvey, 1998);(Bernardin et al., 2005; Isableu et al., 2009), these findings raise the question of its role during unconstrained 3D movements with additional constraints.

From an experimental view, this can lead to the following question:

Does the MIR principle governs throughout experimental setups that test the role of $\mathbf{e_3}$ against velocity-, sensorial- and gravitational constraints.

In Chapter 3, we will introduce the biomechanical model including the computation and calculations performed during this dissertation and it will serve as a working knowledge base before introducing the experimental setups and specific research hypotheses in Chapter 4.

Chapter 3

3 Biomechanical Model

3.1 Introduction

The third chapter is devoted to the presentation of the biomechanical model of the upper-body and the assessment of the upper limb motor coordination identified in the context of our work of the Minimum Inertia Resistance Principle (MIR) (Isableu et al., 2009).

This chapter presents the experimental set-up and the data processing to obtain the relevant biomechanical parameters. These latter are both relative to the upper-limb:

1. kinematics with the joint angle calculation,
2. kinetics with the upper-limb global center of mass position and inertia tensor relative to the shoulder joint center,
3. dynamics including joint torque computation

3.2 Anatomical background

The anatomical structure of the upper body and especially can be composed in the three segments, the upper arm, forearm and hand (Figure 8). The upper arm is connected with the trunk through the shoulder girdle, consisting of the clavicle and the scapula. The clavicle is a long bone of short length located on the anterior and upper part of the thorax and serves as strut between the scapula and the sternum. The scapula is a flat, even and non-symmetrical triangular bone located on the upper and posterior part of the thorax leading to the glenohumeral joint. The glenohumeral joint can be represented as a ball and socket joint with three degrees of freedom that involves the articulation between the scapula and the humeral head. The humerus itself is a long, non-symmetrical bone connecting the scapula and the forearm bones, the ulna and the radius. The arm contains the humerus and the forearm, the ulnar and radius; both segments are connected via the synovial elbow hinge joint. The two long bones of the forearm, the radius and the ulna, form the radioulnar joint. The ulna is on the medial side and is relatively fixed while the radius is on the lateral side and represents the mobile part of the forearm. It allows pronation and supination.

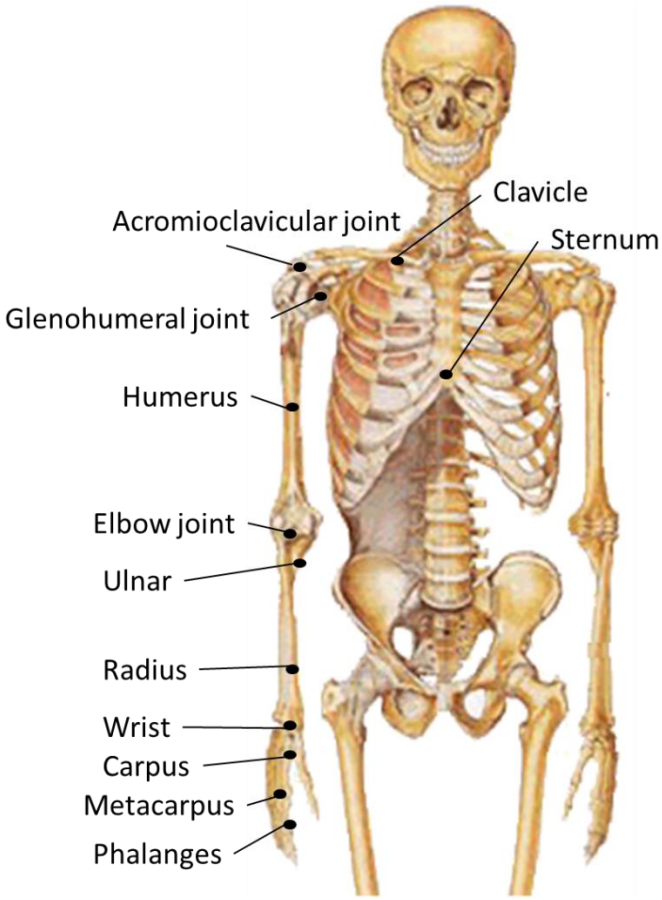

Figure 8 Anatomical model of the human upper body

The forearm bones are distally connected with the first row of the carpal bones of the hand forming the radiocarpal joint or wrist joint. The hand contains 27 bones and can be divided in three parts, the carpus, the metacarpus and the phalanges. The carpus contains eight bones and connects the hand to the forearm and allows for the positioning of the hand and the mobility of the individual carpal bones increase the freedom of movements of the wrist. The metacarpi are the bones of the palm and together with the fourteen phalanx bones of the fingers these metacarpal bones form the skeleton of the fingers.

3.2.1 Measuring human movement

Measuring and quantifying human motions allows for the detailed evaluation and description of human movement. Modern movement analysis is based on the pioneering work by Muybridge (1887). Based on Muybridge's approach using successive series of pictures, he was capable of showing a flight phase during the running stride in the horse gallop. Human motion analysis can be performed in two or three dimensions. Depending on the complexity and detail of the analysis, the choice

of the measurement device is important. The analysis itself is applied in multiple fields of research, such as the medical and the sports field. In gait analysis, the location and orientation of body parts are tracked to estimate joint angles that may identify possible injuries and/or movement disorders (Sutherland, 2002). The choice of the measurement device depends on the application and the budget. Over the last years, different methods have been developed to measure human motion including goniometers (Lim et al., 2011), accelerometers (Chung and Ng, 2012), inertia based and electromagnetic sensors (Lee and Park, 2011), active and passive optical motion capture systems (Richards, 1999);(Lorin et al., 2007) and even markerless optical motion capture devices (Corazza et al., 2010), as well as ultrasound motion capture devices (Malmström et al., 2003).

3.2.2 Motion Capture Measurement Devices

Optical Motion Capture technology is a valuable tool when quantifying human movements (Nigg et al., 2012). Moreover, clinical, biomechanical, and industrial applications require high system accuracy. Recurrent research has been conducted to report characteristics of selected systems and/or to validate new technical devices for human movement analysis (Richards, 1999); (Lorin et al., 2007). The evolution of optical motion capture was presented by (Mündermann et al., 2006) Manufactures usually provide accuracy values for their system, which have also been reviewed (Windolf et al., 2008); (Hansen et al., 2012a). The accuracy of passive motion capture systems strongly depend on the number of cameras, the size and quality of used markers, the distance from the cameras to the marker, the quality of the calibration, the calibration volume, the camera resolution and external infrared disturbances (Richards, 1999); (Lorin et al., 2007); (Windolf et al., 2008) (Chung and Ng, 2012). Putting markers on the human body often leads to soft-tissue artifacts (STA) between skin-mounted markers and the underlying bones. In various studies, the meaning and consequences of the STA have been shown (Cappozzo et al., 1996); (Tsai et al., 2009).

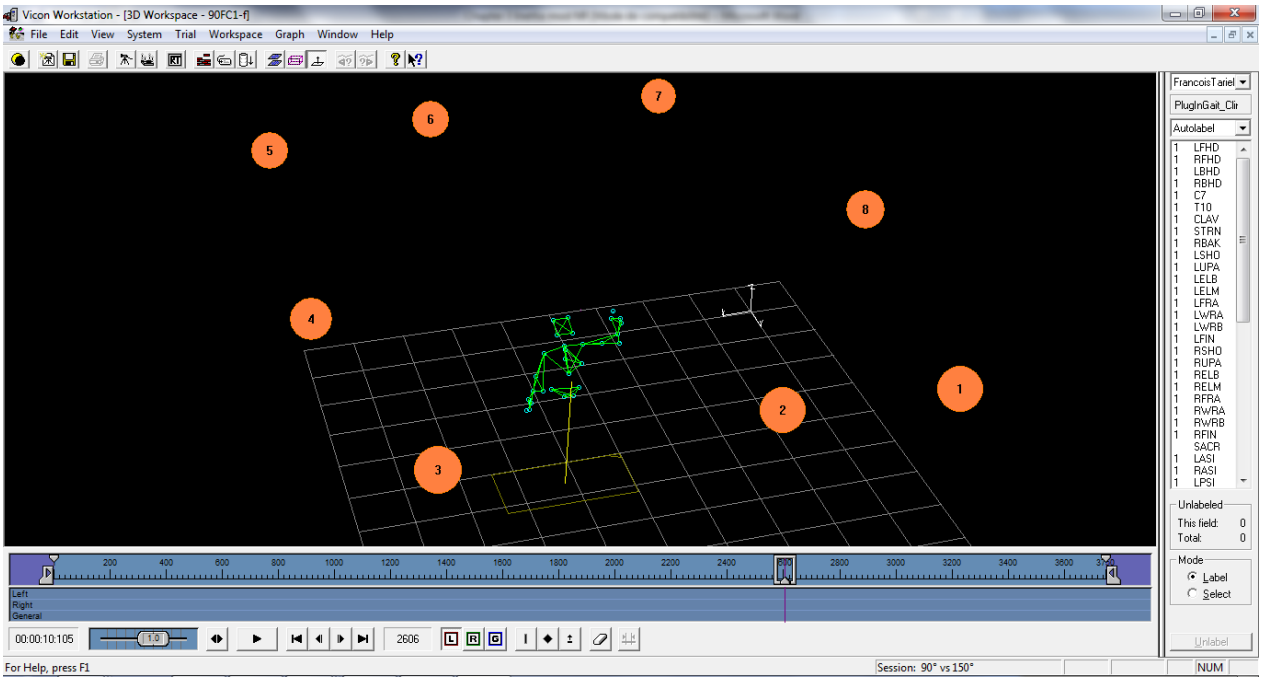

Figure 9 Example of a motion capture session including eight cameras and one force plate.

Using bone pins may avoid the occurrence of STAs (Reinschmidt et al., 1997); (Benoit et al., 2006), but the feasibility of drilling pins in the bone of subjects to quantify joint and bone motions remains questionable. Non-invasive procedures such as the use of external fixators (Cappozzo et al., 1996) and percutaneous tracking devices (Holden et al., 1997); (Manal et al., 2000) are an alternative to quantify joint motion in vivo without increasing the STAs. Throughout the experiments of this dissertation, reflective markers are placed on the skin using prominent bony landmarks of the body to avoid large marker displacement during joint rotation. To reduce inter rater errors, the placement of the markers was always performed by the same experimenter.

A classic motion capture laboratory setup is shown in Figure 9. The optoelectronic cameras are usually set up in a circle around the subject with analog devices such as force plates connected via an analog board to guarantee valid measurements.

Force Plate

Force plates or force platforms are measuring devices that measure the ground reaction forces (GRF) generated by a body standing or moving across them. GRFs are the reaction forces supplied by the ground which is the reaction to the forces a body exerts on the ground. The force plates used in the following experiments were equipped with four tri-axial embedded force sensors to measure the force acting between the body and the ground in 3 axes: transverse (X), anteroposterior (Y), and vertical (Z). The point of application of the collective GRFs on the plate is the center of pressure (COP).

3.3 Biomechanical model

In the following subchapter the biomechanical modeling of the human upper-body will be explained in detail. The biomechanical model includes the determination of degrees of freedom of the human body, the modeling aspect itself, the computations of joint kinematics and dynamics as well as the rotation axes computations that are important to evaluate the minimum inertia resistance principle (MIR) during 3D movements.

3.3.1 Degrees of freedom

Joints in the human body usually connect two segments and depending on the function and form, relative movements of the segment to each other are possible. Each movement possibility of a joint is considered as a degree of freedom (DOF). The term DOF can be defined as a way in “which a body may move or in which a dynamic system may change” (Webster's dictionary, (Merriam-Webster, 1986)). In other words the term describes the possibility in which the rigid body is capable of moving. Movements of three-dimensional bodies can have a maximum of six DOF and can be divided into translations and rotation. Rigid bodies can be moved along its proper axis giving three translational DOF or rotated around the three axes respectively.

3.3.2 Shoulder

The shoulder is the most complex joint in the human body and also provides the largest range of motion (ROM). The shoulder joint itself contains four joints, the sternoclavicular articulation, the acromioclavicular joint, the scapulothoracic joint and the glenohumeral joint. The sternoclavicular joint is a saddle joint that serves as a junction of the clavicle and the sternum. It has two rotational DOF one vertical and one anteroposterior. The acromioclavicular is the junction between the acromion and the clavicle. Due to the presence of numerous ligaments around the joint, the ROM is limited. The scapulothoracic joint is a false joint and formed by an articulation of the anterior scapula and the posterior thoracic rib cage. The glenohumeral joint is a synovial ball and socket joint that unites the head of the humerus and the glenoid fossa of the scapula allowing three degrees of freedom in rotation.

3.3.3 Elbow

The elbow synovial hinge joint is located between the upper arm and the forearm. It combines the humerus and the radius and ulna in the forearm forming a total of two joints: the humeral-ulnar joint and the humeroradial joint. The humeroradial joint is located between the head of the radius and the capitulum of the humerus and is a hinge synovial joint. The humeroulnar joint is the second part of the elbow-joint and is composed of the humerus and ulna. Together, both joints allow two DOF, one the flexion/extension motion of the elbow and the axial rotation (pronation / supination).

3.3.4 Wrist

The wrist is the link between the radius and ulna of the forearm and the carpus of the hand and contains of multiple joints due to the eight bones of the carpus. The radiocarpal joint is a saddle joint offering two DOF rotation, flexion/extension and abduction/adduction called radio-ulnar deviation.

3.3.5 Global Reference System and Marker Set

The global reference frame was chosen such that the x axis pointed in the anterior direction, the y axis in the upward direction, and the z axis laterally to the right (Wu et al. 2005), see Figure 10.

Marker Set: The marker set was adapated depending on the experiment. However, a base marker set of ten anatomical markers were always applied to the participants according to the following anatomic landmarks: 7th cervical vertebrae (C7), 10th thoracic vertebrae (T10), jugular notch where the clavicles meet the sternum (CLAV), xiphoid process of the sternum (STRN), right acromio-clavicular joint (RSHO, LSHO), lateral and medial epicondyle elbow (RELB, RELM), wrist bar thumb and wrist side and the hand (RWRA, RWRB) and the hand place on the dorsum of the hand just below the head of the second metacarpal (RFIN).

Trunk

1. C7 = 7th Cervical vertebrae spinous process of the 7th cervical vertebrae
2. T10 = 10th thoracic vertebrae spinous process of the 10th thoracic vertebrae
3. CLAV = Clavicle jugular notch where the clavicles meet the sternum
4. STRN = Sternum xiphoid process of the Sternum
5. RSHO = right shoulder marker placed on the acromio-clavicular joint

Upper-limb

6. RELB = right elbow placed on lateral epicondyle approximating elbow joint axis
7. RELM = right elbow placed on lateral epicondyle approximating elbow joint axis
8. RWRA = right wrist marker A right wrist bar thumb side
9. RWRB = right wrist marker B right wrist bar pinkie side
10. RFIN = right fingers actually placed on the dorsum of the hand just below the head of the second metacarpal

Joint Center

1. RHUP = Right Shoulder Joint Center
2. RHUO = Right Elbow Joint Center
3. RRAO = Right Wrist Joint Center

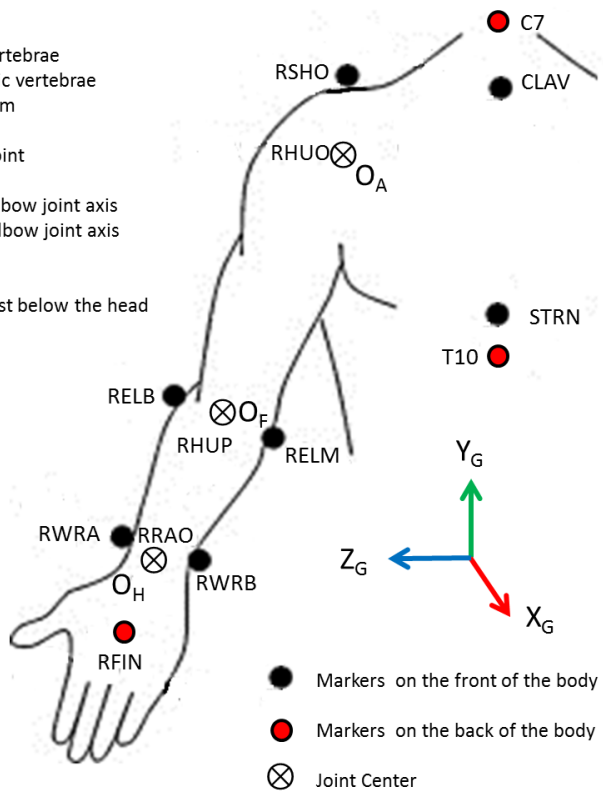

Figure 10 Example Marker Setup of the Upper-Body

3.3.6 Upper-body model segments

The upper-body model is composed of rigid segments linked by revolute joints that allow relative rotation between the segments. The next section is dedicated to the definitions of the segment coordinate systems (SCS) in accordance with the recommendations of the International Society of Biomechanics (ISB). If changes were made to the proposed SCS, it will be indicated and is done to maintain simplicity of the model, experimentation and computation.

Trunk model: Ot: The origin coincident with the CLAV marker. The Yt line connecting the midpoint between STRN and T10 and the midpoint between CLAV and C7, pointing upward. Zt line perpendicular to the plane formed by CLAV, C7, and the midpoint between STRN and T10, pointing to the right. Xt: The common line perpendicular to the Zt- and Yt-axis, pointing forwards.

Humerus model: Oh2: The origin coincident with GH. Yh2: The line connecting GH and the midpoint of RELB and RELM, pointing to GH. Zh2: The line perpendicular to the plane formed by Yh2 and Yf pointing to the right. Xh2: The common line perpendicular to the Zh2- and Yh2-axis, pointing forward.

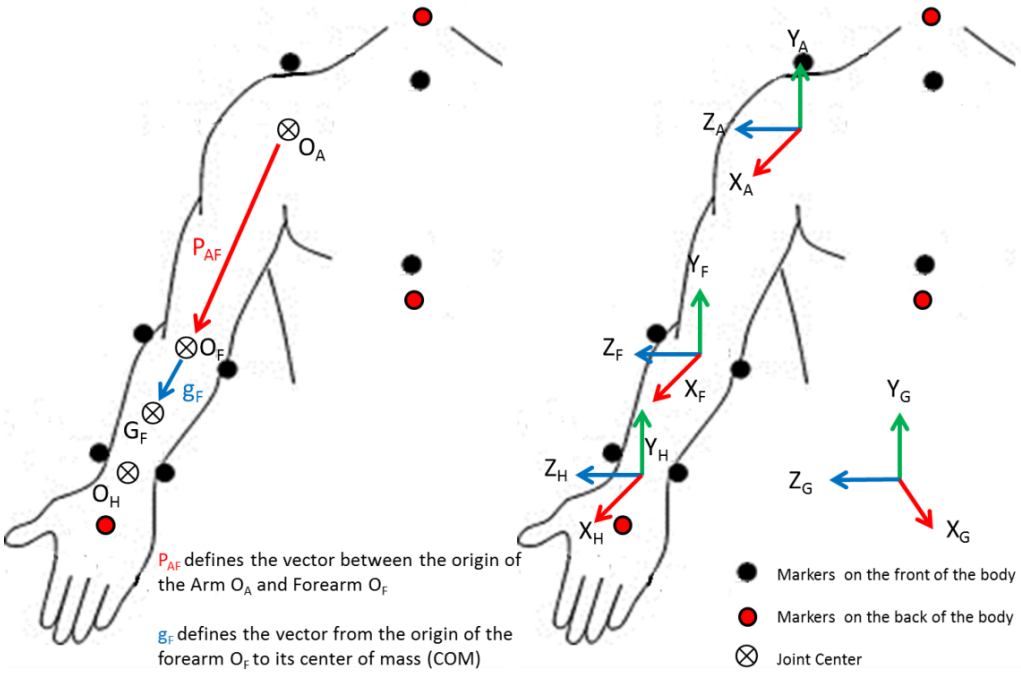

Figure 11 Reference frames and notations to describe the upper-limb kinematics (Wu et al., 2005) (A—arm, F—forearm, H—hand). Oi designs the origin of segment i (i_A, F, or H). pij designs the vector between the origins of segment i and j. Vector gi defines the vector from the origin of segment i to its center of mass (CoM) Gi expressed in the frame of segment i. Ggi defines the position of the CoM of segment i in the global frame. Rij denotes the rotation matrix from frame i to frame j.

Forearm Model: The origin coincident with RRAO. Yf : The line connecting RRAO and the midpoint between RELB and RELM, pointing proximally. Xf : The line perpendicular to the plane through RWRA, RWRB, and the midpoint between RELB and RELM, pointing forward. Zf : The common line perpendicular to the Xf and Yf -axis, pointing to the right.

The ISB-adapted Hand model: Om: The origin coincident with RFIN. Yf: The line connecting RFIN and the midpoint between RWRA and RWRB, pointing distal. Xf : The line perpendicular to the plane through the midpoint of RWRA and RFIN, and the midpoint between RFIN and RWRB, pointing forward. Zf: The common line perpendicular to the Xf and Zf -axis, to the right.

3.3.7 Upper-body model joints

The next section is dedicated to the definitions of the segment and joint coordinate systems in accordance with the ISB recommendations (Wu et al., 2005). To make a kinematic description of the elbow joint useful and practical, we use the following anatomical approximations:

Shoulder: The shoulder joint was modeled with three degrees of freedom (DOF). According to the ISB recommendation (Wu et al., 2005), the first one corresponds to a rotation around a vertical axis coincident with YG of the torso SCS (see Figure 11). The corresponding movement is called “plane of elevation” (PE) because it indicates in which plane the subsequent movement called “elevation” (EL) (second degree of freedom - DOF) is executed. This latter is done around the XA axis rigidly attached to the arm segment. Finally, the third DOF corresponds to the humerus “axial rotation” (AR) around YA rigidly attached to the arm segment.

Elbow: The elbow joint has two DOFS: “flexion – extension” (FE) around ZA rigidly attached to the arm followed by “pronation - supination” (PS) around the YF axis rigidly attached to the forearm.

Wrist: Finally, the wrist has two DOFS: “radio-ulnar deviation” (RUD) around XF rigidly attached to the forearm followed by “flexion-extension” (PE) around ZH rigidly attached to the hand.

The joint center calculation was performed using Matlab and the elbow joint (RHUO) is considered as the midpoint of the RELM and the RELB marker position. The wrist joint center (RRAO) is the midpoint of the RWRA and the RWRB marker and the shoulder joint center defined by a vertical offset from the base of the acromion marker (RSHO) to shoulder joint of seventy three millimeters (Dumas et al., 2007).

3.3.8 Joint Angles Computation

Joint Angles: From the 3D position of the markers, the evolution of the arm joint angles and joint center positions were obtained using inverse kinematics. In order to calculate joint angles, we consider each upper limb segment such as a rigid body. We use an inverse kinematics approach using the recorded trajectories of each marker with the motion capture system. A rigid body is defined by minimum three markers which define the segment coordination frames.

To create a reference frame for each segment two vectors are defined from the three chosen markers. The first vector is denoted **x** and the second vector is its intermediary **a** and together they form a plan. The cross product of **x** ∧ **a** will lead to its resultant the vector **z** which perpendicular to x and a. The cross product of **z** ∧ **x** is the vector y, which is perpendicular to x and z. The vectors are normalized and an orthogonal segment coordinate system is created based on the three initial markers. This segment coordinate system (SCS) has the form of a 3x3 matrix containing the coordinates of each unit vector in the global coordinate system.

To calculate the rotation matrix, the upper-arm and the forearm are considered with its respective SCS. $\mathbf{R_{01}}$ is the SCS of the upper arm and $\mathbf{R_{02}}$ is the SCS of the forearm. Both SCSs (upper-arm $\mathbf{R_{01}}$ and the forearm $\mathbf{R_{02}}$) are expressed in the global reference system $\mathbf{R_{00}}$.

The matrix multiplication of $\mathbf{R_{01}}\ \mathbf{R_{02}^{T}}$ leads to $\mathbf{R_{12}}$ and represents a transition of the SCS of the forearm to express the position and orientation of the forearm in relation to the upper-arm.

Following the recommendations of the ISB (Wu, et al. 2005) Euler rotation sequences are applied on the transformed SCS $\mathbf{R_{12}}$ and angles are obtained relative to each axis forming three angles between each segment (Table 1). In total seven DOFs were used in the biomechanical model, the humerus plane of elevation, humerus elevation, humerus axial rotation, elbow flexion-extension, forearm pronation-supination, wrist abduction-adduction and flexion-extension.

Table 1 Anatomical landmarks and sequences used for the calculation of the relative angles between each segment. The coordinate system Xg, Yg, Zg is the global coordinate system according to Wu et al (Wu et al., 2005).

Segment	Anatomical Landmarks	Rotation Sequence
Trunk		
	Origin : CLAV	
	Yt : midpoint of [STRN-T10] → midpoint of CLAV-C7].	
	Xt : midpoint of [STR-T10] → CLAV ∧ midpoint of	
	[STRN-T10] → C7.	
	Zt : Xt ∧ Yt.	
	Rotation	
	e1 : Flexion (-) / Extension (+)	
	e2 : Lateral rotation right (+) / left (-)	
	e3 : Axial rotation left (+) /right (-)	
Arm		**Y-X-Y**
	Origin : Rotation Center of the Shoulder (RHUP)	
	Yh : midpoint of [RELM-RELB] → Rotation Center of the shoulder	
	Xh : RHUP → RELB ∧ RHUP → RELM	
	Zh : Xh ∧ Yh.	
	Rotation	
	e1 : Plan of Elevation	
	e2 : Elevation (-)	
	e3 : Axial rotation MEDIAL (+) / LATERAL (-)	
Forearm	Origin : RRAO.	**Z-X-Y**
	Yf : RRAO → midpoint of [RELB-RELM].	
	Xf : RRAO → RELM ∧ RRAO → RELB	
	Zf : Xf ∧ Yf.	
	Rotation	
	e1 : Flexion (+) / Hyper-extension (-)	
	e2: Pronation (+) / Supination (-)	

Wrist	Origin : RFIN.	**Z-X-Y**
	Yf : RRAO → midpoint of [RWRA-RWRB].	
	Xf : RRAO → RWRA-RFIN ∧ RWRB-RFIN	
	Zf : Xf ∧ Yf.	
	Rotation	
	e1 :Abduction (+) / Adduction (-)	
	e2 : Flexion (+) / Hyper-extension (-)	

The deflection angle in the frontal plane between the humerus and the bones of the forearm, also called the "carrying angle" (Paraskevas et al., 2004) and the axial rotation of the hand relative to the forearm have been excluded from the model.

3.4 Inertia tensor

The rotational inertia parameters of any object indicate the relationship between the mass elements of the object and the squared distance of these mass elements to the rotation point, axis or plane. The inertia tensor is a 3x3 matrix expressed in Cartesian space.

$$I = \begin{bmatrix} Ixx & Iyx & Izx \\ Ixy & Iyy & Izy \\ Ixz & Iyz & Izz \end{bmatrix} \text{ (1)}$$

The diagonal matrix elements Ixx, Iyy and Izz are called the principal moments of inertia. They are defined in kg.m² and can be calculated by the following equation:

$$Ixx = \iiint (y^2 + z^2) dm \text{ (2)}$$
$$Iyy = \iiint (x^2 + \mathrm{z}) dm \text{ (3)}$$
$$Izz = \iiint (x^2 + y^2) dm \text{ (4)}$$

A moment of inertia around an axis is equal to the 3D integral of the squared distance between the axis of rotation and a small element multiplied by its mass dm. It can be also calculated according to the following formula $I = \mathrm{m}\rho^2$ where m represents the mass of the segment (kg), and ρ the radius of gyration (m) with respect to the rotation axis. The radius of gyration can be expressed as a fraction of

the segment length when considering an axis passing through the center of mass, the proximal end and the distal end of the segment. The value of I depends on the axis around which the rotation is taking place and for parallel axes is a minimum when the rotation takes place around and axis passing through the center of mass.

The inertia tensor elements outside the diagonal are the products of inertia. They are defined by the following relationship:

$$Ixy = \iiint xydm \quad (5)$$

$$Iyz = \iiint yzdm \quad (6)$$

$$Izx = \iiint zxdm \quad (7)$$

The inertia tensor is defined with respect to a particular set of axes and to calculate the diagonal matrix of the inertia tensor, the axes of rotation are reoriented. They are reoriented such that the masses of the segments are symmetrically distributed and the products of inertia are equal to zero. The magnitude and direction of the moment inertia are given by the eigenvalues (I_1, I_2, I_3) and eigenvectors $\mathbf{e_1}$, $\mathbf{e_2}$, $\mathbf{e_3}$ of the inertia tensor. The expression of the diagonal matrix in the eigenspace is the following:

$$\mathrm{I} = \begin{bmatrix} I_1 & 0 & 0 \\ 0 & I_2 & 0 \\ 0 & 0 & I_3 \end{bmatrix} \quad (8)$$

The principal moments of inertia, $I_1 = I_{xx}$, $I_2 = I_{yy}$ and $I_3 = I_{zz}$ of each segment are calculated.

3.4.1 Body Segment Inertial Parameters (BSIP)

Calculating BSIP as the mass, COM and the inertia tensor, has been shown to be very important for clinical and biomechanical research (Rao et al., 2006), (Pai, 2010). The measurement of inertia and the position of the COM of each body part allow monitoring the variations in muscle-mass during hospitalization, rehabilitation or neurological examination. The better the inertial estimation of those segments, the better are the resulting joint loads (force and moment) obtained by inverse dynamics (Pearsall and Costigan, 1999), (Pàmies-Vilà et al., 2012). Three main BSIP estimation methods currently exist in the literature, a regression based, a geometric and a dynamic estimation approach.

3.4.1.1 Regression model

One approach to estimate BSIP is to use scaling functions based on numerous anthropometric measurements from cadaver studies (Dempster, 1955); (Chandler et al., 1975). The equation-based technique is limited by the measurement techniques and the sample population. Using the equations outside the sample population will lead to large estimation errors. However, scaling functions are based on total body mass and segment length, are very convenient and timesaving. For example the scaling equations of de Leva (1996) even distinguish between genders, and provide the inertia tensor of the segments. Recently, Dumas et al. (2007) provided adjusted scaling functions based on the data of McConville et al. (1980) and of Young et al. (1983) providing the 3D locations of the segment centers of mass, the principal moments of inertia and the orientations of the principal axes of inertia with respect to the conventional segment coordinate systems (SCS).

3.4.1.2 Geometric model

In contrast to the regression-based models, the geometric models are based on either numerous anthropometric measurements (Hanavan Jr., 1964) or body scanning methods. 3D imaging techniques vary from using a 3D scanner, IRM or Xray absorptiometry. In contrast to the regression method, the 3D imaging technique estimates or measures personalized 3D BSIPs (Cheng et al., 2000);(Ganley and Powers, 2004); (Mungiole and Martin, 1990) but the methods are very time consuming and subjects are exposed to radiation. Nonetheless, they give detailed information about the distribution of internal structures such as tissues and bones density values it is possible to calculate the BSIP (Kodek and Munih, 2006). However, the results can only be compared to plane by plane and not directly applicable in the conventional SCSs without restrictive assumptions.

3.4.1.3 Dynamic estimation models

With technological progress other non-invasive identification methods have also become available. Recently, identification methods used in robotics to determine mechanical structures inertial parameters began to be applied to the estimation of human BSIP (Atchonouglo et al., 2008); (Venture et al., 2009b; Venture et al., 2009a); (Kodek and Munih, 2006). These methods are based on human body

mechanical models which parameters are tuned to match kinematic and dynamic recorded data. Therefore, they allow evaluating BSIP on a subject-by-subject basis using an optoelectronic motion capture system and a force platform. The BSIP are identified based on the fact that the dynamics of the human system can be written using the Newton-Euler formalism (Venture et al., 2009b; Venture et al., 2009a). This approach however is rather new, and the methods have yet not been validated against other methods. To apply the methods a motion capture system including a force plate is necessary for this estimation technique.

3.4.2 Chosen BSIP estimation technique

The estimation of the BSIP throughout this dissertation is based on the scaling functions proposed by Dumas et al. (2007). The scaling functions adjust the data of McConville et al. (1980) and of Young et al. (1983) and are expressed directly in the conventional segment coordinate systems (SCS) and do not restrain the position of the center of mass and the orientation of the principal axes of inertia. Besides the abovementioned, the method proposed by Dumas et al. (2007) is easy to apply in the laboratory and the subjects are not exposed to radiation kept for a long period time in the laboratory.

3.5 Computation of the rotation axes

In the present dissertation, the role of three candidate axes that could be exploited during the control of voluntary limb movements, involving complex elbow and shoulder configurations, are exemplarily computed. The axes investigated include i) the axis of inertia tensor, i.e., $\mathbf{e_3}$, ii) the axis extending from the shoulder through the center of mass of the whole arm (SH-CM) , and iii) the articular axis extending from the shoulder through the elbow (SH-EL).

On the basis of research results of Dumas et al. (2007), the following subchapter explains the application of the proposed scaling functions on one male exemple for the upper limb segments.

Table 2 Scaling factors for the position of the center of mass (Dumas et al., 2007)

Segment	Gender	*mass m (%)*
Arm	M	2.4
	F	2.2
Forearm	M	1.7
	F	1.3
Hand	M	0.6
	F	0.5

Given the whole body mass of a subject and the appropriate scaling one can estimate the segment mass:

m_A is the mass of the arm (A), m_F the mass of the forearm (F), m_H the mass of the hand (H), and m the mass of the subject.

The scaling factors to determine the position of the center of mass (CoM) of segment i (i = A, F, or H) in its local frame are given in the following table:

Table 3 Scaling factors for the position of the center of mass (Dumas et al., 2007)

Segment	Gender	*X* (%)	*Y* (%)	*Z* (%)
Arm	M	1.7	-45.2	-2.6
	F	-7.3	-45.4	-2.8
Forearm	M	1	-41.7	1.4
	F	2.1	-41.1	1.9
Hand	M	3.5	-35.7	3.2
	F	3.3	-32.7	2.1

Given these factors and the length of the segments (L_i), the position of the segment CoM in the local frame can be defined by using the following equation:

$$^{i}\boldsymbol{g_i} = \boldsymbol{L_i}\,[\boldsymbol{X}(\%) \quad \boldsymbol{Y}(\%) \quad \boldsymbol{Z}(\%)]^{\boldsymbol{T}} \quad (9)$$

The scaling factors to define the inertia tensor of each segment in its local frame located at the CoM are given in the following table (i denotes the complex number such that $i^2 = -1$). These values are valid for male and female subjects.

Table 4 Scaling factors for tensor of inertia (Dumas et al., 2007).

Segment	Gender	r_{XX} (%)	r_{YY} (%)	r_{ZZ} (%)	r_{XY} (%)	r_{XZ} (%)	r_{YZ} (%)
Arm	M	31	14	32	6	5	2
	F	33	17	33	3	5(i)	14
Forearm	M	28	11	27	3	2	8*i*
	F	26	14	25	10	4	13(i)
Hand	M	26	16	24	9	7	8*i*
	F	41	45	36	15(i)	0	0

Given these scaling factors, the terms of the inertia tensor are obtained by the following equation:

$$I = \begin{bmatrix} I_{xx} & I_{yx} & I_{zx} \\ I_{xy} & I_{yy} & I_{zy} \\ I_{xz} & I_{yz} & I_{zz} \end{bmatrix} \quad (10)$$

$$\boldsymbol{I_{jk} = m_i \left(r_{jk} L_i\right)^2} \quad (11)$$

m_i and L_i (i = A, F, or H) denote the mass and length of segment i, respectively. The r_{jk} (j = X, Y, and Z, k = X, Y, and Z) coefficients are presented in Table 5.

Table 5 Mass, length, COM and inertia tensor for one subject

Male	Arm	Forearm	Hand
Mass (kg)	1.8	1.275	0.45
length(m)	0.33	0.26	0.20
COM x,y,z (m)	0.0056, -0.1482, -0.0085	0.0026, -0.1082, 0.0036	0.0026, -0.1082, 0.0036
Ixx (kg.m²)	0.0186	0.0067	0.0012
Iyy (kg.m²)	0.0038	0.0010	0.0005
Izz (kg.m²)	0.0198	0.0063	0.0010
Ixy (kg.m²)	0.0007	0.0001	0.0001
Ixz (kg.m²)	0.0005	0.0000	0.0001
Iyz (kg.m²)	0.0001	-0.0005	-0.0001

3.5.1 Upper-limb inertia tensor and center of mass position in the global frame

The COM position and the inertia tensor at the COM have been now expressed in the SCS (arm, forearm & hand). To express the inertia tensor and the COM in the global frame both will be transformed to the shoulder joint center. Following the initial description of the human model, the upper-limb is composed of three rigid segments linked by revolute joints that allow relative rotation between these segments (Wu et al., 2005). To transform the segment coordinates into the global coordinates expressed at the shoulder joint center, segment-specific rotations and translations have to be computed. It is considered that the origin of the global frame is coincident with the origin of the arm frame (shoulder joint center). As previously described, the upper-limb model consists of seven DOF and the transformation from the segment COM to the shoulder joint follows a translation about the segment length and the specific rotation sequence presented previously.

Given the transformed coordinates of the local COM expressed at the shoulder joint the global COM can be expressed in the global frame. Following the same approach, the segments inertia tensors are expressed in the global frame. To express the inertia tensor at the shoulder the generalized Huygens theorem is used.

$$ {}^{G}I_i^{SH} = {}^{G}I_i^{COM} + \begin{bmatrix} m_i({}^{G}g_{Yi}^2 + {}^{G}g_{Zi}^2) & -m_i\,{}^{G}g_{Xi}\,{}^{G}g_{Yi} & -m_i\,{}^{G}g_{Zi}\,{}^{G}g_{xi} \\ -m_i\,{}^{G}g_{Xi}\,{}^{G}g_{Yi} & m_i({}^{G}g_{Xi}^2 + {}^{G}g_{Zi}^2) & -m_i\,{}^{G}g_{Yi}\,{}^{G}g_{Zi} \\ -m_i\,{}^{G}g_{Zi}\,{}^{G}g_{Xi} & -m_i\,{}^{G}g_{Yi}\,{}^{G}g_{Zi} & m_i({}^{G}g_{Xi}^2 + {}^{G}g_{Yi}^2) \end{bmatrix} \quad (12) $$

Finally the upper-limb inertia tensor at the shoulder expressed in the global frame is:

$$ {}^{G}I^{SH} = {}^{G}I_A^{SH} + {}^{G}I_F^{SH} + {}^{G}I_H^{SH} \quad (13) $$

After having calculated the global COM and the inertia tensor of the upper-limb model, the rotation axes are computed. $\mathbf{e_3}$ corresponds to the eigenvector of the upper-limb inertia tensor associated with the smallest eigenvalue. SH-CM corresponds to the vector of the upper-limb COM and SH-EL corresponds to the articular axis, from the shoulder joint center to the elbow joint center. These parameters are defined from the length of the segments, the joint angles vector $[\boldsymbol{\theta_1, \theta_2, \theta_3, \theta_4, \theta_5, \theta_6, \theta_7}]^T$ at each time step, the mass of the segments, the position of the CoM and the inertia tensors defined in the local frames using the scaling factors of (Dumas et al., 2007).

3.5.2 Upper-limb forward model

To construct the upper-limb forward model, the rigid transformation $\mathbf{T}_{ij}$ (4x4) that gives the pose (position and orientation) of frame *j* with respect to frame *i* is used (*i* = G, A, F, or H, *j* = G, A, F, or H). Its general form is as follows:

$$T_{ij} = \begin{bmatrix} R_{ij} & p_{ij} \\ 0 & 1 \end{bmatrix} \qquad (14)$$

$\mathbf{R}_{ij}$ denotes the rotation matrix from frame *i* to frame *j* (the columns of $\mathbf{R}_{ij}$ represent the coordinate of base vectors $\mathbf{X}_j$, $\mathbf{Y}_j$, $\mathbf{Z}_j$ with respect to vectors $\mathbf{X}_i$, $\mathbf{Y}_i$, $\mathbf{Z}_i$). $\mathbf{p}_{ij}$ denotes the position of the origin of frame *j* expressed in frame *i*.

The $\mathbf{R}_{ij}$ matrices are constructed from the multiplication of rotation matrices around a single axis. If the rotation of an amount $\boldsymbol{\theta}$ is executed around the **X**, **Y**, or **Z** axis, the elementary rotation matrices are:

$$R_x(\theta) = \begin{bmatrix} 1 & 0 & 0 \\ 0 & \cos\theta & -sin\theta \\ 0 & \sin\theta & cos\theta \end{bmatrix} R_y(\theta) = \begin{bmatrix} cos\theta & 0 & sin\theta \\ 0 & 1 & 0 \\ -sin\theta & 0 & cos\theta \end{bmatrix} R_z(\theta) = \begin{bmatrix} cos\theta & -sin\theta & 0 \\ sin\theta & \cos\theta & 0 \\ 0 & 0 & 1 \end{bmatrix} (15)$$

The transformation from the global frame to the arm frame after the 3 shoulder rotations of an amount $\boldsymbol{\theta}_1$ (plane of elevation), $\boldsymbol{\theta}_2$ (elevation), $\boldsymbol{\theta}_3$ (axial rotation) is:

$$T_{GA} = \begin{bmatrix} R_{GA} & p_{GA} \\ 0 & 1 \end{bmatrix} (16) \qquad \text{With } R_{GA} = R_y(\theta_1)R_x(\theta_2)R_y(\theta_3) \quad (17)$$

$$\text{and } p_{GA} = [0 \quad 0 \quad 0]^T \qquad (18)$$

It is considered that the origin of the global frame is coincident with the origin of the arm frame (shoulder joint center); therefore $\mathbf{P}_{\mathbf{GA}}$ is the null vector.

The transformation from the frame of the arm to the frame of the forearm after 2 elbow rotations of an amount $\boldsymbol{\theta}_4$ (elbow flexion - extension) and $\boldsymbol{\theta}_5$ (forearm pronation-supination) is:

$$T_{AF} = \begin{bmatrix} R_{AF} & p_{AF} \\ 0 & 1 \end{bmatrix} \quad (19) \text{ with } R_{AF} = R_z(\theta_4)R_y(\theta_5) \ (20)$$

$$\text{and } p_{AF} = [0 \quad -L_A \quad 0]^T \qquad (21)$$

L_A represents the arm length.

The transformation from the frame of the forearm to the frame of the hand after the 2 wrist rotations of an amount $\boldsymbol{\theta}_6$ (wrist radio-ulnar deviation) and $\boldsymbol{\theta}_7$ (wrist flexion - extension) is:

$$T_{FH} = \begin{bmatrix} R_{FH} & p_{FH} \\ 0 & 1 \end{bmatrix} \quad (22) \text{ with } R_{FH} = R_x(\theta_6)R_z(\theta_7) \ (23)$$

$$\text{and } p_{FH} = [0 \quad -L_F \quad 0]^T \quad (24)$$

L_F represents the forearm length.

Finally, a reference frame **Fg** (for fingertip) is attached to the hand extremity and the transformation between the hand frame and **Fg** is simply

$$T_{HFg} = \begin{bmatrix} R_{HFg} & p_{HFg} \\ 0 & 1 \end{bmatrix} \text{ (25) with } R_{HFg} = \begin{bmatrix} 1 & 0 & 0 \\ 0 & 1 & 0 \\ 0 & 0 & 1 \end{bmatrix} \text{ (26)}$$

$$\text{and } p_{HFg} = [0 \quad -L_H \quad O]^T \quad (27)$$

L_H represents the hand length.

3.5.3 Upper-limb COM position in the global frame

Given $\mathbf{T_{GA}}$, $\mathbf{T_{AF}}$, and $\mathbf{T_{FH}}$, it is possible to express in the global frame any quantity defined in the local frames. In particular, the position of the CoM can be expressed by the following equations (the superscript $^{\mathbf{G}}$ on the right side of a vector denotes the fact that the vector is expressed in the global frame):

$$\begin{bmatrix} {}^G g_A \\ 1 \end{bmatrix} = T_{GA} \begin{bmatrix} g_A \\ 1 \end{bmatrix} \quad (28)$$

$$\begin{bmatrix} {}^G g_F \\ 1 \end{bmatrix} = T_{GA} T_{AF} \begin{bmatrix} g_F \\ 1 \end{bmatrix} = T_{GF} \begin{bmatrix} g_F \\ 1 \end{bmatrix} \quad (29)$$

$$\begin{bmatrix} {}^G g_H \\ 1 \end{bmatrix} = T_{GA} T_{AF} T_{FH} \begin{bmatrix} g_H \\ 1 \end{bmatrix} = T_{GH} \begin{bmatrix} g_H \\ 1 \end{bmatrix} \quad (30)$$

To obtain $^{\mathbf{G}}\mathbf{g}$, the position of the upper-limb CoM in the global frame, the following relation is used:

$$^G g = \frac{m_A \, {}^G g_A + m_F \, {}^G g_F + m_H \, {}^G g_H}{m_A + m_F + m_H} \quad (31)$$

3.5.4 Upper-limb inertia tensor at the shoulder expressed in the global frame

The procedure used to construct the upper-limb inertia tensor is done in three steps.

The first step consists in expressing the segments inertia tensor in the global frame with the following formula (*i* = A, F, and H):

$$ {}^{G}I_i^{COM} = R_{Gi}\ {}^{i}I_i^{COM}\ R_{iG} \text{ with } R_{iG} = R_{Gi}^{T} \quad (32) $$

$\mathbf{R}_{Gi}$	Rotation matrix from the global frame to frame *i*.
${}^{G}\mathbf{I}_i^{CoM}$	Inertia tensor of segment *i* at the segment CoM expressed in the global frame (superscript ^{G}).
${}^{i}\mathbf{I}_i^{CoM}$	Inertia tensor of segment *i* at the segment CoM expressed in the local frame (superscript ^{i}).

Then, using the generalized Huygens theorem, the segment inertia tensors are evaluated at the shoulder center. To do this, the following equation is used for each segment (*i* = A, F, and H):

$$ {}^{G}I_i^{SH} = {}^{G}I_i^{COM} + \begin{bmatrix} m_i({}^{G}g_{Yi}^2 + {}^{G}g_{Zi}^2) & -m_i\,{}^{G}g_{Xi}\,{}^{G}g_{Yi} & -m_i\,{}^{G}g_{Zi}\,{}^{G}g_{Xi} \\ -m_i\,{}^{G}g_{Xi}\,{}^{G}g_{Yi} & m_i({}^{G}g_{Xi}^2 + {}^{G}g_{Zi}^2) & -m_i\,{}^{G}g_{Yi}\,{}^{G}g_{Zi} \\ -m_i\,{}^{G}g_{Zi}\,{}^{G}g_{Xi} & -m_i\,{}^{G}g_{Yi}\,{}^{G}g_{Zi} & m_i({}^{G}g_{Xi}^2 + {}^{G}g_{Yi}^2) \end{bmatrix} \quad (33) $$

${}^{G}\mathbf{I}_i^{SH}$	Inertia tensor of segment *i* at the shoulder expressed in the global frame.
${}^{G}\mathbf{I}_i^{CoM}$	Inertia tensor of segment *i* at its CoM expressed in the global frame.
m_i	Mass of segment *i*.
${}^{G}\mathbf{g}_i$	${}^{G}\mathbf{g}_i = \begin{bmatrix} {}^{G}g_{Xi} & {}^{G}g_{Yi} & {}^{G}g_{Zi} \end{bmatrix}^T$

Finally the upper-limb inertia tensor at the shoulder expressed in the global frame is:

$$ {}^{G}I^{SH} = {}^{G}I_A^{SH} + {}^{G}I_F^{SH} + {}^{G}I_H^{SH} \quad (34) $$

3.5.5 e_3, SH-CM and SH-EL axes computation

e_3 corresponds to the eigenvector of the upper-limb inertia tensor associated with the smallest eigenvalue. If the smallest eigenvalue was found to be negative, | **e_3** | was considered as the eigenvector of the upper-limb inertia tensor associated with the smallest eigenvalue.**SH-CM** corresponds to

$$\frac{{}^{G}g}{\|{}^{G}g\|} \quad (35)$$

SH-EL corresponds to $\frac{P_{GF}}{\|P_{GF}\|}$ (36)

with $\begin{bmatrix} R_{GF} & p_{GF} \\ 0 & 1 \end{bmatrix} = T_{GF} = T_{GA}T_{AF}$ (37)

These parameters are defined from the length of the segments, the joint angles vector [$\boldsymbol{\theta}_1$, $\boldsymbol{\theta}_2$, $\boldsymbol{\theta}_3$, $\boldsymbol{\theta}_4$, $\boldsymbol{\theta}_5$ $\boldsymbol{\theta}_6$, $\boldsymbol{\theta}_7$]^T at each time step, the mass of the segments, the position of the COM and the inertia tensors defined in the local frames using the scaling factors of (Dumas et al., 2007).

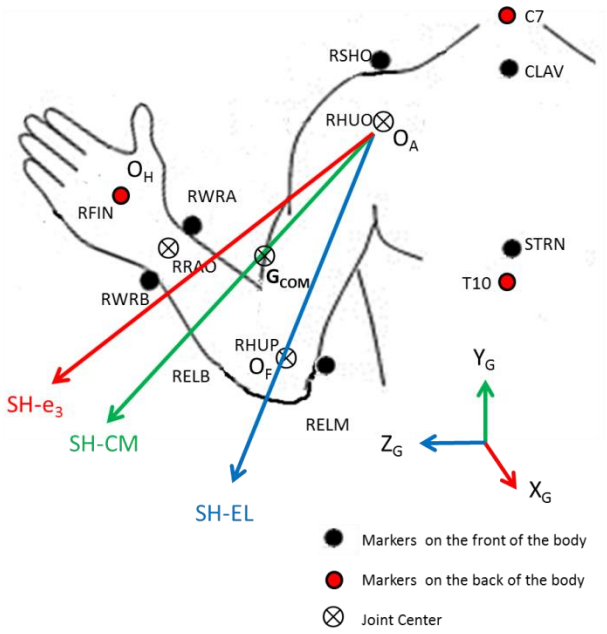

Figure 12 shows the directions of the principal moments of inertia of each upper body segment.

The SH-CM and SH-EL vectors were made unitary at each time step (**e_3** already is) for comparison and statistical analyses (Figure 12). To do this, the coordinates of SH-CM and SH-EL vectors were divided by their respective norm. In order to quantify the

variability of the normalized $\mathbf{e_3}$, SH-CM, and SH-EL axes, we calculated the elevation and azimuth angles in the reference frame of the torso. The calculated variability is the square root of the trace of the two angles covariance matrix.
Among the potential rotational axes that can be exploited during arm movements ($\mathbf{e_3}$, SH-CM and SH-EL), the one for which the variability is minimal will be considered as the one organizing or constraining the control of the arm movements.

3.6 Inverse dynamics

Based on the previously performed kinematic computation of the mass and the inertial properties of a body, torques can be calculated. The analysis is usually conducted in multi-articulated systems to estimate the load or internal moment on joints during movements. Inverse dynamics allows for the evaluation of joint torque, joint reaction torque and joint reaction forces from the movement kinematics and the limb geometric and inertial parameters.

The first inverse dynamic results are based on Fischer and Braune (1899). Technological progresses led to new research in the field of inverse dynamics (see (Robertson, 2004).

The evolution of motion capture systems including synchronized force plates and analog devices made the movement analysis and the processing time an interesting tool for the research community. Bastian et al. (1996) calculated the total torque (NET) as the product of the moment of inertia of the involved segments (including the segment under consideration and all segments distal to it) and the angular acceleration around the joint under consideration. Inverse dynamic studies have been applied to multiple human movements such as walking (Shamaei et al., 2013), running (Bonacci et al., 2013), multi joint movements of the upper body (Topka et al., 1998) during table tennis (Iino Y. and Kojima T., 2011) and 3D overarm throwing (Hirashima et al., 2008).

Following this, the torque can be decomposed in (1) the gravity torque, (2) the resultant joint torque arising from muscles, ligaments, and other connective tissues, and (3) the interaction torque due to rotations at other joints (Hollerbach and Flash,

1982). The equation of motion is represented as the second-order differential equation, as follows:

$$M(\theta)\ddot{\theta} = \left[\tau - V\left(\theta, \dot{\theta}\right) - G(\theta)\right] \quad (38)$$

$$\tau = M(\theta)\ddot{\theta} + V\left(\theta, \dot{\theta}\right) + G(\theta) \quad (39)$$

Where θ is the vector of the joint angle, $\dot{\theta}$ is the vector of joint angular velocity, $\ddot{\theta}$ is the vector of joint angular acceleration, τ is the vector of the torque, $M(\theta)$ is the inertia matrix in joint coordinate space, $V\left(\theta, \dot{\theta}\right)$ is the vector of centrifugal and Coriolis terms and $G(\theta)$ is the vector of gravity terms. Clear definitions and in-depth explanations of each torque component have been given in several studies (Bastian et al., 1996); (Cooper et al., 2000); (Hollerbach and Flash, 1982).

In our work, the inverse dynamics were computed using a recursive Newton-Euler Scheme. It is a two-step process. Firstly the acceleration and the angular momentum derivate are assessed recursively at each segment center of mass by starting from the base link (the scapula/torso) and going to the end-effector (hand). Secondly, the joint forces and torques are computed recursively starting from the hand and going to the shoulder joint. This formalism can be implemented by modeling the kinematic chain with the Denavit-Hartenberg (DH) convention. In this work, the original DH convention is used. The source code for the inverse dynamics was written in Matlab© code (The Mathworks, Inc) and the “Robotics Toolbox” (Peter I. Corke) (Corke, 2011) was used for visualization only.

3.6.1 DH convention

The DH convention is a mathematical method based on homogeneous matrices. They describe the transfer of local coordinate systems (LCS) between each segment of the kinematic chain. Thus, they facilitate the calculation of the direct kinematics (forward kinematics) and have become the standard procedure, especially in robotics.

According to this convention, we assume that the kinematic chain consists of n+1 bodies linked by n revolute or prismatic joints. Each body is associated with its segment coordinate system (SCS) Ri. The SCS are numbered from 0 to n. The ith

joint, which the associated angle is denoted qi is the body which connects link i-1 and i.

The following requirements are necessary to correctly define the kinematic chain using the DH convention. The z_{n-1} axis lies along the axis of movement of the nth joint, the x_n axis is the cross product of z_n axis and z_{n-1} axis and the y_n axis is perpendicular to them creating a right-handed coordinate system. It is possible to represent the coordinate system R*i* against the coordinate system R_{i-1} using four parameters and constraining two of them.

Using four elementary transformations one gets four parameters to move from R_{i-1} to R_i:

Rotation R around zi-1 at an angle θi.

Translation along zi-1 (di),

tTranslation along xi (ai),

Rotation R around xi at an angle αi.

Following this principle, we have chosen a three segment model (arm, forearm and hand) with three joints (glenohumeral, elbow and wrist) representing the upper part of the human body (Figure 13).

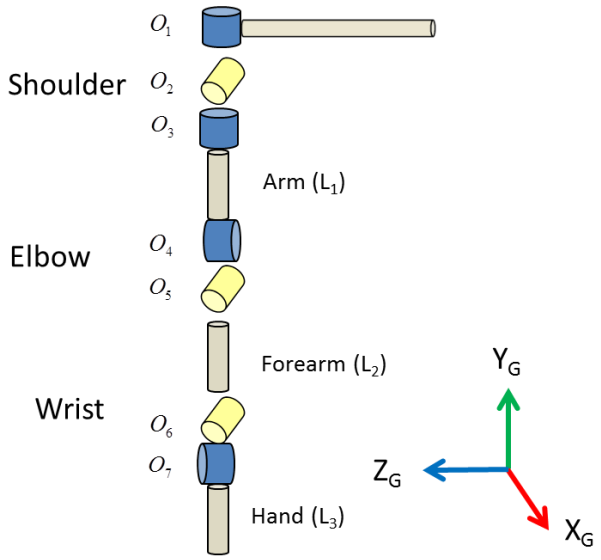

Figure 13 Schematic representations of the biomechanical multi-articulated upper limb model

The order of rotation sequences directly influences the results of the joint angle calculation (Senk and Chèze, 2006). To remain consistent with previous work, we chose to configure our model following the recommendations of the ISB (Wu et al., 2005) using the second convention for the forearm.

Table 6 Table of Denavit-Hartenberg parameters associated with each DOF of the model

Segment	Rotation Sequence	Angles	θ	d	a	α	Offset
Arm	YXY	Plan of elevation	Θ_1	0	0	π /2	π /2
		Elevation / Depression	Θ_2	0	0	- π /2	0
		Axial Rotation	Θ_3	-L(1)	0	π /2	- π /2
Forearm	ZXY	Flexion / Extension	Θ_4	0	0	- π /2	0
		Pronation Supination	Θ_5	-L(2)	0	π i/2	π /2
Hand	YXZ	Abduction Adduction	Θ_6	0	0	- π /2	π /2
		Flexion / Extension	Θ_7	0	L(3)	0	0

The multi-articulated model includes seven degrees of freedom. Table 6 shows the DH parameters for each degree of freedom. The column "offsets" has been added in the biomechanical model to indicate if all angles are equal to zero and are corresponding to the anatomical reference position.

The parameters L1, L2 and L3 correspond to the respective lengths of the arm, forearm and hand. The column parameters θ DH values correspond to each of the joint angles expressed in radians. Their implementation of the poly-articulated model reproduces the corresponding position visually. (cf. (Jacquier-Bret, 2009)).

3.6.2 Decomposition of the inverse dynamics computation

The net torque can be expressed as the sum of the joint muscle torque (MUS), gravitational torque (GRAV) and interaction (INT) torque (Sande de Souza et al., 2009), (Yamasaki et al., 2008):

$$NET = MUS + INT + GRAV \quad (40)$$

GRAV is the term with the gravitational acceleration, INT at each joint is the sum of the terms with the angular accelerations of the other joint (inertial torque), the terms

with the product of the angular velocities of the same joint (centripetal torque), the terms with the product of the angular velocities of the different joints (Coriolis torque), and the terms with the linear acceleration of the most proximal joint (Hollerbach and Flash, 1982), (Hirashima et al., 2008). The MUS is calculated in residual terms as follows: MUS = NET - GRAV - INT, and for that reason sometimes called “residual torque.” The MUS includes the mechanical contribution of muscle contraction acting at the joint and the passive contributions by muscles, tendons, ligaments, articular capsules, and other connective tissues (Hirashima et al., 2008).

To calculate the torque around specific joints of the human body, a few assumptions have to be made to facilitate the calculation. The body segments are considered as rigid bodies with a fixed mass located at its fixed center of mass interconnected with joints and constant segment length.

As an example the torque around the elbow joint is calculated assuming 2DOF and the movement in a vertical plane. The following parameters are known: I_i = moment of inertia about the center of gravity, r_i = distance to center of mass from proximal joint of the segment, l_i = length, m_i = mass, τ_i = joint torque, r_i = distance between the SCS origin and the segment COM (i = 1: upper arm, 2: forearm). NET, GRAV, INT, and MUS at the elbow and wrist are described as follows:

Upper arm

$$Net_u = +\ddot{\theta}_1[I_1 + I_2 + m_2 l_1^2 + m_1 r_1^2 + m_2 l_2^2 + 2m_2 l_1 r_2 \cos\theta_2] \quad (41)$$

$$Int_u = -\ddot{\theta}_2[I_2 + m_2 r_2^2 + m_2 l_1 r_2 \cos\theta_2] - \dot{\theta}_2^2[m_2 l_1 r_2 \sin\theta_2] - \dot{\theta}_2^2[m_2 l_1 r_2 \sin\theta_2] - \dot{\theta}_1\dot{\theta}_2[2m_2 l_1 r_2 \sin\theta_2] \quad (42)$$

$$Gra_u = g[(m_2 l_1 + m_1 r_1)\sin\theta_1 + m_2 r_2 \sin(\theta_1 + \theta_2)] \quad (43)$$

$$Mus_u = Net_e - Int_e - Gra_e \quad (44)$$

Forearm

$$Net_f = \ddot{\theta}_1[I_2 + m_2 r_2^2] \quad (45)$$

$$Int_f = -\ddot{\theta}_1[I_2 + m_2 r_2^2 + m_2 l_2 r_2 \cos\theta_2] - \dot{\theta}_1^2[m_2 l_1 r_2 \sin\theta_2] \quad (46)$$

$$Gra_f = -g[(m_2 r_2 \sin(\theta_1 + \theta_2)] \quad (47)$$

$$Mus_f = Net_f - Int_f - Gra_f \quad (48)$$

3.6.3 Validation of the inverse dynamics calculations

The inverse dynamics in this dissertation are performed using the DH convention and to validate the abovementioned model we compare it with the analytical model proposed by Hirashima et al. (2008).

We consider a 2 DOF model and evaluate possible differences between the original DH convention and the analytical model using custom written Matlab© codes (The Mathworks, Inc) and the "Robotics Toolbox" (Corke, 2011) for the visualization (Figure 14) to compute both inverse dynamics solutions.

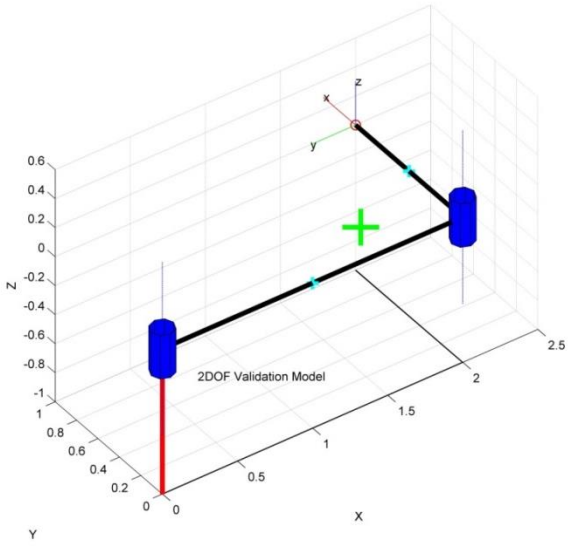

Figure 14 The robot with DOF used for the inverse dynamics computation using the DH convention

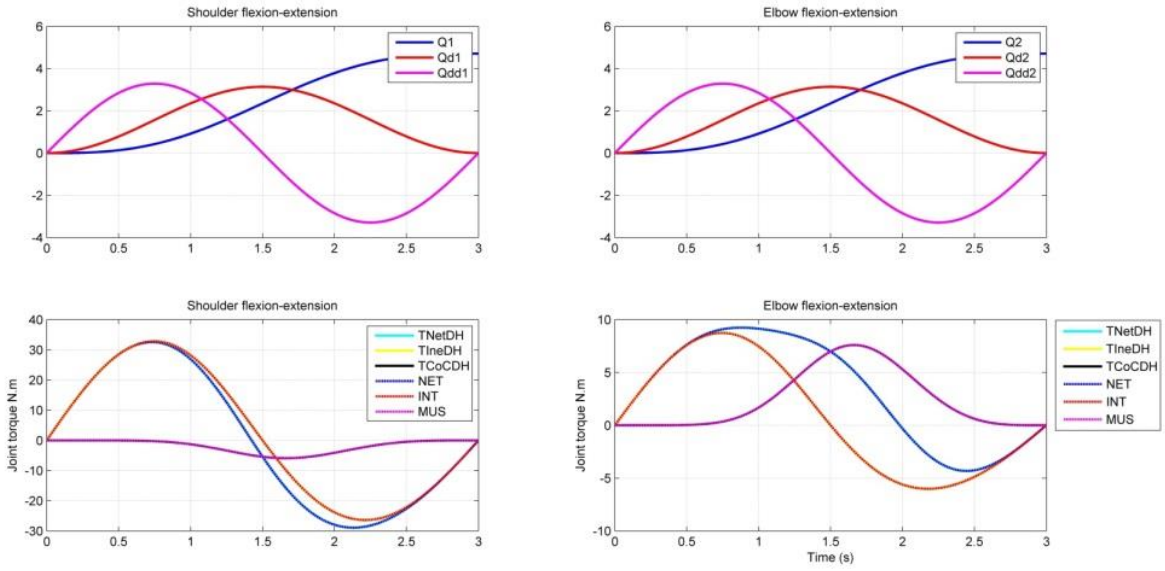

Figure 15 Results of the validation study. No differences could be found between the computations of the DH convention and the analytical model.

The computation of both inverse dynamics computations was consistent between the DH convention and the abovementioned analytical model (Figure 15).

After having introduced the biomechanical model the research hypotheses will be presented and the experimental setups are introduced.

Chapter 4

4 Hypotheses and Transition

Following the theoretical motor control background and the biomechanical model this chapter will present the eight experimental setups which are briefly introduced with the respective research hypotheses. The eight experiments divided into four experimental chapters

Chapter 5 "Effect of velocity, sensory, gravity torque, arm dominance, initial instruction during purposeless (non-athletic) rotation movements' tasks".

In the first experimental chapter, we tested the effect of velocity, sensory, gravity torque, arm dominance, initial instruction during non-athletic rotation movements tasks on the role of the minimum inertia resistance principle. In total three experimental protocols were tested.

We hypothesized that the rotational axes employed by the subjects would change from an articular axis to an inertial axis as the velocity of the arm's movements increased even though the initial starting position was imposed. This is because higher velocities and accelerations amplify the effects of inertia when arm rotations must occur off of the $\mathbf{e_3}$ axis, due to the presence of large inertial products (i.e., higher resistance of the arm to being rotated). Specifically, we hypothesized that at a slow angular velocity (S) the rotation of the arm should spontaneously coincide with the geometrical articular axis SH-EL (given that the effects of inertia remain weak at slower velocities and yield minimum mechanical disturbances). Finally, at a faster angular velocity (F) the arm should become dynamically balanced around $\mathbf{e_3}$ in order to minimize both the inertial resistances and joint muscle torque. We hypothesized also that differences in the control of the upper-limbs occur due to handedness. The third hypothesis of this chapter is that the rotational axes employed by the subjects would change from an articular axis to an inertial axis as the influence of gravity acting on the arm was manipulated.

Experiment 1

While the results of previous studies have shed light to the control of unconstrained upper limb movements the first experimental protocol will test the hypothesis if initial instructions may have an influence on the outcome and change of rotational axes. The first study will test the research question if a velocity-dependent change of rotation axis is an emergent phenomenon (in nonlinear dynamic system theory), reported by (Isableu et al., 2009) regardless of initial instructions. Instructions can be considered as additional constraints that may reduce the number of possible solutions in the coordination of our limbs.

Experiment 2

Following the outcome of the first study the question arises if the initial constraints may prevent the non-dominant arm from rotating around a more efficient rotation axis then the anatomical shoulder elbow axis. In general, the non-dominant arm is less well controlled (Sainburg and Kalakanis, 2000; Bagesteiro and Sainburg, 2002; Sainburg, 2002) compared to the dominant arm, which leads to the assumption that in direct comparison the non-dominant will show larger variability. We hypothesize similar behaviors during rotation tasks of the upper limbs where the control of the arm during internal-external rotations will show larger variability of the employed rotation axis and possibly the absence of a preferred axis.

Experiment 3

The third study covers the final experiment regarding cyclic internal-external arm rotations implementing the idea that that velocity-dependent change of rotation axis toward $\mathbf{e_3}$ should be observed regardless of the gravitational settings. The rotation sequences were performe, changing the influence of the gravitational torque and the hypothesis was posed that a velocity-dependent change of rotation axes toward mass or inertial ($\mathbf{e_3}$) axis would be uncovered regardless of the gravitational torque and postural orientation of the arm. In addition, the initial instruction was avoided and the initial experimental conditions were reproduced as in the paper by (Isableu et al., 2009).

Chapter 6 “Effect of precision demands: “maximizing precision” in athletic skills

In the second experimental chapter we tested the effect of precision in athletic throwing on the role of the minimum inertia resistance principle. Two experimental protocols were chosen to evaluate the role of the minimum inertia resistance axis a precision throwing task.

The first section of the chapter has addressed the impact of initial instructions and the influence of the gravitation torque on the internal-external arm rotations, the second section continue with a precision-dependent task. In other words, this section evaluates if precision demands in a throwing task provoke the use of the inertia tensor axis (minimum inertia resistance axis) during the movement. Since the first experimental attempts failed to provide evidence for a change of axes due to high velocity, this section will focus on the movements that include precision. Lastly, this chapter will explore the impact of expertise comparing novices with experts.

We hypothesized that the stabilization of rotational axes by the subjects would change from the initial control strategy to a different one when the throwing distances and target heights were altered and the influence of gravity acting on the arm changed. Changing the throwing distance should change the velocity profiles of the hand, while the influence of gravity should help the angular acceleration when throwing with gravity and counteract it when throwing against gravity.
Even though dart throwing is a slow movement, stabilizing $\mathbf{e_3}$ should minimize both the inertial resistances and joint muscle torque. We also hypothesized that differences in the control of the upper-limbs occur due to different skill levels.

Experiment 4

The fourth study evaluates different control strategies during a dart throwing task. Different throwing techniques have been observed and stabilizing the $\mathbf{e_3}$ axis has been shown to change the torque decomposition favoring the contribution of MUS to Net torque. Additionally, the first study explores the influence of different target heights and distances on the throwing motion.

Experiment 5

The fifth study deals with the comparison between novice darts players and high performance athletes. Due to the level of expertise, control strategies are expected to differ from novices to the task. The findings of this sector, indeed show different control strategies but inter individual strategies seem to cover generalizable motor control strategies as stabilizing the $\mathbf{e_3}$ to minimize both the inertial resistances and joint muscle torque.

Chapter 7 "Effect of velocity demands: Maximizing velocity in athletic skills".

In the third experimental chapter we tested whether velocity demands in overarm throwing are maximized when the rotation axis of the upper limb coincide with the $\mathbf{e_3}$ axis. One experimental protocol was chosen to evaluate the role of the minimum inertia resistance axis during an overarm throwing task maximizing the velocity profile.

We hypothesized that the stabilization of rotational axes by the subjects would change from an articular axis to an inertial axis during the throwing phases that have a high velocity profile. Higher velocities and accelerations amplify the effects of inertia and arm rotations may occur around the $\mathbf{e_3}$ axis. Moreover, at a faster angular velocity the arm should become dynamically balanced around $\mathbf{e_3}$ in order to minimize both the inertial resistances and joint muscle torque.

Experiment 6

The sixth study tests the MIR principle against velocity constraints during an overarm throwing task. Subjects were asked to throw a ball as fast as possible at a target. Among the three main throwing phases, it has been found that subjects tend to rotate their arm around the $\mathbf{e_3}$ axis during the cocking phase. The cocking phase is the preparation to the acceleration phase and it could be noted that this movement provokes a rotation around this specific axis to minimize the effort and bring the elbow in position for the last phase.

Chapter 8 "Effect of spatial and velocity demands: Maximizing both precision and velocity in athletic skills".

In the fourth and last experimental chapter we tested the effect of maximizing velocity and precision in overarm throwing on the role of the MIR principle. Two experimental protocols were chosen to evaluate the role of the minimum inertia resistance axis during an interception task and a tennis flat serve.

We hypothesized that the stabilization of rotational axes by the subjects would change from an articular axis to an inertial axis during the interception heights and the velocity profiles. We also hypothesized that the stabilization of an inertial axis would be invariant throughout the experimental conditions. Moreover, at faster angular velocities the arm should become dynamically balanced around $\mathbf{e_3}$ in order to minimize both the inertial resistances and joint muscle torque.

Experiment 7

The seventh study is the first of the fourth experimental chapter and tests the MIR principle against velocity and precision constraints during a tennis flat serve. Subjects were asked to perform a tennis flat serve. The subjects were high performance athletes and the serve movement was divided into three distinguishable movement phases.

The findings show that subjects tend to minimize the angular variability of the rotation axes during the cocking phase. However, due to the small sample size no statistical differences could be uncovered. To conclude, subjects tend to rotate around a tradeoff axis around SH-CM and the SH-$\mathbf{e_3}$ during the cocking phase.

Experiment 8

The eighth study is also the last of the fourth experimental chapter and tests the MIR principle against velocity and precision constraints during interception task. Subjects were asked to intercept a ball, in three different velocity and three interception heights. Interestingly the findings show that consequently the rotations during a specific intercepting height are performed around the $\mathbf{e_3}$ axis. To conclude, a change of rotation axis can be observed for specific interception heights independent of the velocity. In other words, the change of rotation axes depends on the given time constraints. Rotation around $\mathbf{e_3}$ may allow for the production of maximal acceleration of the hand to intercept the ball in a short period of time. This could be advantageous when subjects have strong time limiting constraints.

Chapter 5

5 Effect of velocity, sensory, gravity torque, arm dominance, initial instruction during purposeless (non-athletic) rotation movements tasks

The fifth chapter is devoted to the effect of velocity, sensory, gravity torque, arm dominance, initial instruction during non-athletic rotation movement tasks on the role of the minimum inertia resistance principle. The presented experiments in this chapter are structured with an introduction to explain the research question, followed by a short methods section, the results and a discussion

5.1 Velocity-dependent changes of rotational axes during the control of unconstrained 3D arm motions depend on initial instruction on limb position.

5.1.1 Introduction

Controlling both daily motor activities and skilled athletic movements requires complex 3D rotational motions of our upper limbs in different ranges of angular acceleration, often in the absence of visual regulation. The rotation axes around which cyclic rotational movements of the whole arm are performed is an organizational key factor in motor control (Isableu et al., 2009). One assumption is that rotational axes may provide a parsimonious basis for controlling the multiple degrees of freedoms of our upper limbs during 3D movements. It has been shown that the rotational axes are spatial invariants specified in both the dynamics and kinematics of arm movements. This can be shown in the way the various torques (gravity, muscle and interaction) contribute to produce specific angular acceleration profiles and displacements at a given joint (Hirashima et al., 2007b; Hirashima et al., 2003b; Isableu et al., 2009).

Due to different arm configurations involving flexion-extension of the elbow, there is almost always a separation between the axis of minimal inertia ($\mathbf{e_3}$) (Pagano and Turvey, 1995), the shoulder-centre of mass axis (SH-CM) (van de Langenberg et al., 2008) and the shoulder-elbow axis (SH-EL) of the upper-limb (Isableu et al., 2009; Hirashima et al., 2007b; Hirashima et al., 2003a). During cyclic external-internal rotations at the shoulder, the rotation axis of the arm may coincide with one of these rotation axes. The choice of axis has implications on the amount of torque that must be produced, and also may have on the energy costs associated with the task.

Isableu et al., (2009) recently tested which axes of rotation subjects would emerge (SH-EL, SH-CM and $\mathbf{e_3}$) in a task involving an internal-external cyclic rotation of the shoulder performed at different velocities, without vision of the arm or any instruction regarding the axes to be used. The authors found that the rotation axis of a multi-articulated limb system may change from a geometrical articular axis (SH-EL) to a mass or inertia-based axis as the velocity and acceleration of the limb increased. They identified that the relevant mass/inertia-based axis forms a compromise between static and dynamic joint torques; i.e. a SH-CM/$\mathbf{e_3}$ trade-off axis. Higher velocities and accelerations amplify the effects of inertia. When arm rotations are performed around other axes than $\mathbf{e_3}$, the inertia products augment and rotations are performed with higher torque. The authors also showed that rotation axes specifically determine the contribution of muscle, interaction and gravity torque to net torque and the magnitude of joint rotation. The calculations were consistent with multiple studies in movement dynamics (Sande de Souza et al., 2009; Yamasaki et al., 2008). The net torque (NET) corresponds to the part of the muscle (or resultant) torque (MUS) which is proportional to the corresponding joint acceleration. The interaction torque corresponds to the sum of the Coriolis and centrifugal torques plus the torque generated by joint accelerations of other joints. The gravity torque (GRAV) is the torque due to gravity. MUS = NET-INT-GRAV

Isableu (2009) proposed a model of unconstrained 3D arm rotations which predicts that rotational limb movements will occur about the eigenvectors ($\mathbf{e_i}$) of the inertia tensor ($\mathbf{I_{ij}}$), specifically $\mathbf{e_3}$ (the axis of minimum inertial resistance). Rotations about $\mathbf{e_3}$ have been shown to minimize the contribution of muscle torque to net torque by using the interaction torque to assist motion compared to rotations about the center of mass (SH-CM) or joint (SH-EL) axes (Isableu, 2009).

For this experiment, we expected the arm to rotate about $\mathbf{e_3}$ during fast movements. We assumed that rotations about SH-EL, however, require explicit detection and explicit control about that axis, along with the production of additional muscular torques during fast movements. For the task used in this experiment, the use of $\mathbf{e_3}$ is more efficient and requires less intervention of the CNS (Todorov and Jordan, 2002) while the use of SH-EL requires more skill and higher joint torques.

The purpose of this study was to examine whether the minimum inertia resistance (MIR) principle (i.e., the spontaneous velocity-dependent change of rotation axes

toward axes known to reduce inertial resistances and muscle torque) governs internal-external rotations at a fast velocity and when subjects are instructed to maintain the rotation of the arm around the humeral long axis (SH-EL) as closely as possible to horizontal. Specifically, we are interested whether increasing the frequency of the arm rotations would cause the limb to rotate around an axis closely aligned to $\mathbf{e_3}$, in order to minimize inertial resistances, despite the instruction to keep the upper arm horizontal. We also verified whether the combination of sensory inputs, kinaesthetic only (K) vs. visuo-kinaesthetic (VK), improved the extent to which the subjects maintained the rotation of the arm around the instructed rotation axis. More precisely, we expected the VK inputs should minimize the variability of displacements of the instructed axis of rotation, but that K inputs should facilitate the rotation around $\mathbf{e_3}$ at fast velocity. We also hypothesized that the subjects' tendency to rotate around $\mathbf{e_3}$ at fast velocity should be maintained at different elbow angles (i.e.,Elb 90° and Elb140°).

Experimental Procedures

Subjects: 14 subjects (12 men and 2 women) voluntarily participated in the experiment after signing a statement of informed consent pertaining to the experimental procedure as required by the Helsinki declaration and the EA 4532 local Ethics Committee. Twelve participants were right-handed and 3 left-handed. They were aged 22 (± 3) years and all recruited from the university community. Handedness was determined using the ten-item version of the Edinburgh inventory (Oldfield, 1971). They were free of sensory, perceptual, and motor (shoulder and elbow) disorders. They were naïve about the purpose of the experiment.

Procedures:

Participants stood upright in a perimeter delimited on the floor and were instructed to produce cyclic backwards and forwards rotation movements with their dominant arm from upward (about 10° behind the vertical) to downward (slightly below horizontal) (see figure 16).

Sensory conditions

In each of the conditions described below, the upper-limb movements were performed with eyes open to allow for both visual and kinesthetic information (VK), and with the eyes closed to provide only kinesthetic information (K). In the VK condition, subjects were instructed to look at their arm during movements in order to visually monitor the internal-external rotational sequence.

Elbow angular configurations

In each of the sensory conditions (VK and K), participants were instructed to perform cyclic external-internal rotations of the whole arm with the shoulder abducted to the horizontal and the elbow flexed and actively held at 90° (Elb90°) or 140° (Elb140°) relative to the arm outstretched at the horizontal (see Figure 16).

When the arm is fully extended, local centers of mass (hand, forearm and arm) are closely aligned with the longitudinal axis of the whole arm (SH-EL). In this configuration the SH-CM and $\mathbf{e_3}$ axes are aligned very closely with the SH-EL axis. The Elb90° and Elb140° elbow configurations induce geometrical change in the arm's mass distribution (i.e., in the relationships between hand, forearm and arm's centers of mass). The changes in mass distribution provokes a separation between the SH-CM, $\mathbf{e_3}$ and SH-EL rotation axes (see Figure 17) and provide a possibility to asses which axes are employed during the kinaesthetic and visuo-kinaesthetic control of voluntary 3D rotational arm movements. The Elb90° and Elb140° elbow configurations were chosen to yield a constant separation between the SH-EL, SH-CM and $\mathbf{e_3}$ axes of rotation, and to modify the relative positions of SH-CM and $\mathbf{e_3}$ axes with respect to the SH-EL axis.

The Elb140° configuration resulted in different relative positions of the SH-CM and $\mathbf{e_3}$ axes with respect to the SH-EL axis compared to the Elb90° configuration (see, Figure 17). More specifically, Elb90° produced an angle of about 5.40° between $\mathbf{e_3}$

and SH-CM (with the SH-CM axis positioned between $\mathbf{e_3}$ and SH-EL) and Elb140° produced an angle about 5.40° ± 0.4° between $\mathbf{e_3}$ and SH-CM for the mean elbow flexion angle of 137.6° (the differences between subjects morphology led to those differences) (with the $\mathbf{e_3}$ axis positioned between the SH-CM and SH-EL axes), (see Figure 17). $\mathbf{e_3}$ was angled 27° and 15° away from the SH-EL axis at Elb90° and Elb140°, respectively.

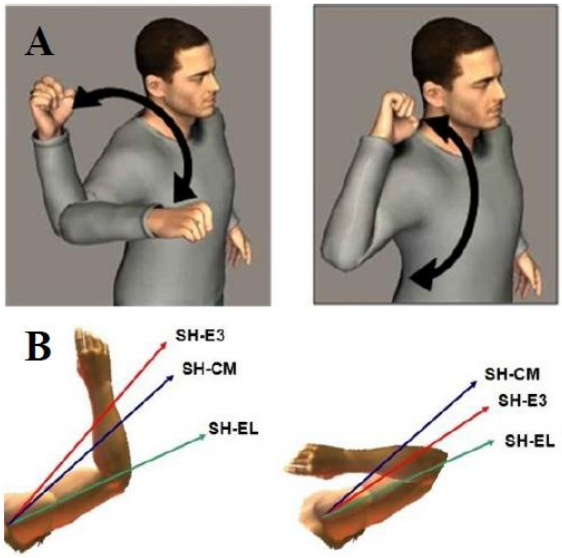

Figure 16 Experimental setup A) shows the Elb90 and the Elb140 configuration B) shows the rotation axes

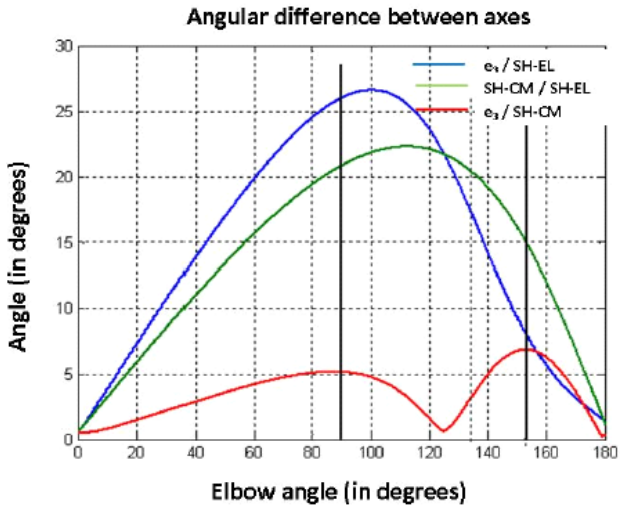

Figure 17 Angular separation between the rotation axes due to the elbow angle.

Velocity conditions

In both angular elbow configurations (Elb90° and Elb140°) and sensory conditions (K and VK), the roles of SH-CM, $\mathbf{e_3}$ and SH-EL were investigated in slow (S) and fast (F) angular velocities of the arm.

In the S velocity condition, participants performed one cycle of the internal-external rotation of the arm per 10 s during a 50 s trial (0.1 Hz). In the F velocity condition subjects were instructed to approach maximal velocity while producing biomechanically comfortable movements during a trial lasting 10 s (corresponding to about 2 Hz). A timed audio signal was used to fix the frequency of the movement cycle prior to each trial. The audio-signal was stopped before the start of the recording in order to avoid a dual-task.

Experimental sessions

Each subject performed three external-internal rotation sequences in the eight different conditions. This results in a total of 24 trials per subject.

The three trials for a given elbow configuration, frequency and sensory condition were presented in succession within a single block, with a 30 s rest period between each trial. The eight conditions were performed in a random order, with a one minute rest period between them.

Prior to the experimental conditions, a training session was completed for each of the two frequency conditions to allow subjects to become familiar with the movement frequencies and the shoulder elevation of 90°. We carefully checked that the instruction to hold the shoulder-elbow axis close to horizontal was clearly understood as the initial position. The learning was visually evaluated by the researcher, with the task being judged as acquired once the participant reproduced 5 successive trials that were synchronized with the signal. Before each of the experimental trials the audio signal was played again to indicate the frequency to be used. Trials were withdrawn and immediately repeated if it appeared to the experimenter that the elbow angles (i.e., 90° and 140°) were not maintained.

The kinematic analysis and the computation of the SH-EL, SH-CM, and $\mathbf{e_3}$ vectors were performed as described in Chapter 3.

Statistical analyses

A multivariate repeated measures analysis of variance (MANOVA, using the GLM module, Statistica 7 software) combining two arm velocities (S vs F) * two angular elbow configurations (Elb90° vs Elb140°) and two sensory conditions (V vs VK) was then applied on the variability of angular displacements of each rotational axes (SH-EL, SH-CM, $\mathbf{e_3}$) with a .05 level of statistical significance.

5.1.2 Results

The means of each variable were determined for each condition and subject (see Table 7), and the data was analyzed using a multivariate analysis of variance (MANOVA, see Table 8), followed by Tukey HSD post hoc comparisons.

Table 7 Mean(SD) rotation axes variability across conditions and subjects.

Axes variability in [rad]			SH-EL	SH-CM	SH-e_3
90	Open	Slow	0.08 ± 0.01	0.16 ± 0.02	0.20 ± 0.02
		Fast	0.17 ± 0.04	0.20 ± 0.06	0.26 ± 0.06
	Closed	Slow	0.09 ± 0.02	0.15 ± 0.03	0.18 ± 0.03
		Fast	0.19 ± 0.03	0.19 ± 0.07	0.24 ± 0.07
140	Open	Slow	0.10 ± 0.02	0.15 ± 0.03	0.12 ± 0.02
		Fast	0.15 ± 0.03	0.17 ± 0.03	0.15 ± 0.03
	Closed	Slow	0.10 ± 0.02	0.13 ± 0.03	0.11 ± 0.02
		Fast	0.14 ± 0.04	0.16 ± 0.02	0.14 ± 0.03

Table 8 Manova results

Source	df	df	F
Axes	2	12	45.95***
Elbow flexion	1	13	19.96***
Sensory conditions	1	13	6.69*
Velocity conditions	1	13	31.97***
Axes x Elbow Flexion	2	12	111.50***
Axes x Sensory conditions	2	12	12.92**
Elbow flexion x Sensory conditions	1	13	0.20
Axes x Velocity conditions	2	12	7.54**
Elbow flexion x Velocity Conditions	1	13	5.98*
Sensory conditions x Velocity conditions	1	13	0.01
Axes x Elbow flexion x Sensory conditions	2	12	12.11**
Axes x Elbow flexion x Velocity conditions	2	12	3.11
Axes x Sensory condition x Velocity conditions	2	12	1.66
Elbow flexion x Sensory conditions x Velocity conditions	1	13	0.02
Axes x Elbow flexion x Sensory conditions x Velocity conditions	2	12	3.42

* $p < 0.05$, ** $p < 0.01$, *** $p < 0.001$

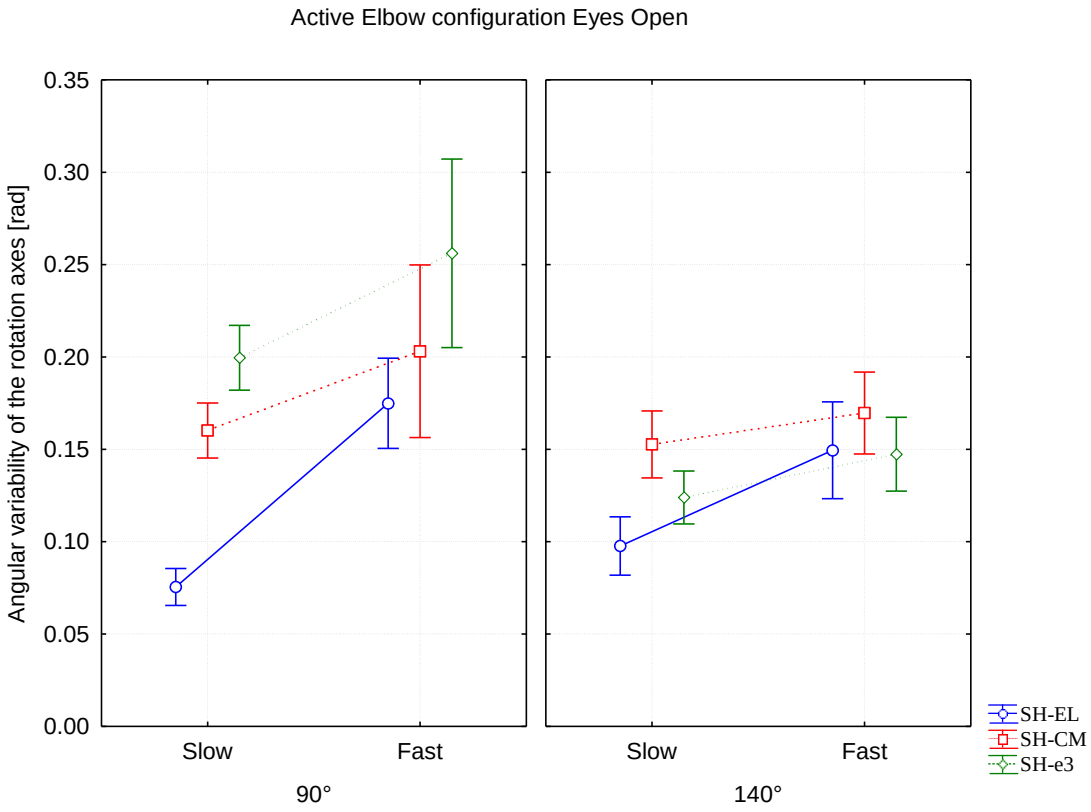

Figure 18 Angular variability of the rotation axes during the eyes open conditions

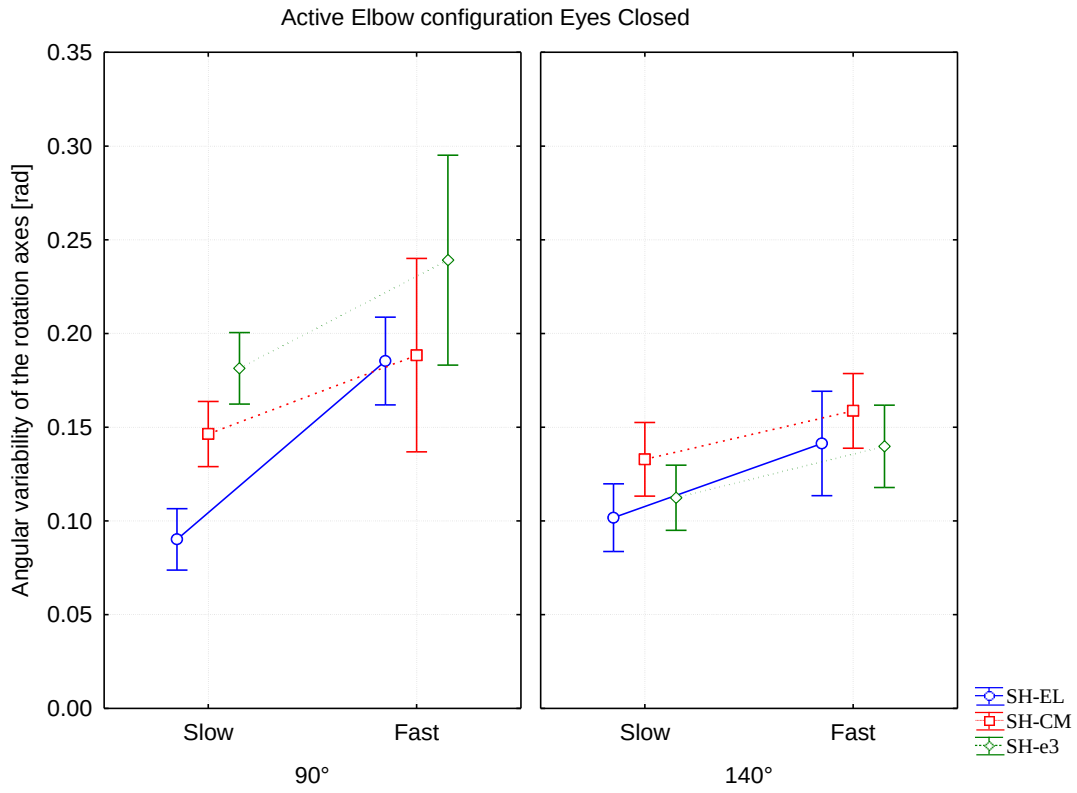

Figure 19 Angular variability of the rotation axes during the eyes closed conditions

To analyze the variability of the 3D angular displacements of the rotation axes, we used the framework of the MIR principle and computed rotation axes of the arm that were affected by the experimental conditions. Across all conditions, subjects showed a tendency to rotate their arm around the SH-EL axis compared to the SH-CM and the SH-e_3 axes (Figure 18 & 19). In other words, subjects showed no change in rotational axis during the experiment.

The variability of the SH-EL (0.13±0.12 rad) was significantly (p <.05) smaller than the variability of the SH-CM (0.16±0.16 rad) and $\mathbf{e_3}$ (0.17±0.17 rad). Furthermore the significant (p <.05) differences in the variability of the axes were due to elbow flexion with (0.18±0.17 rad) for the 90° and (0.14±0.12 rad) for the 140° elbow angle.
In the 90° elbow configuration the variability of the SH-EL (0.13 rad) axis significantly differed from the SH-CM (0.17 rad) and the SH-e_3 (0.22 rad) (p <.05) axes. Moreover, the SH-CM and the SH-e_3 axes significantly differed from each other.

Sensory condition

Across all conditions, subjects showed a tendency to decrease the variability of the movement during the K conditions (see Figures 19&20). In general the variability between the K (0.15±0.15 rad) condition and the VK condition (0.16±0.15 rad) significantly differed.
No differences could be discovered in the displacement of the SH-EL (VK=0.12 & K=0.13) axis in contrast to the SH-CM (VK=0.17 & K=0.16) and the SH-e_3 (VK=0.18 & K=0.17) axes, which showed significant variations between them (p <.05).
For the 90° elbow configuration additional post hoc analysis showed significant difference (p <.05) in the variability of the axes between closed and open eyes conditions for the SH-EL (VK=0.13 & K=0.14 rad), SH-CM (VK=0.18 & K=0.17 rad) and SH-e_3 axis (VK=0.23 & K=0.21 rad).
Furthermore the 140° elbow configuration only the SH-CM axis showed significant differences (p <.05) due to the sensory conditions (VK=0.16 & K=0.15 rad).

Velocity condition

Across all conditions, subjects showed an augmentation of variability when rotating the arm in the fast conditions (see Figures 19&20). In other words higher movement speed increased the variability of the rotational axes displacements.

The analysis revealed significant differences (p <.05) due to the velocity conditions. The variability of the SH-EL, SH-CM and SH-e_3 axis significantly increased (p <.05) during fast velocity conditions (0.18±0.18 rad) compared to the slow velocity conditions (0.13±0.12 rad).

Post hoc tests showed a significant effect of velocity conditions on the variability (p <.05) for the three rotational axes, SH-EL (S=0.09 & F=0.16 rad), SH-CM (S=0.15 & F=0.18 rad), SH-e_3 (S=0.15 & F=0.2 rad).

5.1.3 Discussion

An exact correspondence between the principal axis of inertia and the joint axis in unconstrained 3D movements rarely occurs in everyday activities or during advanced athletic achievements (Hirashima et al., 2007b; Hirashima et al., 2007a). This raises the question of how the CNS identifies the relevant rotation axis that allows motor coordination to be adaptive and proficient in demanding tasks. The proprioceptive role of the inertia tensor ($\mathbf{I}_{ij}$) was initially proposed by (Pagano and Turvey, 1995), and was based on the rationale that $\mathbf{I}_{ij}$ acts on line and is informative of the instantaneous state of limb's disposition independent of any stored or learned representations of the limb's past or potential states. An assumption reinforced by the fact that $\boldsymbol{I}_{ij}$ is a dynamic parameter that is specifically available when the 3D motions and forces are actively produced.

The present experiment was designed to test the hypothesis that increasing the frequency of arm rotations would cause the limb to rotate around an axis closely aligned to $\mathbf{e}_3$, even if the alignment of the shoulder-elbow axis to horizontal was initially imposed by the instructions. In other words, we have tested the hypothesis that biomechanical constraints should overcome the influence of initial instructions (cognitive) and dominate the control of fast 3D rotational movements.

In this experiment, the candidate axes that were tested were i) the geometrical SH-EL axis based on the exploitation of kinematic signals corresponding to the joint angles, ii) the SH-CM axis based on the consideration of the whole upper-limb center

of mass and likely detected on the basis on kinetic positional signals, and iii) $\mathbf{e_3}$, which involves the exploitation of dynamic joint torques and the extraction of invariants in the dynamics of motion about an axis related to mass distribution i.e., through angular acceleration signals (Pagano and Turvey, 1995; Pagano and Turvey, 1998).

Taken together, our results indicated that the velocity increase significantly increased the variability of 3D angular displacements of the rotational axes, but were not sufficient enough to yield a change in the axes around which the whole upper-limb was rotated. Our results provide evidence that the influence of initial instructions regarding the shoulder-elbow positioning to the horizontal and its maintenance during the trial prevented subjects from shifting from a geometrical articular axis at S velocity to a mass or inertia-based axis at the F velocity (Isableu et al., 2009).

These results, emphasizing the role of top-down influences, contrast with earlier results demonstrating a change toward more efficient biomechanical solutions, such as the use of the SH-CM or $\mathbf{e_3}$ axes (when the specific axis of rotation was not strictly indicated) (Isableu et al., 2009), or the use of additional interaction torque to assist motion (Dounskaia et al., 2005; Dounskaia et al., 2002; Dounskaia et al., 1998; Goble et al., 2007; Hirashima et al., 2007b; Hirashima et al., 2003a).

The results showed an increase of the variability of 3D angular displacements of the SH-EL articular axis as velocity increases, which should provoke a change toward either a mass or inertia based axis. The instructions employed in the present experiment may have caused the subjects to take into account the increase of the variability of 3D angular displacements of the SH-EL articular axis and, thus, actively maintain the arms rotation about the SH-EL axis.

Sensory conditions

Given that integration of visuo-kinaesthetic inputs is known to improve the signal-to-noise ratio by reducing uncertainty present in each of the sensory modalities (van Beers et al., 1998; van Beers et al., 1999a; van Beers et al., 1999b; van Beers et al., 1996), we hypothesized that the visuo-kinesthetic (VK) control of arm movements should have led to less scattered displacements of rotational axis used. We also hypothesized that the kinesthetic (K) control of arm movements should have increased the likelihood of the arm's rotation axis to change toward more efficient

rotation axes strategies (SH-CM or $\mathbf{e_3}$) at the faster velocity, even if the initial starting position was imposed. Closer inspection of the results showed that VK inputs reduced the variability of the SH-EL axis across velocity conditions at 90°. Hence, our initial hypothesis according to which the visuo-kinesthetic (VK) control of arm movements should have led to less scattered displacements of rotational axis used is confirmed. However, the results did not confirm the second hypothesis regarding the effect of velocity.

We have hypothesized that rotation around $\mathbf{e_3}$ at the fast velocity should persist at different elbow angles (i.e., Elb90° and Elb140°) although these elbow configurations caused variation of $\mathbf{e_3}$ angle with respect to the SH-EL axis . With this view, the minimum inertia axis $\mathbf{e_3}$ was angled 5.4±0.4° away from the SH-CM axis in both elbow configurations. SH-CM was positioned between $\mathbf{e_3}$ and SH-EL at Elb90°, while $\mathbf{e_3}$ was positioned between SH-CM and SH-EL at Elb140°. The results did not show any evidence that modifying the angle between $\mathbf{e_3}$ or SH-CM with respect to the SH-EL axis allowed the arm to rotate around $\mathbf{e_3}$.

The effect of the initial starting position prevented subjects from using efficient biomechanical strategies in the organization of the movement. The results have not shown an effect of the sensory conditions on the variability of 3D angular displacements of the rotational axes, which might be due to the initial instruction to keep the upper arm horizontal.

Further experiments will be necessary to explore whether instructions related to the minimization of perceived effort for rotating the arm, or simply instructing the subjects to rotate as rapidly as possible with no specific axis being indicated, would result in rotations about $\mathbf{e_3}$. It is possible that a person does not need to detect $\mathbf{e_3}$ in order to rotate the arm about $\mathbf{e_3}$. They just have to set the arm in motion and in the absence of explicit control about some other axis the arm will rotate about $\mathbf{e_3}$ on its own. We assumed that rotations about SH-EL, however, require explicit detection and control about that axis, along with the production of additional muscular torque. The use of $\mathbf{e_3}$ is more efficient in terms of muscular torques produced because it requires less intervention (attention) of CNS (Todorov and Jordan, 2002), while the use of SH-EL requires more skill, higher joint torques and more explicit control. Further experiments will be necessary to explore whether increasing the angle between SH-CM and $\mathbf{e_3}$ is

a necessary condition to constrain the arm to rotate around an axis closely aligned with $\mathbf{e}_3$.

5.1.4 Conclusion

The results showed that the rotational axis of a multi-articulated limb does not change from an articular axis of rotation to either a mass or inertia based axis when instructions corresponding to the articular axis are imposed. This finding was observed for both slow and fast rotations, for rotations made both with and without vision, and in different angular elbow configurations. The elbow configurations employed were close to those observed in many athletic configurations and the absence of an invasive mechanical device to alter the mass distribution of the limb reinforces the external validity of our results. These findings extend our understanding of the influence of instructions on how rotation axes are used to organize action, their relevance, and the proficiency that can be expected when coordinating limbs in tasks requiring fast rotations.

Our results do not contradict the findings of previous research (e.g., (Isableu et al., 2009), but explain the influence of the initial limb configuration and the instructions on the performed movement.

5.1.5 Executive Summary

The velocity-dependent change in rotational axes observed during the control of unconstrained 3D arm rotations may obey the principle of minimum inertia resistance (MIR). Rotating the arm around the minimum inertia tensor axis (**e_3)** reduces the contribution of muscle torque to net torque by employing interaction torque. The present experiment tested whether the MIR principle still governs rotational movements when subjects were instructed to maintain the humeral long axis (SH-EL) as closely as possible to horizontal. With this view, the variability of 3D trajectories of the minimum inertia axis (**e_3**), shoulder-center of mass axis (SH-CM) and shoulder-elbow axis (SH-EL) was quantified using a VICON V8i motion capture system. The axis for which the 3D variability displacement is minimal and is considered as the one constraining the control of arm rotation. Subjects (n=14) rotated their arm in two elbow angular configurations (Elb90° vs. Elb140°), two angular velocity conditions (slow S vs. fast F), and two sensory conditions (kinesthetic K vs. visuo- kinesthetic VK). The minimum inertia axis **e_3** is angled 5.4±0.4° away from SH-CM axis, and varied from 27° to 15° away from de SH-EL axis, for Elb90° and Elb140°, respectively. We tested whether the participants would be able to maintain the instructed SH-EL rotation axis or if increasing the frequency of the arm rotations would override the initial rotation instructions and cause the limb to rotate around an axis closely aligned with **e_3**. We expected that VK inputs would minimize the variability of the SH-EL axis and that K should facilitate the detection and rotation around **e_3** at the faster velocity. Taken together the results showed that the initial instruction, favoring rotation around the SH-EL axis, prevented the velocity-dependent change towards the minimum inertia (**e_3**) and/or the mass axis (SH-CM), i.e., use of the MIR principle. However, the variability of the SH-EL axis was significantly increased in the F condition, confirming that arm rotations around the SH-EL axis produces larger mechanical instabilities in comparison to when the arm is rotated around a mass/inertial axis (Isableu et al., 2009).

Study I	Description
Title	Velocity-dependent changes of rotational axes during the control of unconstrained 3D arm motions depend on initial instruction on limb position.
Subjects	14 subjects recruited from the University community
Hypothesis	The MIR principle overcomes the instruction of trying to maintain the rotation around the SH-EL axis during high movement velocity Kinesthetic cues only may lead to controlled rotations around $\mathbf{e_3}$ at fast motion frequency. Visuo-kinesthetic cues should prevent a change of rotation axes due to the visual control of the movement.
Task	Participants stood upright in a perimeter delimited on the floor and were instructed to produce cyclic backwards and forwards rotation movements with their dominant arm from upward to downward in two different angular elbow (90° vs. 140°), two velocity (Slow vs. Fast) and two sensory (Eyes Open vs. Eyes Closed) configurations. The instruction was given, trying to rotate the arm around SH-EL.
Measurement system	Vicon V8i eight M2 camera passive optical motion capture system, frequency 250Hz
Measured Variables	Displacements of the 13 Markers put on the trunk, arm, forearm and hand
Data Analysis	Filter: Butterworth filter (2nd order) Joint Angle Computation Vector Computation Vector displacement computation
Calculated Variables	Variability of the angular axes displacement
Statistical Analysis	Repeated measured MANOVA Post hoc test (Tukey HSD)
Results	The variability of the angular displacement of the axes augmented with higher movement frequency A decrease of the variability of the rotation axes was found during the K conditions Visual kinesthetic cues improved the stability of the rotation axis around which the arm rotates
Discussion	The MIR principle did not overcome the initial instruction but higher variability was observed Kinesthetic or visual kinesthetic cues do not significantly alter the variability of the rotation axes.

5.2 Differences in the control of unconstrained 3D arm motions of the dominant and the non-dominant arm.

5.2.1 Introduction

In everyday life each person has a preferred hand to perform given tasks. Controlling 3D rotational motions of our upper limbs is complex and is often performed in different ranges of angular velocities and accelerations. The control becomes even more difficult, when the motions are executed in the absence of visual regulation (Isableu et al, 2013) or with the nondominant arm (Dounskaia, 2005);(Sainburg, 2005). Previous research has shown that the control of unconstrained 3D arm motions, like external-internal rotations of the shoulder do depend on kinesthetic cues and the velocity of the performed task (Isableu et al., 2009); (Isableu et al., 2013). Recent research (Sainburg, 2002) showed differences in the dynamic intersegmental control between the dominant and the nondominant arm in a reaching task. Earlier studies have also shown a dominant limb advantage in the use of passive forces like interaction torque during a variety of tasks (Dounskaia, 1998; Dounskaia, 2005; Dounskaia et al., 2010) (Sainburg, 2002). They showed that adaption for new tasks were less effective for the nondominant limbs.

However, some studies have shown advantages of the nondominant arm in reproducing movement distance (Yamauchi et al., 2004) or position accuracy (Lenhard and Hoffmann, 2007); (Goble et al., 2007), even without visual feedback (Bagesteiro and Sainburg, 2002); (Bagesteiro and Sainburg, 2003); (Sainburg, 2002), (Sainburg and Kalakanis, 2000); (Sainburg and Wang, 2002). (Bagesteiro and Sainburg, 2003) also reported that the nondominant arm is more efficient dealing with perturbations acting during the movement.

During different arm configurations involving flexion-extension of the elbow, most often a separation between the axis of minimal inertia ($\mathbf{e_3}$) (Pagano and Turvey, 1995; Pagano and Turvey, 1998), the shoulder-center of mass axis (SH-CM) (van de Langenberg et al., 2007; van de Langenberg et al., 2008) and the shoulder-elbow axis (SH-EL) of the whole upper-limb (Isableu et al., 2009); (Hirashima et al., 2007b), (Hirashima et al., 2007a) occurs. A nontrivial observation is that during most

unconstrained three-dimensional (3D) movements an exact correspondence between the rotation axes of minimum inertial resistance ($\mathbf{e_3}$), minimum center of mass movement (shoulder-center of mass, SH-CM) and minimum elbow movement (shoulder-elbow, SH-EL) very seldom occurs (Hirashima et al., 2007b), (Hirashima et al., 2007a). For the dominant limb, (Isableu et al., 2009) a velocity-dependent change in rotational axes away from the SH-EL axis during the kinesthetic control of unconstrained 3D arm rotations was reported, which allow for the use of the interaction torque in an assistive manner to decrease the necessary muscle torque. More recently, (Isableu et al., 2013) also showed that the weight of initial instruction on limb positioning i) may prevent this velocity-dependent change in rotational axes, ii) reinforce the arm to rotate around the SH-EL, iii) that fast velocity increased the variability of the SH-EL axis leading to larger mechanical instabilities and iv) that visual kinesthetic cues improved the stability of the rotation axis around which the arm rotates.

We questioned whether this velocity-dependent change in rotational axes applies to the nondominant arm as well as for the dominant arm and if it applies when the initial starting position of the upper-limb is strictly defined. We also investigated to what extent the velocity increase and multisensory control cyclic movement of the upper arm (dominant and nondominant) influenced the variability of the center of pressure (CoP) displacements.

Entropic methods have been introduced to explore the non-linear dynamics of the center of pressure movement that describe the systems randomness or unpredictability (Pincus, 1991). New methods like the Multi Scale Entropy algorithm (Costa et al., 2005) and Multivariate Multi Scale Entropy (Lu et al., 2012) have recently been developed to measure and quantify the intrinsic complexity of a signal but also to provide a more meaningful measure of dynamic complexity in general. This method has been widely used to analyze several biological signals such as EEG, heart rate variability, postural sway and is also used to distinguish between physiological and pathological conditions (Mizuno et al., 2010) (Protzner et al., 2010) (Takahashi et al., 2010) (Turianikova et al., 2011) (Trunkvalterova et al., 2008) (Jiang et al., 2011).

The purpose of this study was to examine whether the minimum inertia axis would be exploited during internal-external rotations of the shoulder when subjects are

instructed to maintain the rotation of the arm around the humeral long axis (SH-EL), i) at a fast velocity and ii) regardless of handedness. We also investigated whether the effect of different constraints (velocity, sensory conditions, handedness) on arm movement and rotation axis influenced iii) the variability of COP displacements in upright stance. We hypothesized that velocity increase, sensory impoverishment (K), and handedness (nondominant arm) would lead the arm to rotate around a mass distribution axes (SH-CM or $\mathbf{e_3}$) and more particularly around $\mathbf{e_3}$. Specifically, we are interested whether differences in the control strategies between both arms occur during the experimental conditions. Varying the rotation frequency has been previously shown to result in a change of rotational axis so we also verified whether the combination of sensory inputs, kinesthetic only (K) vs. visuo-kinesthetic (VK), improved the extent to which the subjects maintained the rotation of the arm around the instructed rotation axis. In other words we expected the VK inputs to minimize the variability of angular displacements of the instructed axis of rotation, but that K feedbacks should facilitate the rotation around $\mathbf{e_3}$ at fast velocity.

We also hypothesized that the subjects' tendency to rotate their arms around a specific axis would be alike for both elbow angles (i.e.,Elb 90° and Elb140°).

5.2.2 Methods

Subjects: 15 subjects (13 men and 2 women) voluntarily participated in the experiment after signing a statement of informed consent pertaining to the experimental procedure as required by the Helsinki declaration and the EA 4532 local Ethics Committee. Twelve participants were right-handed and 3 left-handed. They were aged 22 (± 3) years and all recruited from the university community. Handedness was determined using the ten-item version of the Edinburgh inventory (Oldfield, 1971). They were free of sensory, perceptual, and motor (shoulder and elbow) disorders. They were naïve about the purpose of the experiment. The kinematic analysis and the computation of the SH-EL, SH-CM, and $\mathbf{e_3}$ vectors were performed as described in Chapter 3.

Procedures:

Participants stood upright on a force plate (BP6001200-1000, AMTI, Watertown USA) and were instructed to produce the external-internal rotation movements with their

dominant and nondominant arm from upward (about 10° behind the vertical) to downward (weakly below horizontal) (see Experiment 1 and Figure 16). The rotational movement consisted of internal-external rotation of the shoulder

In each of the sensory conditions (VK and K), participants were instructed to perform cyclic external-internal rotations of the whole arm with the shoulder abducted to the horizontal and the elbow flexed depending on the elbow angular configuration. The external rotational movement is directed away from the center of body and the internal rotation is directed towards the center of the body.

Handedness related conditions

In each of the conditions described below, the arm movements were performed with the dominant (d) and the nondominant (n-d) arm to allow testing the hypothesis if the performances change due to handedness.

Sensory conditions

In each of the conditions described below, the arm movements were performed with eyes open to allow for both visual and kinesthetic information (VK), and with the eyes closed to provide only kinesthetic information (K). In the VK condition, subjects were instructed to look at their arm during movements in order to visually monitor the internal-external rotational sequence.

Elbow angular configurations

In each of the sensory conditions (VK and K), participants were instructed to perform external-internal rotations of the whole arm with the shoulder abducted to the horizontal and the elbow flexed and actively held at 90° (Elb90°) or in maximal flexion (Elb140° relative to the arm outstretched at the horizontal (see Experiment 1 Figure 17).

Postural data processing

The postural sway was analyzed in both the anterior-posterior (AP) and in the medio-lateral (ML) direction. Multi-scale entropy (MSE) algorithm was used to calculate the complexity and the interaction between the postural sway (A/P & M/L). The MSE algorithm converts the original time series into coarse-grained time series

corresponding to a scale factor. Depending on the number of scales, Sample Entropy is calculated for every coarse-grained time series. The multi scale entropy curve was drawn by plotting the sample entropy of each coarse-grained time series as a function of time scale. The integral of the MSE curve is the complexity index (CI) which allows easy comparison between subjects or groups of subjects. The higher the CI the higher is the stability of a person (Manor et al., 2010); (Jiang et al., 2011) and the lower is the predictably of the postural sway.

Statistical analyses

A multivariate repeated measures analysis of variance (MANOVA, using the GLM module, Statistica 7 software) combining arm dominance (D vs ND) * two arm velocities (Sl vs Fa) * two angular elbow configurations (Elb90° vs Elb140°) and two sensory conditions (V vs VK) was then applied on the variability of angular displacements of each rotational axes (SH-EL, SH-CM, $\mathbf{e_3}$) with a p=.05 level of statistical significance followed by Tukey HSD post hoc comparisons.

To further analyze the influence of rotating arm conditions of the COP displacements an analysis of variance (ANOVA) using the same factors as the MANOVA was then applied on the variability of the CoP displacement with also a p=.05 level of statistical significance and followed by Tukey HSD post hoc comparisons.

5.2.3 Results

General

To analyze the variability of the 3D angular displacements of the rotation axes, we used the framework of the MIR principle and computed rotation axes of the dominant and the nondominant arm. Across all conditions, subjects showed a tendency to rotate their arm around the SH-EL axis compared to the SH-CM and the SH-e_3 axes. In other words, subjects showed no change in rotational axis during the experiment for both the dominant and the nondominant arm.

Handedness related conditions

The variability of the axes displacements (0.24 ± 0.12 rad) around which the dominant arm rotated was not significantly larger than the variability of the axes (0.22 ± 0.11) in the nondominant arm. Moreover, the variability of the SH-EL (0.12 ± 0.05 rad) was significantly ($p < .05$) smaller than the variability of the SH-CM (0.38 ± 0.12) and $\mathbf{e_3}$ (0.39 ± 0.13 rad) for the dominant arm as well as for the nondominant arm (SH-EL 0.12 ± 0.04 rad), SH-CM (0.37 ± 0.09 rad) & $\mathbf{e_3}$ (0.37 ± 0.10 rad)). This result suggests that the axis around which the arm rotated coincided with the SH-EL axis in both dominant and nondominant arms (Table 9, Figure 20 & 21).

Table 9 Angular Variability of the angular displacement of the axes (mean ± sd)

Angular Variability in [rad]				SH-EL	SH-CM	SH-e_3
dominant	90	Open	Slow	0.07 0.02	0.30 ± 0.05	0.30 ± 0.07
			Fast	0.17 ± 0.05	0.47 ± 0.11	0.49 ± 0.12
		Closed	Slow	0.09 ± 0.03	0.29 ± 0.07	0.28 ± 0.08
			Fast	0.17 ± 0.05	0.48 ± 0.11	0.49 ± 0.11
	140	Open	Slow	0.09 ± 0.03	0.17 ± 0.05	0.18 ± 0.05
			Fast	0.14 ± 0.04	0.26 ± 0.06	0.28 ± 0.07
		Closed	Slow	0.09 ± 0.03	0.15 ± 0.05	0.16 ± 0.05
			Fast	0.13 ± 0.04	0.24 ± 0.06	0.26 ± 0.06
non-dominant	90	Open	Slow	0.08 ± 0.02	0.31 ± 0.06	0.30 ± 0.06
			Fast	0.15 ± 0.04	0.45 ± 0.09	0.45 ± 0.10
		Closed	Slow	0.08 ± 0.01	0.28 ± 0.05	0.27 ± 0.05
			Fast	0.15 ± 0.03	0.45 ± 0.09	0.44 ± 0.09
	140	Open	Slow	0.09 ± 0.02	0.14 ± 0.03	0.15 ± 0.03
			Fast	0.12 ± 0.03	0.21 ± 0.03	0.23 ± 0.04
		Closed	Slow	0.10 ± 0.03	0.14 ± 0.05	0.15 ± 0.05
			Fast	0.12 ± 0.02	0.19 ± 0.04	0.21 ± 0.05

Elbow flexion

The variability of the three axes (0.29 ± 0.14 rad) in the Elb90 condition was significantly ($p < .05$) larger than the variability of the axes (0.17 ± 0.07) in the Elb140° configuration. Further investigations showed that this is the case both for the nondominant arm (0.29 ± 0.11 rad) in the Elb90 condition and in the Elb140° (0.15 ± 0.05) configuration and for the dominant arm (0.30 ± 0.10 rad) in the Elb90 condition and in the Elb140 (0.18 ± 0.07) configuration, see Table 9.

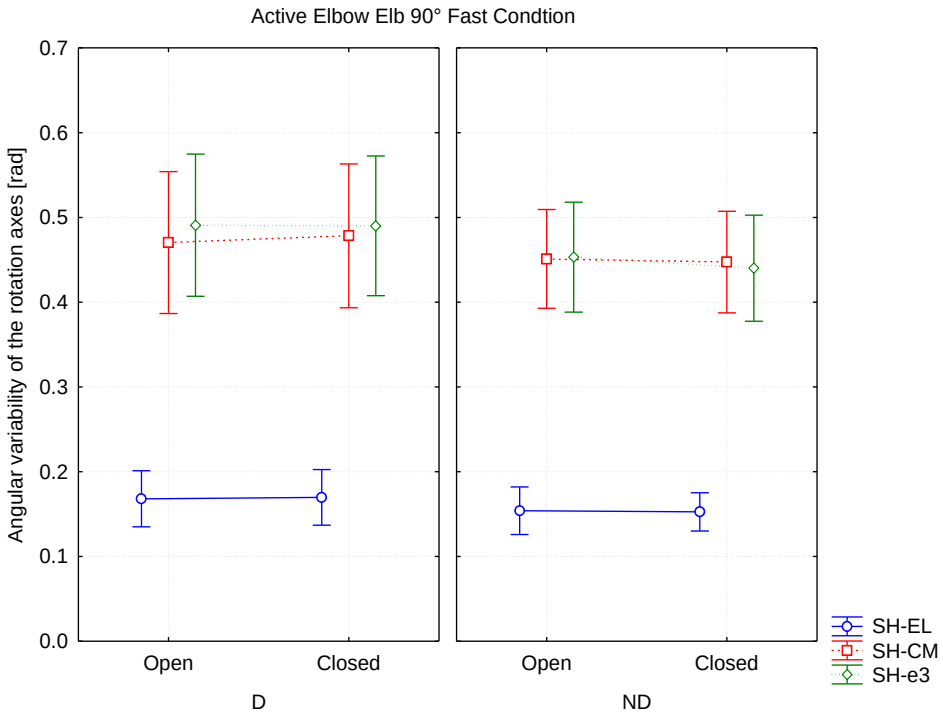

Figure 20 Angular variability of the rotation axes during the active elbow fast condition comparison between dominant and nondominant arm

This result represents the angular separation of both elbow configurations but also shows the lower variability of the SH-EL (0.12 ± 0.05 rad) axis compared to the SH-CM (0.29 ± 0.12 rad) and the SH-e_3 (0.30 ± 0.13 rad) axis for the dominant and the nondominant arm (SH-EL 0.11 ± 0.03 rad ; SH-CM 0.27 ± 0.11 rad ; SH-e_3 0.27 ± 0.11 rad).

Velocity condition

The variability of the axes (0.18 ± 0.09 rad) in the slow condition was significantly ($p < .05$) smaller than the variability of the axes (0.28 ± 0.14) in the fast condition, which is true for the nondominant (Sl 0.18 ± 0.09 rad & Fa 0.26 ± 0.13 rad) and the dominant arm (Sl 0.18 ± 0.09 rad & Fa 0.30 ± 0.15 rad).

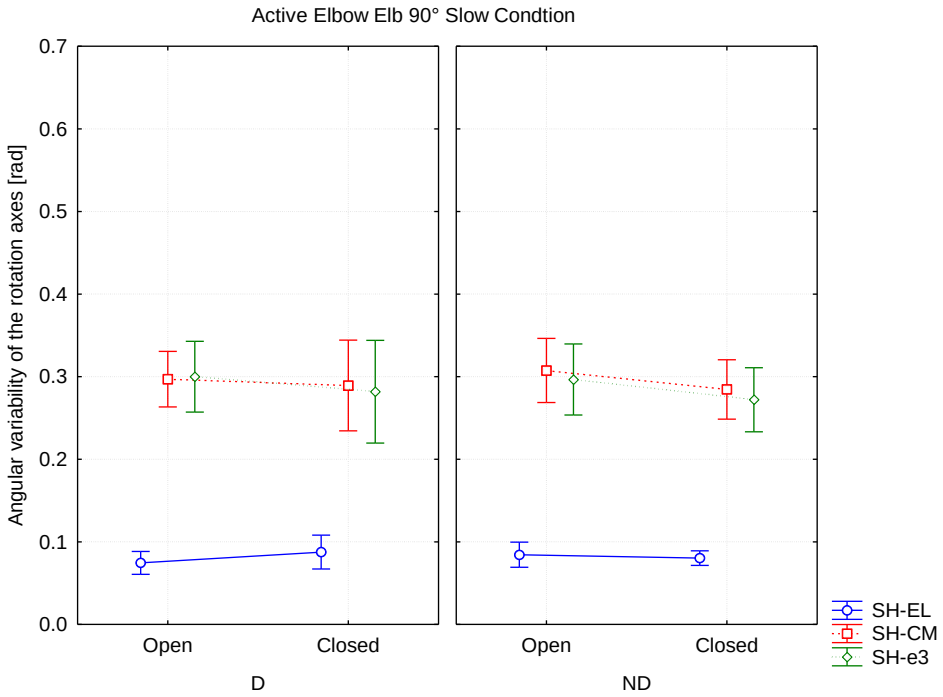

Figure 21 Angular variability of the rotation axes during the active elbow slow condition comparison between dominant and nondominant arm

The analysis shows significant augmentation ($p < .05$) in the variability of the axes in the Fa velocity conditions for both elbow configurations and sensory conditions compared to the Sl condition. These results suggest an increase of the variability of the SH-EL axis at fast velocity in both dominant and nondominant arms (Figure 21&22).

Sensory condition

The variability of the axes (VK 0.23 ± 0.12 rad) in the VK condition shows no differences (K 0.23 ± 0.12) to the K condition neither for the nondominant (K 0.22 ± 0.11 rad & VK (0.22 ± 0.11 rad) nor for the dominant arm (K 0.24 ± 0.13 rad & VK 0.24 ± 0.12 rad).

Likewise, the comparison reveals no differences in the displacement of the SH-EL axis (K 0.11 ± 0.04 rad & VK (0.11 ± 0.04 rad) during both sensory conditions. In contrast the SH-CM (K 0.29 ± 0.11 rad & VK (0.28 ± 0.12 rad) and SH-e_3 (K 0.30 ± 0.12 rad & VK (0.28 ± 0.12 rad) axis show different variations during the sensory conditions ($p < .05$).

Closer investigations did not prove the significant effects of the sensory conditions on the variability ($p < .05$) for the rotational axes in neither the Elb90 conditions nor in the Elb140° conditions. Furthermore, no significant effects of the sensory conditions

could be found for the variability ($p < .05$) of the rotational axes in neither the Elb90 nor the Elb140° conditions. Concluding the analysis, no differences could be found regarding a change in the variability of the axes due to the sensory conditions (see Figure 22 & 23).

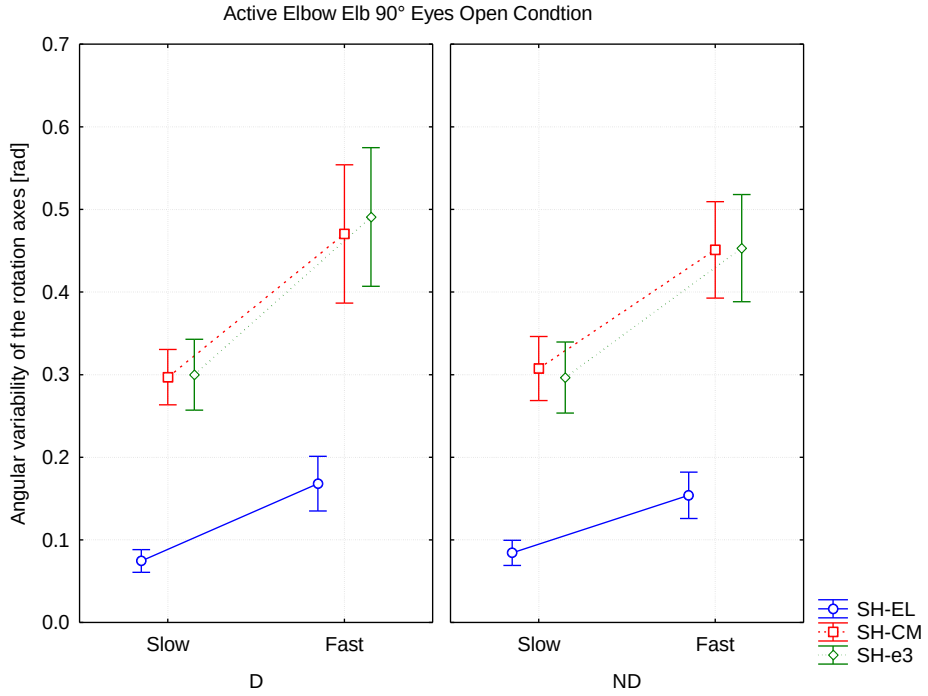

Figure 22 Angular variability of the axes during the active elbow eyes open condition comparison between dominant and nondominant arm

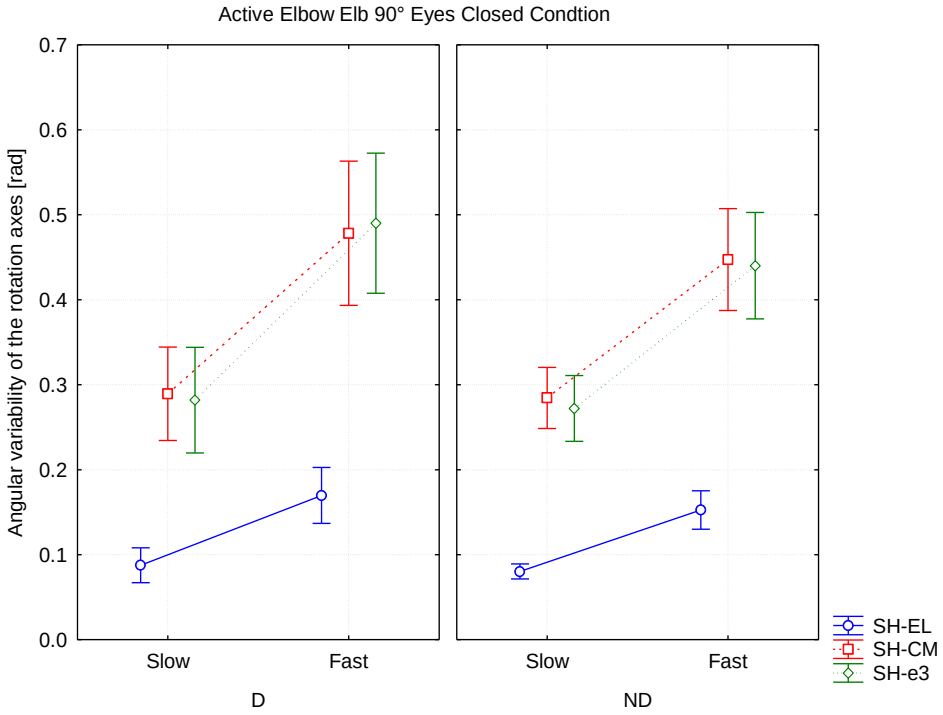

Figure 23 Angular variability of the axes during the active elbow eyes closed condition comparison between dominant and nondominant arm

General Postural Sway Analysis

The postural sway was analyzed twofold. First of all, the CoP movement was analyzed in the medio-lateral (M/L) time series and then in the anterior-posterior (A/P) time series. To analyze the postural variability we computed the complexity index and the Root Mean Square (RMS) for each experimental condition.

An ANOVA combining arm dominance (D vs ND) * two arm velocities (Sl vs Fa) * two angular elbow configurations (Elb90° vs Elb140°) and two sensory conditions (V vs VK) was then applied on the Complexity Indexes of both directions. The A/P direction showed significant main effects for elbow configuration [F(1, 14)=29.928, p<.0001] and for sensory condition [F(1, 14)=7.0015, p<.05], the M/L direction did not show any significant effects.

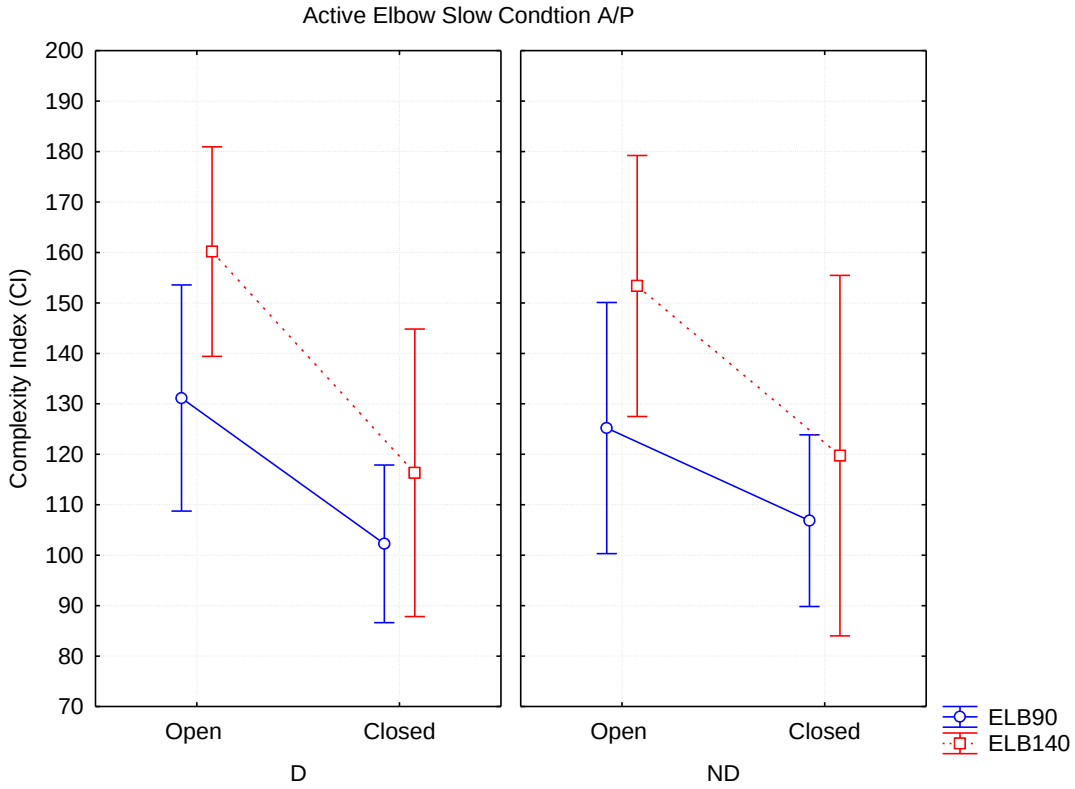

Figure 24 Complexity index of the postural sway in A/P direction during slow arm rotations.

Across all conditions, subjects showed a tendency to increase their CI in the A/P direction during the eyes open conditions. In other words, subjects showed higher postural complexity of the COP movement when performing the rotations with their eyes open A/P CI Op: 142,88 ± 34,29; Cl: 116,27 ± 36,03). Also main effects were discovered due to elbow flexion, A/P CI Elb90°: 121,53 ± 32,20; Cl Elb140°: 137,62 ± 41,61. Higher postural complexity of the COP movement was revealed for the

Elb140° configuration. The findings of the entropic approach are supported by the RMS analysis ($F(1, 14)=5.6545$, $p<.05$) that shows smaller RMS values in the VK condition (RMS A/P Open: 0,40 ± 0,41; Closed: 0,27 ± 0,26 & RMS M/L Open: 0,30 ± 0,11; Closed: 0,15 ± 0,15). Furthermore in the M/L direction a main effect was found for dominance $F(1, 14)=4.6760$, $p<.05$, meaning a lower RMS value for the nondominant arm (RMS M/L D: 0,31 ± 0,32; ND: 0,15 ± 0,13).

5.2.4 Discussion

Regarding handedness, our experimental outcomes do not confirm a different control strategy or differences in the angular variability of the rotation axes throughout all experimental conditions. As such, the original hypothesis was not supported for this experiment. The results do certainly confirm the hypothesis that higher velocity result in higher angular variability of the SH-EL rotation axes throughout all related conditions. Conversely, the findings of the experiment do not confirm a decreased variability of the rotation axis during the multisensory (VK) control of arm movement. In other words, the variability did not increase when the subjects performed the external-internal rotations with their eyes closed.

Handedness conditions

Previous studies have revealed differences between the dominant and the nondominant arm especially during pointing and reaching tasks e.g. greater curvature and large errors in initial direction for the nondominant arm (Przybyla et al., 2012). We did not found the dominant limb hypothesis established by (Sainburg, 2002)and confirmed by (Dounskaia, 2005; Dounskaia et al., 2010) in the control of 3D unconstrained arm movements during external-internal rotations of the shoulder. Changing the sensory input has not lead to a change in rotation axes, neither have the velocity conditions given any proof of different control strategies between the dominant and the nondominant arm. The postural sway analysis, however, shows slightly smaller RMS values for the nondominant arm, which could account for a less well controlled posture during the movement. Subjects may have tried to reduce their whole body movement to focus on the rotation task of the shoulder to avoid possible noise that could influence the goal of the initial task (Todorov and Jordan, 2002). The rotation axes haven’t shown any alterations which could be due to the proposed task.

Velocity conditions

The variability of the rotation axes and, more precisely, of the SH-EL axis showed larger variability during the fast conditions for both the dominant and the nondominant arm, which supports the results reported by (Isableu et al., 2009). Interestingly, the effect of initial positioning of the upper limb to horizontal prevents the velocity-dependent change in rotation axis reported during the experiments by (Isableu et al., 2009), with the dominant arm, and where the subjects initial starting position was not a specified, even though a change toward either a mass or inertia based axis would have led to lower torque values at the shoulder (Isableu et al., 2009). The effect of initial positioning of the upper limb was observed in both dominant and nondominant arm. The biomechanical and dynamical advantage to rotate around $\mathbf{e_3}$, which was thought to become irrepressible at fast velocity in such dynamic nonlinear systems, was not present. Mechanical instabilities arise when rotations are preformed around the SH-EL at a fast velocity, but were not strong enough to produce such changes in axis rotation.

Sensory conditions

Taking into account that that the integration of visuo-kinaesthetic inputs is known to improve the signal-to-noise ratio and, further, to reduce uncertainties in each of the sensory modalities (van Beers et al., 1998; van Beers et al., 1999a; van Beers et al., 1999b; van Beers et al., 1996), we hypothesized that the visuo-kinesthetic (VK) control of arm movements should have led to the reduction of the variability in the angular displacement of the used axis. Subsequently, the kinesthetic (K) control of the arm movements should have increased the probability that the arm's rotational axis changed toward more efficient rotational axes strategies (SH-CM or $\mathbf{e_3}$) at higher velocities, even if the initial starting position was imposed. The results did not confirm either hypothesis.

Interestingly the postural sway analysis reveals higher postural stability during the rotational movements in the visuo-kinesthetic conditions compared to the kinesthetic conditions. The complexity of the COP movement diminishes when subjects performed the task with eyes closed. The reduced RMS values indicate that the variations of the CoP movements are controlled by the subjects freezing the ROM of

the legs and torso slightly to prevent noise that may affect the initial task (Todorov and Jordan, 2002).

Elbow configuration

The variability of the axes did show differences between the displacement of the axes in the Elb90 and the Elb140 conditions. Both angular conditions were precisely chosen to guard constant separations of the axes (SH-EL, SH-CM & SH-e_3). The SH-CM axis was positioned between $\mathbf{e_3}$ and SH-EL at Elb90°, while $\mathbf{e_3}$ was positioned between SH-CM and SH-EL at Elb140°. The results did not show any evidence that modifying the angle between $\mathbf{e_3}$ and SH-CM with respect to the SH-EL axis allowed the arm to rotate around $\mathbf{e_3}$. Results showed no differences in the variability of the axes due to handedness in the Elb140° condition and, thus, did not confirm the hypothesis of a less well controlled nondominant arm during cyclic internal-external rotation movements.

Previous findings from this laboratory have indicated a change of the SH-EL axis to a more efficient rotation axis such as $\mathbf{e_3}$ during conditions involving high velocity profiles. This has led to formulate the MIR (Minimum Inertia Resistance) principle. Taken together, our results indicate that the velocity increase amplified the variability of 3D angular displacements of the rotational axes, but were not sufficient enough to yield a change in the axes around which the whole arm was rotated neither for the dominant nor the nondominant arm. The constraints during the movement, however, should have led to an organization of the rotation around the $\mathbf{e_3}$ axis.

Our results provide evidence that the influence of initial instructions regarding the shoulder-elbow positioning to the horizontal and its maintenance during the trial prevented subjects shifting from a geometrical articular axis at S velocity to a mass or inertia-based axis at the F velocity as previously reported by (Isableu et al., 2009), regardless of the arm used. Also the movement did not involve high precision as reported in multiple studies proposing a dominant limb advantage such as reaching, grasping or pointing (Sainburg, 2002). Furthermore, the cyclic movement character might also play a role as well as the velocity conditions of the task. Further experiments will be necessary to explore whether instructions related to the

minimization of perceived effort for rotating the arm, or simply instructing the subjects to rotate as rapidly as possible with no specific axis being indicated, would result in rotations about $\mathbf{e_3}$. It is possible that a person does not need to detect $\mathbf{e_3}$ in order to rotate the arm about $\mathbf{e_3}$. We assumed that rotations about SH-EL, however, require explicit detection and control about that axis, along with the production of additional muscular torque. Further experiments will be necessary to explore whether increasing the angle between SH-CM and $\mathbf{e_3}$ is a necessary condition to constrain the arm to rotate around an axis closely aligned with $\mathbf{e_3}$.

5.2.5 Conclusion

The results showed that the rotational axis of a multi-articulated limb does not change from an articular axis of rotation to either a mass- or inertia-based axis when instructions corresponding to the articular axis are imposed. This finding was observed for both slow and fast rotations, also for rotations with and without visual cues and for rotations in different angular elbow configurations for both arms. The employed elbow configurations were close to those observed in many athletic configurations and the absence of an invasive mechanical device to alter the mass distribution of the limb reinforces the external validity of our results. These findings extend our understanding of the influence of instructions on how rotation axes are used to organize action, their relevance, and the proficiency that can be expected when coordinating limbs in tasks requiring fast rotations. Our results do not contradict the findings of previous research (e.g., (Isableu et al., 2009), (Bagesteiro and Sainburg, 2002; Sainburg, 2002), but explain the influence of the initial limb configuration and the instructions on the performed movement. Also, no findings could be related to different control strategies due to handedness.

5.2.6 Executive Summary

We examined the role of handedness during unconstrained 3D arm movements. Specifically, we investigated if a velocity-dependent change in rotational axes can be observed for both arms and if the control may obey the principle of minimum inertia resistance (MIR) as shown by (Isableu et al., 2009). Subjects rotated their arms in elbow configurations that yielded a constant separation between the minimum inertia axis ($\mathbf{e_3}$), shoulder-center of mass axis (SH-CM) and the shoulder-elbow axis (SH-EL). The purpose of this study was to test three hypotheses: 1) increasing the motion frequency would result in the limbs' rotational axis to coincide with $\mathbf{e_3}$ in order to minimize rotational resistances; 2) rotations without visual feedback (kinesthetic) would increase the variability of the rotational axes 3) based on the dynamic dominance hypothesis (Sainburg, 2002), the rotation movements are less well controlled for the nondominant arm when the initial instruction favors rotation around the SH-EL axis. Our results showed that the limbs' rotational axis coincide with the SH-EL axis across velocity conditions, although higher variability has been shown at higher motion frequency. Sensory- and handedness-related conditions did not modify the used rotation axis. Even though no change of rotation axis could be uncovered, the arm rotation showed an effect due to handedness on the postural sway variability. Taken together, the results showed that the initial instruction prevented the velocity-dependent, handedness and sensory-dependent change towards the minimum inertia ($\mathbf{e_3}$) and/or the mass axis (SH-CM), i.e., use of the MIR principle.

Study II	Description
Title	Differences in the control of unconstrained 3D arm motions of the dominant and the non-dominant arm
Subjects	15 subjects recruited from the University community
Hypothesis	The non-dominant arm is less well controlled and the MIR principle may overcome the initial instruction maintain the rotation around the SH-EL axis Higher velocities may lead to a change of rotation axis Kinesthetic cues only may lead to controlled rotations around $\mathbf{e}_3$ at fast motion frequency. Visuo-kinesthetic cues should prevent a change of rotation axes due to the visual control of the movement.
Task	Participants stood upright in a perimeter delimited on the floor and were instructed to produce cyclic backwards and forwards rotation movements with their dominant arm from upward to downward in two different angular elbow (90° vs. 140°), two velocity (Slow vs. Fast) and two sensory (Eyes Open vs. Eyes Closed) configurations. The instruction was given, trying to rotate the arm around SH-EL.
Measurement system	Vicon V8i eight M2 camera passive optical motion capture system, frequency 250Hz & AMTI OR-6-1000 force plate to measure the GRF and Moments at 1000Hz
Measured Variables	Displacement of the 13 Markers put on the trunk, arm, forearm and hand
Data Analysis	Filter: Butterworth filter (2nd order) Joint Angle Computation Vector Computation Vector displacement computation Multi-Scale Entropy of the COP movement
Calculated Variables	Variability of angular axes displacement
Statistical Analysis	Repeated measured MANOVA Post hoc test (Tukey HSD)
Results	No differences in the control of the dominant and the non-dominant arm The variability of the angular displacement of the axes augmented with higher movement frequency No differences could be found due to sensory conditions The MSE shows higher complexity values for the dominant arm, associated to larger COP displacements when upper limbs rotation are performed with the non-dominant arm.
Discussion	In contrast to the literature no differences in the variability of the rotation axes were found during the external-internal rotation of the arm. The MIR principle did not overcome the initial instruction but higher variability was observed Kinesthetic or visual kinesthetic cues do not significantly alter the variability of the rotation axes.

5.3 Differences in the control of unconstrained 3D arm motions due to gravitational torque.

5.3.1 Introduction

Getting a cup of coffee from the table or getting it from the overhead shelter are two different things. Gravity does influence the movement of multiple segment limbs and especially the generation of appropriate joint torque including terms arising from dynamic interactions among the moving segments. (Hollerbach and Flash, 1982). (Isableu et al., 2009), (Pagano and Turvey, 1995), (van de Langenberg et al., 2007) showed that a key factor in motor control is the choice of rotation axes around which cyclic external-internal rotational movements of the whole arm are performed. Controlling the multiple degrees of freedom of our upper limbs around specific rotation axis has an influence on both the dynamics and kinematics during 3D movements. This can be shown in the way the various torque components (gravity, muscle and interaction) contribute to produce specific angular acceleration profiles and displacements at a given joint (Hirashima et al., 2003a);(Hirashima et al., 2007b);(Isableu et al., 2009). Almost every arm configurations involving flexion-extension of the elbow, separates the axis of minimal inertia ($\mathbf{e_3}$) (Pagano and Turvey, 1995) , the shoulder-center of mass axis (SH-CM) (van de Langenberg et al., 2008) and the shoulder-elbow axis (SH-EL) of the whole arm (Isableu et al., 2009);(Hirashima et al., 2003a);(Hirashima et al., 2007b). The initially proposed model of unconstrained 3D arm rotations predicts that rotational limb movements would facilitated when they occur around the eigenvectors ($\mathbf{e_i}$) of the inertia tensor ($\mathbf{I_{ij}}$), and specifically around $\mathbf{e_3}$ which is the axis of minimum inertial resistance. Rotations about $\mathbf{e_3}$ have been shown (by inverse dynamic computation) to minimize the contribution of muscle torque to net torque by using the interaction torque to assist motion compared to rotations about the minimum center of mass (SH-CM) or minimum joint (SH-EL) axes (Isableu et al., 2009).The $\mathbf{e_3}$ hypothesis was tested during cyclic external-internal rotations at the shoulder around the horizontal in various conditions of the elbow angles. The result showed that the rotation axis of the arm coincide at fast velocity with a rotation axis that is between SH-CM and $\mathbf{e_3}$, provided that initial instruction did not constrain the shoulder rotation to the horizontal. The objective of this study was to determine whether variations of the

gravity-induced static torque due to different shoulder elevation angles modify the modes of control of cyclic shoulder rotations. Inverse dynamics were computed and the net joint torques, muscular torques, dynamic interaction torques and gravitational torques acting at the elbow and shoulder joint quantified during the movement. Since rotations about SH-EL require the production of larger muscular torques, we hypothesized the arm would rotate about $\mathbf{e_3}$ during fast movements regardless of the variation of the gravity-induced static torque due to different shoulder elevation angles.

The representation of the movement has been shown to depend on the gravitational influence and movement trajectory planning takes into account environmental changes. In other words, the CNS adapts its motor planning with respect to gravitational information and activates internal models optimally adapted to the gravitational environment (Bringoux et al., 2012). (Bennett et al., 1992) showed that small force disturbances could alter the movement when applied to the wrist with an air jet actuator and (Topka et al., 1998) showed that an overshooting when attempting to terminate the movement due to gravitational and dynamic interaction forces. Movements in upward (against gravity) and downward (with gravity) directions provide evidence that gravity is centrally represented in an anticipatory fashion as a driving force during vertical arm movement planning (Papaxanthis et al., 1998). (van de Langenberg et al., 2008), showed during their second experiment an independence of the CM during a pointing movement regardless of the variations of gravity.

However, knowledge of how the rotation movement is executed is lacking. This information is fundamental to investigate the control of the movement. Understanding the relation between the rotation axes, kinematics and kinetics is difficult in multi-joint movements, and a change of rotation axes due to velocity increase (or the maintenance of a rotation axis) regardless of the gravitational setting has, to our knowledge, never been reported. Consequently, the purpose of this study was to examine whether the minimum inertia axis would be advantageously exploited regardless of changes in the gravitational torque influence.

5.3.2 Methods

Subjects: 10 male subjects voluntarily participated in the experiment after signing a statement of informed consent pertaining to the experimental procedure as required by the Helsinki declaration and the EA 4532 local Ethics Committee. Handedness was determined using the ten-item version of the Edinburgh inventory (Oldfield, 1971). They were free of sensory, perceptual, and motor (shoulder and elbow) disorders. They were naïve about the purpose of the experiment.

Procedures

Participants stood upright and were instructed to produce the backwards and forwards rotation movements with their dominant arm from upward (about 10° behind the vertical) to downward (weakly below horizontal) (see Experiment 1 Figure 16). In each condition, participants were instructed to perform cyclic external-internal rotations of the whole arm with the shoulder at different angles and the elbow actively held at a constant 90° angular configuration (Figure 25).

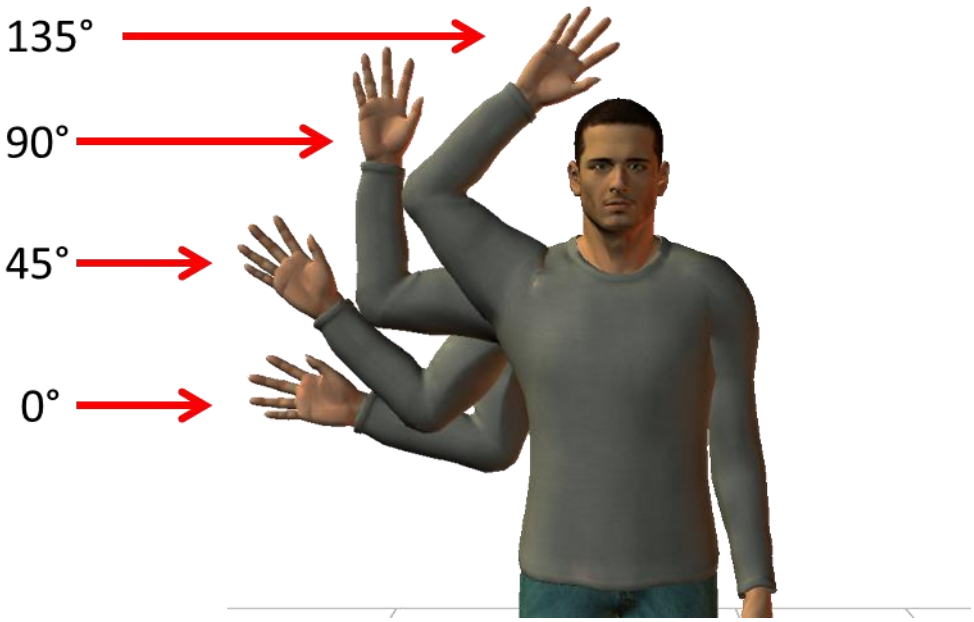

Figure 25 Experimental conditions, from 0° to 135° shoulder elevation

The external rotational movement is directed away from the center of body and the internal rotation is directed towards the center of the body. In the present study we analyzed kinematic and dynamic features of arm rotations in order to understand how

the motor system integrates gravity as an environmental constraint in motor control. We experimentally manipulated the mechanical effects of gravity on the arm while maintaining the mass distribution of the upper-arm and its inertia constant around the shoulder joint.

Sensory conditions

In each of the conditions described below, the arm movements were performed with eyes open to allow visual and kinesthetic information, which should minimize the variability of displacements of the axis of rotation Participants were instructed to perform external-internal rotations of the whole arm with the shoulder abducted a various angles (Figure 25) the elbow flexed and actively held at 90° relative to the arm outstretched at the horizontal (see Figures 16 & 25). The 90° elbow flexion was chosen to constantly separate the rotational axes (Isableu et al., 2009; Isableu et al., 2013).

We experimentally manipulated the gravity components acting on the arm during rotations around the shoulder joint. The participants performed the cyclic external-internal rotations of the whole arm with the shoulder abducted to 135° (above the horizontal), 90° (horizontal), 45° (below the horizontal) and 0° (downward) with the elbow actively held at a constant 90° angle. The subjects performed the rotation around the shoulder joint against (135°) and with gravity (45° and 0°) and the shoulder gravitational torques vary when arm movements are performed within diverse shoulder elevation angles. The overall shoulder torque changes as a function of the shoulder elevation angle due to changing distances from the center of mass of the whole arm to the shoulder joint center. The gravitational influence at the 135° and 45° is reduced to half and in the 0° condition completely reduced, compared to the shoulder abducted to the horizontal (90°) configuration.

Velocity conditions

In all conditions, the roles of SH-CM, $\mathbf{e_3}$ and SH-EL were investigated in slow (S) and fast (F) angular velocities of the arm. In the S velocity condition, participants performed the cycle of internal-external rotation of the arm at a frequency of 0.1 Hz for 60 seconds. In the F velocity condition subjects were instructed to rotate their arm

at a motion frequency of 2 Hz. Each trial lasted 15 s. A timed audio signal was used to fix the frequency of the movement cycle prior to each trial. The audio-signal was stopped before the start of the recording in order to avoid a dual-task.

Experimental sessions

Each subject performed three external-internal rotation sequences in the eight different conditions. This results in a total of 24 trials per subject. The three trials for a given shoulder elevation configuration and frequency condition were presented in succession within a single block, with a 30 s rest period between each trial. The eight conditions were performed in a random order, with a one minute rest period between them.

Prior to the experimental conditions, a training session was completed for each of the two frequency conditions to allow subjects to become familiar with the movement frequencies and the shoulder elevations of 135°, 90°, 45° and 0°.

The learning was visually evaluated by the researcher, with the task being judged as acquired once the participant reproduced 5 successive trials that were synchronized with the signal. Before each of the experimental trials the audio signal was played again to indicate the frequency to be used. Trials were withdrawn and immediately repeated if it appeared to the experimenter that the elbow and shoulder angles (i.e., were not maintained.

5.3.3 Results

The shoulder movement frequency and elbow angles as a function of velocity conditions (S vs. F) are presented in Figure 26. The results showed that movement frequency instructions are well respected. The elbow angle is slightly larger than required. The variability of the 3D angular displacements of the rotation axes in each experimental condition is analyzed in the next section.

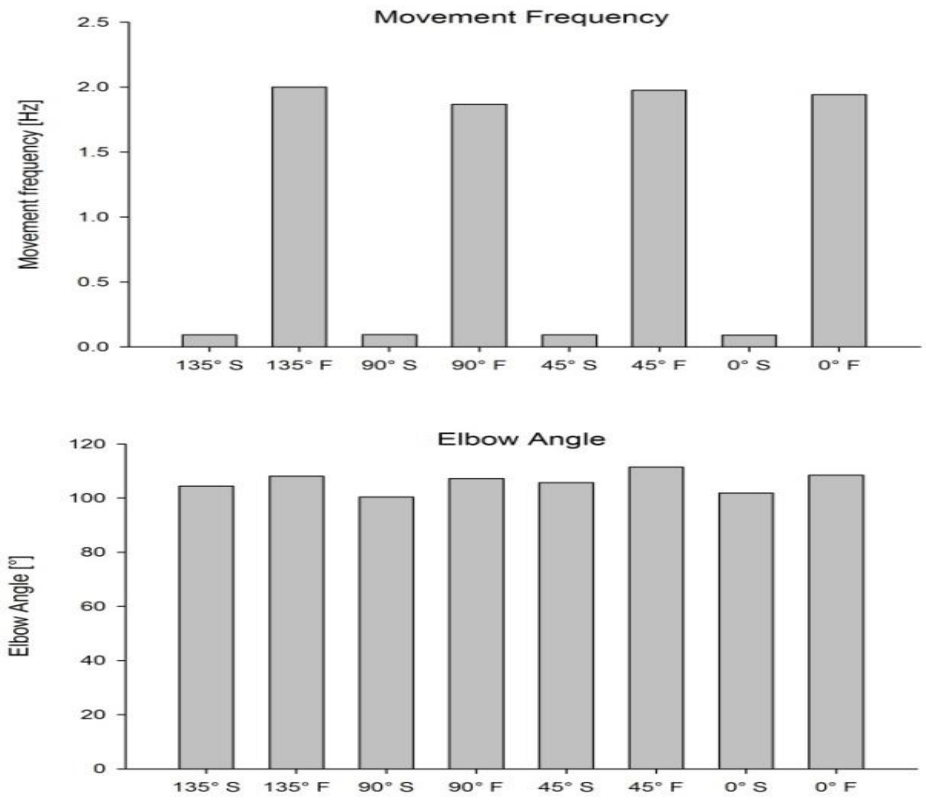

Figure 26 Movement frequency and elbow angle during the eight experimental condition

Statistical analyses

A multivariate repeated measures analysis of variance (MANOVA, using the GLM module, Statistica 7 software) combining arm dominance (135° vs 90° vs 45° vs 0°) * two arm velocities (S vs F) was then applied on the variability of angular displacements of each rotational axes (SH-EL, SH-CM, $\mathbf{e_3}$) with a p=.05 level of statistical significance followed by Tukey HSD post hoc comparisons.

Table 10 MANOVA table

Source	df	df	F
Axes	2	8	67.31***
Height	3	7	5.99*
Velocity	1	9	1.63
Axes x Height	6	4	11.58*
Axes x Velocity	2	8	0.76
Height x Velocity	3	7	0.56
Axes x Height x Velocity	6	4	1.64
* $p < 0.05$, ** $p < 0.01$, *** $p < 0.001$			

Across most conditions, subjects showed a tendency to rotate their arm around the SH-EL axis compared to the SH-CM and the SH-e_3 axes. Only in the 45° fast condition subjects tend to rotate their arm around the SH-CM axis (Table 11).

Table 11 Angular Variability of the angular displacement of the axes (mean ± std)

Angular Variability in [rad]		SH-EL	SH-CM	SH-e_3
135°	Slow	0.12 ± 0.04	0.22 ± 0.06	0.26 ± 0.07
	Fast	0.16 ± 0.06	0.23 ± 0.07	0.27 ± 0.08
90°	Slow	0.11 ± 0.03	0.18 ± 0.05	0.21 ± 0.06
	Fast	0.16 ± 0.06	0.18 ± 0.05	0.21 ± 0.06
45°	Slow	0.16 ± 0.08	0.18 ± 0.08	0.21 ± 0.09
	Fast	0.19 ± 0.06	0.18 ± 0.04	0.20 ± 0.05
0°	Slow	0.16 ± 0.06	0.20 ± 0.12	0.22 ± 0.13
	Fast	0.19 ± 0.06	0.22 ± 0.08	0.25 ± 0.09

Shoulder elevation related conditions

Comparing the angular variability of the rotation axes within the different shoulder elevation conditions a significant main effect was found showing the lowest variability in the 90° configuration (Table 11). The variability of the axes displacements in the 135° condition showed significant differences between the SH-EL axis and the SH-CM and SH-$\mathbf{e_3}$ axes for the slow and fast conditions. In the 90° elbow configuration the variability of the SH-EL axis and the SH-CM and SH-$\mathbf{e_3}$ also significantly differed

in the S conditions. In contrast the variability of the rotation axes in the F conditions do not differ (Figure 27).

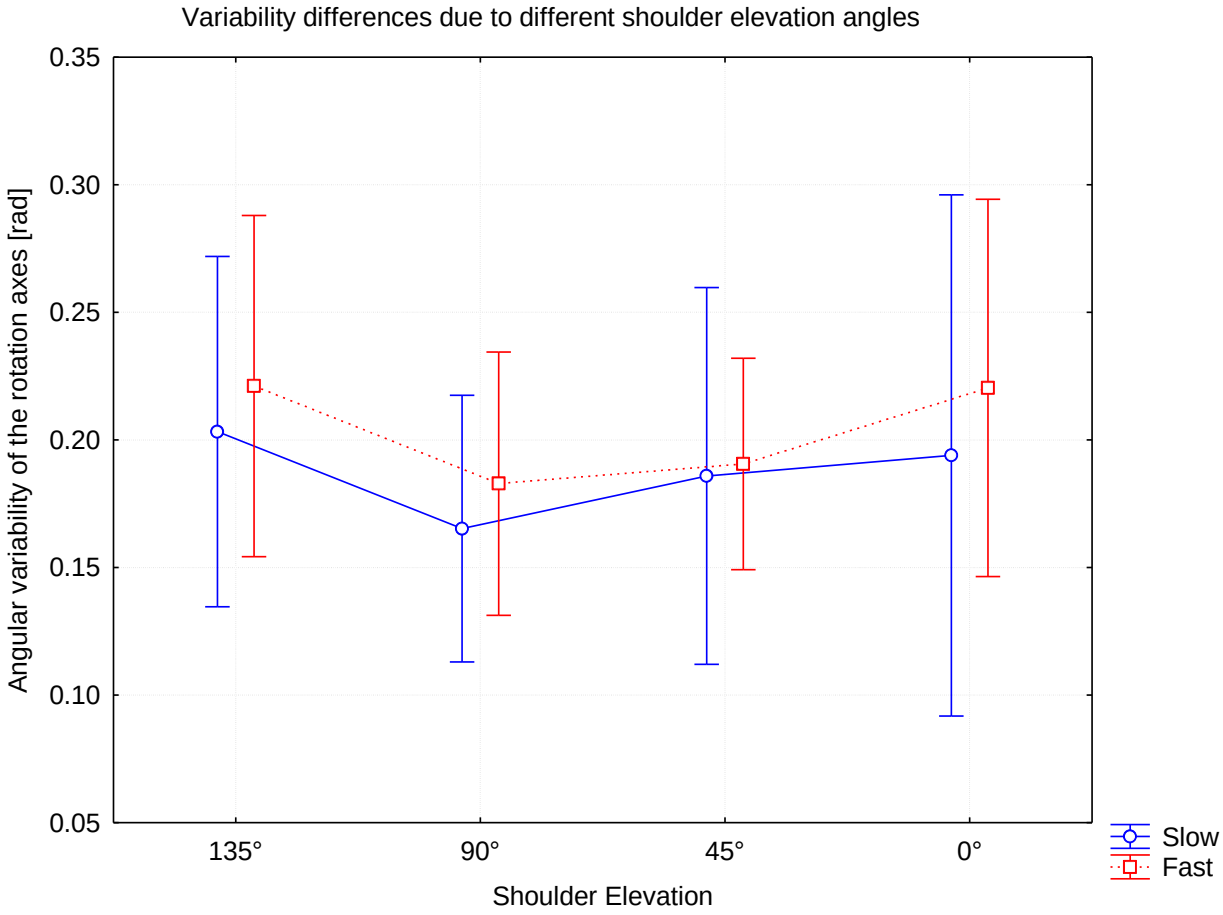

Figure 27 The angular variability of the rotation axes due to the shoulder elevation angles

In the 45° elbow configuration, no differences in the variability of the rotation axes could be observed for neither the S conditions nor for the F conditions. When the shoulder elevation was set to 0°, the variability of the angular displacement of the rotation axes shows no differences between the SH-EL and the SH-CM axes but significant differences between the SH-EL and the SH-$\mathbf{e_3}$ axis. This suggests that the axis around which the arm rotated coincided with the SH-EL axis.

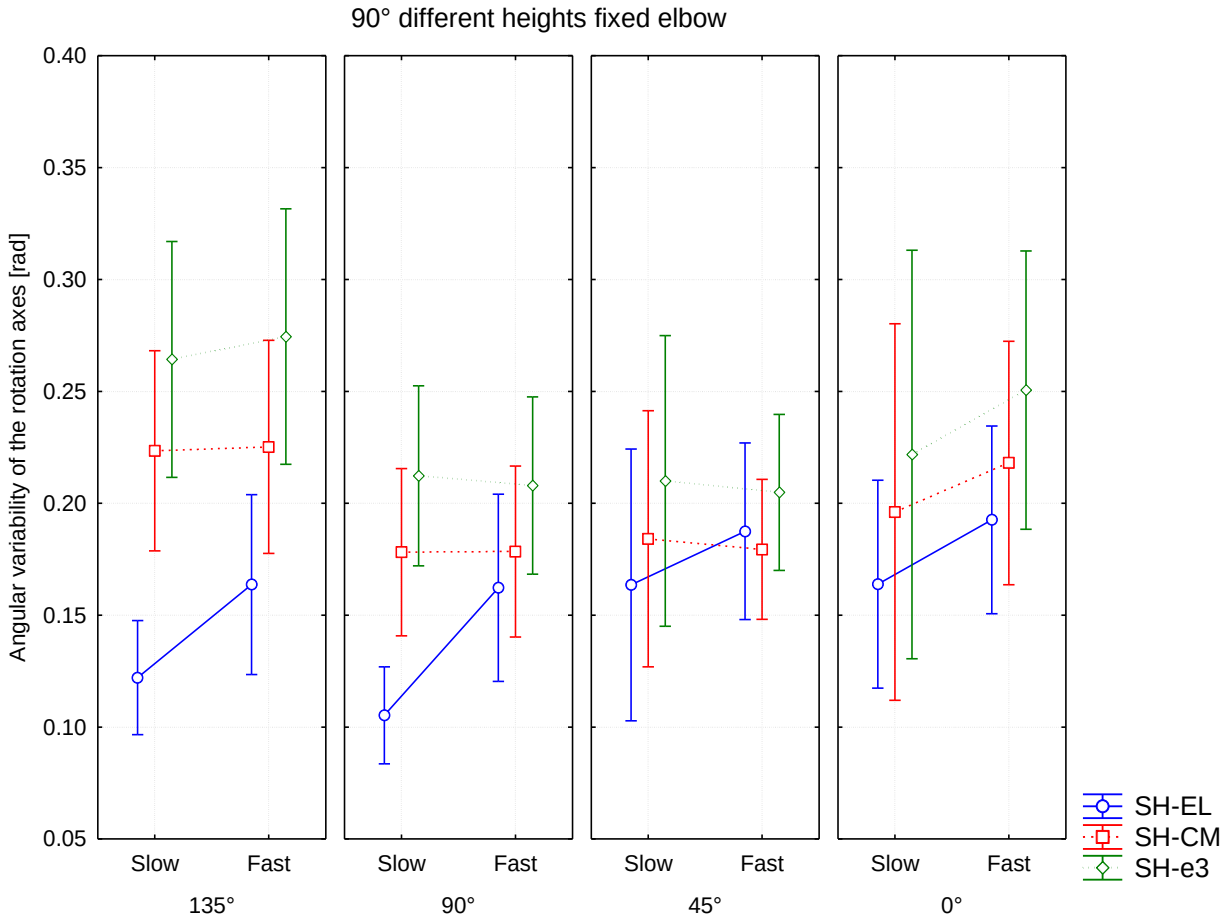

Figure 28 The angular variability of the rotation axes due to the shoulder elevation angles and velocity conditions

Velocity condition

The general variability of the axes in the slow condition showed no differences in comparison to the variability of the axes (0.28 ± 0.14) in the fast condition, which is also true for all shoulder elevation conditions (see Figure 27). Figure 28 shows the amplification of the angular variability of the F conditions compared to the S trials. Nonetheless, the analysis shows one significant increase ($p < .05$) in the variability of the axes in the F velocity conditions in the 90° shoulder elevation compared to the S condition. Even though a general increase of the variability of the SH-EL axis at fast velocity can be observed, only the 90° shoulder elevation condition shows significant changes.

Inter subject variability

The general variability of the axes has not shown any significant differences or even a change of rotation axes. Analyzing the data in more detail, the large variances of the movement patterns may be due to inter individual differences (Figure 29). During the 135° shoulder elevation configuration when working against gravity, subjects 2 and 10 tend to rotate their arms around the SH-CM axis at fast movement frequency. In the slow 90° elbow elevation where the static gravitational is max, one subject (No.4) exploits the SH-CM axis while in the fast conditions four subjects follow this strategy and a velocity-dependent change of rotation axis appeared in favor to SH-CM (no. 3, 5, 7 & 10). Lowering the arm and working with gravity, in total six subjects rotate their arms around the SH-CM axis, four during slow rotation movements (No. 2, 4, 9, 10) and four in fast conditions (No. 2, 5, 7, 10). It can be stated that due to higher velocity, subjects 5 and 7 change the rotation axis. Subjects 2 and 10 exploit the SH-CM axis in both movement velocities. In the last shoulder elevation configuration five subjects tend to rotate around SH-CM. In the slow conditions four subjects (No. 2, 6, 9, 10) exploit the center of mass axis while in the fast conditions subjects 1, 2 & 10 follow the same strategy. Subject 10 maintained rotation around the CM/$\mathbf{e}_3$ axis across velocity and shoulder angle conditions.

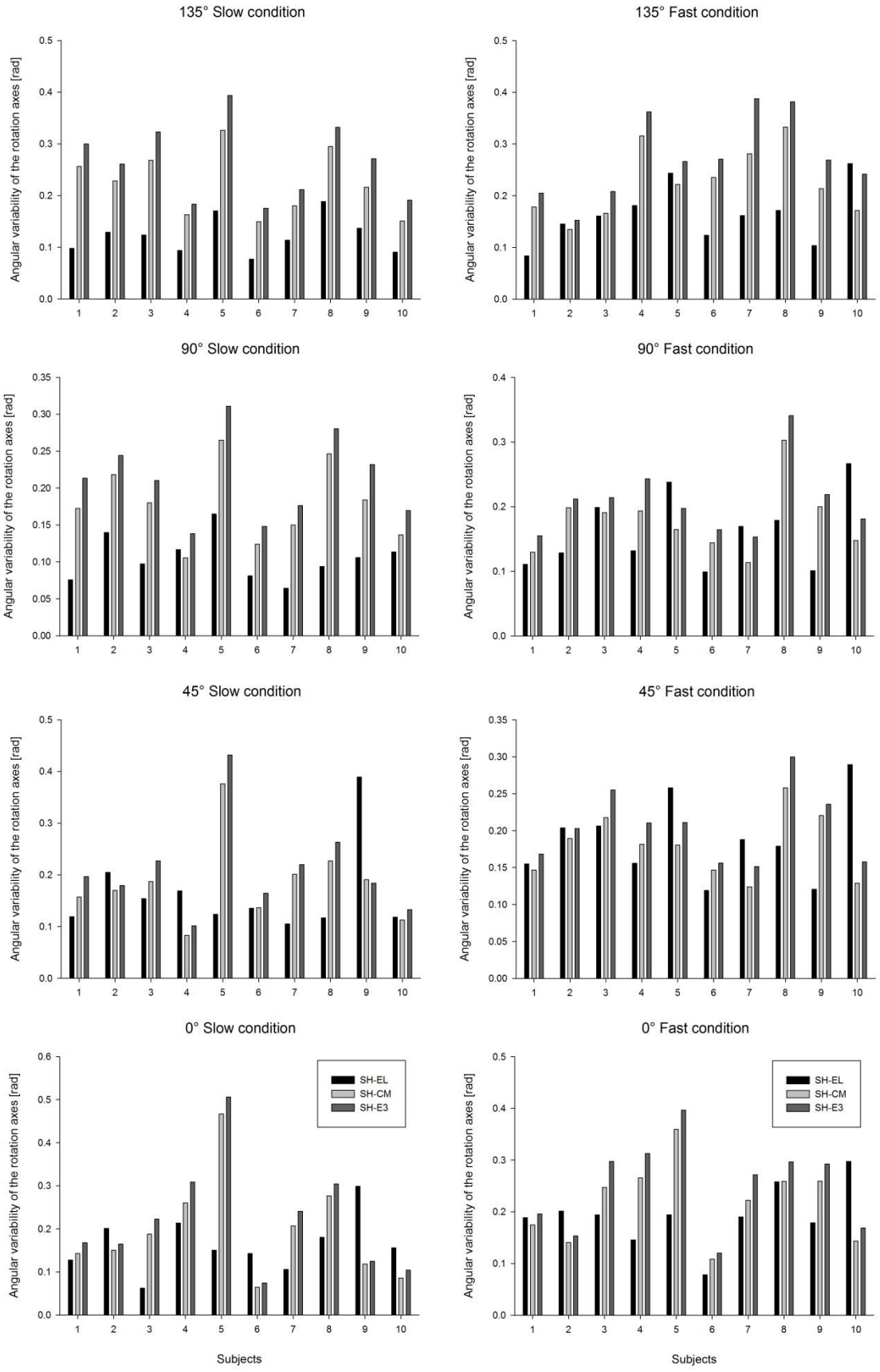

Figure 29 Angular variability of the rotation axes for each subject

5.3.4 Discussion

Regarding the influence of different shoulder elevations on a possible change in rotation axes, our experimental outcomes do not show a global change in control strategy or differences in the angular variability of the rotational axes throughout the experimental conditions. Individual factors played a major role regarding the employed strategies, especially when the elevation angle was lowered.

As such, the original hypothesis was not globally supported for this experiment. The results certainly confirm the hypothesis that higher velocity affects the angular variability of the SH-EL rotation axes throughout conditions but this could only be significantly confirmed in the 90° shoulder elevation condition. The findings of the experiment also confirm different variability of the rotation axes due to the elevation conditions. In other words the variability decreased when the subjects performed the external-internal rotations with at a shoulder elevation angle of 90°. As previously pointed out, close inspection of our data revealed large individual differences regarding which rotational axes were exploited. Our findings show that a spontaneous change of the arm's axis of rotation depends on the individual. Each individual exploits different frames of reference and a change from one frame of reference to another during the movement is possible (Bernardin et al., 2005; Isableu and Vuillerme, 2006; Isableu et al., 2003; Berthoz, 1991; Paillard, 1991; Berthoz, 1991; Bernardin et al., 2005; Bernardin et al., 2005; Isableu and Vuillerme, 2006). Various sensory-motor strategies can exist across subjects (Latash et al., 2002) and multiple modes of spatial referencing controlling reaching tasks (Bernardin et al., 2005; Adamovich et al., 1998) and postural balance (Kluzik et al., 2005; Isableu and Vuillerme, 2006) have been suggested.

Gravity conditions

Previous studies have revealed differences due to gravitational changes especially during pointing and reaching tasks e.g. the shape of velocity profiles movement duration showed transient perturbations initially in microgravity (Papaxanthis et al., 2005). We did not find significantly different strategies in the control of 3D unconstrained arm movements during external-internal rotations of the shoulder. Changing the sensory input has not lead to a change in rotation axes, neither have

the velocity conditions given any proof of the different control strategies between the different shoulder elevation angles. (Pozzo et al., 1998) showed that gravity is represented in the motor command at the planning level as the effect of gravity may initiate or brake arm movements. Three-dimensional arm reaching movements have shown the effect to the central representation of gravity but our experiment has not led to different strategies during the rotation task, when working with or against gravity. Subjects may have tried to reduce their whole body movement to focus on the rotation task of the shoulder to avoid possible noise that could influence the goal of the initial task (Todorov and Jordan, 2002). The rotation axes haven't shown any alterations which may be due to the proposed task.

Velocity conditions

The variability of the rotation axes and more precisely of the SH-EL axis showed larger variability during the fast conditions in all shoulder elevation configurations, which is congruent with results reported by (Isableu et al., 2009; Isableu et al., 2013). During both preceding experiments the variability increased during the shoulder rotations in F velocity. Nonetheless, our results only show a significant variability increase in the 90° shoulder elevation configuration. (Todorov and Jordan, 2002) suggested that the CNS uses a minimal intervention principle in which noise/errors are not corrected if they do not influence the goal of the task, but are quickly corrected if they affect the task. Rotations around the SH-EL axis lead to higher shoulder torque (Isableu et al., 2009) at high motion frequency but in this experiment they were not strong enough to provoke a change of rotation axes. The biomechanical and dynamical advantage to rotate around $\mathbf{e_3}$, which was shown at fast velocity in such dynamic nonlinear systems (Isableu et al., 2009), could not be reproduced and it appears that the rotation axes are confounded. Also the execution of the task itself depends on the subject and its interpretation of the task requirements.

Elbow configuration

The 90° elbow angular condition was chosen to guard a constant separation of the axes (SH-EL, SH-CM & SH-e_3). The SH-CM axis was positioned between $\mathbf{e_3}$ and SH-

EL at Elb90 but no evidence was found that would imply a change of rotation towards a biomechanical and dynamical advantageous rotation axis as $\mathbf{e_3}$.
The initially formulated MIR (Minimum Inertia Resistance) principle that was proposed based on a change of the SH-EL axis to a more efficient rotation axis such as $\mathbf{e_3}$; during conditions involving high velocity profiles could not be confirmed in this experiment.

Our results provide evidence that the influence of gravitational torque was not a constraint that prevented subjects from shifting from a geometrical articular axis at S velocity to a mass- or inertia-based axis at the F velocity as previously reported by (Isableu et al., 2009). The cyclic movement character might also play a role as well as the velocity conditions of the task. As the CNS adapts, its motor planning with respect to gravitational information optimally adapts to the gravitational environment (Bringoux et al., 2012). To effectively explore the influence of gravity on the choice of rotation axes, further experiments will be necessary e.g. in environments with changing gravity such as parabolic flights (Papaxanthis et al., 2005) or zero gravity environments such as space (Lackner and DiZio, 2000), (Papaxanthis et al., 1998) (Pozzo et al., 1998). These conditions allow one to remove the influence of the center of mass while only the inertial cues remain. It is possible that a person does not need to detect $\mathbf{e_3}$ in order to rotate around it. We hypothesized that rotations about SH-EL, require explicit detection and control about that axis, along with the production of additional muscular torque (Isableu et al., 2009). Further experiments will be necessary to explore the MIR principle governs during high velocity movements.

5.3.5 Conclusion

The results showed that the rotational axis of a multi-articulated limb does not change from an articular axis of rotation to either a mass- or inertia-based axis independent of the shoulder elevation angle. This finding was observed for both slow and fast rotations. The employed shoulder configurations were close to those observed in many athletic configurations such as handball throwing. These findings extend our understanding of the influence of shoulder elevation, especially when working with or against gravity. Also, we gain knowledge of how rotation axes are used to organize action and the proficiency that can be expected when coordinating limbs in tasks requiring fast rotations. Our results do not contradict the findings of previous research (e.g., (Isableu et al., 2009), (Isableu et al., 2013),(Garrett et al., 1998; van de Langenberg et al., 2007) but explain the influence of gravitation torque and the shoulder elevation configuration on the performed movement. No findings could be related to different control strategies due to gravity.

5.3.6 Executive Summary

We examined whether the velocity-dependent change in arm rotational axes, in favour to the minimum inertia at fast velocity, remains a robust and efficient control strategy even when the gravity-induced static torque magnitude varied due to different shoulder elevation angles (135°, 90°, 45° & 0°).

We examined if a velocity-dependent change in arm rotational axes, driven by the principle of minimum inertia resistance (MIR) (Isableu et al., 2009) can be observed regardless of the variations of the gravity-induced static torque magnitude provoked by different shoulder elevation angles (135°, 90°, 45° & 0°). Exploiting the minimum inertia axis constitutes an efficient control rule during rotational movements. Subjects rotated their arms in a 90° L-Shape elbow configuration that yielded a constant separation between the minimum inertia axis ($\mathbf{e_3}$), shoulder-centre of mass axis (SH-CM) and the shoulder-elbow axis (SH-EL). To identify the preferentially used rotation axis and its associated dynamic pattern, the angular variability of the rotation axes and inverse dynamics were computed. Taken together, the results showed that the limbs' rotational axis usually coincide with the SH-EL axis across velocity conditions. Variations of the gravity-induced static torque did not generally modify the used rotational axis. However, individual analysis revealed a rotational axis change at fast velocity towards the minimum inertia ($\mathbf{e_3}$) and/or the mass axis (SH-CM) in some subjects, but only for some shoulder elevation angles (135°, 90° & 45°).

Study III	Description
Title	Differences in the control of unconstrained 3D arm motions due to varying gravitational torque
Subjects	10 subjects recruited from the University community
Hypothesis	The rotation axis may depend on the gravitational influence will have an influence on the choice of the rotational axis. Higher velocities may lead to a change of rotation axis
Task	Participants stood upright in a perimeter delimited on the floor and were instructed to produce cyclic backwards and forwards rotation movements with their dominant arm from upward to downward in one angular elbow (90°), two velocity (Slow vs. Fast) and four different shoulder elevation (135°, 90°, 45°,0°) configurations. no instruction was given about rotation axis
Measurement system	Vicon V8i eight M2 camera passive optical motion capture system, frequency 250Hz
Measured Variables	Displacement of the 13 Markers put on the trunk, arm, forearm and hand
Data Analysis	Filter: Butterworth filter (2nd order) Joint Angle Computation Vector Computation Vector displacement computation
Calculated Variables	Angular Axes displacement
Statistical Analysis	Repeated measured MANOVA ANOVA (velocity) Post hoc test (Tukey HSD post hoc test)
Results	Change of rotational axis during the high movement velocity and 90° shoulder elevation The variability of the angular displacement of the axes augmented with higher movement frequency
Discussion	In contrast to earlier findings the MIR principle did not apply to systematically. The angular variability of the rotation axes has been shown to increase with motion frequency, which is congruent with earlier finding. However the gravitational influence has not shown a general effect on the control of the rotation movement which could be due to a lack of experimental constraints.

Chapter 6

6 Effect of precision demands: maximizing precision in athletic skills

The sixth chapter is devoted to the effect of maximizing precision during dart throwing tasks on the role of the minimum inertia resistance principle. The presented experiments in this chapter are structured with an introduction to explain the research question, followed by a short methods section, the results and a discussion.

6.1. Precision throwing tasks and the control of unconstrained 3D arm motions

6.1.1. Introduction

Darts is a popular sport with professional structures spread as a bar sport. The aim of the game is to throw darts on a board and the score depends on its final position. This task requires good eye-hand coordination and accuracy and consistency are important. The final position depends on the combination of throwing technique, direction, release height and speed as well as the moment when the fingers lose contact with the dart. The whole dart throwing movement is redundant because an infinite number of combinations of these variables will lead to exactly the same final position of the dart on the board (Smeets et al., 2002). This phenomenon is very interesting because control strategies may vary between subjects. It has been well documented that novice dart throwers show larger performance (endpoint) variability compared to experts.

Even though different throwing techniques and styles may appear between subjects, the final position inter alia depends on the moment when the fingers lose contact with the dart. Previous studies have been conducted to measure or estimate the time of release (ToR) of the darts (Smeets et al., 2002), (Hansen et al., 2012b) during the throwing task. The ToR could be used to identify if subjects try to stabilize specific rotation axes, joint configurations or even dynamic parameters (Tamei et al., 2011). Previous studies (Pagano and Turvey, 1995);(Pagano et al., 1996b);(Garrett et al., 1998);(Bernardin et al., 2005);(van de Langenberg et al., 2007; van de Langenberg et al., 2008) ; (Isableu et al., 2009) proposed a minimum inertia resistance (MIR) principle that movements will occur about the eigenvectors ($\mathbf{e}_i$) of the inertia tensor

($\mathbf{I_{ij}}$), specifically $\mathbf{e_3}$ (the axis of minimum inertial resistance). It has been shown that rotations about $\mathbf{e_3}$ minimize the contribution of muscle torque to net torque by using the interaction torque to assist motion compared to rotations about the center of mass (SH-CM) or joint (SH-EL) axes (Isableu et al., 2009). Based on this model, there is almost always a separation between the axis of minimal inertia ($\mathbf{e_3}$) (Pagano & Turvey, 1995), the shoulder-center of mass axis (SH-CM) (van de Langenberg et al., 2008) and the shoulder-elbow axis (SH-EL) of the whole arm (Isableu et al., 2009); (Hirashima et al., 2003a; Hirashima et al., 2007b). In other words, the throwing motion can be performed while fixing one of the aforementioned axes and the choice of axis has implications on the amount of torque that must be produced. As Smeets et al. (2002) showed, the throwing motion has a specific pattern and the hand follows a quasi-circular path with non-constant speed, also the throwing time is very short (<150 ms) and cannot be adjusted on the basis of proprioceptive information (Cordo et al., 1995). During regular dart throwing, where the arm is in a ninety degrees angle to the trunk or horizontal to the floor the gravitational influence is maximal. The influence is divided in half when the arms position is changed to either forty five or hundred thirty five degrees. Taking this into account, the control strategies of the subjects may change when they are asked to throw at very high and very low dartboards or in other terms against or in gravity direction respectively. Similar results were reported during an interception task (Cesqui et al., 2013). Moreover, the precision and success of the throwing task also depends on the distance to the target. To investigate the influence on the performance the target distance was also increased to force the subjects to amplify the throwing effort. Considering the ToR and the decomposed torques during throwing, the question arises how the throwing patterns are organized and what control strategies subjects may have. This question is the focus of the present study, in which we analyzed the control strategies of eight subjects in the framework of the MIR principle. Two hypotheses were postulated. The first hypothesis was that throwing is controlled by fixing the $\mathbf{e_3}$ axis to minimize the contribution of muscle torque to net torque and by using the interaction torque to assist the motion as shown by (Tamei et al., 2011);(Hirashima et al., 2008);(Hore et al., 2011). The second hypothesis was that the control strategies, including the torque contribution, alter when the target's position and distance are changed.

6.1.2. Methods

Eight male subjects (age of 24 ± 2) took part in the present research and were recruited from the university community. All subjects were novice darts players and voluntarily participated in the experiment after signing a statement of informed consent pertaining to the experimental procedure as required by the Helsinki declaration and the EA 4532 local Ethics Committee. They were free of sensory, perceptual, and motor (shoulder and elbow) disorders. They were naïve about the purpose of the experiment.

Procedures:

According to the World Darts Federation rules the horizontal distance between the front of the board and any part of the shoes was at least 2.37 m, and the center of the board (the bull) was 1.73 m above the floor.

The height of the dartboard was manipulated and additionally set to 2.46m and 1m. 2.46m was the highest possible position in the research facility to set up the dart board and reducing the original height by 0.73m resulted in a lowest board height of 1m. Within these constraints, subjects were free to choose their posture when throwing. The low target height was chosen to evaluate the throwing pattern when throwing in the gravitation direction, while throwing against the gravitation direction was initiated by setting the dart board at a height of 2.46m. Also the distance was augmented to 2.87m, resulting in two distances with three target heights respectively (Figure 30). The increased distance should lead to higher velocity profiles causing different control strategies and torque patterns.

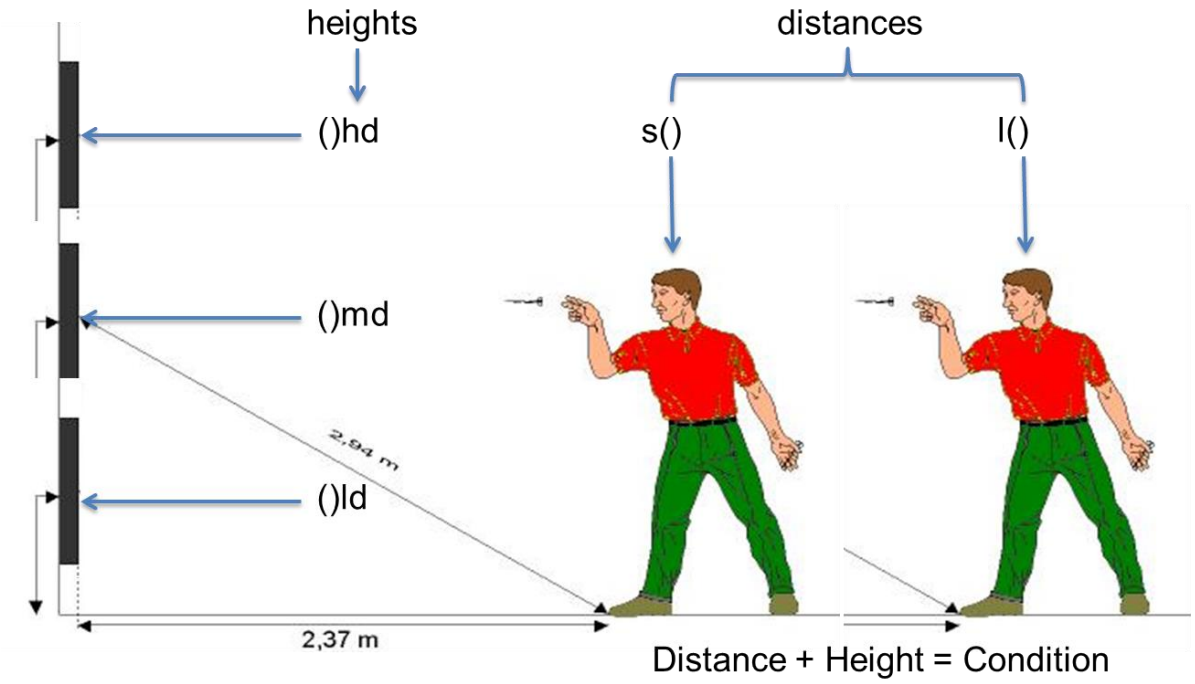

Figure 30 Experimental setup

To conclude two distances (s = 2.37m; l = 2.87m) were tested with three dart board heights (l = 1m; m = 1.73m; h = 2.43m). Throughout the remainder of this text, the six conditions will be described using the acronyms lld, lmd, lhd, smd, lmd and lhd where e.g. smd stands for the close distance of 2.37m (s) and the medium target height 1.73m (m) (see Figure 30).

In contrast to normal dart practice, subjects were asked to repeatedly aim for the bull. The dart players performed the task with the same darts (18gr.) and no manipulation or instruction was given on how the task should be performed. The throwing posture and technique should not vary (Edwards and Waterhouse, 2009) throughout the trials. Following a 10 minute warm-up, each subject was instructed to perform 10 dart throws at the indicated dartboard. No further constraints were given and subjects were allowed the amount of time that they wanted to execute the throwing motion.

The kinematic and dynamic analysis as well as the computation of the SH-EL, SH-CM, and $\mathbf{e}_3$ vectors were performed as described in Chapter 3.

Time of release (ToR)

In order to evaluate the ToR subjects wore a small FSR (Force Sensor Resistor) on their Index finger to measure the precise moment of release. The FSR was synchronized via an Analogue board of the Vicon V8i system (Hansen et al., 2012b).

Data reduction

The data, all trials were aligned on the ToR and the analyses were performed over the whole throwing trial. In other words, the data was analyzed over the whole throwing period of 250ms. The data was aligned to the ToR, i.e. 150ms before and 100ms after its occurrence.

Statistical analyses

A multivariate repeated measures analysis of variance (MANOVA, using the GLM module, Statistica 7 software) combining two distances (s vs l) * three target heights (low vs medium vs high) was then applied on the variability of angular displacements of each rotational axes (SH-EL, SH-CM, $\mathbf{e_3}$) with a .05 level of statistical significance.

6.1.3. Results

The means of each variable were determined for each condition and subject and the data was analyzed using either multivariate analysis of variance (MANOVA) or univariate analysis of variance (ANOVA), followed by Tukey HSD post hoc comparisons.

Before investigating the rotational axes associated with the throwing condition, the relative performance scores (the score hit on the dartboard) were determined. Across subjects, no consistent differences in the performance were uncovered [$F(5, 395)=2.1576$, $p>.05$]. However, the performance seems to decrease when the distance of the target is greater (see Figure 31).

Overall, our observation was that across throws, the most difficult condition was aiming at the high target in the long distance but this could not be reliably quantified for all subjects.

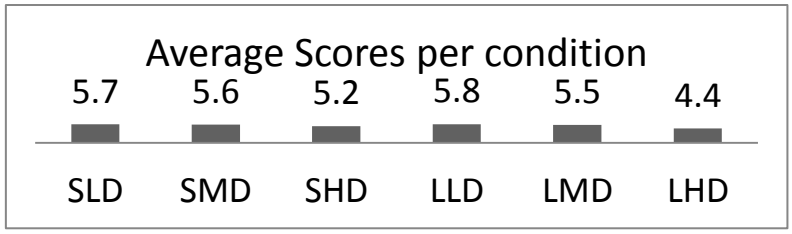

Figure 31 Average scores of the subjects throwing performance

Kinematics of the shoulder joint

Understanding the control patterns due to the different conditions may come from the knowledge of the joint kinematics.

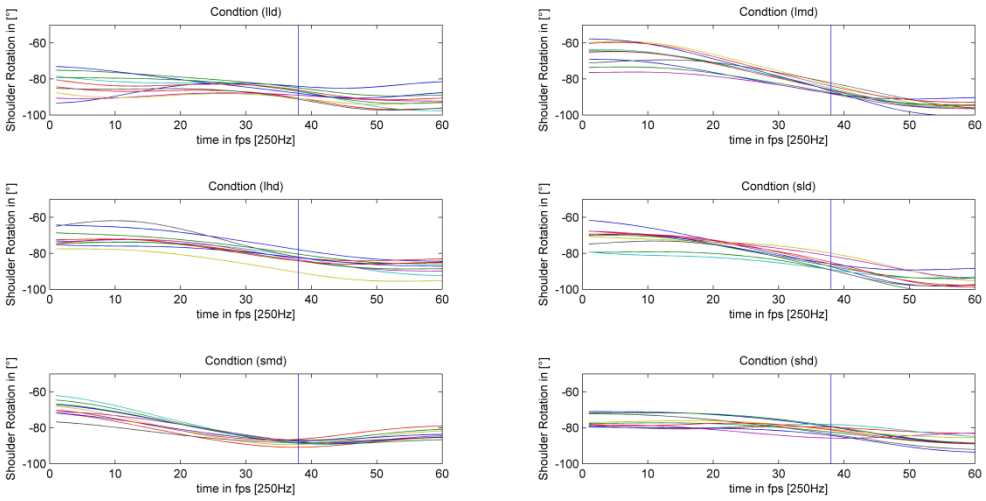

Figure 32 shows the axial shoulder rotation kinematic parameters of 10 representative throws made by subject 8 aligned on the moment of darts release indicated by the vertical line.

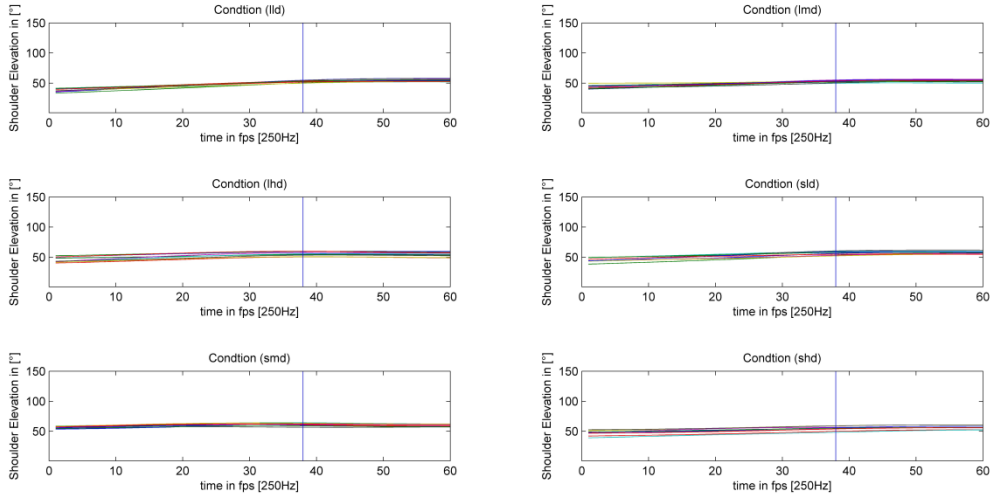

Figure 33 shows the shoulder elevation kinematic parameters of 10 representative throws made by subject 8 aligned on the moment of darts release indicated by the vertical line.

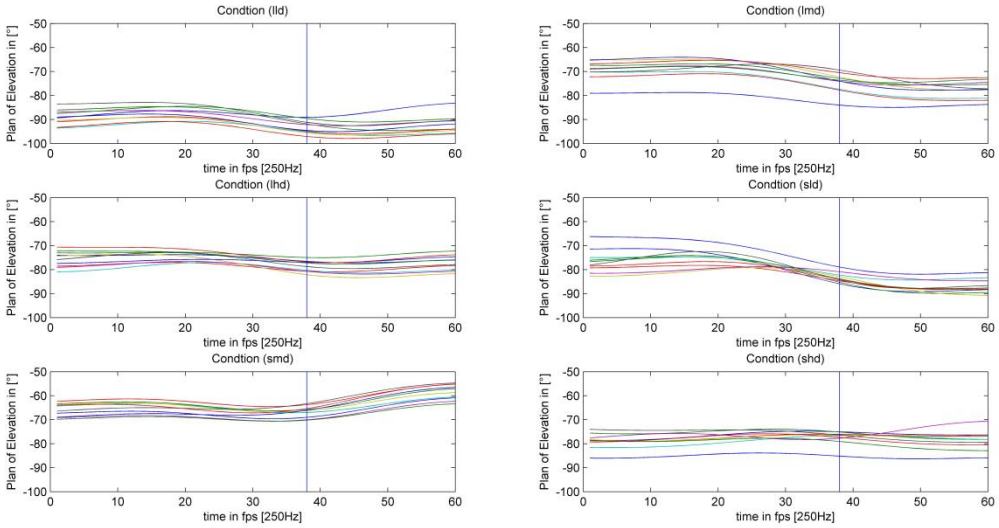

Figure 34 shows the plan of elevation kinematic parameters of 10 representative throws made by subject 8 aligned on the moment of darts release indicated by the vertical line.

The shoulder plan of elevation [*F(5, 35)=1.3541,* p>.05] and the shoulder elevation [*F(5, 35)=.67150,* p>.05] do not show different patterns when comparing the maximal angular amplitude of the six throwing conditions (Figure 33 & 34). The kinematic patterns of the shoulder remain constant throughout the conditions. However the axial shoulder rotation [*F(5, 35)=3.1415*, p<.05] shows differences due to the throwing height and especially the axial rotation the angular amplitude is significantly

larger in the smd condition compared to the sld and shd conditions (p<.05) (Figure 32).

Kinematics of extension of the elbow joint

Understanding the control patterns due to the different conditions may come from the knowledge of the joint kinematics.

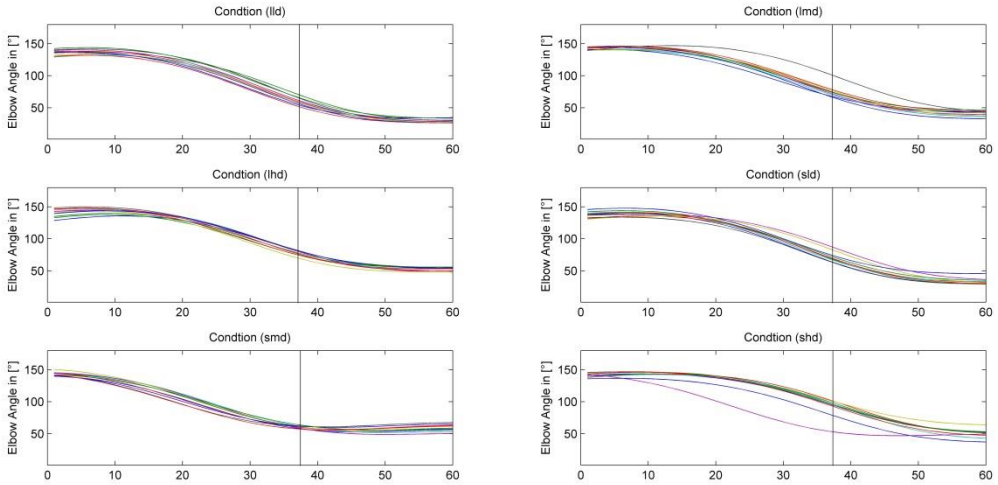

Figure 35 shows the elbow kinematic parameters of 10 representative throws made by subject 8 aligned on the moment of darts release indicated by the vertical line.

The elbow extension angles do not show different patterns when comparing the conditions and the amplitude of elbow extension remain constant (Figure 35). No significant differences could be uncovered for the mean/max elbow extension amplitude using a one-way ANOVA (Mean Amplitude (averaged) [F(5, 35) = 1.0412, p>.05] Max Amplitude [*F*(5, 35) =1.6888, p>.05] nor for the mean/max hand velocities Mean Velocity [*F*(5, 35) =.76538, p>.05] nor for the Max Velocity [*F*(5, 35)) =1.2005, p>.05]. However, the vertical hand position at ToR differ due to the conditions [*F*(5, 35)=7.92, p<.05] and the differences are illustrated in Figure 36.

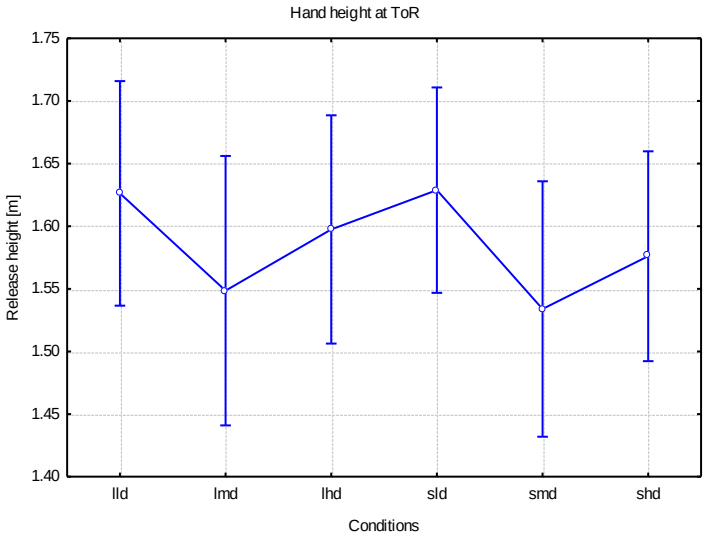

Figure 36 Mean hand heights at ToR during the six throwing conditions

Tukey HSD post hoc tests revealed significant differences between the short and the long throwing distances ($p<.05$) as well as between the three throwing heights ($p<.05$) for each distance.

Throws and torque generation

The results described so far showed no differences in the amplitude of the kinematics even though six different targets combinations were used. The shoulder angles have been shown to be quite indifferent. Therefore, the following analyses will focus on the elbow joint. It could be argued that the throwing patterns do not vary regarding time-space parameters and the kinematics, but that differences may be hidden in the dynamic parameters of the throws (Debicki et al., 2010);(Debicki et al., 2004). Furthermore, it is of interest to determine whether the relation between the rotational axes and the decomposed torque signatures also applies in the more complex situations where the target position and distance changes. As the movement is mainly performed by the elbow joint, a prediction from the hypothesis is that the decomposed torque at the elbow will vary due to the throwing conditions because of the target heights and distances. To test this prediction, elbow dynamics were computed using inverse dynamics. The computed elbow torques for the representative subject is shown in Figure 37 as a function of time.

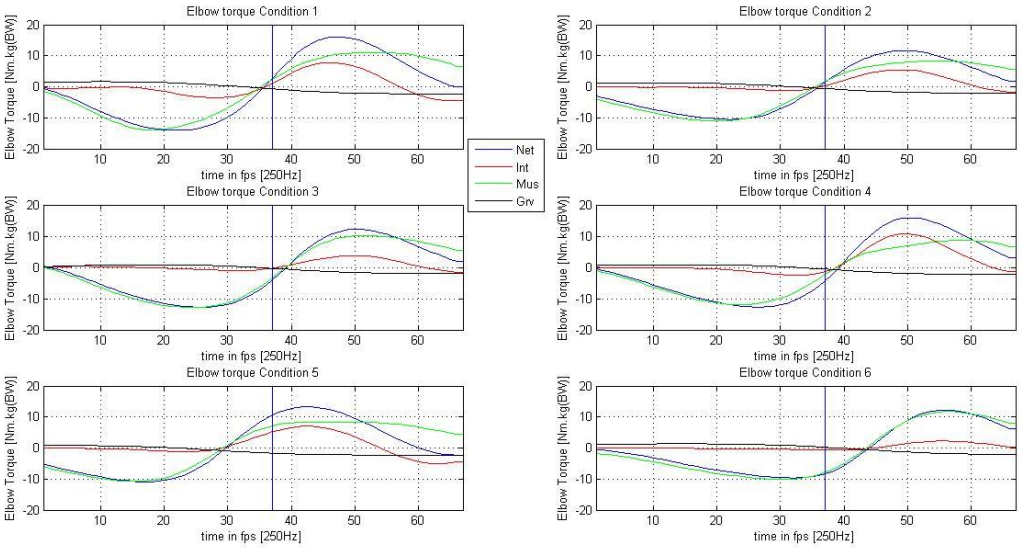

Figure 37 Decomposed torque at the elbow joint. The trials are aligned on the ToR, indicated by the vertical black line.

The relative contributions of MUS and INT to NET were quantified as INT impulses over movement time was divided by the absolute impulse of NET to yield a contribution index of INT to NET in each trial similar for the contribution index of MUS to NET (Yamasaki, 2008).

One-way ANOVAS for the relative contributions of MUS and INT to NET torque were quantified but did not reveal differences between the conditions neither for MUS/NET [$F(5, 35)=.94808$, $p>.05$] nor the INT/NET [$F(5, 35)=.29217$, $p>.05$] contribution index.

Rotational Axes

To analyze the variability of the 3D angular displacements of the rotational axes, we used the framework of the MIR principle and computed rotational axes of the arm that were affected by the experimental conditions.

Table 12 Angular variability of the rotation axes during the six throwing conditions.

Angular variability in [rad]	SH-EL	SH-CM	SH-e_3
sld	0.21± 0.13	0.39 ± 0.37	0.47 ± 0.54
smd	0.15 ± 0.04	0.30 ± 0.16	0.33 ± 0.18
shd	0.18 ± 0.10	0.32 ± 0.23	0.38 ± 0.25
lld	0.24 ± 0.09	0.47 ± 0.53	0.49 ± 0.53
lmd	0.14 ± 0.07	0.28 ± 0.12	0.31 ± 0.13
lhd	0.17 ± 0.09	0.30 ± 0.23	0.33 ± 0.24

Across all conditions, subjects showed a tendency to fix the SH-EL axis during the throw compared to the SH-CM and the SH-e_3 axes (Table 12). In other words, subjects showed no change in rotational axis used during the experiment.

Table 13 MANOVA table

Source	df	df	F
Axes	2	14	8.24*
Condition	5	35	0.87
Axes x Conditions	10	70	0.20

* $p < 0.05$

The variability of the SH-EL axis significantly differs from the variability of the SH-CM and e_3 axes (Table 13). Moreover no significant differences could be uncovered due to the distance and height conditions on the variability of the SH-EL and the SH-CM and e_3 axes (p <.05) respectively (Figure 38).

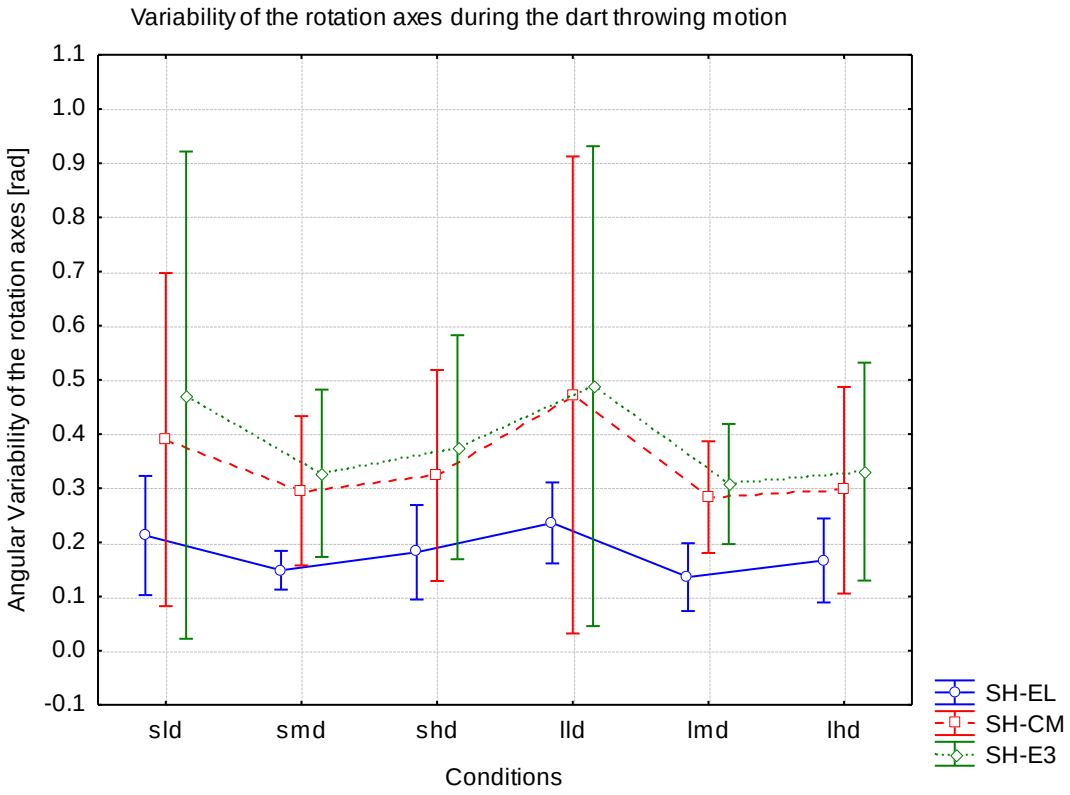

Figure 38 Angular variability of the rotation axes during the six throwing conditions

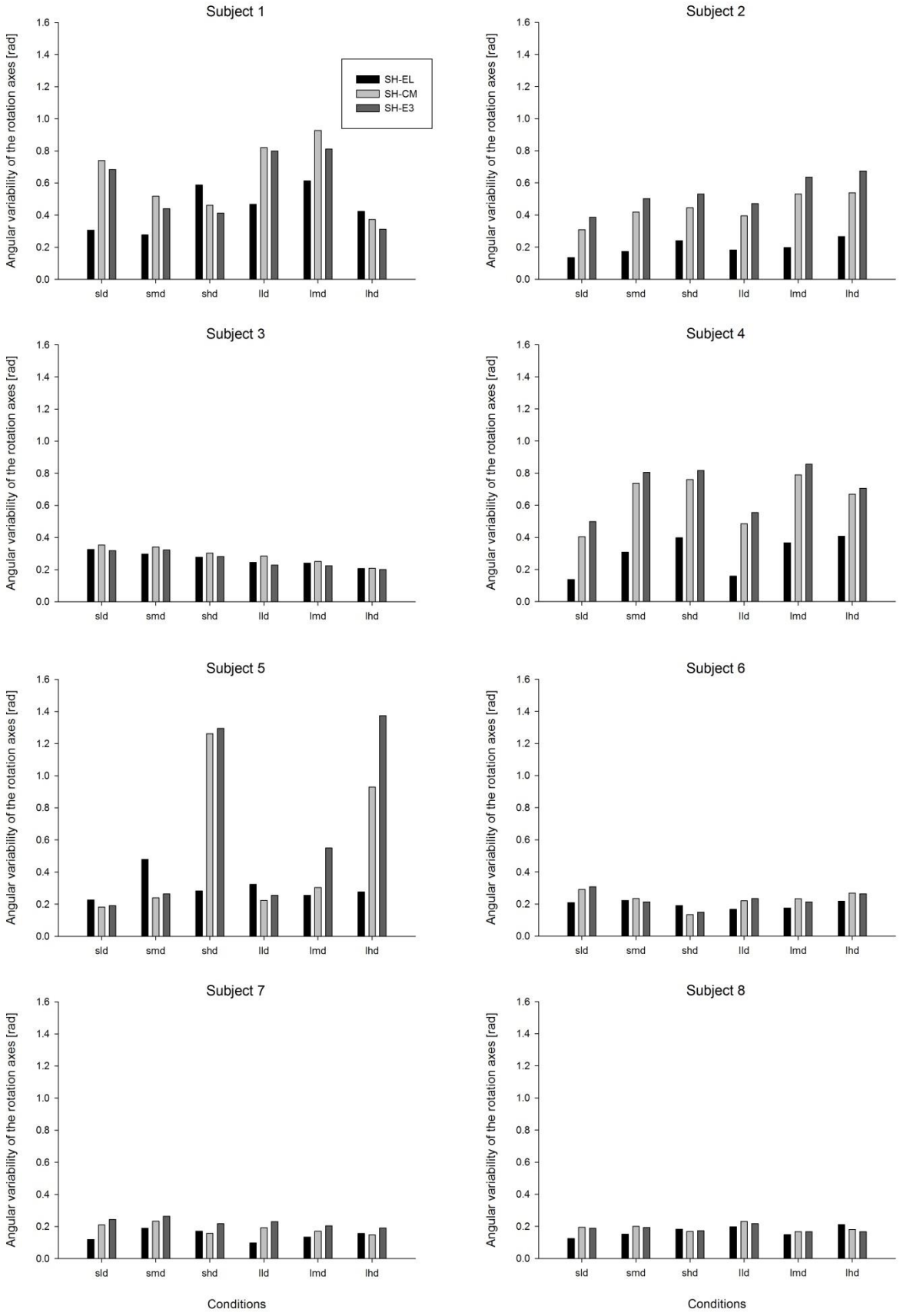

Figure 39 Individual angular variability of the rotation axes during the six throwing conditions

Further analysis of the angular variability on an individual basis shows that during certain conditions a change of rotation axes occurs (Figure 39). Subject 6 for example exploits on average the SH-e_3 axis during the shd condition. Nonetheless it has to be stated, that no different control strategies can be uncovered when comparing the individual subjects. Thus, subjects tend to fix the SH-EL axis to control the dart throwing motion regardless the target height or distance. However, some subjects show very small differences between the variability of the axes thus, it can be pointed out that some subjects do not stabilize one specific axis (see Subject 1).

6.1.4. General discussion

How does the CNS identify relevant rotation axes that allow motor coordination to be adaptive and proficient in precision throwing task? Concerning the results of dart throwing this experimental results showed that subjects choose individual control strategies that may be affected and changed due to changing conditions and constraints.

However, novice subjects tend not to take dynamics into account when performing the throwing task. Even though the proprioceptive role of the inertia tensor ($\mathbf{I}_{ij}$) and its advantages in terms of the instantaneous state and representation of the limb's disposition (Pagano and Turvey, 1995) has been subject of various experiments (Isableu et al., 2009; Isableu et al., 2013) dart throwing may not be as important in terms of actively produced forces as shoulder rotations. Regarding the outcome of our experimental conditions different control strategies or differences in the angular variability of the rotation axes could be uncovered throughout subjects and experimental conditions. The results confirm that some subjects change their strategies during conditions.

Target heights

Previous studies have revealed differences in the performance comparing different throwing distances. The target height though has not been reported to change the control strategy during precision throwing tasks. Our results do not confirm a general change of rotation axis due to the target heights but the variability changes over conditions (Figure 38). It seems that throwing on the medium dart board, results in lower angular variability of the rotational axes. This raises the question if subjects that

have been used to throwing darts on a regular dart board or throwing against or with gravity direction changes the control strategy. It could be claimed that throwing at different heights leads to less well controlled posture and technique during the throwing motion.

Target distance

The variability of the rotation axes and more precisely of the SH-EL axis did not show larger variability during the longer throwing distance conditions. The throwing scores were not different when comparing the short and the long distance,s which is contradictory to the findings of (Edwards and Waterhouse, 2009), but may be due to the small differences of 0.5m. Even though the angular variability of the rotation axes and performance score variability do not confirm distance-related changes, difference could be uncovered for the throwing speed and the maximal torque values generated by the subjects.

In contrast to findings from this laboratory that have indicated a change of the SH-EL axis to a more efficient rotation axis such as $\mathbf{e_3}$, during conditions involving high velocity profiles the dart throwing task did not show a consistent change of rotation axes for all subjects. However, subjects showed that different target heights may influence the choice of the rotation axes to possibly generate higher angular velocities to successfully hit the dart on the high board, regardless of the throwing distance.

Our results provide evidence that the influences of target heights are more relevant to the choice of motor control strategy then the throwing distance. Changing the target heights and forcing the subjects to throw in and against gravity direction changed the angular variability of the rotation axes, of the rotation shoulder angle and also led to changes in the exploited rotation axes (e.g. from Subject 6 from the SH-EL in the sld condition to a SH-CM/$\mathbf{e_3}$ axis in the shd condition). Also the movement did not involve high velocity as reported in multiple studies proposing a shift in rotation axes (Isableu et al., 2009);(Isableu et al., 2013). Further experiments will be necessary to explore whether movements involving high precision and high velocity profiles with no specific axis being indicated, would yield in a change towards $\mathbf{e_3}$.

6.1.5. Conclusion

The results showed that the rotational axis of a multi-articulated limb does not generally change from an articular axis of rotation to either a mass- or inertia-based axis during a precision throwing task with different target heights and distances. Individual strategies of subjects however have shown that a change of rotational axes occurs with target height (e.g. Subject 6). This was observed for both throwing distances. The employed long distance was close to original distance, which could explain why no observable differences were found. In contrast to the distances, target height led to individual strategies involving variability of the rotation axes. These findings extend our understanding of the influence of target heights on how rotation axes are used to organize action, their relevance, and the proficiency that can be expected when coordinating limbs in tasks requiring precision. The results do not contradict the findings of previous research (e.g., (Isableu et al., 2009), (Edwards and Waterhouse, 2009), but explain the influence of target heights and distances on the performed movement.

6.1.6. Executive Summary

We examined the role of target height and distance during unconstrained 3D precision throwing movements. Specifically, we investigated if subjects stabilize rotational axes to steady the throwing motion and if the control of the principle of minimum inertia resistance (MIR) as shown by (Isableu et al., 2009) could play a role during the throwing task. Subjects threw darts at dartboards at three different heights and two different distances. The general darts throwing movement is performed using mostly the elbow joint and during the throwing motion, separations between the minimum inertia axis ($\mathbf{e_3}$), shoulder-center of mass axis (SH-CM) and the shoulder-elbow axis (SH-EL) could be observed. The purpose of this study was to test two hypotheses: 1) subjects may follow specific strategies such as stabilizing rotational axes in a precision throwing task, and 2) changing the target heights and distances may lead to a change in their motor control strategy. Our global results showed that the limbs' rotational axis coincide with the SH-EL axis across conditions. Nonetheless although the variability of the SH-EL changes with constraints, throwing against or with gravitational acceleration did not modify the exploited rotation axis. Taken together, the results showed that inter individual differences covered global effects and prevented the generalization of the used rotational axis that was used in each condition. Individual changes from the SH-EL towards the minimum inertia ($\mathbf{e_3}$) and/or the mass axis (SH-CM), i.e., use of the MIR principle could be observed.

Study IV	Description
Title	Differences in the control of dart throwing motion in novices due to different target heights and distances
Subjects	8 subjects recruited from the University community
Hypothesis	Changing the distance and height of the target will change the performance A change of rotation axis occurs due to different heights and target distance
Task	Participants stood upright on a marked line and performed 10 throws in two distances and three target heights respectively.
Measurement system	Vicon V8i eight M2 camera passive optical motion capture system, frequency 250Hz
Measured Variables	Displacement of the 13 Markers put on the trunk, arm, forearm and hand Scores on the dart board
Data Analysis	Filter: Butterworth filter (2nd order) Joint Angle Computation Vector Computation Vector displacement computation Torque Time of Release
Calculated Variables	Angular Axes displacement Performance Scores Torque
Statistical Analysis	Repeated measured MANOVA ANOVA Post hoc test (Tukey HSD)
Results	Subject specific control strategies and throwing signatures
Discussion	Based on the different control strategies and among the different parameters (kinematic or dynamic) analyzed, it can be considered, that subjects simply tend to stabilize their elbow during the throw. Even though the different target heights vary the gravitational influence, no changes could be uncovered in the rotation axis used. The same has to be stated for the different target distances.

6.2. Differences between experts and novices in the control of unconstrained 3D throwing motions Darts Novices vs. Experts

6.2.1. Introduction

Experience and training are often key factors for succeeding in sportive tasks. Based on the performance, each person implements individual strategies (in intercepting see (Cesqui et al., 2012)) that optimize their possible outcome. Besides the differences in strategies used between novices and experts, various studies (Wagner et al., 2010) have shown differences between the two groups in terms of performance, kinematics, kinetics, muscles activity and even injuries.

Taking the example of darts, the aim of the game is to throw darts on a board and the score depends on its final position. Also, the success of the throwing depends on the combination of throwing technique, direction, release height and speed. However, the almost infinite number of combinations of these variables shapes various motor equivalent solutions that lead to exactly the same final position of the dart on the board (Smeets et al., 2002). This phenomenon is very interesting because redundancy in control strategies may vary between novices and experts and optimal robust solutions should be observed in the latter group. Earlier studies have been conducted to identify control strategies due to target distances and the effect of fatigue (Edwards and Waterhouse, 2009).

Isableu et al. (2009) proposed a minimum inertia resistance (MIR) principle that rotational movements will occur about the eigenvectors ($\mathbf{e_i}$) of the inertia tensor ($\mathbf{I_{ij}}$), specifically $\mathbf{e_3}$ (the axis of minimum inertial resistance). It has been shown that rotations about $\mathbf{e_3}$ minimize the contribution of muscle torque to net torque by using the interaction torque to assist motion compared to rotations about the center of mass (SH-CM) or joint (SH-EL) axes (Isableu et al., 2009). During reaching task, subject move their arm in a multi articulated manner, meaning that the moment of inertia is controlled. Elbow flexion implies that there is almost always a separation between the axis of minimal inertia ($\mathbf{e_3}$), the shoulder-center of mass axis (SH-CM) (van de Langenberg et al., 2008) and the shoulder-elbow axis (SH-EL) of the whole arm (Isableu et al., 2009); (Hirashima et al., 2007b), (Hirashima et al., 2007a). In other words, the throwing motion can be performed while fixing one of the

aforementioned axes and the choice of axis has both kinematic and kinetic implications that may have mechanical influence on the variability of (dart release) the task. It has been hypothesized (Isableu et al., 2009; Isableu et al., 2013) that rotating around $\mathbf{e_3}$ could be skill dependent and novices may not take advantage of the kinetic benefits. It is well known that elite athletes have higher performance in perception, planning, and execution in sports activities relative to novices so the question arises if both groups exploit different control strategies.

Performance differences in shooting and throwing have led to different theories how unskilled subjects may compensate their lack of skill and general learning theories fortify the observed differences. Knowledge of how the throwing movement is executed is unknown and information if certain rotation axes are fixed because they optimally minimize mechanical instabilities due to passive torque at dart release is severely lacking although fundamental to investigate the motion.

Understanding the relation between the rotational axes, the kinematics and kinetics is difficult in multi-joint movements, and quantifying the rotational axes during a precision throwing task has, to our knowledge, never been reported before. The purpose of this study was to examine whether the minimum inertia axis would be exploited during the dart throwing movement and if differences in the control of the movement are due to the level of expertise of the thrower. We examined the variations in dart-throwing performance with novice and high performance athletes under regular conditions in the laboratory using optical motion capture to quantify the throwing motion.

6.2.2. Methods

Eight male novice subjects (age of 24 ± 2) took part in the present research and were recruited from the university community. 13 expert male dart players (age of 34 ± 10) were recruited at the French Open of Darts. All subjects voluntarily participated in the experiment after signing a statement of informed consent pertaining to the experimental procedure as required by the Helsinki declaration and the EA 4532 local Ethics Committee. They were free of sensory, perceptual, and motor (shoulder and elbow) disorders and naïve about the purpose of the experiment.

Procedures:

According to the World Darts Federation rules the horizontal distance between the front of the board and any part of the shoes was at least 2.37 m, and the center of the board (the bull) was 1.73 m above the floor. In contrast to the common darts games, the subjects were asked to repeatedly aim for the bull. The novice dart players performed the task with the same darts (18gr.) and no manipulation or instruction was given on how the task should be performed. The throwing posture and technique though should not vary (Edwards and Waterhouse, 2009) throughout the trials. The athletes on the other hand played with their personal darts to avoid perturbations in their performance due to manipulated darts.

Following a 10 minute warm-up, each subject was instructed to perform 10 dart throws at a dartboard positioned at a wall. No further constraints were given and subjects were allowed the time that they wanted to execute the throwing motion.

The kinematic and dynamic analyses as well as the computation of the SH-EL, SH-CM, and $\mathbf{e_3}$ vectors were performed as described in Chapter 3. Due to the sensitivity of the athletes, only one marker was attached to the hand which hinders a detailed kinematic and dynamic analysis, so the analysis focuses on the elbow and the shoulder joint.

Torque prediction

Throwing a darts on a dartboard was simulated using the above mentioned method and it was previously shown (Isableu et al., 2009) that fixing the rotation around the minimum inertia resistance axis $\mathbf{e_3}$ led to lower Net torque values during the throwing motion of the elbow and the shoulder.

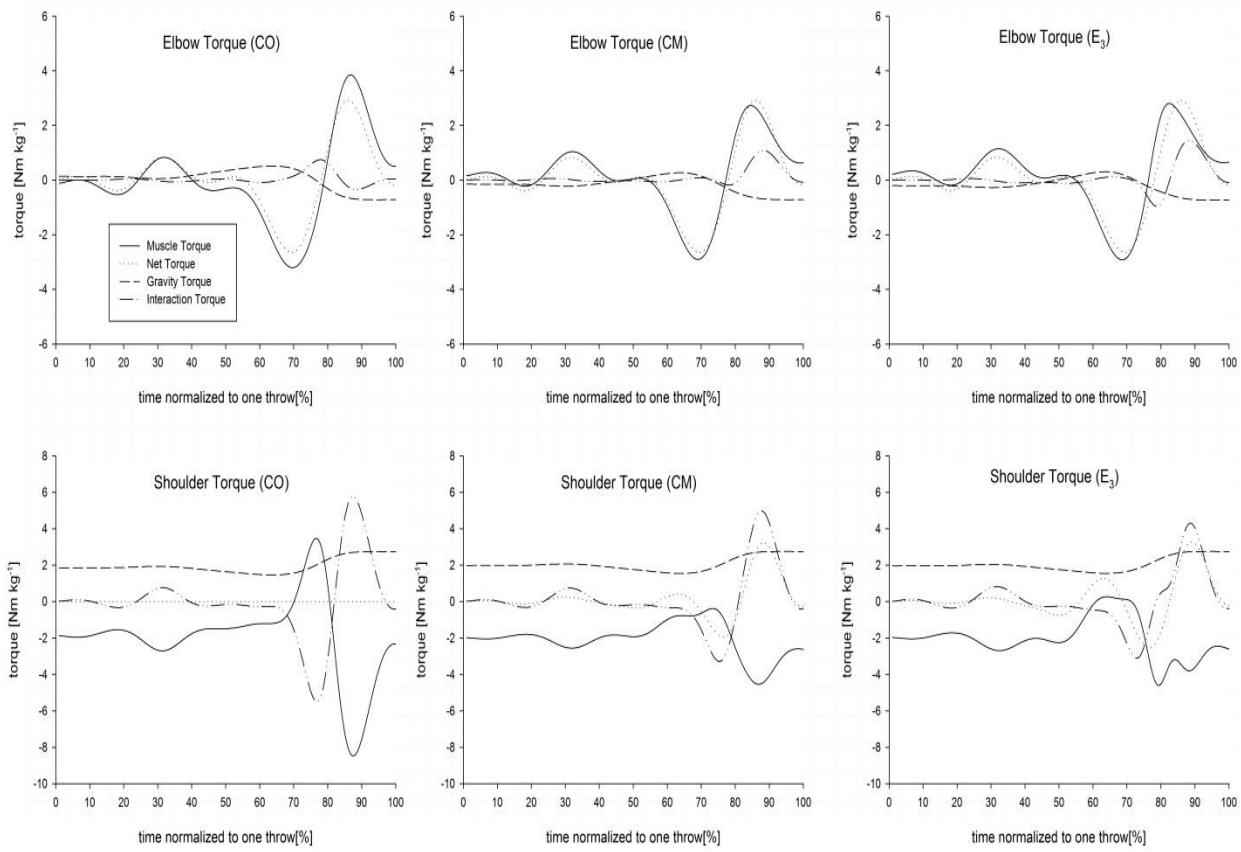

Figure 40 Torque predictions of a dart throwing movement while stabilizing the SH-EL, SH-CM and the SH-e_3 axis

Therefore fixing one of the above axes will result in different torque distributions and the dynamic efficiency depends on the control strategy and the rotation axis (Figure 40).

Data reduction

The darts throwing motion can be divided in four phases. The first phase is the aiming phase, which is followed by a backward move also called “take back” (Tamei et al., 2011) of the hand to prepare for the acceleration phase. During the acceleration phase the release occurs and the follow through phase takes place. The time of release has been subject of previous research (Smeets et al., 2002); (Hansen et al., 2012b) but unfortunately when working with athletes, manipulation of the fingers or the dart will lead to performance differences. The throwing motion was declared as finished when the elbow extension angle reached its maximum.

Statistical analyses

A multivariate repeated measures analysis of variance (MANOVA, using the GLM module, Statistica 7 software) combining two groups (Experts vs. Novices) was then applied on the variability of angular displacements of each rotational axes (SH-EL, SH-CM, $\mathbf{e_3}$) with a .05 level of statistical significance followed by Tukey HSD post hoc comparisons. To further analyze the differences between both groups, an analyses of variance (ANOVA) using the same factors as the MANOVA was then applied on the variability of the joint kinematics and dynamics with also a p=.05 level of statistical significance and followed by Tukey HSD post hoc comparisons.

6.2.3. Results

Kinematics

One-way ANOVAs were performed to quantify kinematic differences between the groups using the shoulder joint and elbow angles [F(1, 7=0.41168, p>.05]. The angular velocity [F(1, 7)=0.13148, p>.05] and acceleration [F(1, 7)=0.32284, p>.05] has not shown significant differences respectively (Figure 41).

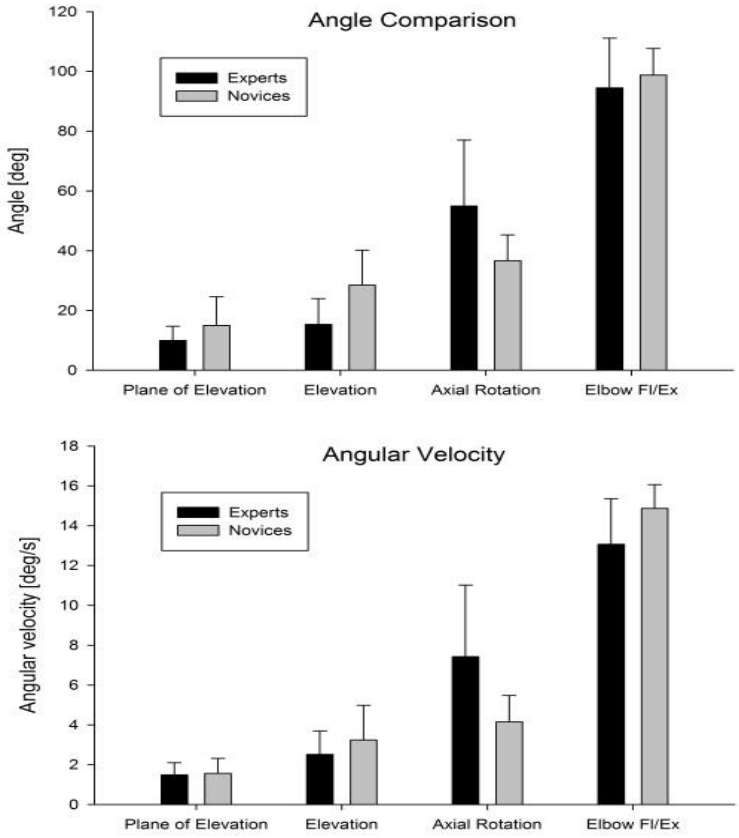

Figure 41 Differences the angular amplitude and the angular velocity amplitude between the novice and expert dart throwers

However, Tukey HSD post hoc comparisons did not show kinematic differences for the elbow flexion/extension angle, the shoulder plane of elevation and the elevation angles ($p>.05$) but significant differences could be uncovered for the shoulder axial rotation ($p<.05$).The same results are obtained for the angular velocity profiles.

Throws and torque generation

The results described so far, across groups showed differences in the amplitude of the axial rotation. Experts tend to rotate their arm more significantly and also faster compared to novice dart throwers. Following the kinematic analysis, inverse dynamics calculations for the upper arm were computed (Debicki et al., 2010);(Debicki et al., 2004) to uncover possible differences between the groups. A prediction from the hypothesis is that the decomposed torque at the elbow will vary due to skill. The maximal torque values were compared to evaluate the differences between the two groups.

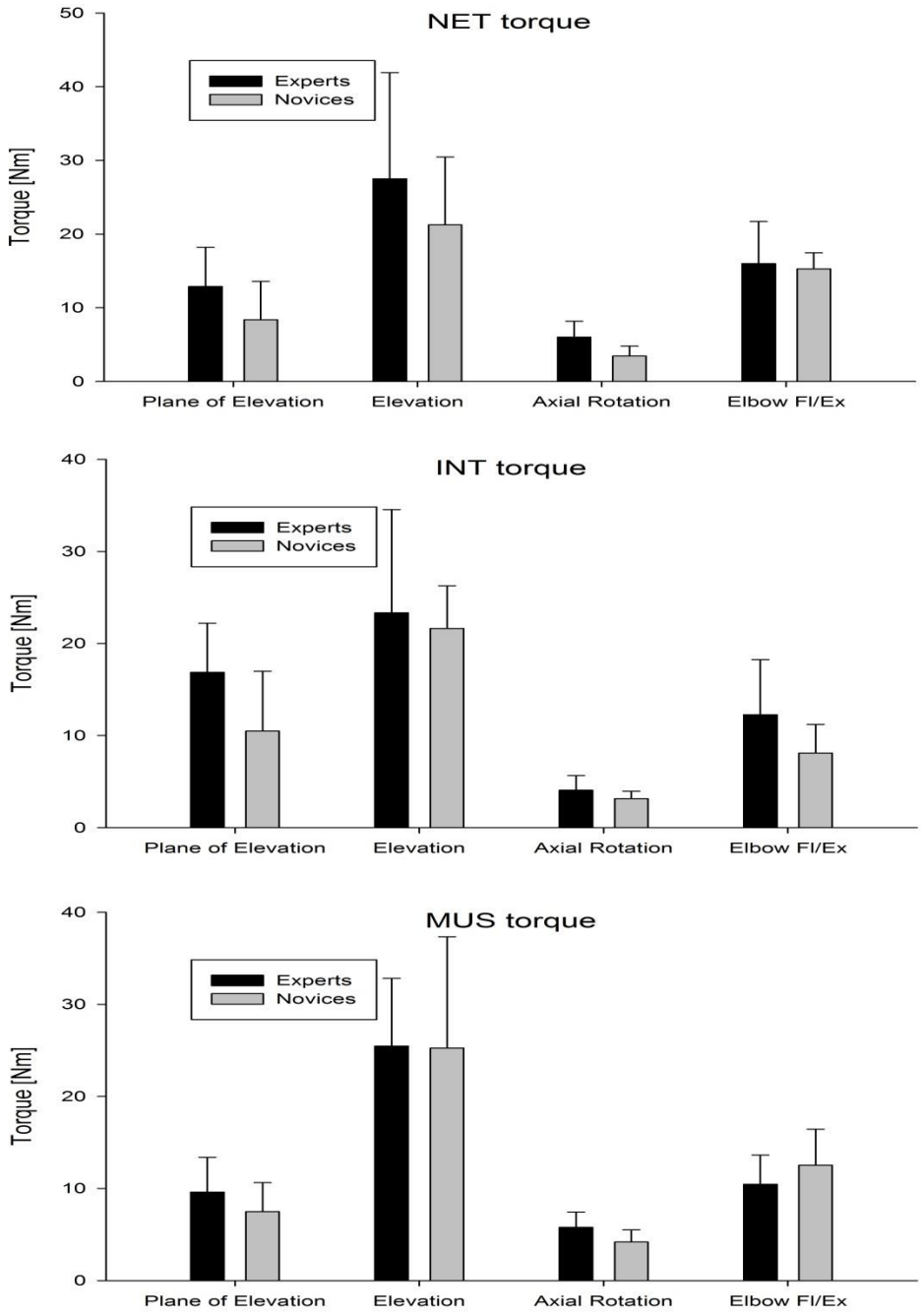

Figure 42 Dynamic differences between novices and experts regarding the maximal torque values during the throwing movement

One-way ANOVAS for the relative contributions of MUS and INT to NET torque (Figure 42) were quantified but did not reveal differences between the two groups for the elbow flexion [F(1, 7)=. 31290, p>.05], shoulder plane of elevation [F(1, 7)= 4.1448, p>.05] and the shoulder elevation [F(1, 7)= .46744, p>.05].

In contrast significant differences could be uncovered for the shoulder rotation torque [F(1, 7)= 15.738, p<.05], see Figure 43.

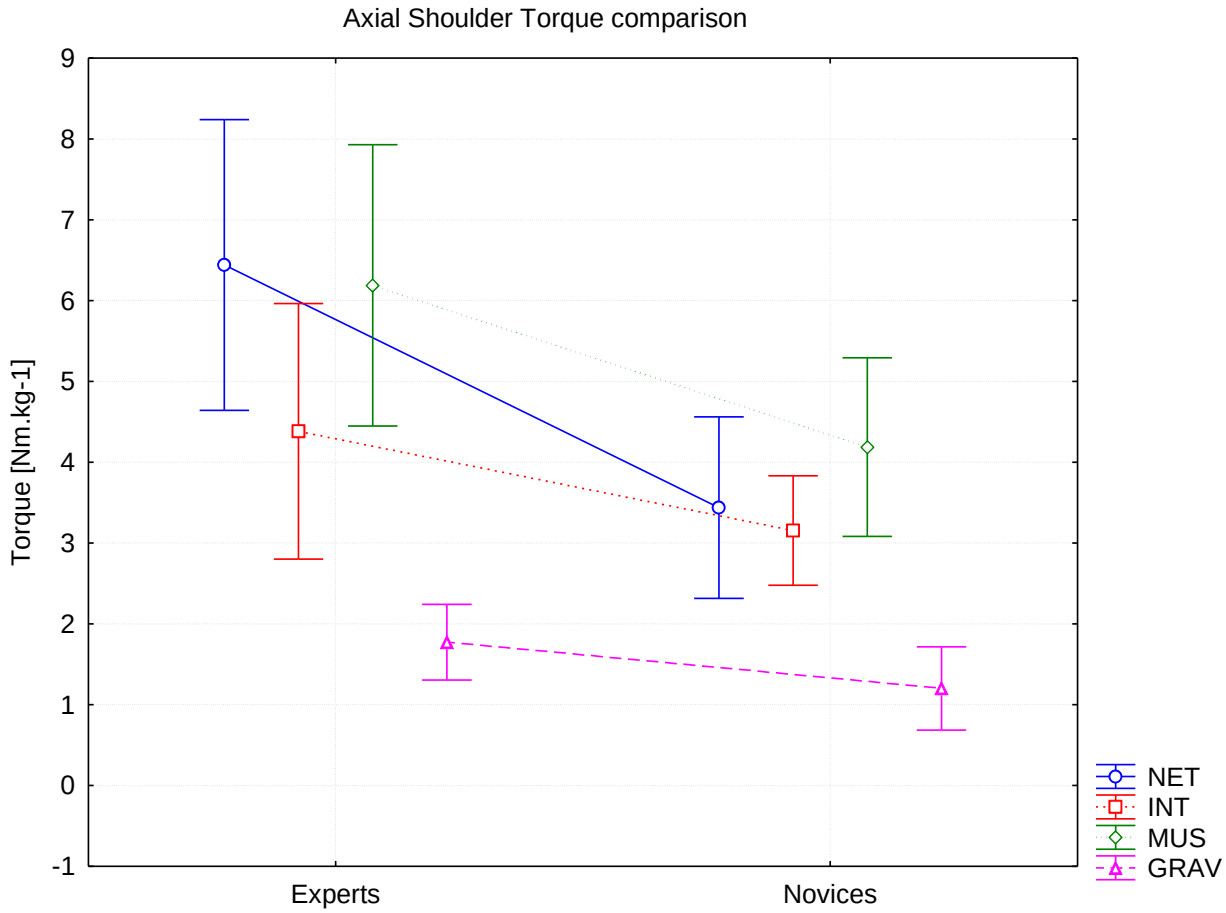

Figure 43 Differences between novices and experts regarding the axial shoulder net torque

Rotational Axes

To analyze the variability of the 3D angular displacements of the rotational axes, we used the framework of the MIR principle and computed rotation axes of the arm that were affected by the experimental conditions.

Table 14 Angular variability of the rotation axes during the dart throwing

Angular variability in [rad]	SH-EL	SH-CM	SH-e_3
Experts	0.21± 0.13	0.39 ± 0.37	0.47 ± 0.54
Novices	0.15 ± 0.04	0.30 ± 0.16	0.33 ± 0.18

Across all conditions, subjects showed a tendency to rotate their arm around the SH-EL axis compared to the SH-CM and the SH-$\mathbf{e_3}$ axes. In other words, subjects showed no change in rotational axis during the experiment.

Table 15 MANOVA table

Source		df	df	F
Axes		2	14	8.24*
Experts Novices	vs.	5	35	0.87

* $p < 0.05$

The variability of the SH-EL axis significantly differs from the variability of the SH-CM and $\mathbf{e_3}$ axes (Table 15). Moreover no significant differences could be uncovered due to skill on the variability of the SH-EL and the SH-CM and $\mathbf{e_3}$ axes ($p < .05$) respectively (Table 14).

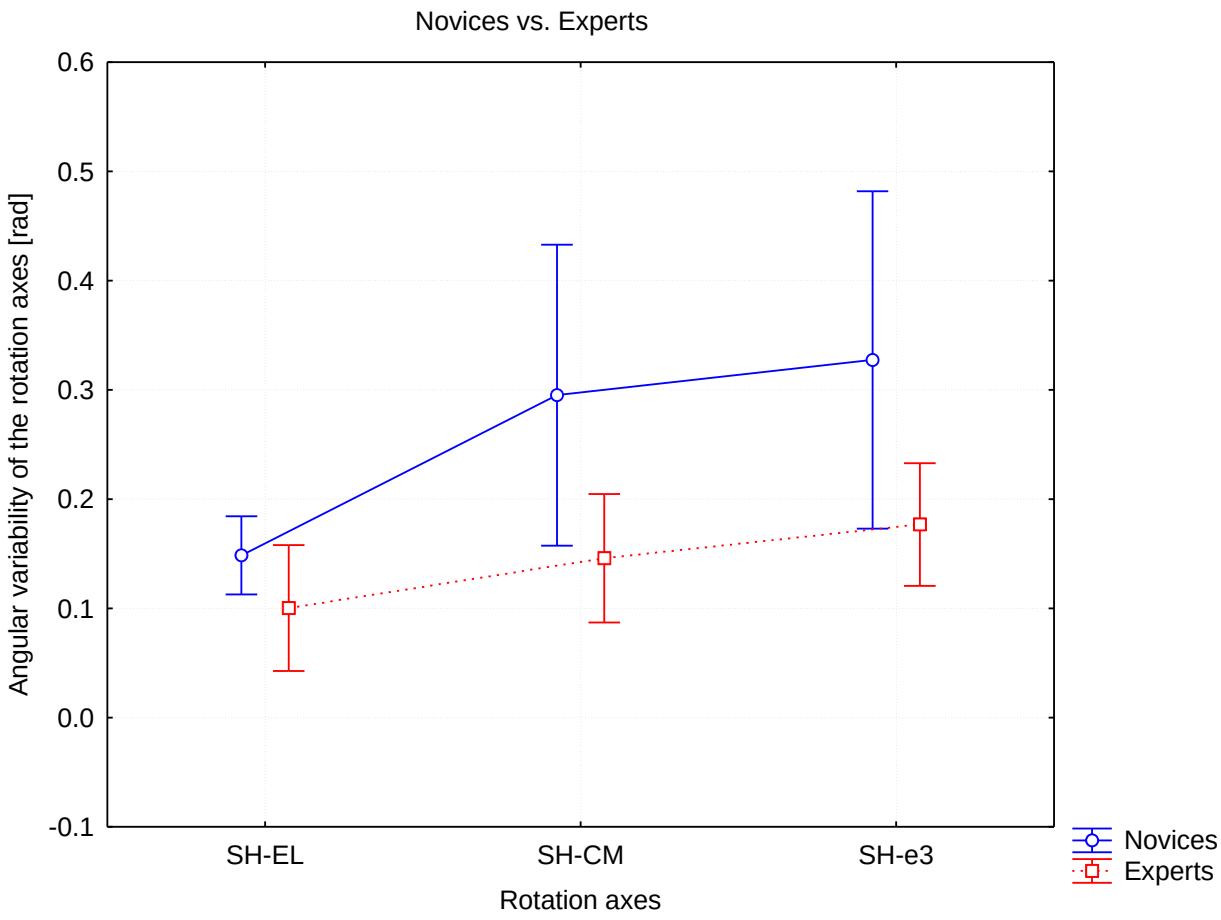

Figure 44 Differences of the angular variability of the rotation axes between novices and experts

Further analysis of the angular variability on an individual basis shows that certain subjects exploit different rotation axes besides SH-EL e.g. Subject 5 of the experts and Subjects 5 and 8 of the novices (Figure 45).

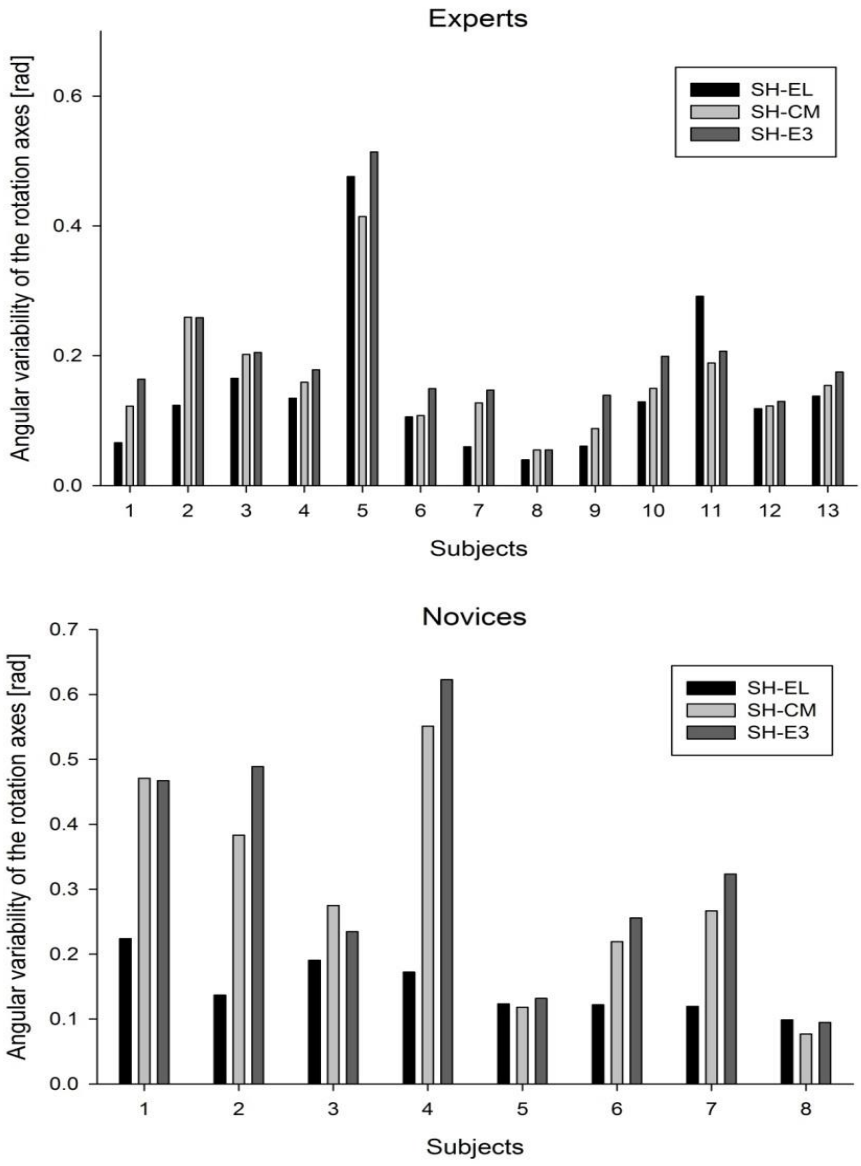

Figure 45 Angular variability of the rotation axes of each subject

Nonetheless it has to be stated, that no different control strategies can be uncovered when comparing the individual subjects. Thus, subjects fix the SH-EL axis to control the dart throwing motion regardless the skill level.

6.2.4. Discussion

Comparing novice and expert dart throwers is a very interesting research field that could reveal how the CNS identifies control strategies or changes them due to training and skill level. Previous research has shown changes due to skill level in sports such as baseball, tennis and handball (Schorer et al., 2007; Müller and Abernethy, 2012; Wagner et al., 2010). Significant differences could be uncovered in time space parameters, performance outcome, kinematics and the dynamics.

Also, the relation between the joint torque components and the skill level of subjects has been reported to differ for the elbow joint (Tamei et al., 2011), which could not be confirmed with the results of this experiment.

Novice and expert dart throwers choose individual control strategies and fixing the SH-EL axis is the most common strategy even though the simulated movements have shown lower Net torque profiles when fixing the $\mathbf{e_3}$ axis. However, neither the novice subjects nor the experts tended to take dynamics into account when performing the throwing task. Even though the proprioceptive role of the inertia tensor ($\mathbf{I_{ij}}$) and its advantages in terms of the instantaneous state and representation of the limb's disposition (Pagano and Turvey, 1995; Pagano and Turvey, 1995) has been subject of various experiments (Isableu et al., 2009; Isableu et al., 2013), dart throwing may not be as important in terms of actively produced forces as, for example, shoulder rotations at high velocity (Isableu et al., 2009; Isableu et al., 2013).

In general no differences in the angular variability of the rotation axes could be uncovered across subjects and skill level. As such, this experiment shows that all subjects follow their individual strategies but mostly the SH-EL axis was stabilized during the throwing motion.

Skill differences

The variability of the rotational axes showed no differences between novice and expert dart throwers. No skill-related rotational axes choice could be uncovered. The kinematics and torque analysis, on the other hand, showed that experts make more use of the axial shoulder rotation, which could be related to a specific follow through or deceleration phase. (Hore et al., 2011) reported that the interaction torque was also used to decelerate the throwing movement and (Tamei et al., 2011) described higher elbow interaction torque values for skilled dart players. Based on the initial hypothesis our data does not confirm different control strategies between novice and expert dart throwers regarding the choice of a rotational axis.

Throwing techniques

The task itself is a goal-directed movement and the CNS has to realize the throwing movement according to the initial state of the body, the location of the board, and the DOF available (Berret et al., 2011). Taking the DOF as an example shows the redundancy in the throwing motion. The movement could be performed, freezing some DOFs except the elbow joint. However in dart throwing, individual techniques and possibilities allow one to throw equally successful shots. This makes comparisons between groups difficult when focusing on rotational axes.

The choice of rotational axes directly influences the movement pattern. Stabilizing the SH-EL axis is a strategy to control the elbow as the only joint involved during the throwing motion. In contrast the stabilization of the SH-CM and e_3 axes is more complex because the shoulder and the elbow have to be controlled during the throwing motion. Focusing on one joint may be less complex attention-wise and, therefore, may be a convenient strategy during dart throwing. Unfortunately. the identification of the rotational axes was limited by the fact that the ToR could not be identified for the experts. Additional equipment on the hand would alter the performance and throwing patterns. However, earlier studies have already evoked this problem (Smeets et al., 2002);(Hansen et al., 2012b) and further experiments could uncover which rotation axis was stabilized at the ToR.

General discussion

Dart throwing is a relatively slow movement and stabilizing the rotational axes towards an efficient rotational axis such as $\mathbf{e_3}$ may not be necessary due to the specific velocity profiles. Even though the MIR principle is a motor control model that may lead to changes of the rotational axes in higher velocity profiles (Isableu et al., 2009; Isableu et al., 2013) the CNS does not necessarily change the motor control strategy or intervene during the throwing motion. The minimal intervention principle (Todorov and Jordan, 2002) leads to improved strategies if noise affects the motion, but may not be possible during a discrete movement over a short time period.

However, neither the skilled nor the novice dart throwers tended to stabilize the $\mathbf{e_3}$ axis despite the fact that the torque contribution may be advantageous. Throwing darts is not a physically exhausting task and saving energy may not be an issue. Fixing the elbow and performing the throwing motion while freezing DOF could be the preferred solution, besides the limiting effect of the freezing make the motion vulnerable for external errors. On the other hand, it would be interesting if the same results are reproducible when subjects are physically exhausted.

Taken together, our results indicate that the subjects don't follow the MIR principle, which may be a result of the low velocity profile and low physical demand but variances in the kinematic profiles show differences between the novice and the expert dart throwers.

Our results provide evidence that the subjects followed individual strategies during a precision throwing task. The choice of rotation axes has an impact on the inverse dynamics of the arm during the throwing movement and each axis will show slightly different decomposed torque patterns. Also the movement did not involve a high velocity profile which has led to a shift in rotation axes (Isableu et al., 2009; Isableu et al., 2013) stabilizing the $\mathbf{e_3}$ or SH-CM axis during a precision throwing task may be the best way to increase the performance but at the same time may be a strategy that is vulnerable for internal or external perturbations, while fixing the SH-EL axis and freezing degrees of freedom is very resistant to external perturbations. Further experiments would be necessary to explore whether movements involving high precision and high velocity profiles with no specific axis being indicated, would yield in a change towards $\mathbf{e_3}$. Also simulating the kinematics and dynamics of the throwing

motion with fixed rotation axes could help to understand the vulnerability of the strategy to noise.

6.2.5. Conclusion

The results showed that the rotational axis of a multi-articulated limb does not generally change from an articular axis of rotation to either a mass- or inertia-based axis during a precision throwing task, neither for experts nor for the novice dart throwers. Individual strategies are presented in this study but no global differences could be found regarding the control strategies between novice and expert dart throwers. In contrast to the rotational axes, the kinematic parameters were found to differ between the groups and do indicate different throwing patterns with skill level. These findings extend our understanding of differences between novice and expert dart players and how rotational axes are used when coordinating limbs in tasks requiring precision. The results do not contradict the findings of previous research (e.g., (Isableu et al., 2009), (Edwards and Waterhouse, 2009), but explain the influence of the role of the MIR principle during movements that require precision and a low velocity profile. These conclusions are important to our understanding of how movements are performed and executed in precision throwing sports with different skill level.

6.1.1 Executive Summary

We examined the role of skill during unconstrained 3D precision throwing movements. Specifically, we investigated if subjects stabilize rotational axes to facilitate the throwing motion and if experts show different strategies compared to novice thowers. The control of the principle of minimum inertia resistance (MIR) as shown by (Isableu et al., 2009) could play a major role during throwing. Subjects threw darts at a dartboard following the rules of the International Darts Federation. The general darts throwing movement is performed using mostly the elbow joint and during the throwing separations between the minimum inertia axis ($\mathbf{e_3}$), shoulder-center of mass axis (SH-CM) and the shoulder-elbow axis (SH-EL) can be observed. The purpose of this study was to test two hypotheses: 1) subjects may show different control strategies in a precision throwing task, preferentially fixing certain rotation axes and 2) motor control strategy (either at the kinematic or dynamics levels or both) may vary between groups with different skill level and experience. Our global results showed that the limbs' rotational axis coincide with the SH-EL axis across subjects. Nonetheless, the differences in the kinematics were observed between both groups. Even though no change of the rotational axis could be globally uncovered, a few subjects show the exploitation of the SH-CM and the $\mathbf{e_3}$ axis. Taken together the results showed that inter individual differences covered global effects and prevented the generalization of the axis of rotation that was exploited for both groups. No change from the SH-EL towards the minimum inertia ($\mathbf{e_3}$) and/or the mass axis (SH-CM), i.e., use of the MIR principle could be observed.

Study V	Description
Title	Differences in the control of dart throwing motion in novices and experts
Subjects	8 novice subjects recruited from the University community and 13 high performance athletes recruited during the French Darts Open
Hypothesis	Novices should show higher angular variability during the throwing Different control strategies are expected due to the different skill level
Task	Participants stood upright on a marked line and performed 10 throws.
Measurement system	Vicon V8i eight M2 camera passive optical motion capture system, frequency 250Hz for the novices Natural Point twelve OptiTrack 250e passive optical motion capture system, frequency 250Hz for the experts
Measured Variables	Displacement of the 13 Markers put on the trunk, arm, forearm and hand
Data Analysis	Filter: Butterworth filter (2nd order) Joint Angle Computation Vector Computation Vector displacement computation Torque
Calculated Variables	Variability of angular axes displacement
Statistical Analysis	Repeated measured MANOVA ANOVA Post hoc test (Tukey HSD post hoc)
Results	Subject specific control strategies and throwing signatures. Novices and experts show slightly different patterns at the kinematic at dynamics level (axial rotation angular velocity and torque) but no generalizable throwing strategy could be uncovered for both groups.
Discussion	Based on the different control strategies it can be considered, that subjects reduce the dimensionality of the throwing task and stabilize their elbow during the throw.

Chapter 7

7 Effect of velocity demands: Maximizing velocity in athletic skills. The axis of rotation changes during overarm throwing.

The seventh chapter is devoted to the effect of maximizing velocity during an overarm throwing task on the role of the minimum inertia resistance principle. The presented experiments in this chapter are structured with an introduction to explain the research question, followed by a short methods section, the results and a discussion.

7.1 The axis of rotation changes during the over arm throwing.

7.1.1 Introduction

Throwing objects in everyday life varies from casual actions like throwing a balled up paper into the trash to sportive activities. Throwing has been shown to be a hugely complex task, where performance depends on various variables including (Whiting et al., 1991) joint kinematics (van den Tillar and Ettema, 2004; van den Tillar and Ettema, 2007),; (Wagner et al., 2010), joint torques (Hirashima et al., 2008); (Fleisig et al., 1999) and muscle activity (Hirashima et al., 2002). Controlling 3D rotational motions of one's upper limbs in different ranges of angular velocities and accelerations is quite difficult and also skill dependent (Isableu et al., 2009). The control becomes even more difficult when the motions are executed in the absence of visual regulation or with low preparation time.

General throwing is a goal-related task, as passing a ball or shooting a goal directly has an influence on the velocity and kinematic profile (Hore et al., 1996); (Smeets et al., 2002). A transfer of momentum from proximal to distal is critical to maximize performance in javelin (Whiting et al., 1991) baseball (Hong et al., 2001), team-handball (van den Tillar and Ettema, 2009), and tennis (Marshall and Elliott, 2000). The end effector velocity profiles depend on the summation effects on the velocity of elbow extension and internal rotation of the shoulder. (van den Tillar and Ettema, 2004) quantified this influence on 67% of the total velocity. (Jöris et al., 1985) showed that a high ball velocity also depends on an optimal proximal to distal movement sequence, but especially on the skill level of the thrower (Fradet et al.,

2004).This is supported by findings of (Wagner et al., 2010), who compared the kinematics of handball players of varying skill level. In team handball, various research has evaluated the influence of different throwing techniques on the kinematics and end effector velocity (Fradet et al., 2004); (Jöris et al., 1985); (van den Tillar and Ettema, 2004; van den Tillar and Ettema, 2007) (Wagner and Müller, 2008). Also, the shoulder internal rotation has an influence on the ball velocity in baseball (Fleisig et al., 1999); (Hong et al., 2001); (Stodden et al., 2001), team handball throw (van den Tillar and Ettema, 2004; van den Tillar and Ettema, 2007), (Wagner et al., 2010), volleyball spike (Coleman et al., 1993), and tennis serve (Elliott et al., 1995b), (Marshall and Elliott, 2000).

The control of unconstrained 3D arm motions like external-internal rotations of the shoulder has been shown to depend on kinesthetic cues and the velocity of the performed task (Isableu et al., 2009; Isableu et al., 2013). Understanding how the body organizes and which rotational axes are exploited during an overarm throwing task is crucial and fundamental for understanding, improving and maintaining an athlete's performance. Moreover during different arm configurations involving flexion-extension of the elbow, most often a separation between the axis of minimal inertia ($\mathbf{e_3}$) (Pagano and Turvey, 1995), the shoulder-center of mass axis (SH-CM) (van de Langenberg et al., 2008) and the shoulder-elbow axis (SH-EL) of the whole arm (Isableu et al., 2009; Hirashima et al., 2007b; Hirashima et al., 2003a) occurs. Rotation of one's upper limb around $\mathbf{e_3}$, the minimum inertia axis, is biomechanically more efficient because less inertial resistance facilitates humeral internal-external rotations (Pagano and Turvey, 1995), (Isableu et al., 2009) while the use of SH-EL results in higher joint torques. However, (Isableu et al., 2013) also showed that the weight of initial instruction on limb positioning when it reinforces the arm to rotate around the SH-EL i) may prevent subjects from using biomechanically more efficient solutions, ii) that fast velocity increased the variability of the SH-EL axis leading to larger mechanical instabilities and iii) that VK cues improved the stability of the rotation axis around which the arm rotate.

However, knowledge of how the rotation movement is executed is severely lacking, although it is fundamental to investigate the motion. Depending on the research question, throwing actions can be divided from three (Wagner et al., 2010) to seven

(Meister, 2000) different phases. However all phases can be separated in a preparation, cocking, acceleration and follow through phase (Wagner et al., 2011; van den Tillar and Ettema, 2007). Understanding the relation between the rotation axes, the kinematics and kinetics is difficult in multi-joint movements, but may provide new insight in to how the CNS coordinates multiple DOFs regarding the control of throwing actions. To our knowledge, the contribution of rotational axes and their associated dynamic and kinematic relationships during the different phases of overarm throwing has never been reported before. Previous research with the goal to investigate high velocity throwing motions reduced the dimensionality of the task to one plane and analyzed a quasi 2D movement (Debicki et al., 2011; Hore and Watts, 2011; Hore et al., 2011).

The purpose of this study was to examine whether the minimum inertia axis would be exploited during the throwing phases when internal-external rotations of the shoulder are particularly important.

7.1.2 Methods

Subjects: 10 male subjects voluntarily participated in the experiment after signing a statement of informed consent pertaining to the experimental procedure as required by the Helsinki declaration and the EA 4532 local Ethics Committee. All participants were right-handed and aged 21 (± 3) years. They were free of sensory, perceptual, and motor (shoulder and elbow) disorders and naïve about the purpose of the experiment.

Experimental procedures

Each subject performed twenty overarm throws and was asked to throw as fast as possible to a target in three meter distance with a height of 2 meters. Ball height defined the angle of shoulder extension at ball release. The ball was a small synthetic ball that had the same size and weight as a regular tennis ball but showed a less bouncy behavior. The twenty trials were presented in succession within two blocks. The two blocks of ten throws were performed with a five minute rest period between them. Prior to the experimental conditions, a training session was completed for the throwing task to allow subjects to become familiar with the movement and the

ball. The learning was visually evaluated by the researcher, with the task being judged as acquired once the participant reproduced 5 successful trials. Trials were withdrawn and immediately repeated if it appeared that the throw was not performed at maximal velocity.

Throwing Phases

In order to better understand the relative contribution of biomechanical, kinematic and dynamic variables involved during throwing, it is helpful to divide the throw into phases (see (Meister, 2000)). In this study the throwing was divided into three phases, the preparation phase, the cocking phase and the acceleration/follow through phase (see Figure 46). A kinematics description of the arm movement during each phase is provided below.

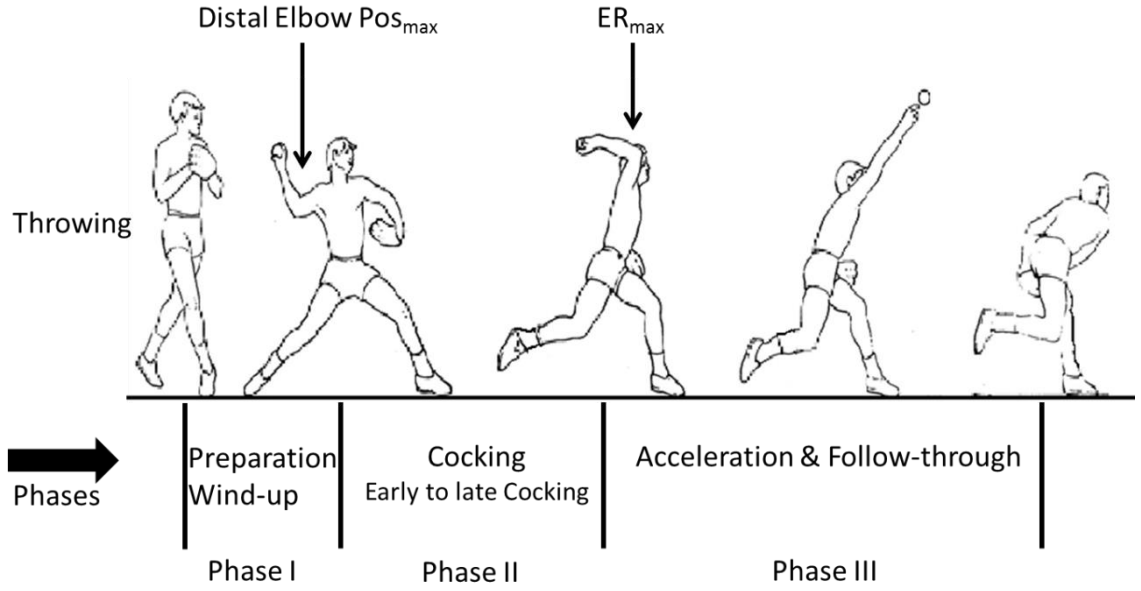

Figure 46 An example of the overarm throw in team handball of the different phases and characteristic points during the throw (Modified from (Meister, 2000))

In the preparation phase the participants initiated their throwing movement. The start of the throwing movement was defined as the beginning of the arm movement because this event was easily detectable and always occurred early in preparing for the goal-directed movement. During the early phase, subjects move the upper extremity and ball backwards and this phase ended when the maximum distal

position of the elbow was reached and could be also declared as early cocking (Meister, 2000). After, this event the cocking phase starts from the most distal point of the elbow and it ends when the throwing arm reaches its maximum external rotation. The acceleration phase starts when the throwing arm reaches maximum external rotation and the hand moves forward. During this phase the release of the ball occurs around the maximal elbow extension and the phase ends when the subject brakes the movement, also called the follow through.

Kinematic analysis

A T160 VICON eight camera (Nexus) motion capture system was used to record the resulting arm movements at a rate of 250 Hz (Vicon motion systems Inc., Oxford, UK). The kinematic and dynamic analysis as well as the computation of the SH-EL, SH-CM, and $\mathbf{e_3}$ vectors were performed as described in Chapter 3. The mass of the ball was not implemented in the inverse dynamic computation.

We also compute an index to assess the relative contribution of active vs. passive forces to net torque during the different throwing phases. We hypothesize that subjects should increase the contribution of passive torque and interaction torque (Hirashima et al., 2008), (Debicki et al., 2011; Hore et al., 2011) throughout the throw to reach the highest velocity of the hand at ball release. We expect a velocity-dependent change of rotation axes to occur to maximize the contribution of interaction torque to net torque.

Statistical analyses

A multivariate repeated measures analysis of variance (MANOVA, using the GLM module, Statistica 7 software) combining the three throwing phases (Preparation vs Cocking vs. Acceleration & Follow through) was then applied on the variability of angular displacements of each rotational axes (SH-EL, SH-CM, $\mathbf{e_3}$) with a .05 level of statistical significance.

7.1.3 Results

To analyze the variability of the 3D angular displacements of the rotation axes, we used the framework of the MIR principle and computed rotation axes of the arm that were affected by the experimental conditions.

Kinematics and SH, EL, WR displacement/velocity

The velocity profiles of the subjects did not show any differences regarding the intra subject variability. The maximal velocity of the hand was always reached during the acceleration & follow-through phase and the mean velocity for the two hundred trials was to be found 15.41± 1.92 m/s.

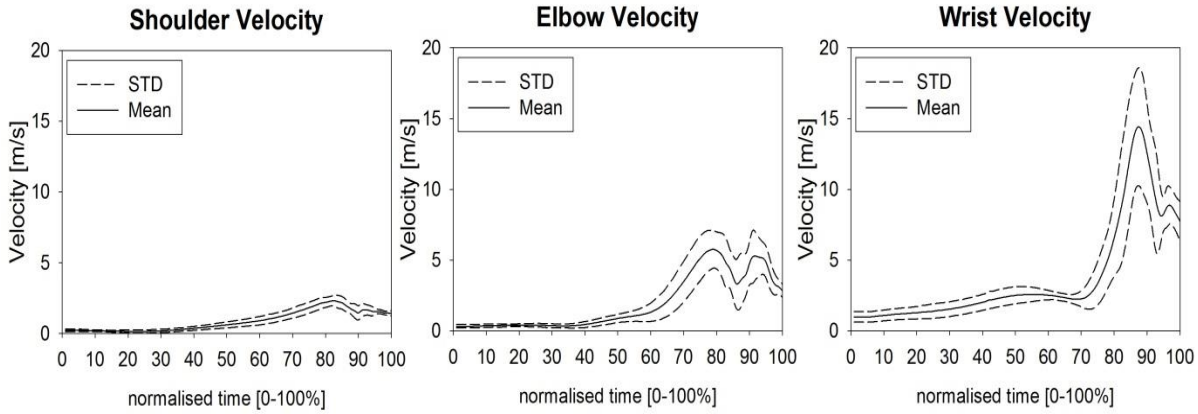

Figure 47 Velocity profiles of the hand of a representative subject over the 20 trials

Figure 48 shows that across subjects, shoulder peak velocity was smaller than the wrist and elbow velocity. Wrist peak acceleration was also shown to be larger than elbow and shoulder peak acceleration as did the jerk profiles.

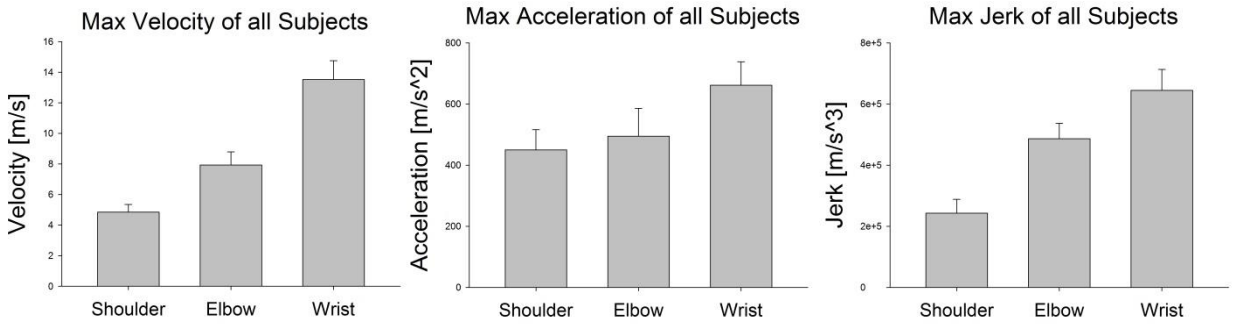

Figure 48 Peak velocity, acceleration and jerk profiles of the shoulder, elbow and the hand

Joint velocity over time

During the throwing motion the shoulder, elbow and wrist joint do show specific velocity patterns. Thus the velocity profiles are represented graphically for one subject during the three throwing phases (see Figure 47).The highest joint velocity values were found during the acceleration and follow through phase and the wrist shows the highest velocity profiles.

Figure 47 also revealed that the proximo-distal upper-limb coordination reported in expert throwers in earlier studies is not yet well mastered in the novice subjects of this study (Wagner et al., 2010) since the shoulder peak appeared later then the elbow velocity peak. However the wrist velocity peak occurs at the end of the throwing motion.

Throwing patterns

Close inspection of our data revealed large individual differences regarding the throwing patterns and the control strategies when throwing at maximal velocity. Figure 49 shows axial rotation angle of the shoulder as a function of the elbow flexion/extension angle. These individual kinematic patterns are likely due to different throwing experiences and techniques. Figure 50 shows axial rotation net torque as a function of the elbow flexion/extension net torque.

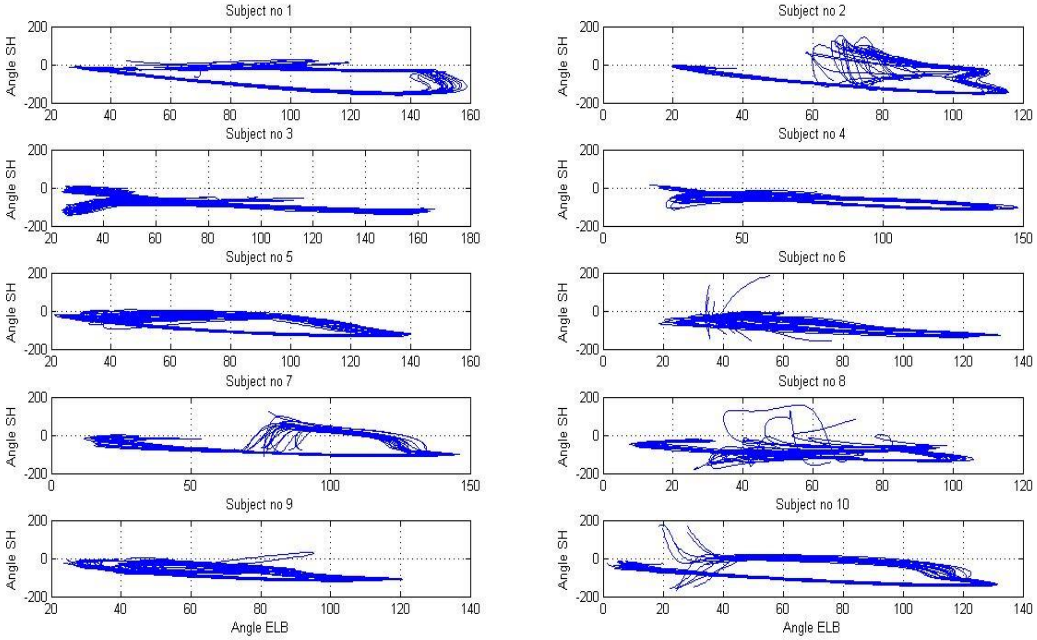

Figure 49 Axial shoulder rotation angle as a function of elbow flexion/extension angle [°]. This figure shows the individual throwing patterns of each subject.

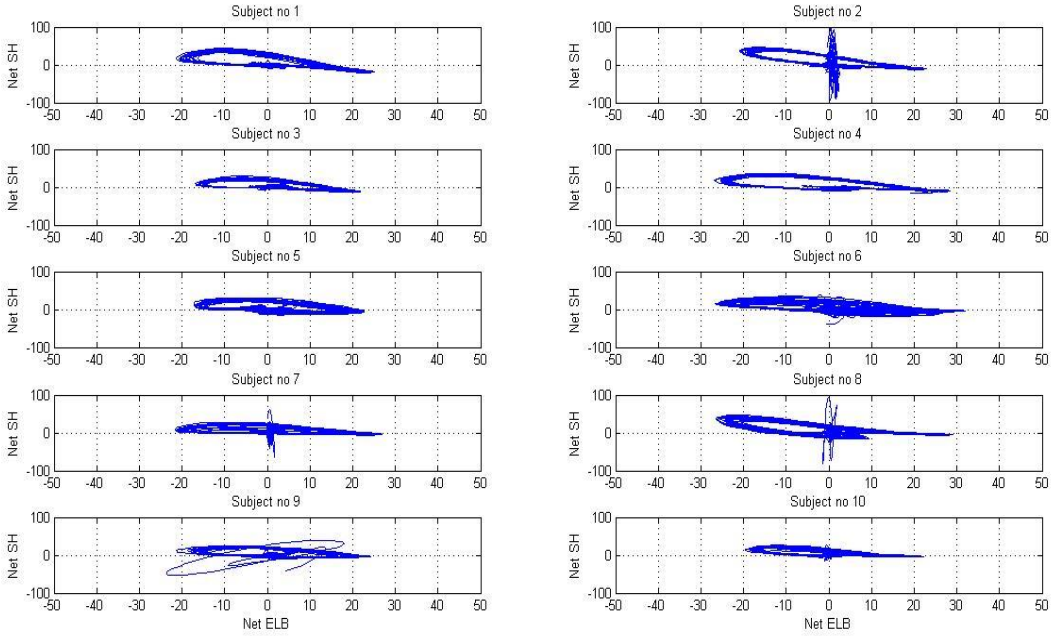

Figure 50 Axial shoulder rotation net torque as a function of elbow flexion/extension torque. This figure shows the individual throwing patterns of each subject.

Rotational Axes

The means of each variable were determined for each condition and subject (see Table 17), and the data was analyzed using a multivariate analysis of variance (MANOVA, see Table 16) followed by Tukey HSD post hoc comparisons.

Table 16 MANOVA table

Source	df	df	Value	F
Axes	2	8	0.19	17.28**
Phases	2	8	0.34	7.64*
Axes x Phases	4	6	0.02	70.46***

* $p < 0.05$, ** $p < 0.01$, *** $p < 0.001$

We analyzed whether the rotation of one's upper limbs coincide with a specific axis. With this view, the variability of the 3D angular displacements of the rotational axes was computed and then analyzed to identify the axis preferentially used in each throwing phases. Across the throwing phases, subjects showed changed the rotational axis over time. In other words, subjects showed a change in rotational axis during the experiment due to the specific characteristics of each phase.

Table 17 Mean (SD) rotation axes variability across conditions and subjects.

Angular variability in [rad]	SH-EL	SH-CM	SH-e_3
Preparation	0.78 ± 0.24	0.77 ± 0.17	0.76 ± 0.16
Cocking	0.43 ± 0.13	0.33 ± 0.09	0.32 ± 0.08
Acceleration & Follow Through	0.52 ± 0.19	0.80 ± 0.21	0.82 ± 0.23

During the preparation phase the variability of the SH-EL (0.78 ± 0.24) did not differ ($p < .05$) from the variability of the SH-CM (0.77 ± 0.17) and $\mathbf{e_3}$ (0.76 ± 0.16). In contrast, the variability of the SH-EL (0.43 ± 0.13 rad) during the cocking phase was significantly ($p < .05$) larger than the variability of the $\mathbf{e_3}$ (0.32 ± 0.08 rad) and subjects tend to rotate their arm around a compromise between the SH-CM and the e_3 axis. Post hoc tests showed a significant difference between the SH-EL and the e_3 axis. No differences could be uncovered between SH-CM (0.33 ± 0.09) & e_3 (0.32 ± 0.08 rad).

During the follow through phase subjects accelerated the arm and the variability of the SH-EL (0.52 ± 0.19) was significantly (p <.05) smaller than the variability of the SH-CM (0.80 ± 0.21) & e3 (0.82 ±0.23 rad) axes. In other words subjects tend to rotate their arm around the SH-EL axis (Figure 51).

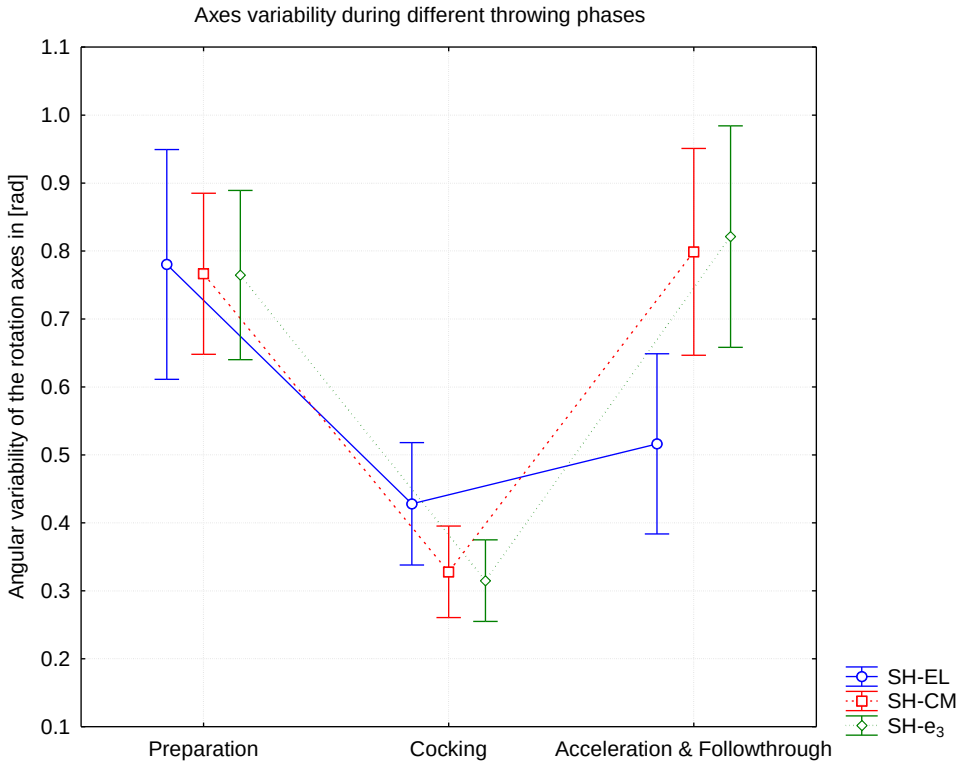

Figure 51 Angular variability of the rotation axes during each throwing phase.

Regarding the individual variability of the rotational axes in more detail, it was noticed that nine of ten subjects tended to rotate their arm around a tradeoff between SH-CM & $\mathbf{e_3}$ axes during the cocking phase. During the preparation phase, subjects tend to rotate their arm very individually in contrast to the follow through phase. In this acceleration & follow through phase all subjects rotate their arm around the geometric SH-EL axis (Figure 52).

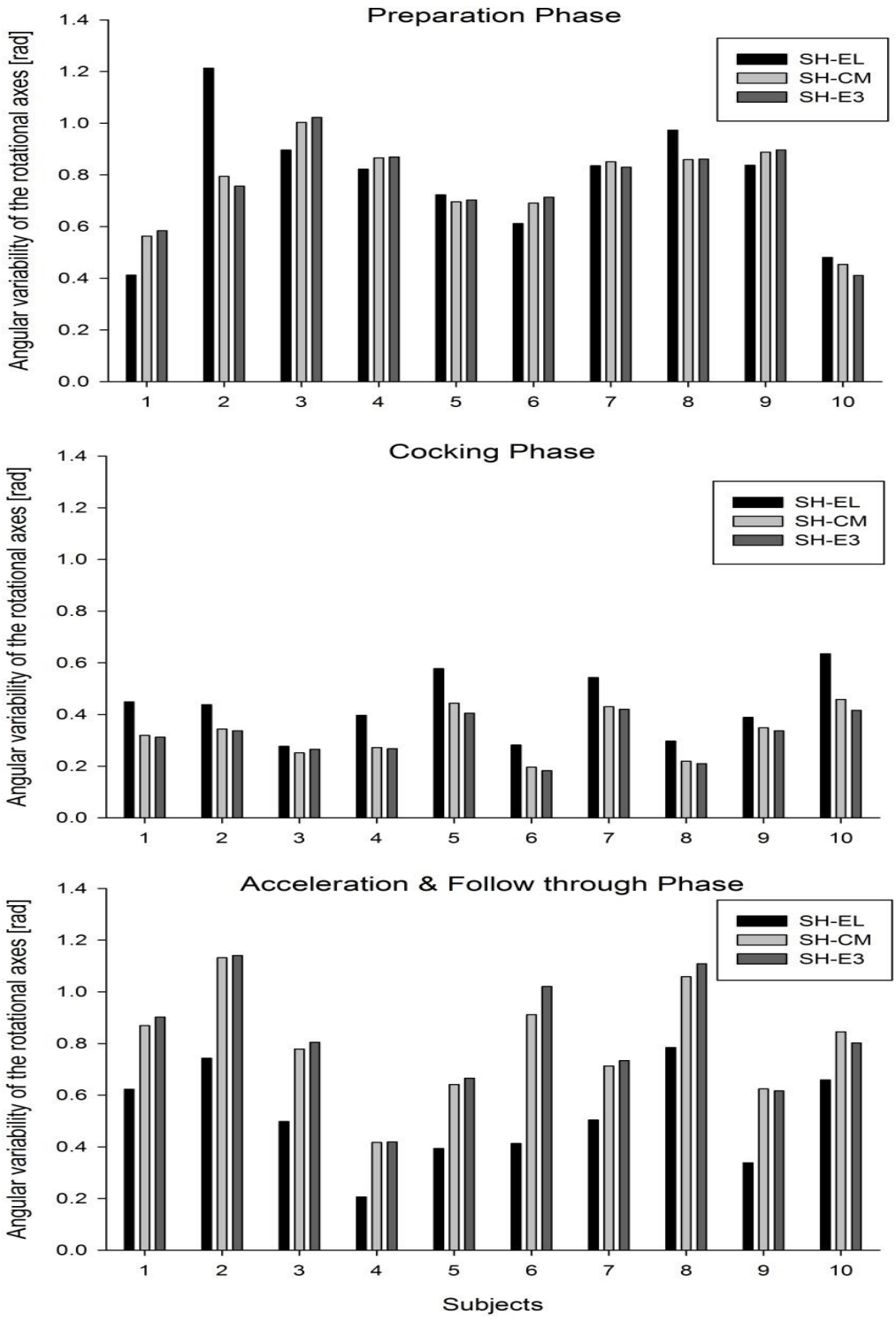

Figure 52 Individual angular variability of the rotation axes for each subject in each throwing phase.

Dynamics / Contribution Indexes

A one way ANOVA with the three throwing phases as factors followed by Tukey HSD post hoc comparisons showed significant differences in the contribution of the INT and MUS to Net torque for the shoulder axial rotation [$F(1, 9)=7.9141$, $p<.05$] and the throwing phases [$F(2, 18)=3.6602$, $p<.05$] and also an interaction effect was found to be significant combining INT and MUS x Phases ($p<.05$) (Figure 53). As expected, subjects increase the contribution of passive torque and more specifically interaction torque (Hirashima et al., 2003b; Hirashima et al., 2003a; Hirashima et al., 2007b; Debicki et al., 2011; Hore et al., 2011) throughout the throw. The rotation of the trunk and arm rotation also produced centrifugal forces that may have increased the hand velocity. This could explain the maximal contribution of the interaction torque during the acceleration & follow through phases.

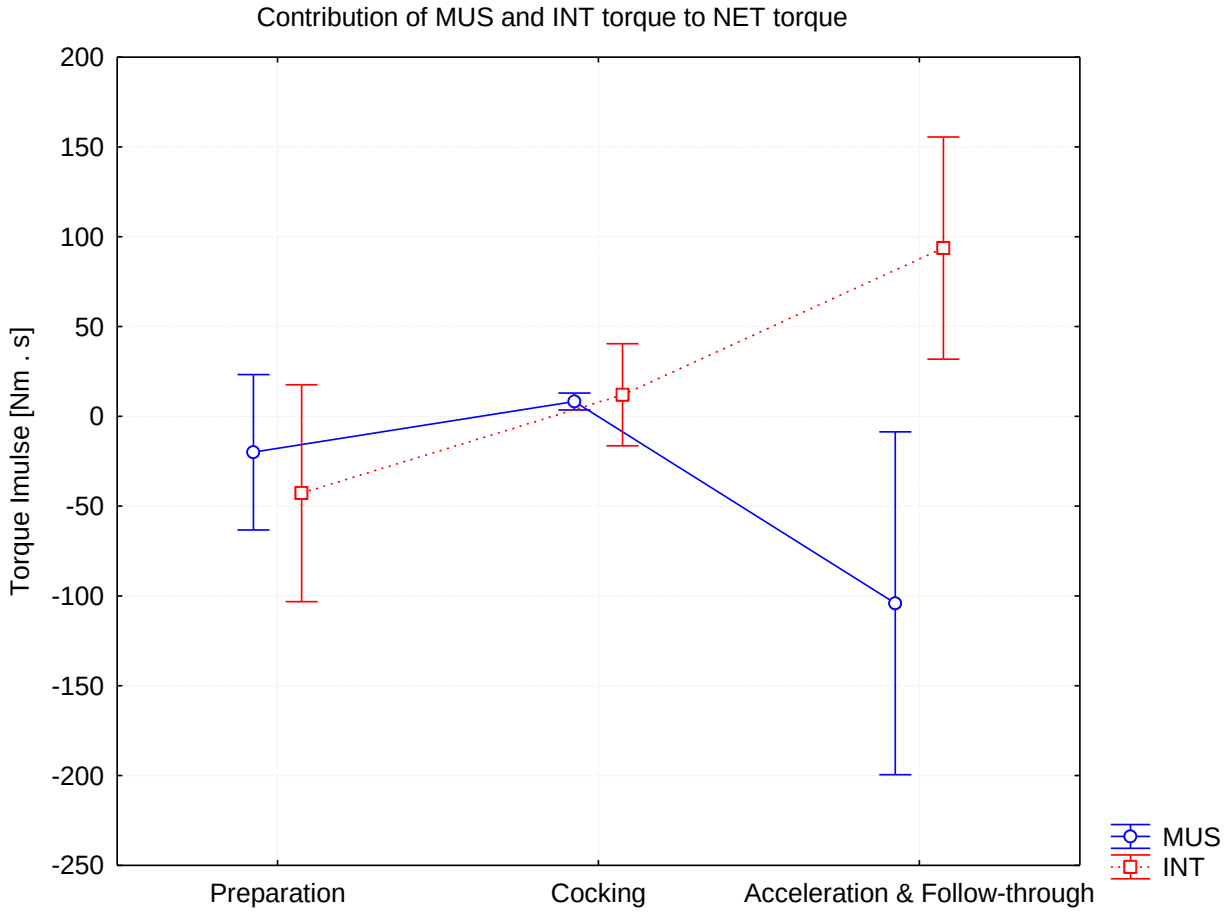

Figure 53 Contribution of the INT and MUS to NET torque during the three throwing phases shown for the shoulder axial rotation

7.1.4 Discussion

Regarding the influence of different throwing phases on a possible change in rotation axes, our experimental outcomes do show a global change in control strategy or differences in the angular variability of the rotation axes especially during the cocking phase. Our results are the first to provide evidence that the rotation axis of a multi-articulated limb system change from a mass- or inertia-based axis to a geometrical articular axis during different throwing phases. It was hypothesized that rotation of one's upper limb around $\mathbf{e_3}$ should facilitate internal-external axial humeral rotation. A change of rotation axis occured in the cocking phase of the throwing movement. The nature of the cocking phase would make rotations about the geometric SH-EL axis more difficult and, thus, relying either on the SH-CM or even better on the $\mathbf{e_3}$ rotational axes would be more likely to occur in that phase.

Inter individual differences

The individual kinematic and dynamic patterns of the shoulder and elbow joint have shown that subjects tend to have different throwing techniques. As previously pointed out, the subjects were novice throwers with no sport background in overarm throwing. The individual differences might be due to throwing skill but may also likely involve the exploitation of different frames of references and/or change from one frame of reference to another (Bernardin et al., 2005; Isableu and Vuillerme, 2006; Isableu et al., 2003; Berthoz, 1991; Paillard, 1991; Berthoz, 1991). The kinematic and dynamic parameters showed differences in the control of the movement (see Figure 51, 52). The differences may be due to different throwing techniques and skill of the subjects. However the exploitation of the rotation axes was consistent across subjects. Interestingly, the $\mathbf{e_3}$ axis was exploited throughout all subjects, which indicates that during the cocking phase subjects obey the MIR principle and tend towards the SH-CM/$\mathbf{e_3}$ trade-off axis regardless of the throwing technique. The acceleration phase is mainly organized on the basis of SH-EL rotation axis. While rotating around the SH-EL axis the contribution of passive interaction torque to net torque can be maximized when blocking the elbow distal to proximal movement.

Throwing phases

Previous studies have revealed differences in throwing technique, evaluating the space time parameters, the kinematics and dynamics during the throwing phases. To

our knowledge no study evaluated a possible change in rotation axis due to different throwing phases in overarm throwing. Previous research has shown a change of rotational axis in the control of 3D unconstrained arm movements during external-internal rotations of the shoulder at high velocities (Isableu et al., 2009). The nature of the cocking phase is quite similar to external-internal rotations of the shoulder and it is a crucial part of the throwing motion, bringing the arm in position for the acceleration and follow-through phase. Simulations of shoulder rotations (Isableu et al., 2009), have shown that rotations around the SH-EL axis reduce the contribution of interaction torque to net torque and as a consequence, the rotation of the arm is entirely determined by joint muscle torque (MUS=NET), which requires a greater energy expenditure. Also, the axial rotation torque patterns of the humerus showed that the interaction and muscle torques act in phase. In contrast to the cocking phase, the acceleration and follow-through phase depended on the passive interaction torque to increase the throwing velocity. The net torque corresponds to the sum of muscle, interaction and gravity torques. When the arm is rotating around $\mathbf{e_3}$, the interaction torque is acting favorably to decrease the necessary muscle torque.

The biomechanical and dynamical advantage to rotate around $\mathbf{e_3}$ was presented previously by (Isableu et al., 2009) during external-internal shoulder rotations and these results could be reproduced. It appears that the preferred rotation axis in the cocking phase is the $\mathbf{e_3}$ axis indicating that subjects tend towards an optimal mechanical solution.

7.1.5 Conclusion

Depending on the throwing phase, our results showed that the rotational axis of a multi-articulated limb does change from an articular axis of rotation to either a mass- or inertia-based axis during the cocking phase. This finding was observed throughout all subjects. The individual throwing styles of the subjects were consistent and the shoulder configurations were close to those observed in many athletic configurations such as handball over arm throwing or baseball. These findings extend our understanding of the influence of how subjects perform and control their limbs in a 3D unconstrained throwing task. Furthermore we gained additional insight in the organization of how rotation axes are used to organize sport actions and movement. Also we expanded our knowledge about the outcome that can be expected when coordinating limbs in tasks requiring fast rotations. Our results confirm the findings of previous research (e.g., (Isableu et al., 2009)) that showed a change of rotation axes due to high velocity profiles. The results of this study are essential and will improve the understanding of how sport movements such as throwing are performed, learned and executed.

7.1.6 Executive Summary

We examined whether the minimum inertia rotation axis ($\mathbf{e_3}$) is a key factor in motor performance and more specifically during unconstrained 3D overarm throwing. Subjects performed an overarm throwing task and were asked to throw a tennis ball at maximal velocity at a goal. The purpose of this study was to test the hypothesis that a change of rotational axes occurs due to the different throwing phases. A motion capture system was used to evaluate the contribution of the minimum inertia axis ($\mathbf{e_3}$), shoulder-center of mass axis (SH-CM) and the shoulder-elbow axis (SH-EL) to the performance in the different phases (preparation, cocking and follow through) of the throwing. The results showed that the limb's rotational axis coincided with the e_3 axis across the cocking phase of the overarm throw. Even though individual throwing strategies were exposed, including the kinematics and dynamics of the subjects' performance, all subjects showed an effect due to the cocking phase and changed the rotational axis during the task. Taken together, the results showed that despite the inter-individual differences all subjects obeyed to the MIR principle and changed the rotational axis towards the minimum inertia ($\mathbf{e_3}$) and/or the mass axis (SH-CM) during the cocking phase. To increase the interaction torque during the acceleration & follow-through phase, subjects tended to exploit the SH-EL axis to slow down the elbow and make use of the passive torque generated by the trunk and whole body.

Study VI	Description
Title	Change of rotation axes during overarm throwing
Subjects	10 subjects recruited from the University community of Tokyo
Hypothesis	Different throwing phases lead to a change of rotational axis
Task	Participants threw balls at maximal velocity at a target
Measurement system	Vicon T160 eight camera passive optical motion capture system, frequency 250Hz
Measured Variables	Displacement of the 13 Markers put on the trunk, arm, forearm and hand
Data Analysis	Filter: Butterworth filter (2nd order) Joint Angle Computation Vector Computation Vector displacement computation Torque
Calculated Variables	Angular Axes displacement
Statistical Analysis	Repeated measured MANOVA Post hoc test (Tukey HSD Post hoc)
Results	Different coordination patterns of the subjects during the throwing task however all subjects change the rotation axis towards the SH-e_3 axis obeying the MIR principle. During the acceleration phase subjects tend to rotate around the geometric rotation axis.
Discussion	Based on the different phases of the overarm throwing it can be considered, that subjects change the rotational axes during the throw and exploit the SH-e_3 & SH-CM axis during the cocking phase. The general exploitation of one specific rotation axis suggests equal control strategies between the subjects.

Chapter 8

8 Effect of spatial and velocity demands. Maximizing both precision and velocity in athletic skills

The eighth chapter is devoted to the effect of maximizing velocity and precision during an interception and a tennis flat serve task on the role of the minimum inertia resistance principle. The presented experiments in this chapter are structured with an introduction to explain the research question, followed by a short methods section, the results and a discussion.

8.1 The axis of rotation changes during the tennis service.

8.1.1 Introduction

Playing tennis is a very popular sport with many followers. Even though hitting a ball with the forehand may be a challenge to some people, the tennis serve is very complex and difficult (Kovacs and Ellenbecker, 2011). Its performance depends on various variables including (Girard et al., 2005) joint kinematics (Fleisig et al., 2003); (Chow et al., 2003), joint power (Creveaux et al., 2013) and muscle activity (Escamilla and Andrews, 2009). Also individual skill (Del Villar et al., 2007), range of motion (Ellenbecker et al., 2002) and specific control have an influence on the performance.

Controlling 3D rotational motions of one's upper limbs in different ranges of angular velocities and accelerations is quite difficult and also skill dependent (Isableu et al., 2009). The control of unconstrained 3D arm motions like external-internal rotations of the shoulder has been shown to depend on kinesthetic cues and the velocity of the performed task (Isableu et al., 2009; Isableu et al., 2013). Understanding how the body organizes and which rotational axes are exploited during a tennis service is crucial and fundamental for understanding, improving and maintaining athletic performance.

Moreover, during different arm configurations involving flexion-extension of the elbow, most often a separation between the axis of minimal inertia ($\mathbf{e_3}$) (Pagano and Turvey, 1995), the shoulder-center of mass axis (SH-CM) (van de Langenberg et al.,

2008), and the shoulder-elbow axis (SH-EL) of the whole arm (Isableu et al., 2009);(Hirashima et al., 2003a; Hirashima et al., 2007b) occurs. Rotation of one's upper limb around $\mathbf{e_3}$, the minimum inertia axis, is biomechanically more efficient because the reduction of the inertial resistance allows for the facilitation of humeral internal-external rotation (Isableu et al., 2009) while the use of SH-EL results in higher joint torques. (Isableu et al., 2013) also showed that the weight of initial instruction on limb positioning when it reinforces the arm to rotate around the SH-EL i) may prevent subjects from using the more biomechanically efficient solution, ii) that fast velocity increased the variability of the SH-EL axis leading to larger mechanical instabilities and iii) that VK improved the stability of the rotation axis around which the arm rotated.

Depending on the research question, the tennis serve can be divided into three phase and eight stages (Kovacs and Ellenbecker, 2011). Understanding the relation between the rotation axes, the kinematics and kinetics is difficult in multi-joint movements, but may provide new insight of how the CNS coordinates multiple DOFs regarding the control of the service. Also, the shoulder internal rotation has an influence on the ball velocity in baseball (Fleisig et al., 1999), (Stodden et al., 2001), team handball (van den Tillar and Ettema, 2004; van den Tillar and Ettema, 2007); (Wagner et al., 2010)**,** volleyball (Coleman et al., 1993), and tennis (Elliott et al., 1995a).

To our knowledge, the contribution of rotational axes and their associated dynamic and kinematic relationships during the different phases of tennis service has never been reported before. The purpose of this study was to examine whether the minimum inertia axis would be exploited when internal-external rotations of the shoulder are particularly important.

8.1.2 Methods

Subjects: 5 male subjects voluntarily participated in the experiment after signing a statement of informed consent pertaining to the experimental procedure as required by the Helsinki declaration. All participants were high performance athletes, right-handed and aged 28 (± 8) years. They were free of sensory, perceptual, and motor (shoulder and elbow) disorders and were naïve about the purpose of the experiment.

Experimental procedures

Each player completed a standardized 10-minute warm-up that allowed him to become accustomed to the experimental situation by performing several tests service. Each player must complete five successful services flat (without effect given to the ball) in the diagonal equalities with 90 seconds of rest between each attempt. Three tennis serves were recorded following the recommendations of (Mullineaux et al., 2001) to obtain accurate and representative kinematic data. A successful service required that the ball reaches the target of a 1.50 x 1.50 m defined in the service box along the midline (not bullet fault or in the net). The subjects were asked to perform powerful services as if they were real competitive situation using their personal rackets. Trials were withdrawn and immediately repeated if it the service failed and was stopped by the net.

Serving Phases

In order to better understand the relative contribution of biomechanical, kinematic and dynamic variables involved during the tennis serve, the movement was divided into three phases, based on the description of (Kovacs and Ellenbecker, 2011). The serve was divided into three phases: the preparation phase, the cocking phase and the follow through phase. A kinematic description of the arm movement during each phase is provided below.

Preparation Phase:

The preparation phase is defined from the movement initiation until maximal external rotation of the shoulder which coincides at the point when the tip of the racket head points toward the ground. The phase is further divided into the Loading and Cocking phase. The Loading phase coincides with the elbows lowest vertical position and also

maximum knee flexion and at the same time will be the beginning of the analysis. The Cocking phase follows and ends when the maximal shoulder external internal rotation is reached and coincides with the tip of the racket pointing toward the ground.

Acceleration Phase:

The acceleration phase starts from the maximal external rotation of the shoulder until the end of ball contact.

Follow through phase:

The follow through phase begins immediately after the ball contact and continues through the end of the service motion including the deceleration phase.

With the tennis serve phases defined, the analysis will not be performed throughout each precise phase but the focus will lie in specific stages of the movement involving shoulder rotations. As a consequence, the preparation phase will already end with the loading phase. The other phases are not changed but an extra separation will take part leading to a total of four phases, the preparation (ending with the loading phase), the cocking, the acceleration and the follow through phase.

Kinematic analysis

A T40 VICON eight camera motion capture system was used to record the resulting arm movements at a rate of 120 Hz (Vicon motion systems Inc., Oxford, UK). In addition to the usual marker set, the tennis racket was defined with four markers. The main ones are on the handle and two on either side of the head. The fourth was added at the top of the racket head.

Data analysis

The kinematic and dynamic analysis as well as the computation of the SH-EL, SH-CM, and $\mathbf{e}_3$ vectors were performed as described in Chapter 3. The racket was rigidly implemented as a fourth segment to the hand with no additional DOFs. The mechanical parameters of the racket as the mass, COM and the inertial parameters were also implemented in the computations.

Contribution Index

We quantified the contributions of muscle and interaction torques using the method introduced by (Sainburg and Kalakanis, 2000). Intervals during which the interaction torque component acted in the same direction as the net torque were considered to contribute to a positive interaction torque impulse. Intervals during which the INT torque component acted in the opposite direction to NET were considered to contribute to a negative INT torque impulse. All positive and negative integrals were summed to yield a single total INT torque impulse for the entire movement. MUS torque impulse was likewise computed as a contribution to net torque for the entire movement (Sainburg and Kalakanis, 2000).

Statistical analyses

Due to the very small sample size of 5 subjects no statistical analysis will be performed. The analysis however, will focus on the inter-individual differences of the subjects.

8.1.3 Results

To analyze the variability of the 3D angular displacements of the rotation axes, we used the framework of the MIR principle and computed rotation axes of the arm that were affected by the experimental conditions.

Ball velocity

The ball velocity profiles of the subjects did not show any differences regarding the intra subject variability. The mean maximal velocity for the fifteen trials was to be found 39.83±1.80m/s.

Racket velocity

The ball velocity profiles of the subjects did not show any differences regarding the intra subject variability. The mean maximal velocity for the fifteen trials was to be found 39.83±1.80m/s.

Joint velocity

Figure 54 shows that shoulder peak velocity was smaller than the elbow and wrist velocity. The racket velocity was found to be the highest for all subjects.

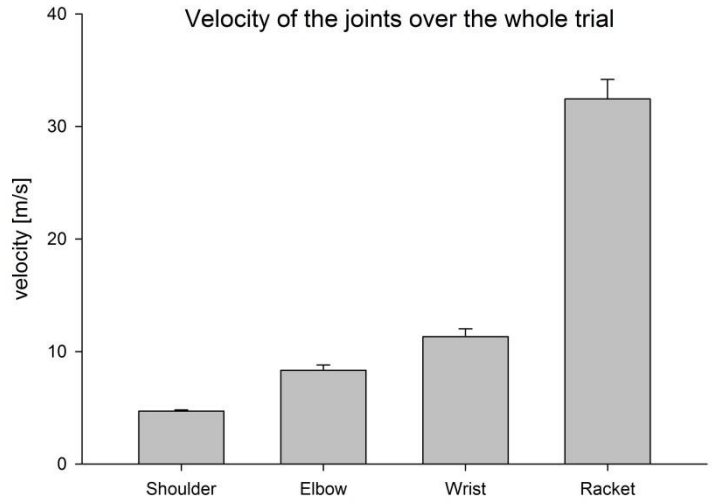

Figure 54 Peak Velocity of the shoulder, elbow, wrist and racket during the tennis serve

The individual velocity profiles are congruent and no large inter-individual differences could be uncovered during the tennis serve for the five subjects (Figure 55).

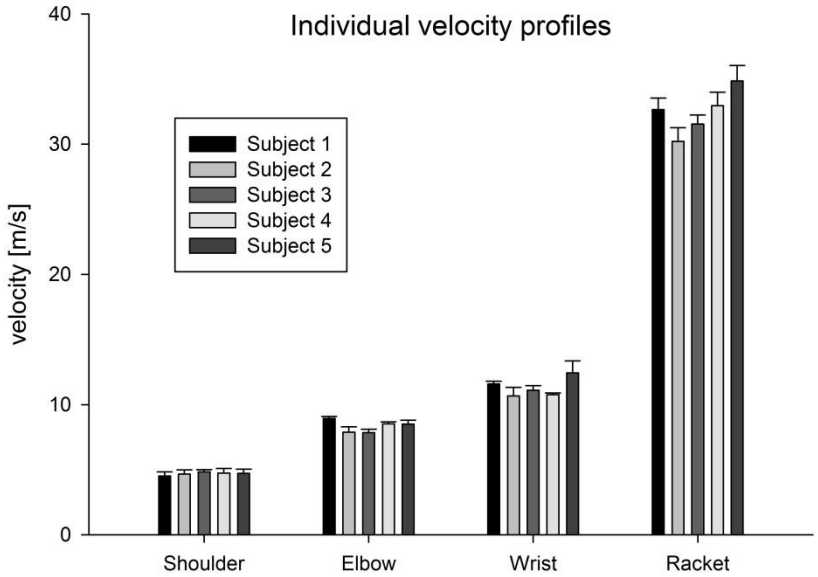

Figure 55 Individual velocity profiles of the shoulder, elbow, wrist and racket

Rotational Axes

The means of each variable were determined for each condition and subject (see table 18). Due to the small sample size no statistical analysis was performed.

We analyzed whether the rotation of one's upper limbs coincide with a specific axis. With this view, the variability of the 3D angular displacements of the rotation axes was computed and then analyzed to identify the axis preferentially used in each throwing phases. Across the throwing phases, subjects changed the rotational axis over time. In other words, subjects showed a change in rotational axis during the experiment due to the specific characteristics of each phase.

Table 18 Mean (SD) rotation axes variability across conditions and subjects

Angular variability in [rad]	SH-EL	SH-CM	SH-e_3
Preparation	1.19 ± 0.21	1.12 ± 0.07	1.14 ± 0.09
Cocking	0.44 ± 0.14	0.21 ± 0.10	0.33 ± 0.12
Acceleration	0.15 ± 0.02	0.14 ± 0.02	0.27 ± 0.05
Follow Through	0.49 ± 0.16	0.56 ± 0.19	0.53 ± 0.18

During the preparation phase the variability of the SH-EL (1.19 ± 0.21) did not seem to differ from the variability of the SH-CM (1.12 ± 0.07) and $\mathbf{e_3}$ (1.14 ± 0.09). In contrast, the variability of the SH-EL (0.44 ± 0.14 rad) during the cocking phase is larger than the variability of the SH-CM (0.21 ± 0.10 rad) and the $\mathbf{e_3}$ (0.33 ± 0.12 rad) axis. Subjects tend to rotate their arm around a compromise between the SH-CM and the e_3 axis.

During the acceleration, the variability of the SH-EL (0.15 ± 0.02 rad) is similar to the variability of the SH-CM (0.14 ± 0.02 rad) but both are smaller than the $\mathbf{e_3}$ (0.27 ± 0.05 rad) axis. Subjects tend to rotate their arm around a compromise between the SH-EL and the SH-CM axis during the acceleration phase.

While accelerating the arm during the follow through phase subjects showed smaller variability of the SH-EL (0.49 ± 0.16) than that of the SH-CM (0.56 ± 0.19) & e_3 (0.53 ± 0.18 rad). In other words, subjects do not seem to prefer a specific axis (Figure 56).

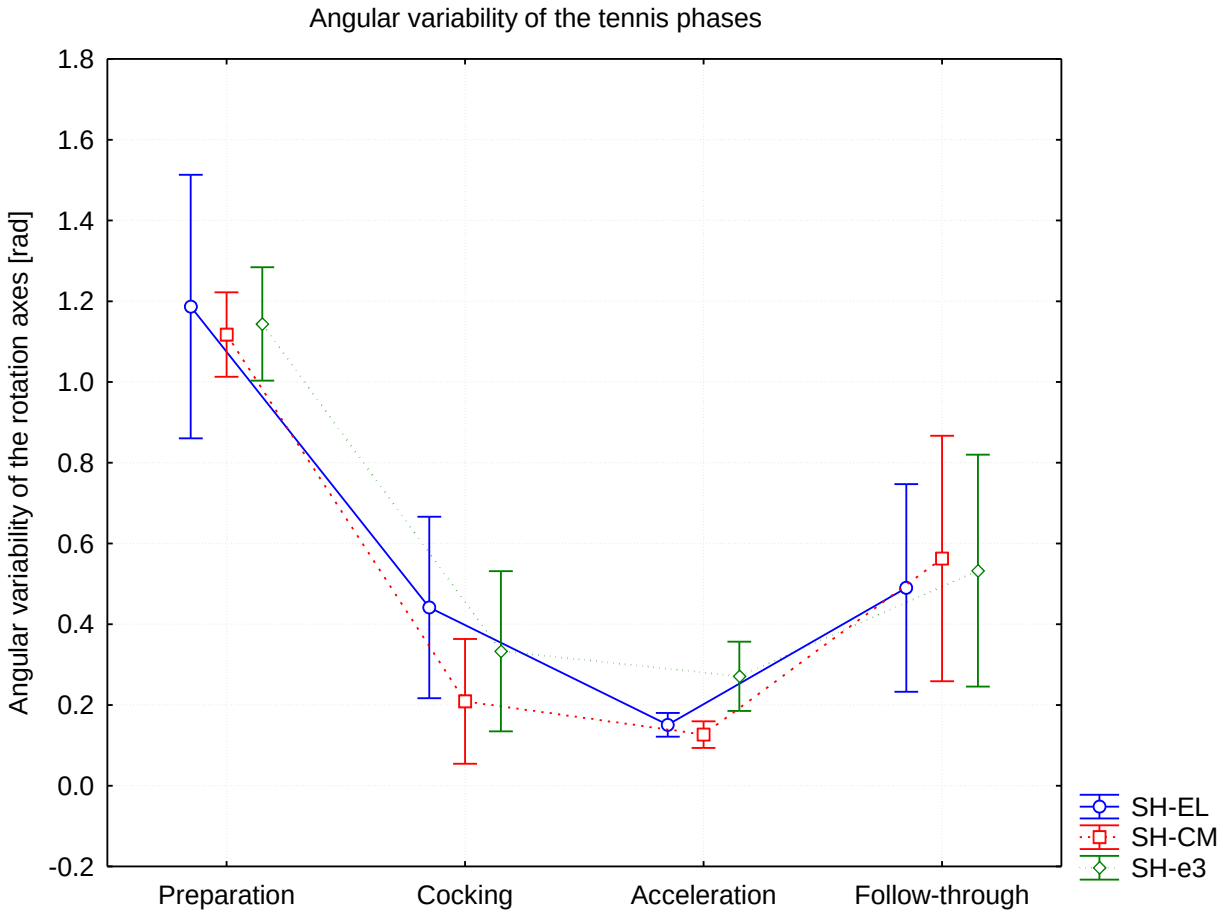

Figure 56 Angular variability of the rotation axes during each tennis serve phase.

Regarding the individual variability of the rotation axes in more detail, it is obvious that during the preparation phase, three of five subjects tend to rotate their arm around the SH-EL axis while during the cocking phase all five subjects tend to rotate either around the SH-CM or the e_3 axis (Figure 57). During the acceleration phase four of the five subjects tend to rotate their arms around the SH-EL axis. In the follow through phase all subjects tend to rotate around the SH-EL axis (see Figure 57) However, the angular variability is large and so no specific rotation axes can be accounted as favored.

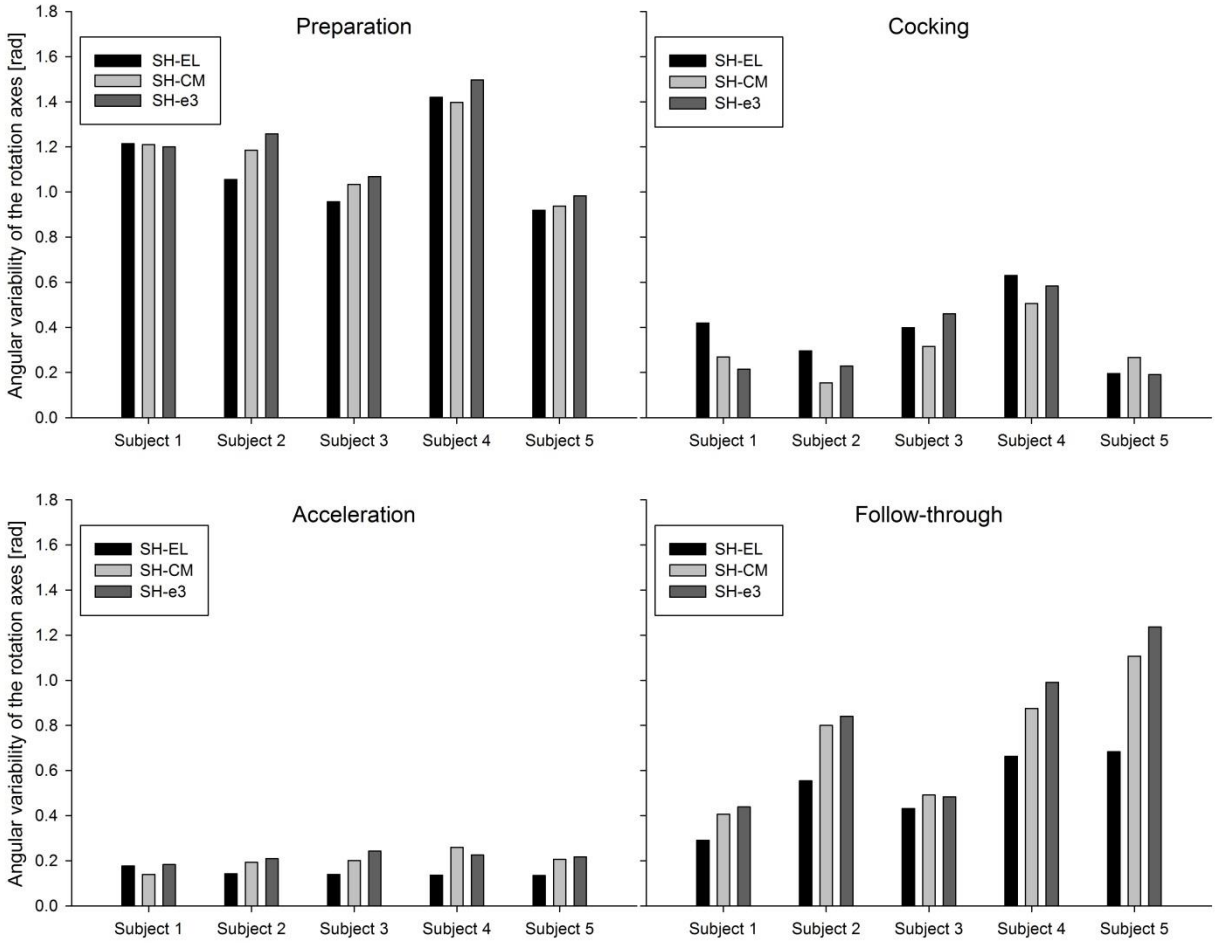

Figure 57 Individual angular variability of the rotation axes for each subject in each tennis serve phase.

Dynamics / Contribution Indexes

Subjects tend to increase the contribution of passive torque and more specifically the interaction torque (Hirashima et al., 2008), (Debicki et al., 2010) in the acceleration phase and keep its contribution constant during the Follow-through phase (Figure 58).

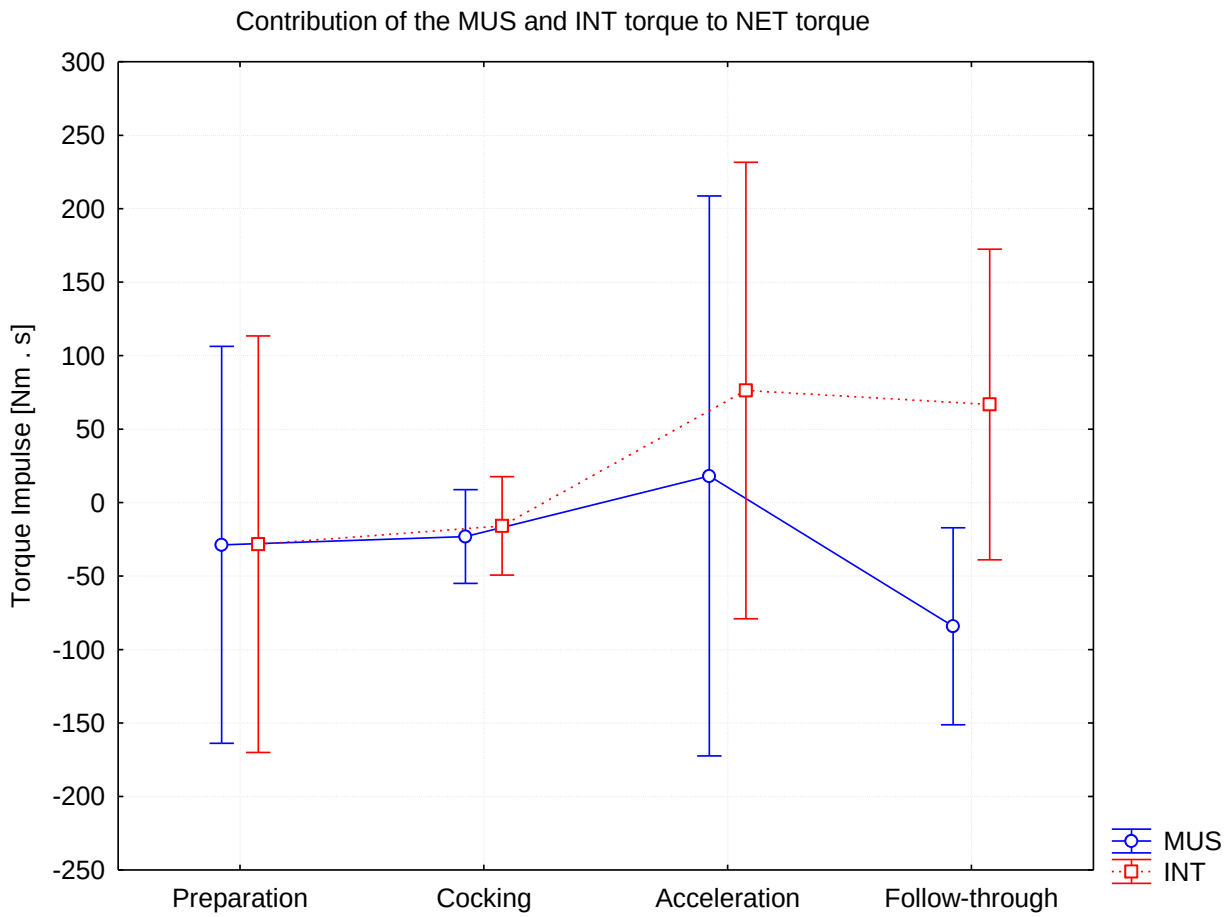

Figure 58 Contribution of the MUS and INT to NET torque during the four tennis serve phases

8.1.4 Discussion

Regarding the influence of different serve phases on a possible change in the rotational axes, our experimental outcomes do show a global change in control strategy or differences in the angular variability of the rotation axes, especially during the cocking phase. The results show that the rotation axis of a multi-articulated limb system changed from a geometrical articular axis to a mass- or inertia-based axis during different serve phases. It was hypothesized that rotation of one's upper limb around $\mathbf{e_3}$, because it is the axis of less inertial resistance, should facilitate internal-external axial humeral rotation. The nature of the cocking phase would make rotations about the geometric SH-EL axis more difficult and, thus, relying either on the SH-CM or $\mathbf{e_3}$ rotational axes would more likely occur in that phase.

Inter individual differences

The individual kinematic and dynamic patterns of the shoulder and elbow joint have shown that subjects tend to exploit similar patterns during the tennis serve. The subjects were all well trained athletes with a highly developed sport background in tennis. No strong individual differences could be uncovered related to the performance velocity however the subjects show differences in the exploitation of the rotation axes during the movement phases. The individual differences might be either due to the serve technique but also likely involve the exploitation of different frames of references and/or change from one frame of reference to another (Bernardin et al., 2005; Isableu and Vuillerme, 2006; Isableu et al., 2003; Berthoz, 1991; Paillard, 1991; Berthoz, 1991).

Interestingly, the SH-CM and e_3 axes were exploited throughout all subjects, which indicates that during the cocking phase subjects obey the MIR principle and tend towards the SH-CM/$\mathbf{e_3}$ trade-off axis regardless the serve technique. The acceleration phase is mainly organized on the basis of SH-EL rotation axis.

Serve phases

Previous studies have revealed differences in serve technique, evaluating the space time parameters, the kinematics and dynamics during the serve phases. To our knowledge, no study has evaluated a possible change in the rotational axis due to different serve phases in tennis. Previous research has shown a change of rotation axis in the control of 3D unconstrained arm movements during external-internal rotations of the shoulder at high velocities (Isableu et al., 2009). The nature of the cocking phase is quite similar to external-internal rotations of the shoulder and it is a crucial part of the throwing motion, bringing the arm in position for the acceleration and follow-through phase. Simulations of shoulder rotations (Isableu et al., 2009), have shown that rotations around the SH-EL axis reduce the contribution of interaction torque to net torque. In contrast to the cocking phase, the acceleration and follow-through phase depends on the passive interaction torque to increase the serving velocity. The net torque corresponds to the sum of muscle, interaction and gravity torques. The highest contribution of the INT was found during the acceleration and the follow-through phase. The high INT contribution during the acceleration

phase could be explained by maximizing the serving velocity and, during the follow-through phase, to actively break the movement as previously shown by (Hore et al., 2011). However, due to the small differences in the angular variability of the subjects, no assumptions can be made regarding the actual contribution of torque linked with the rotation axes.

The biomechanical and dynamical advantage to rotate around $\mathbf{e_3}$ was presented previously by (Isableu et al., 2009) during external-internal shoulder rotations and these results could be reproduced. It appears that the preferred rotatioIn axis in the cocking phase is the e_3 axis indicating that subjects tend towards an optimal mechanical solution.

8.1.5 Conclusion

Depending on the serve phase, our results showed that the rotational axis of a multi-articulated limb does change from an articular axis of rotation to either a mass- or inertia-based axis during the cocking phase. This finding was observed across all subjects. The individual serve styles of the subjects were consistent. These findings extend our understanding of the influence of how subjects perform and control their limbs in a 3D unconstrained tennis serve task. Furthermore, we gained additional insight in the organization of how rotation axes are used to organize sport actions and movement. Also we expanded our knowledge about the outcome that can be expected when coordinating limbs in tasks requiring fast rotations. Our results confirm the findings of previous research (e.g., (Isableu et al., 2009)) that showed a change of rotation axes due to high velocity profiles. The results of this study are essential and will improve the understanding of how sport movements such as throwing are performed, learned and executed.

8.1.6 Executive Summary

We examined whether the minimum inertia rotation axis ($\mathbf{e_3}$) is a key factor in motor performance and more particularly during the unconstrained 3D tennis serve movement. Subjects performed a flat tennis serve task and were asked to serve the ball as fast as possible at a target on the other side of the net. The purpose of this study was to test the hypothesis that change of the rotational axes occurs during the different phases of the tennis serve. A motion capture system was used to evaluate the contribution of the minimum inertia axis (**e**3), shoulder-center of mass axis (SH-CM) and the shoulder-elbow axis (SH-EL) to the performance in the different phases (preparation, cocking, acceleration and follow through) of the serve. The results showed that the limb's rotational axis does not coincide with one specific rotation axis during the preparation phase. However, the subjects show an effect due to the cocking phase and changed the rotation axis during the task and rotated their arm towards the minimum inertia ($\mathbf{e_3}$) and/or the mass axis (SH-CM). The rotation axes exploited during the acceleration phase are the SH-CM for one subject and the SH-EL axis for the other four. During the last phase, all subjects changed the rotational axis back to the geometrical axis.

The individual differences including the kinematics and dynamics of the subjects tend to be quite small and all subjects follow the same strategy during the cocking phase. Taken together, the results showed that all subjects changed the rotational axes during the four serve phases. However, due to the sample size, no general conclusions can be drawn.

Study VII	Description
Title	Change of rotation axes over time during a tennis serve
Subjects	5 subjects recruited from the University community
Hypothesis	Different tennis serve phases lead to a change of rotational axis
Task	Participants were asked to perform a flat tennis serve with the goal to hit the ball in a target area.
Measurement system	Vicon T40 12 camera passive optical motion capture system, frequency 250Hz
Measured Variables	Displacement of the 17 Markers put on the trunk, arm, forearm, hand and tennis racket
Data Analysis	Filter: Butterworth filter (2nd order) Joint Angle Computation Vector Computation Vector displacement computation Torque
Calculated Variables	Angular Axes displacement
Statistical Analysis	Individual analysis due to the small sample size of five subjects
Results	Subjects change the rotation axis due to the different throwing phases Contribution of SH-CM axis for cocking phase more frequent while the SH-EL axis is mainly used for acceleration and follow through phases of the tennis serve
Discussion	Based on the serve phases it can be considered, that subjects change the rotational axes during the movement and it seems that the MIR principle governs during the cocking phase even with an object attached to body. However due to the lack of statistical power no further analyses were performed.

8.2 Intercepting balls and the control of unconstrained 3D arm motions

8.2.1 Introduction

Controlling the 3D movement to catch a ball at the right place and time is very complex and has to be performed in high ranges of angular velocities and accelerations. Previous research has shown that the control of unconstrained 3D arm motions like external-internal rotations of the shoulder do depend the velocity of the performed task (Isableu et al., 2009; Isableu et al., 2013).

Due to different arm configurations involving flexion-extension of the elbow, there is almost always a separation between the axis of minimal inertia ($\mathbf{e_3}$) (Pagano and Turvey, 1995), the shoulder-center of mass axis (SH-CM) (van de Langenberg et al., 2008), and the shoulder-elbow axis (SH-EL) of the whole arm (Isableu et al., 2009);(Hirashima et al., 2003a; Hirashima et al., 2007b). During cyclic external-internal rotations at the shoulder, the rotation axis of the arm may coincide with one of these rotation axes. The choice of axis has implications on the amount of torque that must be produced, and also may have on the energy costs associated with the task. (Isableu et al., 2009) showed that the rotational axis used for controlling unconstrained 3D arm rotations at fast velocity coincide with a trade-off between the eigenvectors (**ei**) of the inertia tensor (**Iij**), specifically $\mathbf{e_3}$ (the axis of minimum inertial resistance) and SH-CM axis.

In everyday life, but especially in sports, one is obliged to react to different situations such as a falling cup in the kitchen or a ball being thrown at us. Intercepting or catching a ball means to place the hand in the trajectory of the ball, to the right place at the right time, to prevent the ball from leaving the interception plane (Peper et al., 1994). It has been shown that interceptive actions strongly depend on the visual cues and consequently the movement initiation and generation (e.g., (Michaels et al., 2006; Jacobs and Michaels, 2006). The longer the visual cues are available, the higher the probability to achieve the task in contrast to short time windows where the catching task can fail (Sharp and Whiting, 1974); (Marinovic et al., 2009).

Also time to contact has been extensively studied and has been shown to be a very important parameter for successfully achieving the interception task (e.g. (Savelsbergh et al., 1992); (Tresilian and Lonergan, 2002; Tresilian et al., 2009). Furthermore, the judgment of time to contact is affected by the speed of approach

and the size of the object (e.g. (McLeod and Ross, 1983);(DeLucia and Warren, 1994). Additionally, it has been shown that movement initiations appear earlier when the time to contact was reduced by higher movement velocity of the ball (Montagne et al., 2000);(Caljouw et al., 2004).

Since an intercepting task depends on a variety of constraints, the room of error may depend on temporal constraints (Senot et al., 2003), as well as individual skill and training (Mann et al., 2010) This chapter focuses on the control of an intercepting task, similar to catching in the lateral interception paradigm (Michaels et al., 2006; Jacobs and Michaels, 2006). As shown by (Arzamarski et al., 2007) a ball is intercepted as it passes on the side one's body. (Cesqui et al., 2012) provided evidence that the right time and place of the collision is not univocally specified by the CNS for a given target motion; instead, different but equally successful solutions can be adopted by different subjects when task constraints are loose.

In hitting tasks (Brenner et al., 2012) showed that the timing precision depended on the prediction of the moment of interest at the last moment at which the timing can still be adjusted (Brenner and Smeets, 2011).

The purpose of this study was to examine whether the minimum inertia resistance (MIR) principle (i.e., the spontaneous velocity-dependent change of rotation axes toward axes known to reduce inertial resistances and muscle torque) governs internal-external rotations at a fast velocity.

Rotating the arm around a specific axis also has an influence on the end effector or hand position during the interception task. Specifically, we are interested whether shortening the interception time window and the interception height would cause the limb to rotate around an axis closely aligned to $\mathbf{e_3}$, in order to minimize inertial resistances.

8.2.2 Methods

Subjects: 10 male subjects voluntarily participated in the experiment after signing a statement of informed consent pertaining to the experimental procedure as required by the Helsinki declaration and the EA 4532 local Ethics Committee. All participants were right-handed. They were aged 24 (± 3) years and all recruited from the university community. Handedness was determined using the ten-item version of the Edinburgh inventory (Oldfield, 1971). They were free of sensory, perceptual, and

motor (shoulder and elbow) disorders. They were naïve about the purpose of the experiment.

Procedures:

Participants sat on a chair and were instructed to intercept a ball, thrown at them by a ball throwing machine. The subjects were instructed to laterally intercept the ball as it passes on the side of the head. The initial starting position was set that the shoulder was abducted to the horizontal and the elbow flexed in a ninety degree angle with the forearm being parallel to the floor (Figure 59b).

The distance from the ball throwing device to the sternoclavicular joint was set to 2.5 meters (Figure 59a). Subjects were instructed to look at the ball throwing device and start the intercepting task as soon as they saw the ball. After each interception the subjects started over in the initial starting position.

The kinematic and dynamic analyses as well as the computation of the SH-EL, SH-CM, and $\mathbf{e}_3$ vectors were performed as described in Chapter 3.

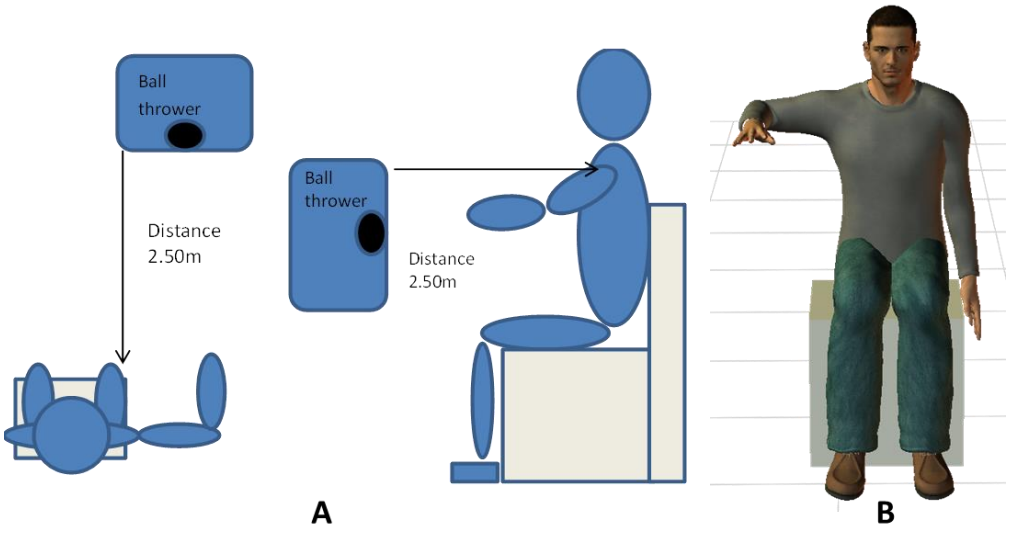

Figure 59 Initial set up of the subjects

Height related conditions

Three height related conditions were chosen to test different movement strategies during the lateral intercepting task. The first height was set to the chin of each subject, the second the ear and the third height was chosen to be the top of the head. The three heights were chosen twofold. First it gave individual anthropometric references that could be easily compared afterwards and second the movement pattern may vary due to the different heights (Figure 60).

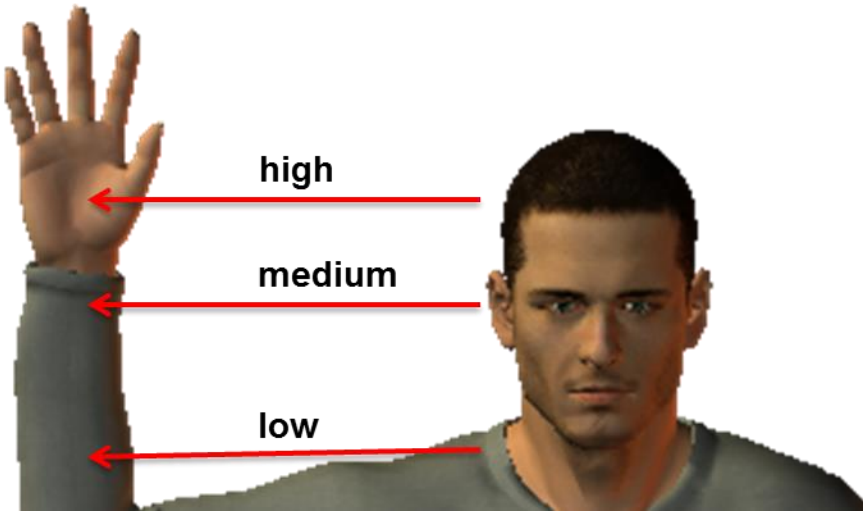

Figure 60 Interception heights of the experimental setup

The chin or low (l) height provokes the subject to intercept the ball rather low and obliges the subject to move the elbow downwards while the interception task. The ear or medium (m) height is an objectively neutral height and subjects could intercept the ball without the previous discussed downward movement of the elbow but could only be achieved by performing an external rotation of the arm. The high (h) height was chosen, to provoke a slight upward movement of the elbow during the interception.

Velocity related conditions

In each of the conditions described above, the interception task was performed in three different velocities (Table 19). The first condition was set to 7.15m/s, which left the subjects around 350ms to intercept the ball.

Table 19 Velocity conditions and time to contact

Velocity conditions			
mph	km/h	m/s	time to contact in [ms]
16.00	25.75	7.15	349.52
18.00	28.97	8.05	310.69
20.00	32.19	8.94	279.62

Additionally the velocity was increased to 8.05m/s , which left the subjects around 310ms to intercept the ball and finally the velocity of the ball thrower was set to 8.94m/s which left the subjects 280ms (Mazynn et al., 2007) to intercept the ball.

Statistical analyses

The individual parameters used in this paper were analyzed in separate analyses of variance (ANOVAs). Post hoc comparison of cell means was done using the Tukey method. A multivariate repeated measures analysis of variance (MANOVA, using the GLM module, Statistica 7 software) combining two three velocities (16mph vs. 18mph vs. 20mph) * three intercepting heights (low vs. medium vs. high) was then applied on the variability of angular displacement of each rotational axes (SH-EL, SH-CM, $\mathbf{e_3}$) with a .05 level of statistical significance.

8.2.3 Results

To analyze the variability of the 3D angular displacements of the rotation axes, we used the framework of the MIR principle and computed rotation axes of the arm that were affected by the experimental conditions.

Joint Amplitude and Joint velocity

A two way ANOVA (heights × speed) found no significant differences in the joint motion amplitude of the shoulder axial rotation for the different heights [$F(2, 18)=.216$, $p>.05$] and the velocities [$F(2, 18)=2.334$, $p>.05$] This indicates that the subjects regulated their interception movement such that the movement amplitude was kept constant regardless of the interception height and throwing speed. A two way ANOVA (heights × speed) found no significant differences in the contribution of the maximal angular joint velocity for the shoulder axial rotation for different heights [$F(2, 18)=.145$, $p>.05$] and velocities [$F(2, 18)=1.883$, $p>.05$]. Figures 61 & 62 shows representative trials made throughout the nine conditions by subject 1. The different hand path curvatures reflect different elbow and shoulder joint coordination patterns.

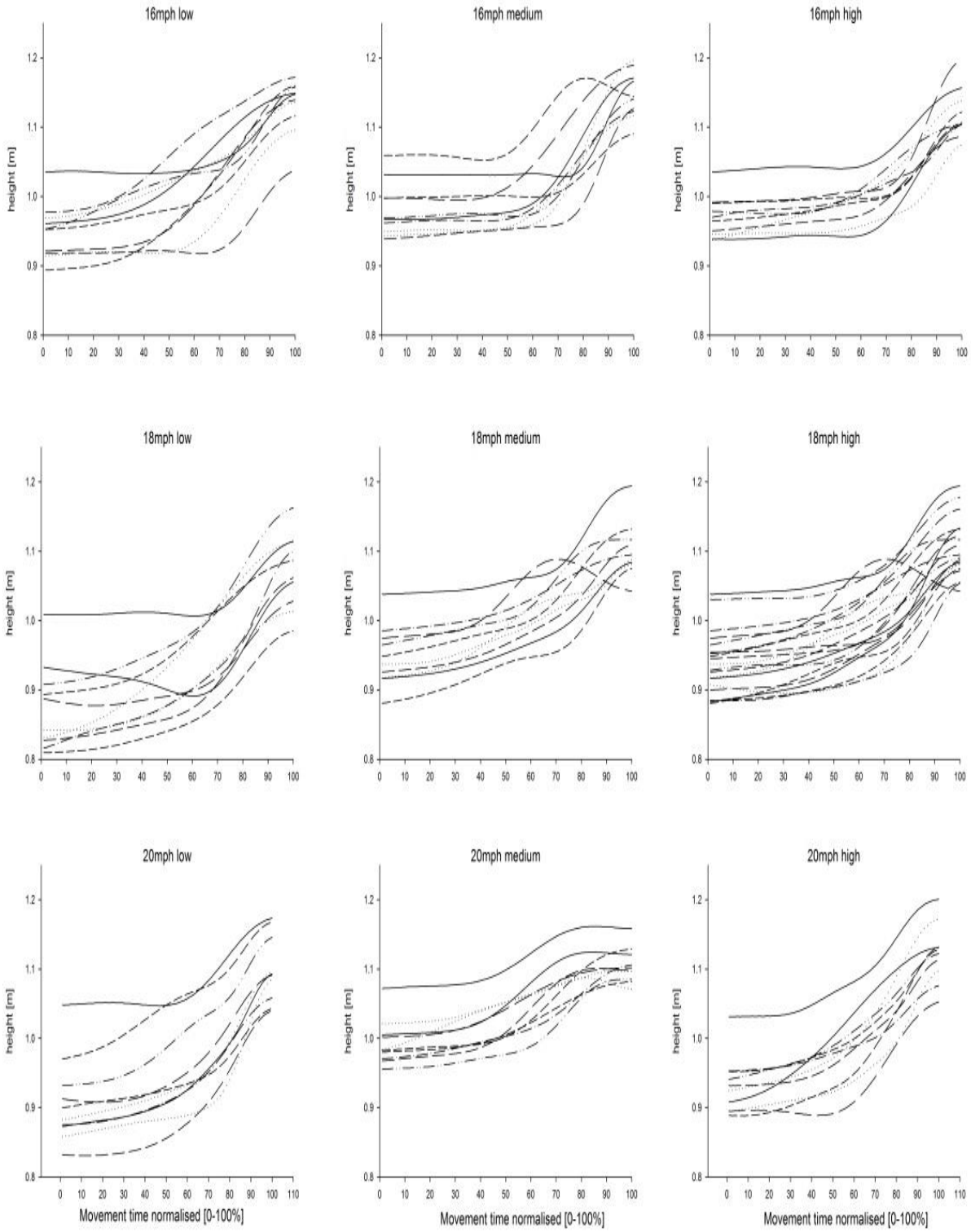

Figure 61 Subject 1 Hand movement traces

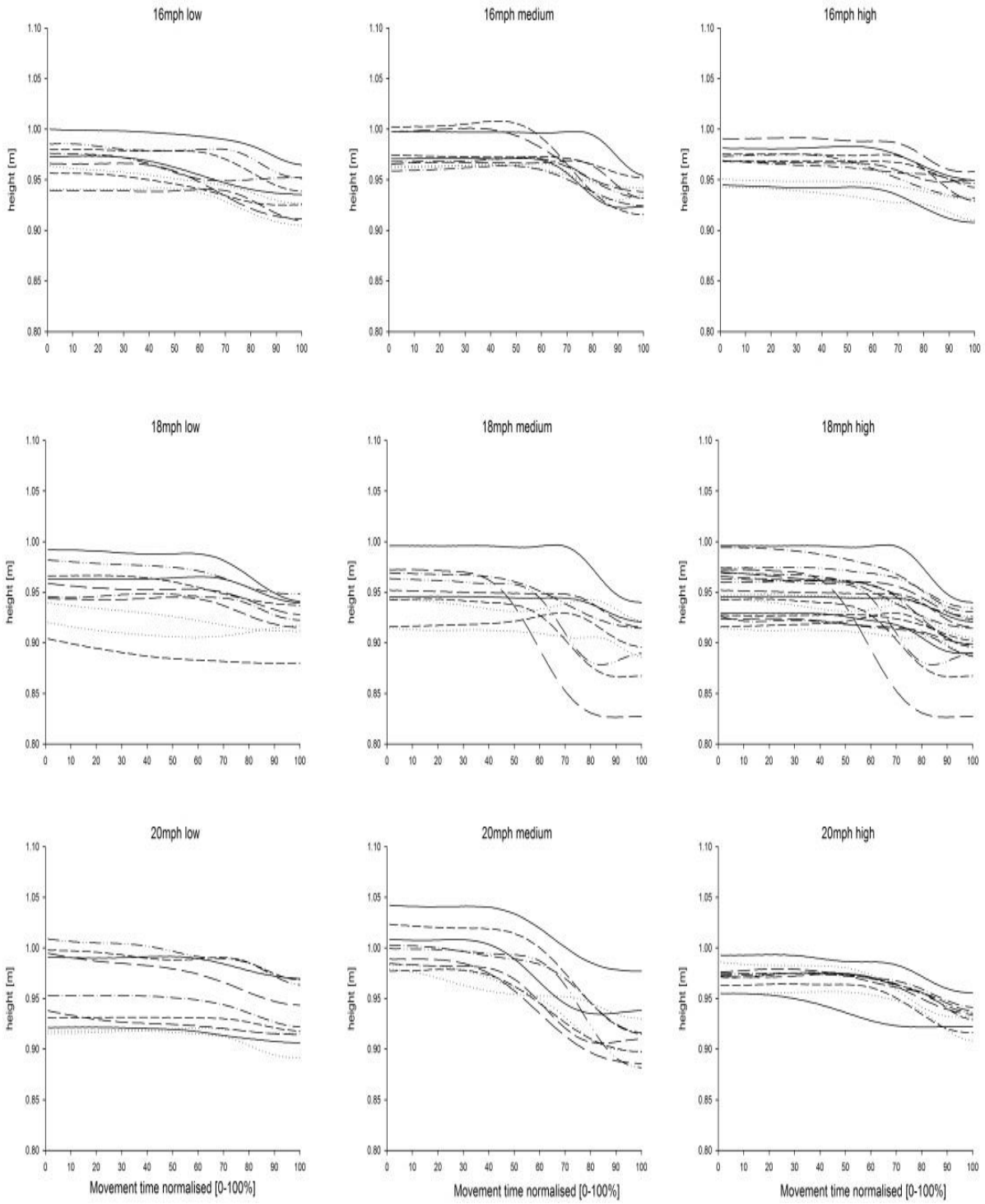

Figure 62 Subject 1 Elbow movement traces

Dynamics / Contribution Indexes

A two way ANOVA (heights × speed) followed by Tukey HSD post hoc comparisons showed significant differences in the contribution of the INT to NET torque for the shoulder axial rotation angle for the different velocities [$F(2, 18)=1.52$, $p<.05$] and the heights [$F(1, 7)=8.38$, $p<.05$] and also significant differences could be uncovered for the shoulder axial rotation ($p<.05$), see Figure 63.

A two way ANOVA (heights × speed) followed showed no significant differences in the contribution of the MUS to NET torque for the shoulder axial rotation angle for the different heights [$F(2, 18)=2.31$, $p>.05$] and the velocities [$F(2, 18)=6.54$, $p<.05$].

For the MUS contribution significant differences could be uncovered in the 16mph configurations and intercepting seemed different between the low and the medium height but also between the medium and the high interception height ($p<.05$). For the 20mph significant differences could be uncovered between the low and the medium height.

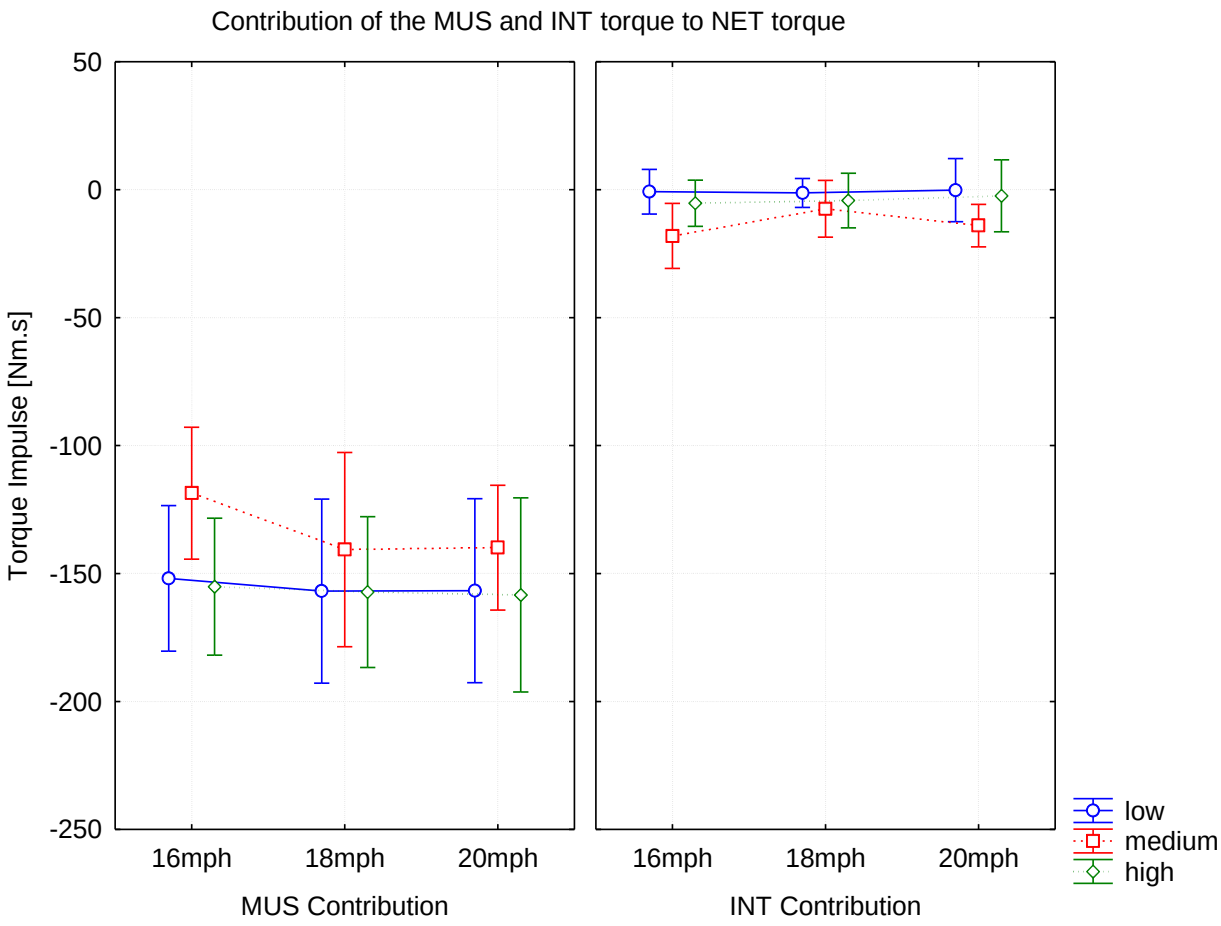

Figure 63 Contribution of the INT and MUS torque do the interception task

Tukey HSD post hoc comparisons revealed significant differences of the INT in the 16mph configurations and the contribution also changes between the low and the medium height ($p<.05$) but also between the medium and the high interception height ($p<.05$).

Rotation axes

The means of each variable were determined for each condition and subject (Table 21), and the data was analyzed using a multivariate analysis of variance (MANOVA) (Table 20), followed by Tukey HSD post hoc comparisons.

Table 20 MANOVA table

Manova Table	df	df	F
Axes	2	8	12.54**
Velocity	2	8	1.34
Heights	2	8	3.81
Axes x Velocity	4	6	0.33
Axes x Heights	4	6	19.85**
Velocity x Heights	4	6	3.10**
Axes x Velocity x Heights	8	2	1.90
* p < 0.05, ** p < 0.01, *** p < 0.001			

Velocity condition

Table 21 shows the mean angular variability of the axes in the three velocity conditions and the three height configuration respectively.

Mean angular displacement		**SH-EL**	**SH-CM**	**SH-e_3**
350ms (16mph)	low	0.15 ± 0.05	0.07 ± 0.02	0.07 ± 0.02
	medium	0.12 ± 0.06	0.08 ± 0.03	0.09 ± 0.04
	high	0.09 ± 0.06	0.07 ± 0.04	0.08 ± 0.05
310ms (18mph)	low	0.16 ± 0.08	0.10 ± 0.04	0.09 ± 0.04
	medium	0.13 ± 0.07	0.09 ± 0.04	0.10 ± 0.05
	high	0.07 ± 0.04	0.07 ± 0.04	0.08 ± 0.04
280ms (20mph)	low	0.13 ± 0.05	0.07 ± 0.02	0.06 ± 0.02
	medium	0.11 ± 0.06	0.08 ± 0.05	0.09 ± 0.05
	high	0.08 ± 0.06	0.08 ± 0.05	0.09 ± 0.05

16mph: In the slow velocity conditions, the variability of the SH-EL axis (0.15 ± 0.05 rad) in the low interception height condition was significantly ($p < .05$) larger than the variability of the SH-CM (0.07 ± 0.02 rad) and the e_3 (0.07 ± 0.02 rad) axis (variability between the two last axes did not differ). In the medium height condition the SH-EL (0.12 ± 0.06 rad) axis was also significantly larger than the variability of the SH-CM (0.08 ± 0.03 rad) axis and the e_3 (0.07 ± 0.04 rad) axis (variability between the two last axes did not differ). No differences could be found in the high interception configuration.

18mph: In the 18mph velocity conditions, the variability of the SH-EL axis (0.15 ± 0.08 rad) in the low interception height condition was significantly ($p < .05$) larger than the variability of the SH-CM (0.10 ± 0.04 rad) and the e_3 (0.09 ± 0.04 rad) axis. In the medium height condition the SH-EL (0.13 ± 0.07 rad) axis significantly differed from the SH-CM (0.09 ± 0.04 rad) and the e_3 (0.10 ± 0.05 rad) axis. No differences could be found in the high interception configuration.

20mph: In the fast velocity conditions, the variability of the SH-EL axis (0.13 ± 0.05 rad) in the low interception height condition was significantly ($p < .05$) larger than the variability of the SH-CM (0.07 ± 0.02 rad) and the e_3 (0.06 ± 0.02 rad) axis. In the medium height condition the SH-EL (0.11 ± 0.06 rad) axis significantly differed from the SH-CM (0.08 ± 0.05 rad) the e_3 (0.09 ± 0.05 rad) axis. No differences could be found in the high interception configuration, see Figure 64.

Height conditions

In the slow velocity conditions, the variability of the SH-EL axis (0.15 ± 0.05 rad) in the low interception height condition was significantly ($p < .05$) larger than the variability of the SH-EL axis in the high SH-EL (0.09 ± 0.06 rad) interception height. Also the angular variability of the SH-EL axis (0.15 ± 0.08 rad) was found to be significantly larger in the 18mph (0.07 ± 0.04 rad) and also in the 20mph the SH-EL (0.13 ± 0.05 rad) is larger than in the high interception height SH-EL (0.08 ± 0.06 rad) condition.

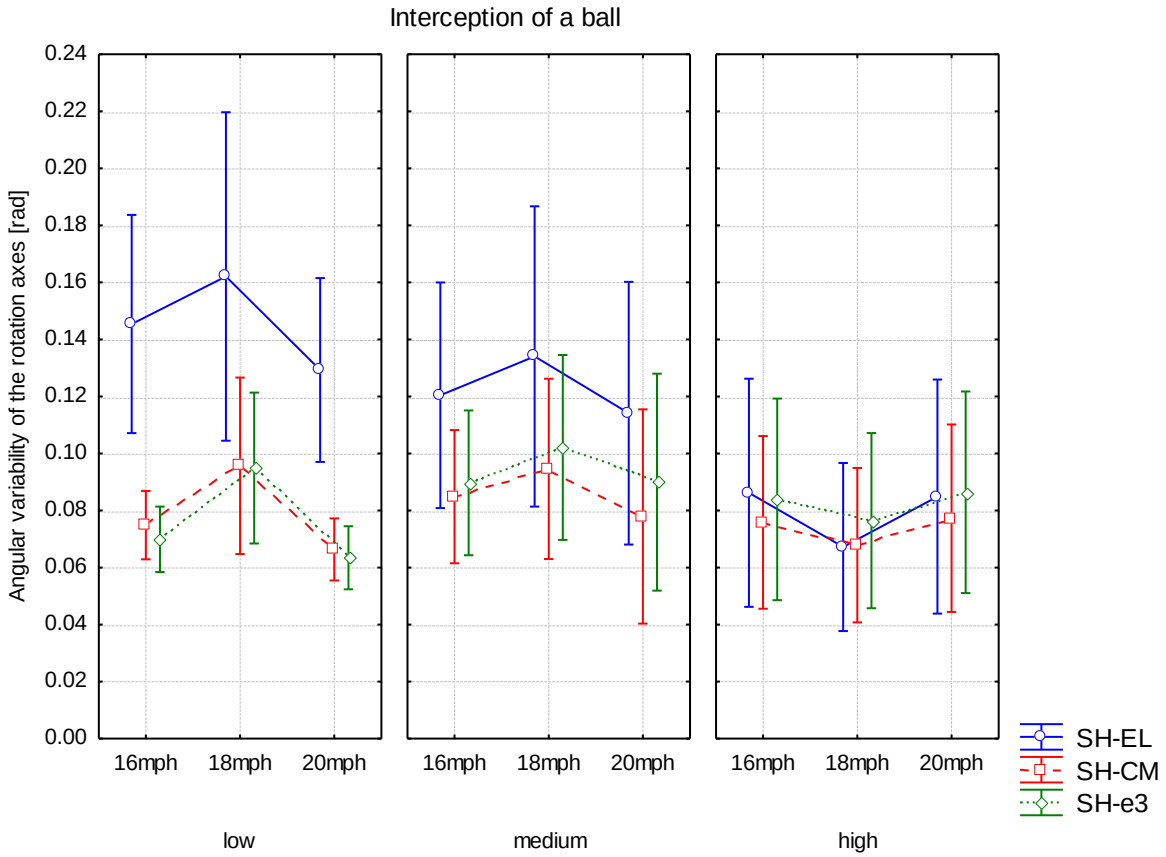

Figure 64 Angular variability of the rotational axes throughout the nine conditions

Individual strategies

Close inspection of our data also revealed that the $\mathbf{e_3}$ strategy is maintained across velocity and height conditions in some subjects (Figure 65). Other subjects showed a change of the rotational axis from $\mathbf{e_3}$ to SH-EL at fast velocity (contrary to (Isableu et al., 2009) results and predictions). Changes in modes of motor control can be due to sensory processing limitation imposed by $\mathbf{e_3}$, which provides a smaller interception window. However, it seems that the interception height has a larger impact on the exploited rotation axis than ball speed. Subjects were obliged to move to the arm upwards and no general control strategy could be uncovered. Subjects tend to rotate their arms around a trade-off axis between the three proposed rotation axes. .

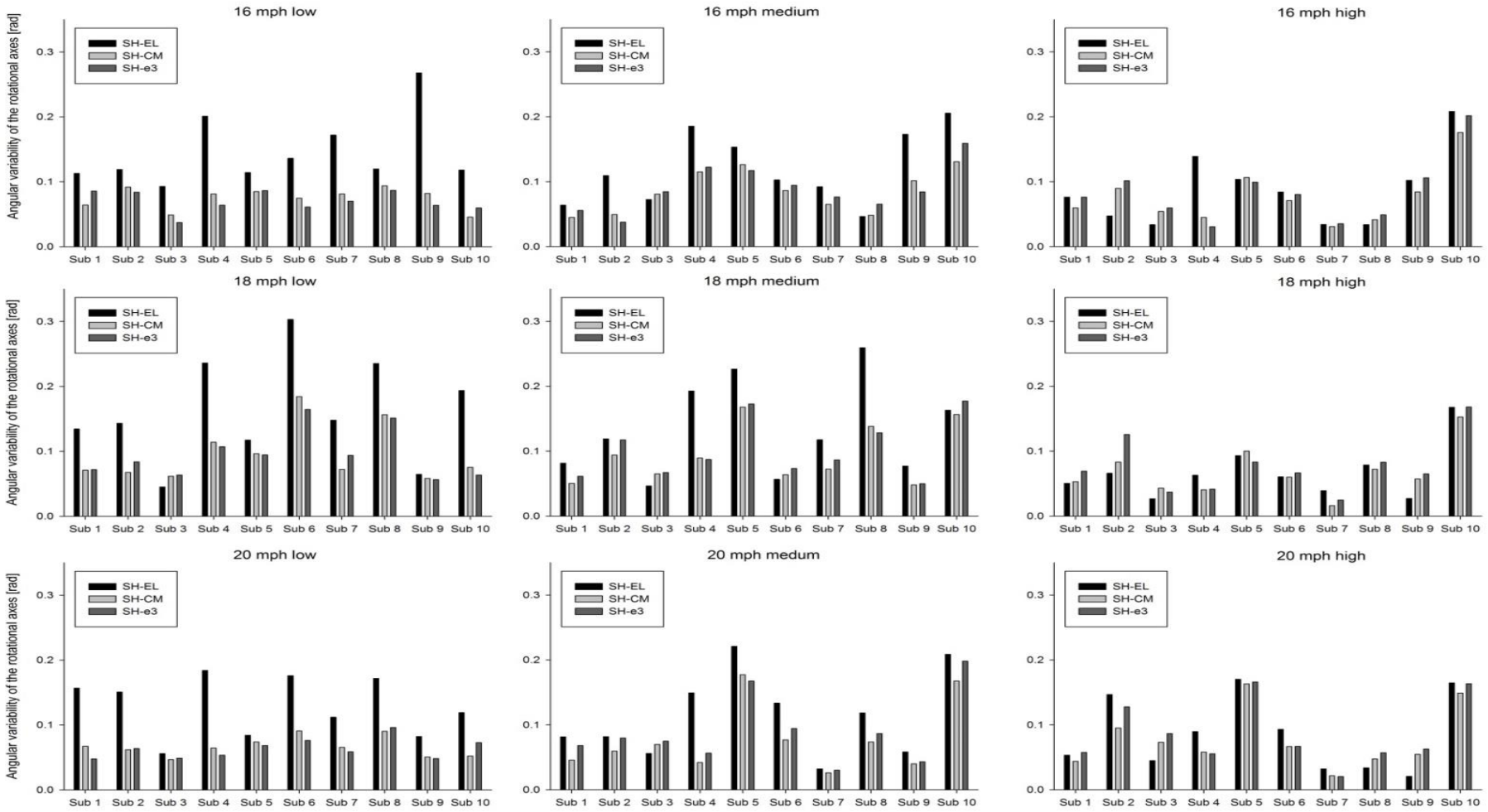

Figure 65 Inter individual differences throughout conditions

As the statistical analysis already showed, differences exist between certain interception conditions. The individual presentation of the MUS & Int torques revealed that the $\mathbf{e_3}$ strategy is maintained across velocity and height conditions in some subjects. Other subjects showed a change of the rotational axis from $\mathbf{e_3}$ to SH-EL at fast velocity (contrary to (Isableu et al., 2009) results and predictions). Changes in modes of motor control can be due to sensory processing limitation imposed by $\mathbf{e_3}$, which provides a smaller interception window. However, it seems that the interception height has a larger impact on the exploited rotation axis then ball speed. Subjects were obliged to move to the arm upwards and no general control strategy could be uncovered. Subjects tended to rotate their arms around a trade-off axis between the three proposed rotation axes.

8.2.4 Discussion

The aim of the study was to verify whether a change of rotation axes occurs when intercepting a moving object. In order to successfully answer this question, we examined whether interception height and time to contact play major roles in the choice of the rotational axes. The results of the experiment showed that subjects tend to rotate their arm around the e_3 axis obeying the MIR principle. Otherwise, no changes in the kinematics or the dynamics could be uncovered, which means that all subjects tended to follow the same control strategy. However, the movement amplitude simultaneously remained constant, which might be due to a decreased time to contact and subjects tended to moderate their movement or don't follow specific control pattern but simply react automatically.

Height related conditions

The angular variability of the rotation axes diminishes when the ball is intercepted in the highest condition and the subjects tend to rotate their arms in a tradeoff between the SH-EL, SH-CM & SH-e_3 axes. All subjects except for subject 2 tended to rotate their arms around either the SH-CM or e_3 axis, which seemed to be the preferred control strategy. Also, it has to be taken into account that the movement condition almost forces subjects to rotate around either the CM or $\mathbf{e_3}$ axis because the movement involves a downwards movement of the elbow. When intercepting the ball at the medium height, subjects tended to have different approaches and rotated their

arm either around the SH-EL axis or a tradeoff between the SH-CM & e_3 axes. However, in contrast to the low and medium interception heights, the high interception configuration forced the subjects to move the elbow upwards to successfully stop the ball. This change may lead to a different control pattern and, therefore, no rotational axis is consistently preferred.

Velocity-related conditions

As it has been previously reported, a change of rotation axes occurs during high velocity shoulder rotations (Isableu et al., 2009; Isableu et al., 2013) and this can be confirmed for the three velocity conditions. It seems that the configurations left enough time to voluntarily rotate the arm, obeying the MIR principle.

Torque contribution

The contribution of the muscle torque showed that it actively helped to bring the arm in the right position. As it has been previously reported, a change of the rotational axes occurs during high velocity shoulder rotations (Isableu et al., 2009; Isableu et al., 2013) and this can be confirmed for the three velocity conditions.

General discussion

Intercepting a ball or an object occurs in sport movement or when catching something in everyday life. The movement depends on multiple constraints such as the time window and position. In other words, the interception may change with stronger time constraints (Savelsbergh et al., 1992); (Tresilian and Lonergan, 2002; Tresilian et al., 2009) and will eventually fail when the time to contact is too short (Sharp and Whiting, 1974); (Marinovic et al., 2009). The specific velocity profiles of the ball were quite high and reducing the time to contact to under 250ms still led to specific control patterns in these configurations and the preferred rotation axis coincides with the SH-CM/e_3 axes and no temporal dependent failure was observed (Sharp and Whiting, 1974); (Marinovic et al., 2009).

The MIR principle is a motor control model that may lead to changes of rotation axes in higher velocity profiles (Isableu et al., 2009; Isableu et al., 2013). The velocity and height constraints of the task may have provoked a different strategy to intercept the ball.

The choice of the rotational axes depends on the nature of the movement and moving the elbow downwards may lead to preferences to rotate around $\mathbf{e_3}$ while moving the elbow upwards may prevent the exploitation of the $\mathbf{e_3}$ axis. Taken together, our results indicate that the subjects follow the MIR principle in two of three interception heights, regardless of the velocity profile.

Our results provide evidence that the subjects follow individual strategies during an interception task and that the high velocity profiles of the movement provoked a shift in the rotational axes (Isableu et al., 2009; Isableu et al., 2013). Cesqui et al. (2012) also provided evidence that a ball can be caught using various motor strategies. Inter-individual differences in motor control can appear due to the abundance of DOF. Task constraints provide various sensorimotor modes of catching a ball that are both equally efficient, i.e., vicarious. Further experiments will be necessary to explore whether interceptions involving different end positions with no specific axis being indicated, would yield in a change towards $\mathbf{e_3}$.

Also we expanded our knowledge about the outcome that can be expected when coordinating limbs in tasks requiring fast rotations. Our results confirm the findings of previous research (e.g., (Isableu et al., 2009) that showed a change of the rotational axes due to high velocity profiles.

8.2.5 Executive Summary

We examined the role of the minimum inertia resistance (MIR) axis in the control of unconstrained 3D catching movements in various ranges of velocity and catching hand height. Subjects were asked to catch a flying ball in three dimensional space at three different velocities, and at the three interception heights (Isableu et al., 2009) showed that shoulder joint rotations with elbow flexed leads to separations between the minimum inertia axis ($\mathbf{e_3}$), shoulder-center of mass axis (SH-CM) and the shoulder-elbow axis (SH-EL). Humeral axial rotation around $\mathbf{e_3}$ axis is facilitated due to the combined use of muscle and Int torque to net torque and is mostly exploited at fast velocity. The purpose of this study was to test the hypothesis that subjects should take advantage of rotating the arm around the $\mathbf{e_3}$ axis to catch a fast moving ball, and this is regardless of the height conditions. The results showed different control strategies in an interception task, fixing certain rotational axes and changing the interception height and ball velocity may lead to a changes in their motor control strategy. The results showed that the limb's rotational axes coincided with the SH-CM and e_3 axes across conditions except for the high interception configuration. The choice of rotational axes changes with height. Throughout all velocity profiles, the subjects tended to obey the MIR principle even though the SH-EL axis was exploited in the high interception configuration. Taken together, the results showed that subjects have the tendency to use the minimum inertia ($\mathbf{e_3}$) and/or the mass axis (SH-CM) when intercepting at lower height but rotate around a trade-off axis in the high configuration.

Study VIII	Description
Title	Velocity and height dependent changes of rotational axes during an interception task
Subjects	10 subjects recruited from the University community
Hypothesis	High velocity and interception heights will lead to a change of rotational axis
Task	Participants sat upright on a chair and intercepted balls in three different velocities and three target heights respectively.
Measurement system	Vicon V8i eight M2 camera passive optical motion capture system, frequency 250Hz
Measured Variables	Displacement of the 13 Markers put on the trunk, arm, forearm and hand
Data Analysis	Filter: Butterworth filter (2nd order) Joint Angle Computation Vector Computation Vector displacement computation Torque Time of contact
Calculated Variables	Angular Axes displacement
Statistical Analysis	Repeated measured MANOVA Post hoc test (Tukey HSD post hoc)
Results	Subjects do not change the rotation axis due to the different velocity profiles but due to different interception heights
Discussion	Based on the different interception heights subjects tend to change their interception strategy. In contrast to the height differences, no difference in the strategies could be observed during the experiment.

Chapter 9

9 General Discussion

The research described in this dissertation investigated the role of the minimal inertia axis in the kinesthetic control of unconstrained 3D rotational movements. Unconstrained 3D movements were both goal-directed as in athletic movements or following fundamental research protocols as proposed by (Isableu et al., 2009). A synthesis of the eight experimental protocols is shown Table 22.

Table 22 Task dependent experiments

Task movement	Conditions	Internal-external rotation of the shoulder	
Athletic movements maximizing		With	without
precision	3 different target heights 2 target distances	/	**Dart throwing**
precision	Official Rules of the International Darts Federation	/	**Dart throwing Novices vs. Experts**
precision and velocity	3 interception heights 3 ball speeds	**Interception task**	/
precision and velocity	Flat tennis serve with maximal precision and velocity	**Tennis serve**	
Velocity	Throwing a ball as hard as possible	**Overarm throwing**	/
Non-athletic movements maximizing		**Internal-external rotation of the shoulder**	
the angle between the SH-CM & SH-e_3	2 sensory conditions 2 motion frequencies	**Internal-external rotation**	/
	2 sensory conditions 2 motion frequencies Task was performed with both arms	**Internal-external rotation handedness**	/
	4 shoulder elevation angles 2 motion frequencies	**Internal-external rotation gravitational torque**	/

Pagano and colleagues (Garrett et al., 1998; Pagano and Turvey, 1995; Pagano et al., 1996b; Pagano, 2000; Pagano and Turvey, 1998; Riley and Turvey, 2001) initially introduced the role of the inertia tensor as a major spatial invariant of egocentric perception of one's limbs during movement. Perceiving and controlling the direction of the limbs, without visual cues may be constrained by invariants tied to the mass distribution as the eigenvector of the inertia tensor (Garrett et al., 1998; Pagano and Turvey, 1995; Pagano et al., 1996b; Pagano, 2000; Pagano and Turvey, 1998; Riley and Turvey, 2001).

The conclusions of these earlier conducted studies are still limited because systematic evaluation of the differences between the CM and $\mathbf{e_3}$ was not carried out. This led to the conclusion that the perception and the control of the limbs in mono and multi-articulated movements were mainly constrained by the center of mass. The conclusions and findings have to be revisited because the contribution of $\mathbf{e_3}$ is not relevant since no rotations are involved in the movement (van de Langenberg et al., 2007). Another drawback in the initial theories is the fact that the movements are performed at slow motion frequencies and to perceive the effect of inertia; high movement accelerations are necessary. This led to the assumption that high acceleration or motion frequencies maximize the role and the way inertial cues are perceived. Introducing rotations to an arbitrary movement as in external-internal rotation of the arm about the shoulder, showed the influence of $\mathbf{e_3}$ in the control of multi-articulated movements (Isableu et al., 2009).

Within these constraints the main objective of this work was to extend the knowledge of the role of the minimal inertia axis in the kinesthetic control of unconstrained 3D movements in both non athletic and athletic arm rotation tasks.

9.1 Role of minimal inertia axis $\mathbf{e_3}$

The role of $\mathbf{e_3}$ was first studied in the context of non-athletic gestures as pointing or reaching (Pagano et al., 1994; Pagano and Turvey, 1995). Isableu et al. (2009) showed the role of the minimum inertia resistance axis during cyclic shoulder rotations at different motion frequencies.

The first three experiments followed the initial and promising experiment of Isableu, (2009) and examined the role of $\mathbf{e_3}$ during external-internal shoulder rotations. The

experimental setup allows for the separation of the rotational axes of the arm naturally without the use of external masses. However, throughout the first three experiments of this dissertation, no global change of the rotational axes towards the minimum inertia resistance axis was observed. The added constraints to investigate the MIR principle were manifold. Neither conditions that involved kinesthetic vs. visuo-kinesthetic feedback nor changing the motion frequency or the static gravity torque reproduced the same results as initially proposed. Global effects were usually covered by inter-individual strategies. Large individual differences have also been reported in past experiments investigating the role of the inertia tensor in pointing or wielding tasks (Garrett et al., 1998); (Kingma et al., 2004); (Bernardin et al., 2005); (Withagen and Michaels, 2005);(van de Langenberg et al., 2008).

We expect that individual differences may be evident in our results due to the fact that subjects are free to make cyclic rotations of their arm coincident with the different axes of rotation (SH-EL; SH-CM or $\mathbf{e_3}$). Earlier studies have shown that subjects do not always behave in accordance with the most appropriate physical parameters (see tasks (Garrett et al., 1998));(Bernardin et al., 2005) ; (Bray et al., 2004) ; (Isableu et al., 2003; Isableu and Vuillerme, 2006); (Withagen and Michaels, 2005).

The question arises if the relevant rotational axes are mechanically controlled or if the rotational axes are an emergent phenomenon constraining perception and the control of DOF when the task demands increase. Multiple solutions have been proposed over time and the CNS may depend on invariants such as the rotational inertia, static torques or geometrical invariants such as joint angles. The CNS has to identify the relevant rotational axis that allows motor coordination to be adaptive and proficient in demanding tasks (Darling and Hondzinski, 1999; Worringham and Stelmach, 1985; Soechting, 1982; Pagano and Turvey, 1998; Pagano and Turvey, 1995).

It appears that the participants of the three studies individually chose their solution to succeed. Following this thought, one of the initial hypotheses is that only high accelerations maximize the role and the way inertial cues are perceived. We theorize that velocity demands in fast movement conditions should lead all subjects towards an axis of rotation that minimizes rotational resistances (i.e., $\mathbf{e_3}$) which also has a

consequence on the contribution of interaction, joint muscle and gravitational to net torque.

Thus, the choice has a significant impact on the motor coordination proficiency. It is still under discussion if the CNS controls movements as a consequence of an interaction between limb mechanics and motor commands (Flanagan and Lolley, 2001); (van de Langenberg et al., 2007; van de Langenberg et al., 2008) or if the CNS predictively compensates for stability loss due to the mechanical effects of interaction torque (INT) (Dounskaia et al., 2002; Dounskaia et al., 2005), (Goble et al., 2007); (Hirashima et al., 2003a; Hirashima et al., 2007b).

During the experiments involving high acceleration profiles as in overarm throwing and flat tennis serve, the mechanical effects of the movements are very important. Throwing is a goal-related task and the velocity and kinematic profiles change respectively (Hore et al., 1996);(Smeets et al., 2002) and may also provide new insights into how the CNS coordinates multiple DOF in the control of throwing and hitting actions.

Both experiments involve large internal-external rotations of the shoulder as previously reported in the initial experiment of Isableu (2009) and as the cocking phase is quite similar to the presented experiment a trade-off between CM and the $\mathbf{e_3}$ axes was found to be the preferred control strategy. The cocking phase is crucial and the goal of this phase is to move the elbow forward with maximum external shoulder rotation to initiate the acceleration phase with the ball release. Similar results were found during the tennis serve and it seems that the MIR principle governs during specific phases of the high velocity movements that involve large shoulder rotations. Large shoulder rotations also occur during spontaneous interception tasks. Following the same idea, the interception experiment limited the movement of the whole body to impose additional constraints on the subjects.

The participants of the study were asked to laterally intercept a ball at three different heights and three velocities. The choice of the rotational axes during the low and medium interception height was unaffected by the velocity of the ball and the rotations were also performed around a trade-off axis between CM and $\mathbf{e_3}$. An

exploitation of this axis could be explained by the velocity profiles of the movement and reducing the products of inertia may be the best control strategy to successfully intercept a ball. However, when intercepting the ball in the high condition subjects tended to not follow a specific axis but show individual patterns as in the first three experiments.

The results are very promising but at the same time they have to be interpreted carefully. Is the perception of the the center of mass (van de Langenberg et al., 2007) or the inertia tensor (Pagano and Turvey, 1995); (Solomon and Turvey, 1988; Turvey et al., 1989) (Pellionisz, 1985) responsible for this specific control strategy or are the movements already constraining the possible solutions?

Wouldn't it be also possible that the movements constrain the participants in such a way that they are obliged to follow specific strategies? So far the principle of self-organization cannot be excluded in the possible explanations. In mechanics, rotations around the minimum inertia resistance axis are very efficient and in motor control the tensor network theory claims that the CNS extracts information from the geometric vectors and tensors but also the shape, length, weight and weight distribution to gather haptic information of an object or even a limb (Burton et al., 1990); (Pagano et al., 1993); (Turvey et al., 1989; Solomon and Turvey, 1988; Kingma et al., 2000).

Also certain control theories may depend on the skill level of the subject (Isableu et al., 2009) or even on the anthropometry (Chiari et al., 2002). However, the in the dart throwing task no differences could be uncovered between novice and expert dart players. During both dart experiments subjects seem to stabilize the SH-EL axis to improve the throwing outcome. The exploitation of the SH-EL axis has been shown to reduce the mechanical effects of interaction torque at higher velocities, changing the contribution of the joint muscle torque totally to the net torque. Moreover, the high contribution of joint muscle torque to interaction torque modifies the appropriate scaling of joint muscle torque and the processing of proprioceptive inputs (Ebaugh et al., 2006b; Ebaugh et al., 2006a). However, exploiting specific rotation axes may not only be due to the proprioception but to the frames of references used by each subject. The choice of the reference frames is task dependent but especially reliant

on the subjects preference. McIntyre et al. (1998) showed the use different frames of reference during aiming tasks. In pointing tasks the regulation of the shoulder angle is interpreted as a geometric centered reference frame of the limb (Soechting and Flanders, 1989). The hand can also become a reference frame, as the target itself (Soechting and Flanders, 1992). Asch and Witkin (1948), showed the existence of a strong inter individual variability when exploiting visual information. The issue of inter individual variability is largely emphasized in the literature, especially during spatial orientation (Isableu et al., 1998), pointing (Adamovich et al., 1998) and postural control tasks (Amblard and Cremieux, 1976; Isableu et al., 1997) ; (Guerraz et al., 2000).

Throughout the experiments the MIR principle has not shown its generalizability and as long as not further experiments show its applicability, the principle has to be used carefully.

Chapter 10

10 Limitations

10.1 Technological Limitations

One of the major drawbacks in human movement analysis are the multiple sources of error. Starting with the motion capture system, the absolute precision of the 3D marker tracking strongly depends on the quality of the system itself, the size of the markers, the camera setup and the calibration. If the setup of the hardware is not appropriate the errors will be accumulated and finally lead to large errors in the marker raw data. The positioning of the markers on the human body is also a very delicate part in the experiment and small deviations of the real position may lead to large calculation errors in the kinematics or the computation of joint torque.

The analysis of raw marker data can yet be another source of error. Filtering the 3D positions or applying other signal processing techniques may hide relevant information and the calculations will be affected. Furthermore the analysis of the data in general involves custom written codes or third party software and both need to be validated before one can analyze real datasets.

10.2 BSIP Estimation

The estimation of BSIP is a crucial step in the analysis of inverse dynamics and, in the case of this dissertation, the computation of the SH-CM and the e_3 axis. To estimate individual BSIP it is either very cost or time intensive or the estimation is reduced to validated regression methods including scaling functions based on previous databases. The regression methods have a few downsides since the BSIP are not individualized and are scaled for specific ethnic populations. During this dissertation, seven of the eight conducted studies fit the sample population but the overarm throwing experiment was conducted in Japan using local students as participants. New BSIP estimation techniques have been developed (Venture et al., 2009b; Venture et al., 2009a) that may help to improve the inverse dynamics and the rotation axes computations conducted in this dissertation.

10.3 Rotation axes computation

In the initial experiment of (Isableu et al., 2009) the MIR principle is based on the role of the inertia tensor during unconstrained 3D movements and, more specifically, $\mathbf{e_3}$ the principal axes of inertia with the minimal resistance to rotational acceleration. As it was originally proposed, three particular vectors were considered: SH-EL corresponding to the upper-arm geometrical axis defined between the centers of the shoulder and the elbow joints, SH-CM linking the shoulder joint center to the center of mass of the entire arm, and $\mathbf{e_3}$ is the eigenvector corresponding to the smallest eigenvalue of the arm's inertia tensor expressed at the shoulder joint.

The computation of the rotation axes depend on the subjects' measured body mass, limb segment lengths, the estimation of BSIP (mass, center of mass position relative to the proximal end of the segment, inertia tensor at the centre of mass expressed in the segment coordinate frame) using the regression equation proposed by (Dumas et al., 2007). The estimation of these parameters is under ongoing research but the computation of the rotational axes could be influenced and change the results gained in this dissertation.

The decision around which axis the movement is performed is also critical. To quantify the variability of the three vectors ($\mathbf{e_3}$, SH-CM, and SH-EL) using the elevation and azimuth angles in the reference frame of the torso and considering the axis with the minimal variability as the exploited rotation axis could also be questioned.

Another point to keep in mind is the real and instant axis of rotation. The proposed rotation axes may not coincide with the real axis of rotation leading to wrong interpretations when only focusing on the three proposed rotational axes.

10.4 Biomechanical model

The biomechanical model described in Chapter 3 also has some limitations and drawbacks. The anatomical movement of the shoulder is not simply limited to the glenohumeral joint with its three rotational DOF but a total of four joints in the shoulder complex allow additional DOF as translational movements. This is a very important point to consider because the center of rotation (CoR) is influenced by the DOF and its estimation technique. Estimating the CoR of the shoulder is quite complex and during this dissertation a regression rather than a functional approach

was used. The CoR estimation is specifically crucial in this case because it is the origin of the rotation axes. False estimations strongly influence the computation of the axes but also the interpretation of the results. Adding DOF to the model to analyze the movements in more detail could be a solution to improve the results of this work. Additionally, the implementation of objects to the body as the ball in the overarm throwing experiment or the tennis racket during experiment 7 will influence the computations. The decision to implement an object to the hand is directly related to the movement of the object in the hand. In the case of the tennis serve, the racket was rigidly modeled to the hand which may be a loss of information. The small synthetic ball was neglected in the computations of the overarm throwing task because the instant when the ball leaves the hand could not be determined.

10.5 Experimental limitation

Pagano & Turvey (1995) and van de Langenberg et al. (2007) proposed a method to separate the SH-CM and the e_3 axis during movements. As initially proposed, attaching masses to the arm via an exoskeleton may have multiple advantages when studying pointing movements or the proprioceptive role of the inertia tensor. Unfortunately this method is not possible to apply in the control of unconstrained 3D movements with large amplitudes and changing joint configurations. The first three experiments evaluating the role of the MIR principle in the control of unconstrained 3D shoulder rotations were chosen to guard a constant separation between the SH-CM and e_3 vector. The other experiments did not allow for a constant separation between the axes.

10.6 Simulations

To gain a deeper understanding of the role of $\mathbf{e_3}$ during unconstrained 3D movements, multi-body simulation should be developed to gain an insight of the choice of the rotation axes and the kinematic and dynamic consequences. In other words, simulations are necessary to evaluate the choice of the rotational axes due to a given dynamic or kinematic parameter. The model could predict results but also help in the planning of the experimental setup. Musculoskeletal modeling could improve the understanding of the choice of the rotation axes in 3D movements. The technological progress over the last few years has led to very sophisticated

musculoskeletal multi-body models that could shed light on to tne recruitment of specific muscle groups. An observed change of the rotation during a movement could then be explained by the simulated results but also in a more physiological way in terms of muscle recruitment and energy consumption.

10.7 Inter individual differences

Large individual differences have been reported in the experiments conducted in this dissertation. The large inter-individual differences may have masked differences in control strategies as previously reported (Isableu et al., 2009). Another alternative would be to increase the sample size to properly cluster the subjects. Furthermore, the sample size of the conducted experiments does not allow a cluster analysis to separate participants showing individual differences suggesting alternative sensory-motor strategies. A possibility to reduce the effect of inter-individual differences is to prescreen the participants. This could be as simple as limiting the recruitment of the participants to sportsmanship, fitness level or motor control capacities.

Chapter 11

11 Perspective

This project aimed to investigate the role of rotation axes in motor control and specifically the proprioceptive detection and exploitation of $\mathbf{e_3}$ (Isableu et al., 2009) during the control of 3D unconstrained multi-joint movements in biological limbs.

The investigation of the proprioceptive detection and exploitation of $\mathbf{e_3}$ can be extended to hybrid limbs (exoskeleton or automated prosthesis) and to subjects with reduced mobility due to aging, central disorders (proprioceptive deficits, neuropathy) or handicaps (limb amputation). Moreover, further research will shed light into the ways in which the CNS limits biomechanical instabilities

1) to prevent the risk of injuries,
2) to improve the performance in elite athletes,
3) to facilitate and decrease the duration of learning
4) to facilitate learning of complex multi-joint coordination in athletic activities.

Improving the abovementioned limitations of this dissertation and restraining the margin of error to a minimum, could improve the results gained so far, but also improve the understanding of the control and learning of 3D multi-joint movements of biological limbs (e.g., in athletic subjects, in patients with altered mobility) and hybrid limbs for amputees (motorized prosthetic devices).

Chapter 12

12 Conclusion

Motor activities in both sport and everyday life require the production of complex 3D rotational movements of the upper limbs. Unconstrained 3D movements can be controlled around different rotational axes including i) the geometrical articular axis, ii) the principal axis of inertia or iii) an axis through the arm's center of mass (Isableu et al., 2009). Each one of these axes belongs to a distinct spatial frame of reference. The axis around which the arm rotates defines the contribution of muscle, interaction and gravitational torques. The choice also influences the proprioceptive and motor consequences for the regulation of movement and the proficiency with which 3D movements can be controlled in demanding situations. Given that various limbs or body configurations typically require flexion of the joints, there is almost always a separation between these axes of rotation and optimal motions may involve the employment of one axis over the others.

The results of the experiments reveal that rotations around the minimum inertia resistance axis $\mathbf{e_3}$ occur and that the MIR principle can be accounted as a valid motor control strategy. However, the chosen experiments and the lack of predictions from multi-body simulations only provide little evidence of the generalizability of the MIR principle.

The elbow configurations employed during the experiments are very close to many athletic configurations and the absence of invasive mechanical devices used to alter the mass distribution of the limb reinforces the ecological validity of the results for some participants. The large inter-individual differences may have masked a more global motor control strategy. However, these findings extend our understanding of the rotational axes used to organize action but also show their relevance and the proficiency that can be expected when coordinating limbs in tasks requiring fast rotations.

13 References

Adamovich, S. V., Berkinblit, M. B., Fookson, O., Poizner, H., (1998). Pointing in 3D space to remembered targets. I. Kinesthetic versus visual target presentation. J.Neurophysiol. 79, 2833-2846.

Admiraal, M. A., Keijsers, N. L., Gielen, C. C., (2004). Gaze affects pointing toward remembered visual targets after a self-initiated step. J Neurophysiol 92, 2380-2393.

Amazeen, P. G., Schmidt, R. C., Turvey, M. T., (1995). Frequency detuning of the phase entrainment dynamics of visually coupled rhythmic movements. Biol.Cybern. 72, 511-518.

Amblard, B., Cremieux, J., (1976). Role of visual information concerning movement in the maintenance of postural equilibrium in man. Agressologie. 17, 25-36.

Anderson, K. N., (1994). Mosby's Medical, Nursing and Allied Health Dictionary. Mosby, St. Louis.

Araújo, D., Davids, K., Bennett, S., Button, C., Chapman, G., (2004). Skill Acquisition in Sport: Research, Theory and Practice. In: Williams, A. M., Hodges, N. J. (Eds.), Taylor & Francis, London: Routledge, pp. 409-433.

Aruin, A., Ota, T., Latash, M. L., (2001). Anticipatory postural adjustments associated with lateral and rotational perturbations during standing. Journal of Electromyography and Kinesiology 11, 39-51.

Arya, A. P., (1998). Classical mechanics. Prentice-Hall International., London.

Arzamarski, R., Harrison, S. J., Hajnal, A., Michaels, C. F., (2007). Lateral ball interception: hand movements during linear ball trajectories. Exp Brain Res 177, 312-323.

Asch, S. E., Witkin, H. A., (1948). Studies in space orientation. II. Perception of the upright with displaced visual fields and with body tilted. J.Exp.Psychol. 38, 455-475.

Assaf, D., (2004). Space representation using multiple references frame in the motor system. The senate of the Hebrew University.

Atchonouglo, E., Vallée, C., Monnet T., (2008). Identification of the ten inertia parameters of a rigid body. Journal of Applied Mathematics and Mechanics 72, 22-25.

Atkeson, C. G., Hollerbach, J. M., (1985). Kinematic features of unrestrained vertical arm movements. J Neurosci 5, 2318-2330.

Bagesteiro, L. B., Sainburg, R. L., (2002). Handedness: dominant arm advantages in control of limb dynamics. J.Neurophysiol. 88, 2408-2421.

Bagesteiro, L. B., Sainburg, R. L., (2003). Nondominant arm advantages in load compensation during rapid elbow joint movements. J.Neurophysiol. 90, 1503-1513.

Bastian, A. J., Martin, T. A., Keating, J. G., Thach, W. T., (1996). Cerebellar ataxia: abnormal control of interaction torques across multiple joints. J.Neurophysiol. 76, 492-509.

Batista, A. P., Buneo, C. A., Snyder, L. H., Andersen, R. A., (1999). Reach plans in eye-centered coordinates. Science 285, 257-260.

Bennett, D. J., Hollerbach, J. M., Xu, Y., Hunter, IW., (1992). Time-varying stiffness of human elbow joint during cyclic voluntary movement. Exp Brain Res 88, 433-442.

Benoit, D. L., amsey, D. K., amontagne, M., Xu, L., retenberg, P., enstrom, P., (2006). Effect of skin movement artifact on knee kinematics during gait and cutting motions measured in vivo. Gait Posture 24, 152-164.

Berkinblit, M. B., Fookson, O. I., Smetanin, B., Adamovich, S. V., Poizner, H., (1995). The interaction of visual and proprioceptive inputs in pointing to actual and remembered targets. Exp.Brain Res. 107, 326-330.

Bernardin, D., (2005). Contribution du tenseur d'inertie à la perception et au contrôle de l'orientation d'un geste pluri-articulé de pointage. Thèse de 3ème cycle 1-230.

Bernardin, D., Isableu, B., Fourcade, P., Bardy, B. G., (2005). Differential exploitation of the inertia tensor in multi-joint arm reaching. Exp.Brain Res. 167, 487-495.

Bernstein, N., (1967). The coordination and regulation of movements. Pergamon, Press, London.

Berret B, Darlot C, Jean F, Pozzo T, Papaxanthis C, et al. (2008) The inactivation principle: mathematical solutions minimizing the absolute work and biological implications for the planning of arm movements. PLoS Comput Biol 4: e1000194.

Berret, B., Chiovetto, E., Nori, F., Pozzo, T., (2011). Evidence for Composite Cost Functions in Arm Movement Planning: An Inverse Optimal Control Approach. PLoS Comput Biol 7, e1002183.

Berthoz, A., (1991). Reference frames for the perception and control of movement. In: Paillard, J. (Ed.), Brain and Space. Oxford University Press, Oxford, pp. 81-110.

Bonacci, J., Saunders, P. U., Hicks, A., Rantalainen, T., Vicenzino, B. G., Spratford, W., (2013). Running in a minimalist and lightweight shoe is not the same as running barefoot: a biomechanical study. Br J Sports Med 47, 387-392.

Bray, A., Subanandan, A., Isableu, B., Ohlmann, T., Golding, J. F., Gresty, M. A., (2004). We are most aware of our place in the world when about to fall. Curr.Biol. 14, R609-R610.

Brenner, E., Smeets, J. B. J., (2011). Continuous visual control of interception. Human Movement Science 30, 475-494.

Brenner, E., van Dam, M., Berkhout, S., Smeets, J. B. J., (2012). Timing the moment of impact in fast human movements. Acta Psychologica 141, 104-111.

Bringoux, L., Blouin, J., Coyle, T., Ruget, H., Mouchnino, L., (2012). Effect of gravity-like torque on goal-directed arm movements in microgravity. J Neurophysiol 107, 2541-3548.

Brown, L. E., Rosenbaum, D. A., (2002). Motor Control: Models. In: Nadel, L. (Ed.), Encyclopedia of Cognitive Science. London, pp. 127-133.

Bryson, A. E. Jr., Ho, Y.-C., (1975). Applied Optimal Control: Optimization, Estimation and Control. Wiley, New York.

Burton, G., Turvey, M. T., Solomon, H. Y., (1990). Can shape be perceived by dynamic touch? Percept.Psychophys. 48, 477-487.

Caljouw, S. R., van der Kamp, J., Savelsbergh, G. J. P., (2004). Timing of goal-directed hitting: impact requirements change the information-movement coupling. Experimental Brain Research 155, 135-144.

Cappozzo, A., Catani, F., Leardini, A., enedetti, M., roce, U. D., (1996). Position and orientation in space of bones during movement: experimental artefacts. Clinical Biomechanics 11, 90-100.

Carello, C., Turvey, M. T., (2000). Rotational dynamics and dynamic touch. In: Heller, M. (Ed.), Touch, representation and blindness. Oxford University Press, Oxforf, pp. 27-66.

Carello, C., (2004). Perceiving Affordances by Dynamic Touch: Hints From the Control of Movement. Ecolog Psychol 16, 31-36.

Cesqui, B., D'Avella, A., Portone, A., Lacquaniti, F., (2012). Catching a Ball at the Right Time and Place: Individual Factors Matter. PLoS ONE 7, e31770.

Chandler, W. K., Schneider, M. F., Rakowski, R. F., Adrian, R. H., (1975). Charge movements in skeletal muscle. Philos Trans R Soc Lond B Biol Sci. 10, 501-505.

Cheng, C.-K., Chen, H.-H., Chen, C.-S., Lee, C.-L., Chen, C.-Y., (2000). Segment inertial properties of Chinese adults determined from magnetic resonance imaging, Clinical Biomechanics, Volume 15, Issue 8, October 2000, Pages 559-566. Clinical Biomechanics 15, 559-566.

Chiari, L., Rocchi, L., Cappello, A., (2002). Stabilometric parameters are affected by anthropometry and foot placement. Clinical Biomechanics 17, 666-677.

Chow, J. W., Carleton, L. G., Lim, Y. T., (2003). Comparing the pre- and post-impact ball and racquet kinematics of elite tennis players' first and second serves: a
preliminary study. J Sports Sci. 7, 529-537.

Chung, PY., Ng, GY., (2012). Comparison between an accelerometer and a three-dimensional motion analysis system for the detection of movement. Physiotherapy. P3, 256-259.

Coleman, S. G. S., Benham, A. S., Northcott, S. R., (1993). A three-dimensional cinematographical analysis of the volleyball spike. J Sport Sci 11, 295-302.

Cooper, M. M., Carello, C., Turvey, M. T., (2000). Perceptual independence of whole length, partial length, and hand position in wielding a rod. J.Exp.Psychol.Hum.Percept.Perform. 26, 74-85.

Corazza, S., Mündermann, L., Gambaretto, E., Ferrigno, G., Andriacchi, TP., (2010). Markerless Motion Capture through Visual Hull, Articulated ICP and Subject Specific Model Generation . INTERNATIONAL JOURNAL OF COMPUTER VISION A 87, 156-169.

Cordo, P., Gurfinkel, V. S., Bevan, L., Kerr, G. K., (1995). Proprioceptive consequences of tendon vibration during movement. J.Neurophysiol. 74, 1675-1688.

Corke, P. I., (2011). Robotics, Vision & Control. Springer.

Costa, M., Goldberger, A. L., Peng, C. K., (2005). Multiscale entropy analysis of biological signals. PHYSICAL REVIEW E 71, 021906.

Craig, C. M., Bourdin, C., (2002). Revisited: the inertia tensor as a proprioceptive invariant in humans. Neurosci.Lett. 317, 106-110.

Creveaux, T., Dumas, R., Hautier, C., Macé, P., Chèze, L., Rogowski, I., (2013). JOINT KINETICS TO ASSESS THE INFLUENCE OF THE RACKET ON A TENNIS PLAYER'S SHOULDER. Journal of Sports Science and Medicine 12.

Darling, W. G., Hondzinski, J. M., (1999). Kinesthetic perceptions of earth- and body-fixed axes. Exp Brain Res 126, 417-430.

de Leva, P., (1996). Adjustments to Zatsiorsky-Seluyanov's segment inertia parameters. Journal of Biomechanics 29, 1223-1230.

Debicki, D. B., Gribble, P. L., Watts, S., Hore, J., (2004). Kinematics of wrist joint flexion in overarm throws made by skilled subjects. Exp Brain Res 154, 382-394.

Debicki, D. B., Gribble, P. L., Watts, S., Hore, J., (2011). Wrist muscle activation, interaction torque and mechanical properties in unskilled throws of different speeds. Exp Brain Res 208, 115-125.

Debicki, D. D., Watts, S., Gribble, P. L., Hore, J., (2010). A novel shoulder-elbow mechanism for increasing speed in a multijoint arm movement. Exp Brain Res 203, 601-613.

Del Villar, F., García González, L., Iglesias, D., Perla Moreno, M., Cervelló, E. M., (2007). Expert-novice differences in cognitive and execution skills during tennis competition. Percept Mot Skills 104, 355-365.

DeLucia, P. R., Warren, R., (1994). Pictorial and motion-based depth information during active control self-motion: size arrival effects on collision avoidance. J Exp Psychol Hum PerceptPerform 20, 783-789.

Dempster, W. T., (1955). Space requirement of the seated operator. Ohio: Aerospace Medical Research Laboratories.

Desmurget, M., Prablanc, C., (1997). Postural control of three-dimensional prehension movements. J.Neurophysiol. 77, 452-464.

Diederichsen, L. P., Winther, A., Dyhre-Poulsen, P., Krogsgaard, M. R., Nørregaard, J., (2009). The influence of experimentally induced pain on shoulder muscle activity. Exp Brain Res. 194, 329-337.

Dounskaia, N., (2005). The internal model and the leading joint hypothesis: implications for control of multi-joint movements. Exp.Brain Res. 166, 1-16.

Dounskaia, N., Nogueira, K. G., Swinnen, S. P., Drummon, E., (2010). Limitations on Coupling of Bimanual Movements Caused by Arm Dominance: When the Muscle Homology Principle Fails. Neurophysiol 103, 2027-2038.

Dounskaia, N., Wisleder, D., Johnson, T., (2005). Influence of biomechanical factors on substructure of pointing movements. Exp.Brain Res. 164, 505-516.

Dounskaia, N. V., (1998). Artificial potential method for control of constrained robot motion. IEEE Trans.Syst.Man.Cybern.B Cybern. 28, 447-453.

Dounskaia, N. V., Ketcham, C. J., Stelmach, G. E., (2002). Influence of biomechanical constraints on horizontal arm movements. Motor Control 6, 366-387.

Dounskaia, N. V., Swinnen, S. P., Walter, C. B., Spaepen, A. J., Verschueren, S. M., (1998). Hierarchical control of different elbow-wrist coordination patterns. Exp.Brain Res. 121, 239-254.

Dumas, R., Cheze, L., Verriest, J. P., (2007). Adjustments to McConville et al. and Young et al. body segment inertial parameters. J.Biomech. 40, 543-553.

Ebaugh, D. D., McClure, P. W., Karduna, A. R., (2006a). Effects of shoulder muscle fatigue caused by repetitive overhead activities on scapulothoracic and glenohumeral kinematics. J.Electromyogr.Kinesiol. 16, 224-235.

Ebaugh, D. D., McClure, P. W., Karduna, A. R., (2006b). Scapulothoracic and glenohumeral kinematics following an external rotation fatigue protocol. J.Orthop.Sports Phys.Ther. 36, 557-571.

Edin, B. B., (2001). Cutaneous afferents provide information about knee joint movements in humans. J Physiol 531, 289-297.

Edwards, B. J., Waterhouse, J., (2009). EFFECTS OF ONE NIGHT OF PARTIAL SLEEP DEPRIVATION UPON DIURNAL RHYTHMS OF ACCURACY AND CONSISTENCY IN THROWING DARTS. Chronobiology International 26, 756-768.

Ellenbecker, T. S., Roetert, E. P., Baillie, D. S., Davies, G. J., Brown, S. W., (2002). Glenohumeral joint total rotation range of motion in elite tennis players and baseball pitchers. Med Sci Sports Exerc. 34, 2052-2056.

Elliott, B., Marshall, R., Noffal, G. J., (1995a). Contributions of upper limb segment rotation during the power serve in tennis. J Appl Biomech 11, 433-442.

Elliott, B. C., Marshall, R. N., Noffal, G. J., (1995b). Contributions of upper limb segment rotations during the power serve in tennis. J Appl Biomech 11, 433-442.

Escamilla, R. F., Andrews, J. R., (2009). Shoulder muscle recruitment patterns and related biomechanics during upper extremity sports. Sports Med. 39, 569-590.

Faisal, A. A., Selen, L. P., Wolpert, D. M., (2008). Noise in the nervous system. Nat.Rev.Neurosci. 9, 292-303.

Fajen, B. R., Warren, W. H., (2007). Behavioral dynamics of intercepting a moving target. Exp Brain Res. 180, 303-319.

Firestone, C. Z., Warren, W. H., (2010). Why does the rabbit escape the fox on a zig-zag path? Predator-prey dynamics and the constant bearing strategy. J.Vision 10, 10-49.

Fischer, O., Braune, C. W., (1899). Der Gang des Menschen.

Fitzpatrick, P., Carello, C., Turvey, M. T., (1994). Eigenvalues of the inertia tensor and exteroception by the "muscular sense". Neuroscience 60, 551-568.

Flanagan, J. R., Lolley, S., (2001). The inertial anisotropy of the arm is accurately predicted during movement planning. J.Neurosci. 21, 1361-1369.

Flanders, M., Soechting, J. F., (1992). Kinematics of typing: parallel control of the two hands. J.Neurophysiol. 67, 1264-1274.

Fleisig, G., Nicholls, R., Elliott, B., Escamilla, R., (2003). Kinematics used by world class tennis players to produce high-velocity serves. Sports Biomech. 2, 51-71.

Fleisig, S. G., Barrentine, S. W., Zheng, N., Escamilla, R. F., Andrews J.R., (1999). Kinematic and kinetic comparison of baseball pitching among various levels of development. Journal of Biomechanics 32, 1375.

Fradet, L., Botcazou, M., Durocher, C., Cretual, A., Multon, F., Prioux, J., Delamarche, P., (2004). Do handball throws always exhibit a proximal-to-distal segment sequence? Journal of Sport Science 5, 447.

Franklin, D. W., Burdet, E., Osu, R., Kawato, M., Milner, T. E., (2003). Functional significance of stiffness in adaptation of multijoint arm movements to stable and unstable dynamics. ExpBrain Res, 151, 145-157.

Ganley, K. J., Powers, C. M., (2004). Determination of lower extremity anthropometric parameters using dual energy X-ray absorptiometry: the influence on net joint moments during gait. Clinical Biomechanics 19, 50-56.

Garrett, S. R., Pagano, C., Austin, G., Turvey, M. T., (1998). Spatial and physical frames of reference in positioning a limb. Percept.Psychophys. 60, 1206-1215.

Ghez, C., Gordon, J., Ghilardi, M. F., (1995). Impairments of reaching movements in patients without proprioception. II. Effects of visual information on accuracy. J.Neurophysiol. 73, 361-372.

Gibson, J. J., (1966). The senses considered as perceptual systems. Houghton Mifflin company, Boston.

Gibson, J. J., (1979). The ecological approach to visual perception. Houghton Mifflin company, Boston.

Gielen, S., (2009). Review of models for the generation of multi-joint movements in 3-D. Adv.Exp.Med.Biol. 629, 523-550.

Girard, O., Micallef, J. P., Millet, G. P., (2005). Lower-limb activity during the power serve in tennis: effects of performance level. Med Sci Sports Exerc. 37, 1021-1029.

Goble, J. A., Zhang, Y., Shimansky, Y., Sharma, S., Dounskaia, N. V., (2007). Directional biases reveal utilization of arm's biomechanical properties for optimization of motor behavior. J.Neurophysiol. 98, 1240-1252.

Gribble, P. L., Mullin, L. I., Cothros, N., Mattar, A., (2003). Role of cocontraction in arm movement accuracy. J Neurophysiol. 89, 2396-2405.

Gueguen, N., Coyle, T., Craig, C., Bootsma, R., Mouchnino, L., (2004). Is perception of upper body orientation based on the inertia tensor? Normogravity versus microgravity conditions. Exp.Brain Res. 156, 471-477.

Guerraz, M., Shallo-Hoffmann, J., Yarrow, K., Thilo, K. V., Bronstein, A. M., Gresty, M. A., (2000). Visual control of postural orientation and equilibrium in congenital nystagmus. Invest Ophthalmol.Vis.Sci. 41, 3798-3804.

Guigon, E., (2010). Models and architectures for motor control: Simple or complex? In: Danion, F., Latash, M. L. (Eds.), *Motor Control*. Oxford University Press, Oxford, UK.

Haggard, P., Wolpert, D. M., (2005). Disorders of Body Scheme. In: Freund, H. J., Jeannerod, M., Hallett, M., Leiguarda, R. (Eds.), Higher-Order Motor Disorders. University Press.

Hanavan Jr., E. P., (1964). A Mathematical Model Of The Human Body. Amrl-Tr-64-102." Amrl Tr: 1-149.

Hansen, C., Honeine, JL., Gibas, D., Rezzoug, N., Gorce, P., Isableu, B., (2012a). Low-cost motion capture systems in practice. Comput Methods Biomech Biomed Engin. 15, 253-255.

Hansen, C., Rezzoug, N., Gorce, P., Isableu, B., (2012b). Is the time of release during a precision throwing task, predictable? Comput Methods Biomech Biomed Engin 15, 250-252.

Henriques, D. Y., Klier, E. M., Smith, M. A., Lowy, D., Crawford, J. D., (1998). Gaze-centered remapping of remembered visual space in an open- loop pointing task. J.Neurosci. 18, 1583-1594.

Hirashima, M., Kadota, H., Sakurai, S., Kudo, K., Ohtsuki, T., (2002). Sequential muscle activity and its functional role in the upper extremity and trunk during overarm throwing. J.Sports Sci. 20, 301-310.

Hirashima, M., Kudo, K., Ohtsuki, T., (2003a). Utilization and compensation of interaction torques during ball-throwing movements. J.Neurophysiol. 89, 1784-1796.

Hirashima, M., Kudo, K., Ohtsuki, T., (2007a). A new non-orthogonal decomposition method to determine effective torques for three-dimensional joint rotation. J.Biomech 40, 871-882.

Hirashima, M., Kudo, K., Watarai, K., Ohtsuki, T., (2007b). Control of 3D limb dynamics in unconstrained overarm throws of different speeds performed by skilled baseball players. J.Neurophysiol. 97, 680-691.

Hirashima, M., Ohgane, K., Kudo, K., Hase, K., Ohtsuki, T., (2003b). Counteractive relationship between the interaction torque and muscle torque at the wrist is predestined in ball-throwing. J.Neurophysiol. 90, 1449-1463.

Hirashima, M., Yamane, K., Nakamura, Y., Ohtsuki, T., (2008). Kinetic chain of overarm throwing in terms of joint rotations revealed by induced acceleration analysis. Journal of Biomechanics 41, 2874-2883.

Holden, J. P., Orsini, J. A., Siegel, K. L., Kepple, T. M., Gerber, L. H., Stanhope, S. J., (1997). Surface movement errors in shank kinematics and knee kinetics during gait. Gait and Posture 5, 217-227.

Hollerbach, M. J., Flash, T., (1982). Dynamic interactions between limb segments during planar arm movement. Biol.Cybern. 44, 67-77.

Hong, D. A., Cheung, T. K., Roberts, E. M., (2001). A three-dimensional, six-segment chain analysis of forceful overarm throwing. J Electromyogr Kinesiol 11, 95-112.

Hore, J., Debicki, D. B., Gribble, P. L., Watts, S., (2011). Deliberate utilization of interaction torques brakes elbow extension in a fast throwing motion. Exp Brain Res 211, 63-72.

Hore, J., Watts, S., (2011). Skilled throwers use physics to time ball release to the nearest millisecond. J Neurophysiol 106, 2024-2033.

Hore, J., Watts, S., Tweed, D., Miller, B., (1996). Overarm throws with the nondominant arm: kinematics of accuracy. J.Neurophysiol. 76, 3693-3704.

Houghton Mifflin Company (COR), A. H., (2007). Medical Dictionary. Houghton Mifflin Company.

Houk, J. C., Buckingham, J. T., Barto, A. G., (1996). Models of the cerebellum and motor learning. Behav.Brain Sci. 19, 368-383.

Iino Y., Kojima T., (2011). Kinetics of the upper limb during table tennis topspin forehands in advanced and intermediate players. Sports Biomech. 10, 361-377.

Isableu, B., Hansen, C., Rezzoug, N., Gorce, P., (2013). Velocity-dependent changes of rotational axes during the control of unconstrained 3D arm motions depend on initial instruction on limb position. Hum Mov Sci (in press).

Isableu, B., Ohlmann, T., Cremieux, J., Amblard, B., (1997). Effet d'une entrée différentielle sur les performances posturales en fonction de la difficulté de la tâche. In: Lacour, M. (Ed.), Posture et Equilibre. *Pathologies, Vieillissement, Stratégies, Modélisation*. Sauramps Médical, pp. 115-121.

Isableu, B., Ohlmann, T., Cremieux, J., Amblard, B., (1998). How dynamic visual field dependence-independence interacts with the visual contribution to postural control. Human Movement Science 17, 367-391.

Isableu, B., Ohlmann, T., Cremieux, J., Amblard, B., (2003). Differential approach to strategies of segmental stabilisation in postural control. Exp.Brain Res. 150, 208-221.

Isableu, B., Rezzoug, N., Mallet, G., Bernardin, D., Gorce, P., Pagano, C. C., (2009). Velocity-dependent changes of rotational axes in the non-visual control of unconstrained 3D arm motions. Neuroscience 164, 1632-1647.

Isableu, B., Vuillerme, N., (2006). Differential integration of kinaesthetic signals to postural control. Exp.Brain Res. 174, 763-768.

Jacobs, D. M., Michaels, C. F., (2006). Lateral interception I: operative optical variables, attunement, and calibration. J.Exp.Psychol.Hum.Percept.Perform. 32, 443-458.

Jacquier-Bret, J., (2009). Analyse biomécanique du mouvement de préhension contraint et altéré : indices quantitatifs de la gestion de la redondance motrice. Ph.D .

Jiang, B. C., Yang, W. H., Shieh, J. S., Fan, J. S. Z., Peng, C. K., (2011). Entropy-based Method for COP data Analysis. Theoretical Issues of Ergonomics Science 1-20.

Jones, L. A., (1986). Perception of force and weight: theory and research. Psychol Bull 100, 29-42.

Jordan, M. I., Wolpert, D. M., (1999). The Cognitive Neurosciences. MIT Press, Cambridge, MA.

Jöris, H. J. J., Edwards van Muyen, A. J., van Ingen Schenau, G. J., Kemper, H. C. G., (1985). Force, velocity and energy flow during the overarm throw in female handball players. Journal of Biomechanics 6, 409-414.

Kandel, E. R., Schwartz, J. H., Jessell, T. M., (2000). Principles of Neural Science. McGraw-Hill, New York..

Kawato, M., (1999). Internal models for motor control and trajectory planning. Curr Opin Neurobiol 9, 718-723.

Kawato, M., Furukawa, K., Suzuki, R., (1987). A hierarchical neural-network model for control and learning of voluntary movement. Biol.Cybern. 57, 169-185.

Kelso, J. A. S., (1995). Dynamic Patterns: The Self Organization of Brain and Behavior. MIT Press, Cambridge.

Kingma, I., Beek, P. J., van Dieen, J. H., (2000). The inertia tensor vs static moment and mass in perceiving length and heaviness of hand-wielded rods. J Exp Psychol Hum Percept Perform 28, 180-191.

Kingma, I., van de Langenberg, R., Beek, P. J., (2004). Which mechanical invariants are associated with the perception of length and heaviness of a nonvisible handheld rod? Testing the inertia tensor hypothesis. J.Exp.Psychol.Hum.Percept.Perform. 30, 346-354.

Kirk, D. E., (1970). Optimal Control Theory: An Introduction. Prentice-Hall, Eaglewood Cliffs.

Kluzik, J., Horak, F. B., Peterka, R. J., (2005). Differences in preferred reference frames for postural orientation shown by after-effects of stance on an inclined surface. Exp.Brain Res. 162, 474-489.

Kodek, T., Munih, M., (2006). An identification technique for evaluating body segment parameters in the upper extremity from manipulator-hand contact forces and arm kinematics . Clinical Biomechanics 21, 710-716.

Kovacs, M., Ellenbecker, T., (2011). An 8-Stage Model for Evaluating the Tennis Serve: Implications for Performance Enhancement and Injury Prevention. Sports Health 3, 504-513.

Lackner, J. R., DiZio, P., (2000). Human orientation and movement control in weightless and artificial gravity environments. Exp.Brain Res. 130, 2-26.

Lacquaniti, F., Soechting, J. F., Terzuolo, C. A., (1982). Some factors pertinent to the organization and control of arm movements. Brain Res. 252, 394-397.

Lacquaniti, F., Terzuolo, C., Viviani, P., (1983). The law relating the kinematic and figural aspects of drawing movements. Acta Psychol (Amst) 54, 115-130.

Latash, M. L., (2008). Neurophysiological Basis of Movement. Human Kinetics, Leeds.

Latash, M. L., (1998). Progress in Motor Control. Human Kinetics.

Latash, M. L., Scholz, J. P., Schoner, G., (2002). Motor control strategies revealed in the structure of motor variability. Exerc.Sport Sci.Rev. 30, 26-31.

Laursen, B., Jensen, B. R., Sjøgaard, G., (1998). Effect of speed and precision demands on human shoulder muscle electromyography during a repetitive task. Eur J Appl Physiol Occup Physiol. 78, 544-548.

Lee, D. N., (1976). A theory of visual control of braking based on information about time-to-collision. Perception 5, 437-459.

Lee, JK., Park, EJ., (2011). 3D spinal motion analysis during staircase walking using an ambulatory inertial and magnetic sensing system. Medical & biological engineering & computing, 49, 755-764.

Lemay, M., Stelmach, G. E., (2005). Multiple frames of reference for pointing to a remembered target. Exp Brain Res 164, 301-310.

Lenhard, A., Hoffmann, J., (2007). Constant error in aiming movements without visual feedback is higher in the preferred hand. Laterality 12, 227-238.

Lim, CK., Luo, Z., hen, I. M., eo, S. H., (2011). A low cost wearable optical-based goniometer for human joint monitoring. Frontiers of mechanical engineering. 6, 13-22.

Lorin, P., Maletsky, L. P., Sun, J., Morton, N. A., (2007). Accuracy of an optical active-marker system to track the relative motion of rigid bodies. Journal of Biomechanics 40, 682-685.

Lu, C. W., Czosnyka, M., Shieh, J. S., Smielewska, A., Pickard, J. D., Smielewski, P., (2012). Complexity of intracranial pressure correlates with outcome after traumatic brain injury. Brain 135, 2399-2408.

Malmström, E. M., Karlberg, M., Melander, A., agnusson, M., (2003). Zebris versus Myrin: a comparative study between a three-dimensional ultrasound movement analysis and an inclinometer/compass method: intradevice reliability, concurrent validity, intertester comparison, intratester reliability, and intraindividual variability. Spine 1, 433-440.

Manal, K., McClay, I., Stanhope, S., Richards, J., Galinat, B., (2000). Comparison of surface mounted markers and attachment methods in estimating tibial rotations during walking: an in vivo study. Gait and Posture 11, 38-45.

Mann, D. L., Abernethy, B., Farrow, D., (2010). Action specificity increases anticipatory performance and the expert advantage in natural interceptive tasks. Acta Psychol (Amst) 135, 17-23.

Manor, B., Costa, M. D., Hu, K., Newton, E., Starobinets, O., Kang H.G., Peng, C. K., Novak, V., Lipsitz, L. A., (2010). Physiological complexity and system adaptability: evidence from postural control dynamics of older adults. J Appl Physiol 109, 1786-1791.

Marinovic, W., Plooy, A. M., Tresilian, J. R., (2009). The utilisation of visual information in the control of rapid interceptive actions. Exp Psychol 56, 265-273.

Marshall, R. N., Elliott, B. C., (2000). Long-axis rotation: the missing link in proximal-to-distal segmental sequencing. J Sports Sci 18, 247-254.

Massion, J., (1994). Postural control system. Curr.Opin.Neurobiol. 4, 877-887.

Mazynn, L. I., Savelsbergh, G. J., Montagne, G., Lenoir, M., (2007). Planning and on-line control ofcatchingas a function of perceptual-motor constraints. Acta Psychol (Amst) 126, 59-78.

McConville, J. T., Clauser, C. E., Churchill, T. D., Cuzzi, J., Kaleps, I., (1980). Anthropometric relationships of body and body segment moments of inertia. Aerospace Medical Research Laboratory, Wright-Patterson Air Force Base, Dayton, Ohio. AFAMRL-TR-80-119.

McGuire, L. M., Sabes, P. N., (2009). Sensory transformations and the use of multiple reference frames for reach planning. Nat.Neurosci. 12, 1056-1061.

McIntyre, J., Berthoz, A., Lacquaniti, F., (1998). Reference frames and internal models for visuo-manual coordination: what can we learn from microgravity experiments? Brain Res.Brain Res.Rev. 28, 143-154.

McIntyre, J., Stratta, F., Lacquanti, F., (1997). Viewer-centered frame of reference for pointing to memorized targets in three-dimensional space. J.Neurophysiol. 78, 1601-1618.

McLeod, R. W., Ross, H. E., (1983). Optic flow and cognitive factors in time-to-collision. Perception 12, 417-423.

Medendorp, W. P., Crawford, J. D., (2002). Visuospatial updating of reaching targets in near and far space. Neuroreport 13, 633-636.

Medendorp, W. P., Goltz, H. C., Vilis, T., Crawford, J. D., (2003). Gaze-centered updating of visual space in human parietal cortex. J.Neurosci. 23, 6209-6214.

Meister, K., (2000). Injuries to the shoulder in the throwing athlete: part one, biomechanics/pathophysiology/classification of injury. Am J Sports Med 28, 265-275.

Merriam-Webster, (1986). Webster's medical desk dictionary. Merriam-Webster, Springfield, MA.

Miall, R. C., Wolpert, D. M., (1996). Forward models for physiological motor control. Neural Networks 9, 1265-1279.

Michaels, C. F., Carello, C., (1981). Direct perception. Prentice Hall, New York.

Michaels, C. F., Jacobs, D. M., Bongers, R. M., (2006). Lateral interception II: predicting hand movements. J.Exp.Psychol.Hum.Percept.Perform. 32, 459-472.

Mizuno, T., Takahashi, T., Cho, R. Y., Kikuchi, M., Murata, T., Takahashi, K., Wada, Y., (2010). Assessment of EEG dynamical complexity in Alzheimer's disease using multiscale entropy. Clin Neurophysiol 121, 1438-1446.

Montagne, G., Fraisse, F., Ripoll, H., Laurent, M., (2000). Perceptionaction coupling in an interceptive task: first-order time-tocontact as an input variable. Hum Movem Sci 19, 59-72.

Müller, S., Abernethy, B., (2012). Expert anticipatory skill in striking sports: a review and a model. Res Q Exerc Sport 83, 175-187.

Mullineaux, D. R., Bartlett, R. M., Bennett, S., (2001). Research design and statistics in biomechanics and motor control. J Sports Sci. 19, 739-760.

Mündermann, L., Corazza, S., Andriacchi, T. P., (2006). The evolution of methods for the capture of human movement leading to markerless motion capture for biomechanical applications. J Neuroengineering Rehabil 3, 6.

Mungiole, M., Martin, P. E., (1990). Estimating segment inertial properties: comparison of magnetic resonance imaging with existing methods. Journal of Biomechanics 23, 1039-1046.

Nagasaki, H., (1989). Asymmetric velocity and acceleration profiles of human arm movements. ExpBrain Res 74, 319-326.

Newell A., Simon H.A, (1972). Human Problem Solving. Englewood Cliffs, NJ: Prentice-Hall.

Nigg, BM., Baltich, J., Maurer, C., Federolf, P., (2012). Shoe midsole hardness, sex and age effects on lower extremity kinematics during running. Journal of Biomechanics 1, 1692-1697.

Oldfield, R. C., (1971). The assessment and analysis of handedness: The Edinburgh inventory. Neuropsychologia 9, 97-113.

Osu, R., Kamimura, N., Iwasaki, H., Nakano, E., Harris, C. M., Wada, Y., Kawato, M., (2004). Optimal impedance control for task achievement in the presence of signal-dependent noise. J Neurophysiol. 92, 1199-1215.

Pagano, C. C., (2000). The role of the inertia tensor in kinesthesis. Crit Rev.Biomed.Eng 28, 231-236.

Pagano, C. C., Carello, C., Turvey, M. T., (1996a). Exteroception and exproprioception by dynamic touch are different functions of the inertia tensor. Percept.Psychophys. 58, 1191-1202.

Pagano, C. C., Fitzpatrick, P., Turvey, M. T., (1993). Tensorial basis to the constancy of perceived object extent over variations of dynamic touch. Percept.Psychophys. 54, 43-54.

Pagano, C. C., Garrett, S. R., Turvey, M. T., (1996b). Is lims proprioception a function of the limb' inertial eigenvectors? Ecological Psychology, 8, 43-69.

Pagano, C. C., Kinsella-Shaw, J. M., Cassidy, P. E., Turvey, M. T., (1994). Role of the inertia tensor in haptically perceiving where an object is grasped. J.Exp.Psychol.Hum.Percept.Perform. 20, 276-285.

Pagano, C. C., Turvey, M. T., (1995). The inertia tensor as a basis for the perception of limb orientation. J.Exp.Psychol.Hum.Percept.Perform. 21, 1070-1087.

Pagano, C. C., Turvey, M. T., (1998). Eigenvectors of the inertia tensor and perceiving the orientations of limbs and objects. J.Appl Biomech 14, 331-359.

Pai, D. K., (2010). Muscle mass in musculoskeletal models. Journal of Biomechanics 43, 2093-2098.

Paillard, J., (1991). Motor and representational framing in space. In: Paillard, J. (Ed.), Brain and space. Oxford University Press, Oxford, pp. 163-182.

Pàmies-Vilà, R., Font-Llagunes, J. M., Cuadrado, J., Javier Alonso, F., (2012). Analysis of different uncertainties in the inverse dynamic analysis of human gait. Mechanism and Machine Theory 58, 153-164.

Papaxanthis, C., Pozzo, T., McIntyre, J., (2005). Kinematic and dynamic processes for the control of pointing movements in humans revealed by short-term exposure to microgravity. Neuroscience 135, 371-383.

Papaxanthis, C., Pozzo, T., Popov, K. E., McIntyre, J., (1998). Hand trajectories of vertical arm movements in one-G and zero-G environments. Evidence for a central representation of gravitational force [In Process Citation]. Exp.Brain Res. 120, 496-502.

Papaxanthis, C., Pozzo, T., Schieppati, M., (2003). Trajectories of arm pointing movements on the sagittal plane vary with both direction and speed. Exp BrainRes 148, 498-503.

Paraskevas, G., Papadopoulos, A., Papaziogas, B., Spanidou, S., Argiriadou, H., Gigis, J., (2004). Study of the carrying angle of the human elbow joint in full extension: a morphometric analysis. Surg Radiol Anat. 26, 19-23.

Pearsall, DJ., Costigan, P. A., (1999). The effect of body segment parameter error on gait analysis results. Gait & Posture 9, 173-183.

Pellionisz, A., (1985). Tensorial aspects of the multidimensional approach to the vestibulo-oculomotor reflex and gaze. Rev.Oculomot.Res. 1, 281-296.

Pellionisz, A., Llinas, R., (1985). Tensor network theory of the metaorganization of functional geometries in the central nervous system. Neuroscience 16, 245-273.

Peper, L., Bootsma, R. J., Mestre, D. R., Bakker, F. C., (1994). Catching Balls: How to Get the Hand to the Right Place at the Right Time. Journal of Experimental Psychology: Human Perception and Performance 20, 591-612.

Pincus, S. M., (1991). Approximate entropy as a measure of system complexity. Proc Natl Acad Sci USA 88, 2297-2301.

Plamondon, R., Alimi, A. M., Yergeau, P., Leclerc, F., (1993). Modelling velocity profiles of rapid movements: a comparative study. Biol Cybern. 69, 119-128.

Pontryagin, L. S., Boltyanskii, V. G., Gramkrelidze, R. V., Mishchenko, E. F., (1962). The Mathematical Theory of Optimal Processes. Wiley-Interscience, New York.

Pozzo, T., Papaxanthis, C., Stapley, P., Berthoz, A., (1998). The sensorimotor and cognitive integration of gravity. Brain Res.Brain Res.Rev. 28, 92-101.

Proske, U., Wise, A. K., Gregory, J. E., (2000). The role of muscle receptors in the detection of movements. Prog Neurobiol 60, 85-93.

Protzner, AB., Valiante, T. A., Kovacevic, N., McCormick, C., McAndrews, M. P., (2010). Hippocampal signal complexity in mesial temporal lobe epilepsy: a noisy brain is a healthy brain. Arch Ital Biol 148, 289-297.

Przybyla, A., Good, D. C., Sainburg, R. L., (2012). Dynamic dominance varies with handedness: reduced interlimb asymmetries in left-handers. Exp Brain Res 216, 419-431.

Rao, G., Amaratini, D., Berton, E., Favier, D., (2006). Influence of body segments' parameters estimation models on inverse dynamics solutions during gait. Journal of Biomechanics 39, 1531-1536.

Reinschmidt, C., van den Bogert, A. J., Nigg, B. M., Lundberg, A., Murphy, N., (1997). Effect of skin movement on the analysis of skeletal knee joint motion during running. Journal of Biomechanics 30, 729-732.

Richards, L., (1999). The measurement of human motion: A comparison of commercially available systems. Human Movement Science 18, 589-602.

Rigoux, L., Guigon, E., (2012). A model of reward- and effort-based optimal decision making and motor control. PLoS Comput Biol. 8, e1002716.

Riley, M. A., Pagano, C. C., (2003). Inertial Eigenvectors Play a Role in Proprioception: Comment on Craig and Bourdin (2002). Ecological Psychology, 15, 229-240.

Riley, M. A., Shaw, T. H., Pagano, C. C., (2005). Role of the inertial eigenvectors in proprioception near the limits of arm adduction range of motion. Hum.Mov Sci. 24, 171-183.

Riley, M. A., Turvey, M. T., (2001). Inertial constraints on limb proprioception are independent of visual calibration. J.Exp.Psychol.Hum.Percept.Perform. 27, 438-455.

Robertson, D. G. E., (2004). Research methods in biomechanics. Human Kinetics.

Rothwell, J. C., Traub, M. M., Day, B. L., Obeso, J. A., Thomas, P. K., Marsden, C. D., (1982). Manual motor performance in a deafferented man. Brain Sep; 105, 515-542.

Sainburg, R. L., (2002). Evidence for a dynamic-dominance hypothesis of handedness. Exp.Brain Res. 142, 241-258.

Sainburg, R. L., (2005). Handedness: differential specializations for control of trajectory and position. Exerc.Sport Sci.Rev. 33, 206-213.

Sainburg, R. L., Kalakanis, D., (2000). Differences in control of limb dynamics during dominant and nondominant arm reaching. J.Neurophysiol. 83, 2661-2675.

Sainburg, R. L., Lateiner, J. E., Latash, M. L., Bagesteiro, L. B., (2003). Effects of altering initial position on movement direction and extent. J.Neurophysiol. 89, 401-415.

Sainburg, R. L., Wang, J., (2002). Interlimb transfer of visuomotor rotations: independence of direction and final position information. Exp.Brain Res. 145, 437-447.

Sande de Souza, L. A., Dionisio, V. C., Lerena, M. A., Marconi, N. F., Almeida, G. L., (2009). The linear co-variance between joint muscle torques is not a generalized principle. J.Electromyogr.Kinesiol. 19, e171-e179.

Sanes, J. N., Mauritz, K. H., Dalakas, M. C., Evarts, E. V., (1985). Motor control in humans with large-fiber sensory neuropathy. Hum Neurobiol 4, 101-114.

Savelsbergh, G. J., Whiting, H. T., Burden, A. M., Bartlett, R. M., (1992). The role of predictive visual temporal information in the coordination of muscle activity in catching. Exp Brain Res. 89, 223-228.

Scholz, J. P., Schoner, G., (1999). The uncontrolled manifold concept: identifying control variables for a functional task. Exp.Brain Res. 126, 289-306.

Schorer, J., Baker, J., Fath, F., Jaitner, T., (2007). Identification of interindividual and intraindividual movement patterns in handball players of varying expertise levels. J Mot.Behav. 39, 409-421.

Seidler-Dobrin, R. D., Stelmach, G. E., (1998). Persistence in visual feedback control by the elderly. Exp Brain Res. 119, 467-474.

Senk, M., Chèze, L., (2006). Rotation sequence as an important factor in shoulder kinematics. Clinical Biomechanics 21, S3-S8.

Senot, P., Prévost, P., McIntyre, J., (2003). Estimating time to contact and impact velocity when catching an accelerating object with the hand. J Exp Psychol Hum Percept Perform 29, 219-237.

Shadmehr, R., Mussa-Ivaldi, F. A., (1994). Adaptive representation of dynamics during learning of a motor task. J.Neurosci. 14, 3208-3224.

Shamaei, K., awicki, G. S., ollar, A. M., (2013). Estimation of Quasi-Stiffness and Propulsive Work of the Human Ankle in the Stance Phase of Walking. PLoS ONE 8, e59935.

Sharp, R. H., Whiting, H. T. A., (1974). Exposure and occluded duration effects in a ball catching skill. Journal of Motor Behavior 3, 139-147.

Sherrington, C. S., (1906). Integrated Action of the Nervous System. Cambridge University Press, Cambridge, UK.

Shumway-Cook, A., Woollacott, M. H., (2007). Motor Control - Translating Research into Clinical Practice. Lippincott Williams & Wilkins, Philadelphia..

Smeets, J. B. J., Frens, M. A., Brenner, E., (2002). Throwing darts: timing is not the limiting factor. Exp Brain Res 144, 268-274.

Soechting, J. F., (1982). Does position sense at the elbow reflect a sense of elbow joint angle or one of limb orientation? Brain Res. 248, 392-395.

Soechting, J. F., Flanders, M., (1989). Sensorimotor representations for pointing to targets in three-dimensional space. J.Neurophysiol. 62, 582-594.

Soechting, J. F., Flanders, M., (1991). Arm movements in three-dimensional space: computation, theory, and observation. Exerc.Sport Sci.Rev. 19, 389-418.

Soechting, J. F., Flanders, M., (1992). Moving in three-dimensional space: frames of reference, vectors, and coordinate systems. Annu.Rev.Neurosci. 15, 167-191.

Soechting, J. F., Lacquaniti, F., (1981). Invariant characteristics of a pointing movement in man. J.Neurosci. 1, 710-720.

Soechting, J. F., Lacquaniti, F., (1989). An assessment of the existence of muscle synergies during load perturbations and intentional movements of the human arm. Exp.Brain Res. 74, 535-548.

Solomon, H. Y., Turvey, M. T., (1988). Haptically perceiving the distances reachable with hand-held objects. J.Exp.Psychol.Hum.Percept.Perform. 14, 404-427.

Stodden, D. F., Fleisig, G. S., McLean, S. P., Lyman, S. L., Andrews, J. R., (2001). Relationship of pelvis and upper torso kinematics to pitched baseball velocity. J Appl Biomech 17, 164-172.

Stoffregen, T. A., Bardy, B. G., (2001). On specification and the senses. Behav.Brain Sci. 24, 195-213.

Sutherland, D. H., (2002). The evolution of clinical gait analysis. Part II kinematics. Gait and Posture 16, 159-179.

Takahashi, T., Cho, R. Y., Mizuno, T., Kikuchi, M., Murata, T., Takahashi, K., Wada, Y., (2010). Antipsychotics reverse abnormal EEG complexity in drug-naïve schizophrenia: a multiscale entropy analysis. Neuroimage 51, 173-182.

Tamei, T., Obayashi, C., Shibata, T., (2011). Throwing darts utilizes the interaction torque of the elbow joint. Conf Proc IEEE Eng Med Biol Soc 1283-1286.

Todorov, E., (2004). Optimality principles in sensorimotor control. Nat.Neurosci. 7, 907-915.

Todorov, E., (2005). Stochastic optimal control and estimation methods adapted to the noise characteristics of the sensorimotor system. Neural Comput. 17, 1084-1108.

Todorov, E., Jordan, M. I., (2002). Optimal feedback control as a theory of motor coordination. Nat.Neurosci. 5, 1226-1235.

Topka, H., Konczak, J., Schneider, K., Boose, A., Dichgans, J., (1998). Multijoint arm movements in cerebellar ataxia: abnormal control of movement dynamics. Exp Brain Res 119, 493-503.

Tresilian, J. R., Lonergan, A., (2002). Intercepting a moving target: effects of temporal precision constraints and movement amplitude. Exp Brain Res 142, 193-207.

Tresilian, J. R., Plooy, A. M., Marinovic, W., (2009). Manual interception of moving targets in two dimensions: performance and space-time accuracy. Brain Res 1250, 202-217.

Trunkvalterova, Z., Javorka, M., Tonhajzerova, I., Javorkova, J., Lazarova, Z., Javorka, K., Baumert, M., (2008). Reduced short-term complexity of heart rate and blood pressure dynamics in patients with diabetes mellitus type 1: multiscale entropy analysis. Physiol Meas 7, 817-828.

Tsai, T. Y., Lu, T. W., Kuo, M. Y., Hsu, H. C., (2009). Quantification of three-dimensional movement of skin markers relative to the underlying bones during functional activities. Biomedical Engineering: Applications, Basis and Communications 21, 223-232.

Turianikova, Z., Javorka, K., Baumert, M., Calkovska, A., Javorka, M., (2011). The effect of orthostatic stress on multiscale entropy of heart rate and blood pressure. Physiol Meas 32, 1425-1437.

Turvey, M. T., (1990). Coordination. Am.Psychol. 45, 938-953.

Turvey, M. T., Burton, G., Pagano, C. C., Solomon, H. Y., Runeson, S., (1992). Role of the inertia tensor in perceiving object orientation by dynamic touch. J.Exp.Psychol.Hum.Percept.Perform. 18, 714-727.

Turvey, M. T., Carello, C., (2011). Obtaining information by dynamic (effortful) touching. Phil.Trans.R.Soc.B 366, 3123-3132.

Turvey, M. T., Shaw, R. E., Reed, E. S., Mace, W. M., (1981). Ecological laws of perceiving and acting: in reply to Fodor and Pylyshyn (1981). Cognition 9, 237-304.

Turvey, M. T., Shockley, K., Carello, C., (1999). Affordance, proper function, and the physical basis of perceived heaviness. Cognition 73, B17-B26.

Turvey, M. T., Solomon, H. Y., Burton, G., (1989). An ecological analysis of knowing by wielding. J.Exp.Anal.Behav. 52, 387-407.

van Beers, R. J., Baraduc, P., Wolpert, D. M., (2002). Role of uncertainty in sensorimotor control. Philos.Trans.R.Soc.Lond B Biol.Sci. 357, 1137-1145.

van Beers, R. J., Sittig, A. C., Denier van der Gon JJ, (1996). How humans combine simultaneous proprioceptive and visual position information. Exp Brain Res 111, 253-261.

van Beers, R. J., Sittig, A. C., Denier van der Gon JJ, (1998). The precision of proprioceptive position sense. Exp.Brain Res. 122, 367-377.

van Beers, R. J., Sittig, A. C., Denier van der Gon JJ, (1999a). Localization of a seen finger is based exclusively on proprioception and on vision of the finger. Exp Brain Res 125, 43-49.

van Beers, R. J., Sittig, A. C., Gon, J. J., (1999b). Integration of proprioceptive and visual position-information: An experimentally supported model. J Neurophysiol. 81, 1355-1364.

van de Langenberg, R. W., Kingma, I., Beek, P. J., (2007). Perception of limb orientation in the vertical plane depends on center of mass rather than inertial eigenvectors. Exp.Brain Res. 180, 595-607.

van de Langenberg, R. W., Kingma, I., Beek, P. J., (2008). The perception of limb orientation depends on the center of mass. J.Exp.Psychol.Hum.Percept.Perform. 34, 624-639.

van den Dobbelsteen, J. J., Brenner, E., Smeets, J. B., (2001). Endpoints of arm movements to visual targets. Exp.Brain Res. 138, 279-287.

van den Tillar, R., Ettema, G., (2004). A FORCE-VELOCITY RELATIONSHIP AND COORDINATION PATTERNS IN OVERARM THROWING. Journal of Sports Science and Medicine 3, 211-219.

van den Tillar, R., Ettema, G., (2007). A three-dimensional analysis of overarm throwing in experienced handball players. J Appl Biomech 23, 12-19.

van den Tillar, R., Ettema, G., (2009). Is there a proximal-to-distal sequence in overarm throwing in team-handball? J Sports Sci 27, 949-955.

Venture, G., Ayusawa, K., Nakamura, Y., (2009a). A Numerical Method For Choosing Motions With Optimal Excitation Properties For Identification Of Biped Dynamics - An Application to Human. IEEE/RAS-Proc.Int.Conf.on Robotics and Automation 1226-1231.

Venture, G., Ayusawa, K., Nakamura, Y., (2009b). Identification of Human Mass Properties From Motion. Proc.of the IFAC Int.Conf.on Systems Identification 988-993.

Vetter, P., Goodbody, S. J., Wolpert, D. M., (1999). Evidence for an eye-centered spherical representation of the visuomotor map. J.Neurophysiol. 81, 935-939.

Vindras, P., Desmurget, M., Viviani, P., (2005). Error parsing in visuomotor pointing reveals independent processing of amplitude and direction. J Neurophysiol. 94, 1212-1224.

Vindras, P., Viviani, P., (1998). Frames of reference and control parameters in visuomanual pointing. J.Exp.Psychol.Hum.Percept.Perform. 24, 569-591.

Wagner, H., Buchecker, M., von Duvillard, S. P., Müller, E., (2010). Kinematic description of elite vs. low level players in team-handball jump throw. J Sport Sci Med 9, 15-23.

Wagner, H., Müller, E., (2008). The effects of differential and variable training on the quality parameters of a handball throw. Sports Biomechanics 7, 54-71.

Wagner, H., Pfusterschmied, J., von Duvillard, S. P., Müller, E., (2011). Performance and kinematics of various throwing techniques in team-handball. Journal of Sports Science and Medicine 10, 73-80.

Whiting, W. C., Gregor, R. J., Halushka, M., (1991). Body segment and release parameter contributions to new-rules javelin throwing. Int J Sport Biomech 7, 111-124.

Windolf, M., Götzen, N., Morlock, M., (2008). Systematic accuracy and precision analysis of video motion capturing systems-exemplified on the Vicon-460 system. Journal of Biomechanics 41, 2776-2780.

Withagen, R., Michaels, C. F., (2005). The role of feedback information for calibration and attunement in perceiving length by dynamic touch. J.Exp.Psychol.Hum.Percept.Perform. 31, 1379-1390.

Wolpert, D. M., Flanagan, J. R., (2001). Motor prediction. Curr.Biol. 11, R729-R732.

Wolpert, D. M., Ghahramani, Z., (2000). Computational principles of movement neuroscience. Nat.Neurosci. 3 Suppl, 1212-1217.

Wolpert, D. M., Ghahramani, Z., Jordan, M. I., (1995). An internal model for sensorimotor integration. Science 269, 1880-1882.

Worringham, C. J., Stelmach, G. E., (1985). The contribution of gravitational torques to limb position sense. Exp.Brain Res. 61, 38-42.

Wu, G., Van der Helm, F. C., Veeger, H. E., Makhsous, M., Van Roy, P., Anglin, C., Nagels, J., Karduna, A. R., McQuade, K., Wang, X., Werner, F. W., Buchholz, B., (2005). ISB recommendation on definitions of joint coordinate systems of various joints for the reporting of human joint motion--Part II: shoulder, elbow, wrist and hand. J.Biomech 38, 981-992.

Yamasaki, H., Tagami, Y., Fujisawa, H., Hoshi, F., Nagasaki, H., (2008). Interaction torque contributes to planar reaching at slow speed. Biomed.Eng Online. 7, 27.

Yamauchi, M., Imanaka, K., Nakayama, M., Nishizawa, S., (2004). Lateral difference and interhemispheric transfer on arm-positioning movement between right and left handers. Percept Motor Skills 98, 1199-1209.

Young, J. W., Chandler, R. F., Snow, C. C., Robinette, K. M., Zehner, G. F., Lofberg, M. S., (1983). Anthropometric and mass distribution characteristics of the adults female. Technical Report FA-AM-83-16, FAA Civil Aeromedical Institute, Oklaoma City, Oklaoma, 1983.